PROCEEDINGS OF THE 13th SYMPOSIUM ON THE GEOLOGY OF THE BAHAMAS AND OTHER CARBONATE REGIONS

June 8-12, 2006

Edited By
Lisa E. Park and Deborah Freile

Gerace Research Centre
San Salvador, Bahamas
2008

PROCEEDINGS OF THE 13th SYMPOSIUM ON THE GEOLOGY OF THE BAHAMAS AND OTHER CARBONATE REGIONS

Edited By
Lisa E. Park and Deborah Freile

Production Editor
Lisa E. Park

Gerace Research Centre
San Salvador, Bahamas
2008

Front Cover: Rice Bay Formation, looking southwest along Grotto Beach. Photograph by Sandy Voegeli.

Back Cover: Dr. John Milliman, The College of William and Mary. Keynote Speaker for the 13th Symposium. Photograph by Sandy Voegeli.

Produced at
The Department of Geology and Environmental Sciences, The University of Akron

ISBN x-xxxxxx-xx-x

TABLE OF CONTENTS

FORWARD

The Thirteenth Symposium on the Geology of the Bahamas and Other Carbonate Regions (Photo: Sandy Voegeli)

PREFACE

The 13th Symposium on the Geology of the Bahamas and Other Carbonate Regions convened on San Salvador Island from June 8-12, 2006. The meeting continued the long-held tradition of prior conferences with excellent presentations, engaging conversations as well as outstanding field trips. Thirty abstracts were presented on a wide range of topics that included karst and cave formation, GIS databases of karst features, geochemistry and paleoclimatology, paleobiology, sedimentology and stratigraphy, hurricane deposition, coastal geology, and education. Overall, there were twenty-one oral and nine poster presentations. Nine students participated in the meeting; and there were participants from 5 countries and 15 states and territories, creating an exciting and energetic conference.

This year's pre-meeting trip to Cat Island, was a rain-soaked adventure that featured outstanding geology, much of it previously unexamined. Outcrops on the island are dominated by the Rice Bay and Grotto Beach Formations. The field trip began at Mt. Alvernia, the highest point in the Bahamas (63 m) and the Hermitage, an important Bahamian cultural site constructed by Father John Hawes in the early 20th century. Later stops included a seawall to examine coastal erosion, a flank margin cave, and the Holocene deposits on Alligator Point, which contained a new palm frond fossil location—the topic of a chapter in this volume, as well as some problematic subtidal/intertidal outcrops. Once the rain let up, the day was a wonderful introduction to the geology of yet another Bahamian island. Many thanks to the field trip leaders, John Mylroie, James Carew, Al Curran, Deb Freile, Neil Sealey and Vince Voegeli for their efforts to make this an important part of the conference.

Jim Carew (background) and Fred Siewers (foreground at Alligator Point, Cat Island (photo: Lisa Park)

Our Symposium Keynote speaker was Dr. John Milliman, Chancellor Professor of Marine Science, The College of William & Mary, who gave an inspiring address on the global carbonate budget, entitled "Macro to Micro: Reflections from a Former Carbonate-Junkie."

Another noteworthy development of this meeting is the availability of electronic copies of all 13 Symposium volumes. Scanning of volumes 1-12 has been initiated and continues at the Department of Geology and Environmental Science at the University of Akron by Ms. Elaine Butcher. Copies of the 3rd, 4th, 5th, 9th, 12th and 13th volumes will be

available immediately and others will be available as they are completed. This effort is supported by The University of Akron.

The 13th Symposium marked Vincent Voegeli's last as the Gerace Research Centre's Executive Director. Researchers and instructors have appreciated the hard work, care and effort that Vince and his wife, Sandy put into the Centre during their tenure on the island. Vince did much to improve the GRC's physical plant, including adding wi-fi access, a SCUBA shop, rebuilding the main dorm and snack bar after Hurricane Frances, and perhaps the most noticeable for many—the dismantling of the water tower. Besides maintaining the "nuts and bolts" of the station, Vince supported research efforts at the GRC and was involved in research projects that have been presented at these symposia. We thank Sandy for her work with the Bahamas Living Jewels organization. She was instrumental in working with the community to help draft a proposal to the Bahamian National Trust to establish a National Park on San Salvador Island. Her beautiful photos documenting the island's amazing underwater life have drawn attention to San Salvador Island and the need to protect reef environments. The GRC research community welcomes Dr. Thomas Rothfus and his wife Erin, to San Salvador and looks forward to working with him to maintain and enhance the GRC's ever-growing potential for scientific research and effective field-based teaching.

As always thanks and appreciation are extended to Don and Kathy Gerace--without their years of dedicated work to establish the station and provide for its future, this symposium and many of the projects represented in the published papers of this volume would not be possible. LEP also would like to express her gratitude to Tina Niemi for her advice and editorial expertise in preparing this volume. She also thanks Carlton Boush for his patience and understanding.

Vince Voegeli (left) and Al Curran (right) at the 13th Symposium on the Geology of the Bahamas and Other Carbonate Regions (photo: Lisa Park).

Lisa E. Park
Department of Geology and Environmental Science
The University of Akron
Akron, OH 44325 USA

Deborah Freile
Department of Geoscience and Geography
New Jersey City University
Jersey City, NJ 07305 USA

WATER CHEMISTRY ON SAN SALVADOR ISLAND, BAHAMAS

Paul J. Moore and Jonathan B. Martin
Department of Geological Sciences
University of Florida
Gainesville, FL 32611
pjmoore@geology.ufl.edu

ABSTRACT

Surface and groundwater on San Salvador Island originates from two sources: rain water, which is undersaturated with respect to carbonate minerals, and seawater, which is supersaturated with respect to carbonate minerals. Analyses of 63 water samples from surface and groundwater show how San Salvador water evolves from these two sources through mixing and water-rock interactions. Chemical modeling of these analyses show that increases in Ca^{2+} concentrations are controlled primarily by the dissolution of metastable aragonite and that most water samples are supersaturated with respect to calcite. Dissolution of carbonate minerals on San Salvador Island results from two main processes: mixing of fresh water and seawater, and the increase in the partial pressure of carbon dioxide in solution (PCO_2), which is the primary cause for mineral dissolution.

INTRODUCTION

Chemical analysis of surface and ground water can lead to a better understanding of geological processes that occur on carbonate platforms, such as San Salvador Island, Bahamas. Some of these processes include dissolution of the highly soluble carbonate rocks making up the island and its hydrology, as well as the linkages between dissolution and hydrology. On San Salvador Island, dissolution has led to karstification, such as surface sculpturing of exposed rock (e.g., karren) and cave development, including pit caves on the surface, and flank margin caves and banana holes in the subsurface. These dissolution features and caves have been widely described in the literature (e.g. Mylroie and Carew, 1990; Mylroie et al., 1991; Mylroie and Carew, 1995a, b; Mylroie et al., 1995), but direct comparisons on San Salvador Island between modern water chemistry and these features are less common (e.g. Moore et al., 2004). In addition to karstification, understanding island hydrology is critical for wise use and conservation of water resources.

The work of Davis and Johnson (1989) used ground water chemistry to help conceptualize the regional hydrology of San Salvador Island. Their work has led to a better understanding of the hydrodynamics of freshwater lenses and the effects of carbonate dissolution as applied to San Salvador Island. Similar chemical analyses could also be used to identify which water-rock interactions influence water compositions and may lead to a better understanding of the mechanisms and rates of formation of the dissolution features commonly seen across the island. For this reason, we present chemical analyses of 63 water samples collected on San Salvador Island from two flank margin caves, one freshwater spring, three lakes, two blue holes, five groundwater wells, and a catchment pond on four separate occasions from January 2004 to June 2006 (see Appendices) and include a limited discussion of these data.

LOCATION AND GEOLOGIC BACKGROUND

San Salvador Island, Bahamas, is a small, isolated carbonate platform located approximately 650 km southeast of Miami, Florida (Figure 1). The island is tectonically stable and assumed to have an isostatic subsidence of 1-2 m per 100,000 years (Mullins and Lynts, 1977; Carew and Myl-

roie, 1995). The exposed rocks are Holocene and Pleistocene carbonate sediments of subtidal, reef and beach facies at low elevations, and dune facies at elevation above 6 m (Carew and Mylroie, 1985). Eolian dunes dominate the landscape, rising to a maximum of 40 meters above present sea level (masl) with most dunes ranging from 10 to 20 masl. Lying between the dunes are low elevation plains, wetlands and interior, saline-to-hypersaline lakes. Surface streams are absent due to the high porosity (≤ 30%) of the limestone (e.g. Vacher and Mylroie, 2002).

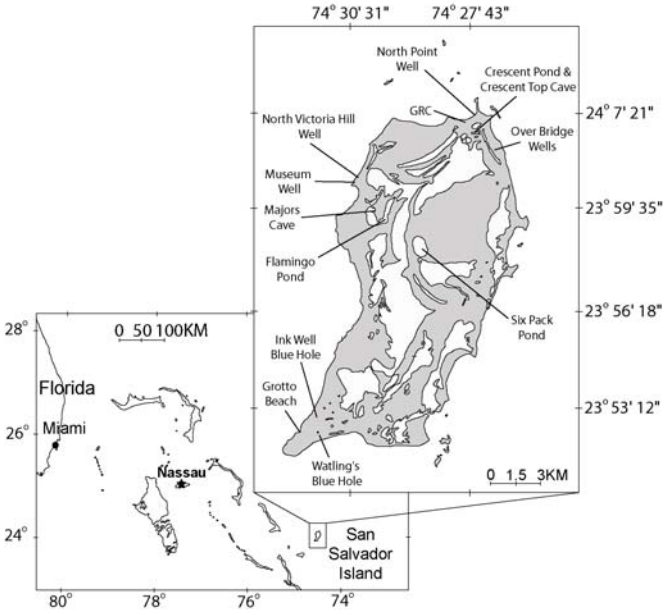

Figure 1. Map of Bahamas showing location of San Salvador Island. Insert of San Salvador Island shows water sampling locations - gray represents land area and white represents water bodies.

San Salvador Island has a subtropical marine climate dominated by northeast trade winds. The island experiences a warm rainy season from May to October, and a cool dry season from November to April (Whitaker and Smart, 1997). Recharge to the freshwater lenses that form below the dune ridges occurs through diffuse infiltration through the vadose zone. Precipitation is delivered by cold fronts during the winter, convective thunderstorms during summer, and transitional stationary fronts. Annual rainfall on San Salvador Island ranges from 1000 to 1250 mm/yr, with potential evapotranspiration (PET) estimated between 1250 and 1375 mm/yr (Sealey, 1994). The negative water budget restricts ground water recharge to rain events that exceed PET.

METHODS

Sixty-three surface and groundwater samples were collected across San Salvador Island during four trips--January through June 2004, April 2005, and June 2006. Samples collected in January 2004 and April 2005 represent water from the dry season, while samples collected in June 2004 and 2006 represent water from the wet season. In the field, we measured pH and temperature using an Orion #250A portable pH/ temperature meter, and conductivity and salinity using an Orion model #130 portable conductivity meter. For samples collected in April 2005 and June 2006, alkalinity was titrated with 0.1N hydrochloric acid (HCl) using the Gran technique within 24 hours of collection (e.g. Drever, 1997). Alkalinity was not measured for the samples collected in January and June 2004. Surface grab samples were collected from inland lakes, tidal pools within Majors Cave (a flank margin cave located on Hog Cay), from a submarine spring at Grotto Beach, and several hand dug wells around the island (Figure 1). One sample was also collected from the catchment pond behind the Gerace Research Centre (GRC) following a torrential rainstorm that occurred the previous day.

In Majors Cave, vertical profiles of water samples were collected with tubing attached to an extendable rod taking care not to mix the water and pumping water to the surface with either a hand-held vacuum pump or a 12 volt GeoTech II peristaltic pump. At the Grotto Beach spring, a horizontal profile of water samples was collected into the spring throat with tubing attached to an extendable rod and pumping water with the peristaltic pump. Samples from most wells were also collected using the peristaltic pump, with exception of two wells located behind the GRC that were pumped using an electric motor-driven pump at a rate of about 23 L/min. At one of the

wells behind the GRC, we collected samples both prior to pumping (GRC1-2006) and following purging the wells of about 1000 L (GRC1PT-2006), or several well volumes, that we assume represents pristine sampling of fresh ground water. These two samples were collected to determine how much water composition changes by remaining stagnant in the numerous hand-dug wells that occur across the island. In the other well behind the GRC, we collected all samples only after purging was completed (GRC2PT-2006).

Samples were pumped into clean dry HDPE bottles for major ions analyses and glass bottles for dissolved inorganic carbon (DIC) analyses, capped and returned to the laboratory. Dissolved inorganic carbon was only collected in June 2006. Major ion and DIC concentrations were measured at Department of Geological Sciences at the University of Florida. Major ion concentrations were measured using an automated Dionex 500 ion chromatograph, and DIC concentrations were measured with a Coulometrics CO_2 coulometer using a 3% silver nitrate scrubber solution, nitrogen as the carrier gas, and 2N HCL to evolve the CO_2 from the water. Precision of the measurements was assessed by replicate measurements of internal standards and was found to be < 5% (1 σ) for major ions and < 3.5% (1 σ) for DIC. Charge balance for samples collected in April 2005 and June 2006 is < 3%. Samples with higher charge balance errors have low salinity, with concentrations close to the detection limit of the instrument.

The geochemical code EQ3NR, Version 8 (Wolery, 1992, 1994), was used to determine the carbonate mineral saturation states of water sampled in April 2005 and June 2006. Saturation states for samples collected in January and June 2004 cannot be determined since these samples lack alkalinity measurements. Activity coefficients of aqueous species were calculated using the extended Debye-Hückle equation of Helgeson (1969). Since all samples were collected at depths ≤ 5 m, fugacity of oxygen was assumed to be in equilibrium with atmosphere at the time of collection. The state of mineral saturation in solution is reported here as the saturation index (*SI*) defined by:

$$SI = \log\left(\frac{Q}{K}\right) \quad (1)$$

where, *Q* is the ion activity product and *K* is the equilibrium constant for the reaction.

RESULTS

Surface and groundwater on San Salvador Island ranges from fresh to hypersaline; specific conductance measured in all of the water samples varied from 0.78 to 196.1 mS/cm, while salinity varied from 0.10 to 156 psu (Appendix 1-4). Temperature of the water samples range from 22.1°C to 32.4°C. Bulk chemical analysis of water samples collected from April 2005 and June 2006 show that San Salvador water evolves through a binary mixing between calcium bicarbonate fresh water and sodium chloride seawater (Figure 2). Samples collected in January and June 2004 are not displayed on Figure 2 due the lack of alkalinity measurements. Regardless, concentrations of these samples correlate with those displayed on Figure 2 by comparison of bulk chemistry, which suggest they also result from binary mixing between the two end-members. The samples collected from the GRC well (i.e., GRC1-2006 and GRC1PT-2006) prior to and following purging show little change in bulk chemistry, PCO_2 and saturation with respect to carbonate minerals. The minimal change in water chemistry, especially PCO_2 and carbonate mineral saturation, suggests there is little exchange of CO_2 between the well water and the atmosphere. Such exchange would be expected to cause CO_2 evasion, thereby increasing saturation with respect to carbonate minerals for the well water compared with formation water pumped into the well. This observation suggests that water from hand-dug wells may represent the chemical composition, including the gasses of unaltered groundwater within freshwater lenses, even if the wells are not purged prior to sampling. This conclusion is also

supported by the high PCO_2 values present in the samples from wells that were not purged (e.g., MW-2006).

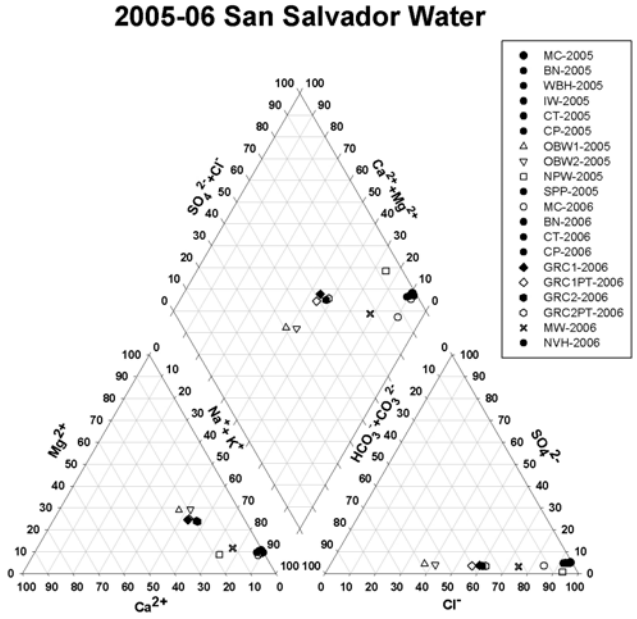

Figure 2. Piper diagram showing San Salvador water chemistry. Projection of water samples suggest water on San Salvador Island evolves from two end-members, calcium bicarbonate fresh water and sodium chloride seawater. Waters with the same symbol (black dot) are of similar water chemistry, i.e., sodium chloride end-member.

Saturation states of carbonate minerals in San Salvador waters were calculated for samples collected in April 2005 and June 2006. Most samples are in equilibrium with respect to aragonite, including those samples with high salinities. In addition to aragonite equilibrium over a broad range of salinity, these samples also vary by about two orders of magnitude in log PCO_2 ranging from -1.83 (GRC2-2006) to -3.73 (WBH-2005) (Appendix 3-4). One possible source of CO_2 is the soil zone, where root respiration and microbially-generated CO_2 can increase vadose water by orders of magnitude above atmospheric values (e.g. Brook et al., 1983; Schwabe et al., 2006).

The PCO_2 in water sampled from the Gerace Research Centre catchment is calculated at log -4.74, which is one order of magnitude lower than atmospheric value. The pH for this sample is 9.13, which suggests rapid equilibration with the carbonate. Total alkalinity for this sample was measured to be 4.99 meq/L, and DIC was measured to be 0.44 meq/L. The difference between total alkalinity and DIC values suggests that dissolved species in addition to carbonate species may contribute to the alkalinity, which could include borate, phosphate and organic anions. Only borate has been measured in the sample, and was found to be a minimal contributor to the total alkalinity. The large charge imbalance of 43% is likely due to its dilute nature, which leads to difficulties associated with accurately measuring low concentration of major ions and the possibility of ions present in solution with concentrations below instrument detection limits.

CONCLUSIONS

Rainwater and seawater are the two sources of water found on San Salvador Island and these two sources have distinct chemical compositions that can be traced through mixing. Rainwater is undersaturated with respect to carbonate minerals, and seawater is supersaturated. The chemistry of water from these sources change from multiple processes, including freshwater—seawater mixing, influx of CO_2 from the soil and the dissolution of limestone, releasing Ca^{2+} and HCO_3^- into solution.

ACKNOWLEDGMENTS

We would like to thank Dr. Donald T. Gerace, Chief Executive Officer, and Vincent Voegeli, Executive Director of the Gerace Research Centre, San Salvador, Bahamas, for logistical support. Thanks go out to all of those who have helped us in the field. Special thanks go out to Jane Gustavson, Cara Gentry, and Don Seale.

REFERENCES

Brook, G.A., Folkoff, M.E., and Box, E.O., 1983, A world model of soil carbon dioxide: Earth Surface Processes and Landforms, v. 8, p. 79-88.

Carew, J.L., and Mylroie, J.E., 1985, The Pleistocene and Holocene stratigraphy of San Salvador Island, Bahamas, with reference to marine and terrestrial lithofacies at French Bay, *in* Curran, H.A., ed., Pleistocene and Holocene Carbonate Environments on San Salvador Island, Bahamas, GSA Annual Meeting (Orlando, FL) Guidebook for Field Trip #2: Ft. Lauderdale, CCFL Bahamian Field Station, p. 11-61.

Carew, J.L., and Mylroie, J.E., 1995, Quaternary tectonic stability of the Bahamian Archipelago; evidence from fossil coral reefs and flank margin caves: Quaternary Science Reviews, v. 14, p. 145-153.

Davis, R.L., and Johnson, J., C.R., 1989, Karst hydrology of San Salvador, *in* Mylroie, J.E., ed., Proceedings, Fourth Symposium on the Geology of the Bahamas: San Salvador, Bahamian Field Station, p. 118-135.

Drever, J.I., 1997, The Geochemistry of Natural Waters: Englewood Cliffs, NJ, Prentice Hall, 437 p.

Helgeson, H.C., 1969, Thermodynamics of hydrothermal systems at elevated temperatures and pressures: American Journal of Science, v. 267, p. 729-804.

Moore, P.J., Martin, J.B., and Gamble, D.W., 2004, Carbonate Water Mixing in a Flank Margin Cave, *in* Gamble. D.W., and Davis, R.L., eds., Proceedings of the Twelfth Symposium on the Geology of the Bahamas: San Salvador Island, Bahamas, p. 123-129.

Mullins, H.T., and Lynts, G.W., 1977, Origin of the northwestern Bahama Platform; review and reinterpretation: Geological Society of America Bulletin, v. 88, p. 1447-1461.

Mylroie, J.E., and Carew, J.L., 1990, The flank margin model for dissolution cave development in carbonate platforms: Earth Surface Processes and Landforms, v. 15, p. 413-424.

Mylroie, J.E., and Carew, J.L., 1995a, Geology and karst geomorphology of San Salvador Island, Bahamas: Carbonates and Evaporites, v. 10, p. 193-206.

Mylroie, J.E., and Carew, J.L., 1995b, Karst development on carbonate islands, *in* Budd, D.A., ed., Unconformities and porosity in carbonate strata: Memoir 63, AAPG, p. 55-76.

Mylroie, J.E., Carew, J.L., Sealey, N.E., and Mylroie, J.R., 1991, Cave development on New Providence Island and Long Island, Bahamas: Cave Science, v. 18, p. 139-151.

Mylroie, J.E., Carew, J.L., and Vacher, H.L., 1995, Karst development in the Bahamas and Bermuda, *in* Curran, H.A., and White, W.B., eds., Terrestrial and Shallow marine Geology of the Bahamas and Bermuda: Boulder, Colorado, Geological Society of America Special Paper 300, p. 251-267.

Schwabe, S.J., Herbert, R.A., and Carew, J.L., 2006, A hypothesis for biogenic cave formation (A study conducted in the Bahamas), *in* Voegeli, V., ed., Abstracts and Program of the 13th Symposium on the Geology of the Bahamas and other Carbonate Regions: San Salvador Island, Bahamas, Gerace Research Center, p. 22-23.

Sealey, N.E., 1994, Bahamian landscapes; an introduction to the physical geography of the Bahamas: Nassau, Bahamas, Media Publishing, 128 p.

Vacher, H.L., and Mylroie, J.E., 2002, Eogenetic karst from the perspective of an equivalent porous medium: Carbonates and Evaporates, v. 17, p. 182-196.

Whitaker, F.F., and Smart, P.L., 1997, Climatic control of hydraulic conductivity of Bahamian limestones: Ground Water, v. 35, p. 859-868.

Wolery, T.J., 1992, EQ3NR, A computer program for geochemical aqueous speciation solubility calculations: Theoretical manual, user's guide, and related documentation (Version 7.0), UCRL-MA-110662-PT-III, Lawrence Livermore National Laboratory, Livermore, California.

Wolery, T.J., 1994, Letter Report: EQ3/6 Version 8: Differences from Version 7, UCRL-ID-129749, Lawrence Livermore National Laboratory, Livermore, California.

APPENDIX

Appendix 1. Water chemistry of samples collected in January 2004.

Samples	Depth (m)	pH	Cond. (mS/cm)	Temp. (C)	Salinity (psu)	Na^+ (mM)	K^+ (mM)	Mg^{2+} (mM)	Ca^{2+} (mM)	Cl^- (mM)	Br^- (mM)
Majors Cave											
MC-A-2004	0.1	7.95	33.80	22.10	23.70	327.51	6.45	37.67	7.81	383.45	0.563
MC-B-2004	0.5	7.89	34.70	22.20	24.60	331.26	6.78	38.31	7.84	393.54	0.573
MC-C-2004	1.0	7.80	35.70	22.40	25.20	350.52	7.17	40.66	8.25	406.41	0.588
MC-D-2004	1.5	7.70	36.80	22.50	26.40	360.42	7.35	41.51	8.36	417.65	0.620
MC-E-2004	2.0	7.68	36.60	22.50	26.00	362.01	7.40	42.03	8.55	418.92	0.611

Samples	SO_4^{2-} (mM)	$SiO_{2(aq)}$ (uM)	$B(OH)_{3(aq)}$ (mM)	Alk. (meq/L)	DIC (meq/L)	Log PCO_2	SI_{cal} (log Q/K)	SI_{arag} (log Q/K)	SI_{dol} (log Q/K)	% Charge Error
Majors Cave										
MC-A-2004	19.74									
MC-B-2004	20.32									
MC-C-2004	21.12									
MC-D-2004	21.77									
MC-E-2004	21.82									

Appendix 2. Water chemistry of samples collected in June 2004

Samples	Depth* (m)	pH	Cond. (mS/cm)	Temp. (C)	Salinity (psu)	Na^+ (mM)	K^+ (mM)	Mg^{2+} (mM)	Ca^{2+} (mM)	Cl^- (mM)	Br^- (mM)
Majors Cave											
MC-1-2004	0.1	7.64	44.30	23.9	29.0	361.16	7.59	42.29	9.08	416.21	0.615
MC-2-2004	1.0	7.59	44.70	24.1	29.3	363.76	7.54	42.54	8.85	419.42	0.643
MC-3-2004	2.0	7.59	45.10	24.1	29.5	367.00	7.87	43.08	9.02	427.01	0.646
MC-4-2004	3.0	7.30	45.70	24.4	29.7	372.77	7.92	43.40	8.93	431.03	0.647
MC-5-2004	4.0	7.41	46.10	24.1	30.2	373.76	7.81	43.62	9.15	437.77	0.653
MC-6-2004	5.0	7.18	46.10	24.1	30.2	369.57	7.61	43.07	9.13	441.53	0.673
BN-1-2004	0.1	7.63	41.50	23.8	27.1	325.69	6.74	37.97	7.94	406.93	0.595
BN-2-2004	0.4	7.60	42.40	23.9	27.6	340.04	6.86	39.44	8.31	395.82	0.571
BN-3-2004	0.8	7.48	43.40	23.9	28.4	354.62	7.11	41.40	8.59	415.58	0.628
BN-4-2004	1.2	7.60	44.00	23.9	28.7	362.35	7.55	42.21	8.88	419.85	0.609
BN-5-2004	1.6	7.53	44.30	23.9	29.0	356.80	7.39	41.70	8.77	421.97	0.631
BN-6-2004	2.0	7.45	44.70	24.1	29.2	358.69	7.45	41.87	8.80	425.43	0.627
Flamingo Pond											
FP-2004	0.1	8.41	109.00	31.6	69.40	841.58	16.56	97.62	17.50	969.44	1.42
OF-2004	0.1	8.25	196.10	28.3	~120	1905.65	38.02	227.91	35.62	2198.32	3.26
Grotto Beach Spring											
GB-1-2004	-1.5	7.52	45.80	27	27.90	350.87	7.16	40.63	7.88	411.49	0.589
GB-2-2004	-1.5	7.39	42.00	27	25.30	320.03	6.43	37.18	7.55	372.09	0.541
GB-3-2004	-2.0	7.37	41.00	26.9	24.90	313.25	6.45	36.47	7.39	364.72	0.532
GB-4-2004	0.0	7.9	54.50	27.8	33.30	419.59	8.71	49.05	9.24	491.43	0.710
GB-5-2004	+3	8.28	64.30	28.4	40.00	502.35	10.64	58.93	11.04	589.86	0.866
North Point Well											
NP-2-2004	0.4	7.63	1.14	27	0.30	4.62	0.26	0.85	0.72	3.55	0.005
NP-1-2004	0.1	7.67	0.78	27.3	0.10	2.79	0.16	0.52	0.58	1.48	0.004

Appendix 2. cont.

Samples	SO_4^{2-} (mM)	$SiO_{2(aq)}$ (uM)	$B(OH)_{3(aq)}$ (mM)	Alk. (meq/L)	DIC (meq/L)	Log PCO_2	SI_{cal} (log Q/K)	SI_{arag} (log Q/K)	SI_{dol} (log Q/K)	% Charge Error
Majors Cave										
MC-1-2004	20.91	6.37	0.280							
MC-2-2004	21.16	0.00	0.264							
MC-3-2004	21.56	18.73	0.305							
MC-4-2004	21.81	7.50	0.265							
MC-5-2004	22.17	0.00	0.271							
MC-6-2004	22.43	0.00	0.292							
BN-1-2004	21.17	20.69	0.232							
BN-2-2004	20.55	20.41	0.249							
BN-3-2004	21.70	19.57	0.256							
BN-4-2004	21.86	19.85	0.256							
BN-5-2004	22.01	19.29	0.271							
BN-6-2004	22.20	19.29	0.262							
Flamingo Pond										
FP-2004	47.32	0.00	0.762							
OF-2004	107.05	0.00	1.346							
Grotto Beach Spring										
GB-1-2004	21.31	0.00	0.273							
GB-2-2004	18.97	29.40	0.231							
GB-3-2004	18.54	26.31	0.221							
GB-4-2004	25.98	7.22	0.338							
GB-5-2004	32.06	0.00	0.443							
North Point Well										
NP-2-2004	0.29	79.37	0.062							
NP-1-2004	0.29	59.15	0.051							

* Depth at Grotto Beach Spring represents sampling interval at the fissure, where negative values represent distance into the fissure. Sample GB-4-2004, at 0.0 m, was collected at the rock wall, and GB-5-2004 represents seawater collected 3 m away from the fissure.

Appendix 3. Water chemistry of samples collected in April 2005.

Samples	Depth (m)	pH	Cond. (mS/cm)	Temp. (C)	Salinity (psu)	Na^+ (mM)	K^+ (mM)	Mg^{2+} (mM)	Ca^{2+} (mM)	Cl^- (mM)	Br^- (mM)
Majors Cave											
MC-0-2005	0.1	7.68	38.70	23.8	27.80	358.26	7.33	41.94	8.82	423.97	0.593
MC-1-2005	1.0	7.68	38.80	23.7	27.80	361.71	7.39	42.19	8.86	423.49	0.606
MC-2-2005	2.0	7.67	38.80	23.7	27.80	361.82	7.38	42.41	9.04	424.60	0.595
MC-3-2005	3.0	7.67	38.80	23.7	27.80	366.59	7.57	42.58	8.79	424.57	0.610
MC-4-2005	4.0	7.59	39.00	23.8	28.00	370.09	7.74	43.13	9.23	429.33	0.609
MC-5-2005	4.5	7.55	39.40	23.9	28.30	379.29	7.59	44.70	9.45	435.89	0.613
BN-0-2005	0.1	7.63	35.70	23.3	25.30	328.49	6.68	38.36	8.21	384.54	0.534
BN-1-2005	0.5	7.55	37.90	23.8	27.10	362.62	7.30	41.96	8.48	412.60	0.660
BN-2-2005	1.0	7.59	38.30	23.8	27.50	363.36	7.25	42.21	8.59	422.19	0.604
Watling's Blue Hole											
WBH-2005	0.1	8.51	43.20	30.6	27.80	368.69	7.39	43.23	9.26	422.23	0.596
Ink Well Blue Hole											
IW-2005	0.1	7.7	9.32	24.2	5.20	66.52	1.29	7.15	3.32	77.82	0.108
Crescent Top Cave											
CT-2005	0.1	7.44	55.80	26.5	35.50	483.06	19.07	51.79	9.80	544.79	0.772
Crescent Pond											
CP-2005	0.1	8.44	61.00	28.4	37.80	491.91	10.31	57.56	11.16	581.47	0.845
Over Bridge Wells											
OBW-1-2005	0.1	7.87	0.99	26.1	0.30	3.08	0.00	1.79	1.56	2.89	0.004
OBW-2-2005	0.1	7.87	1.27	27.8	0.50	4.37	0.00	2.38	1.66	4.32	0.003
North Point Well											
NP-2005	0.1	7.6	3.79	26.1	1.90	18.82	0.19	2.15	4.89	30.15	0.048
Six Pack Pond											
SPP-2005	0.1	8.37	74.60	25.3	51.70	679.01	13.73	78.29	15.28	780.68	1.091

Appendix 3. cont.

Samples	SO_4^{2-} (mM)	$SiO_{2(aq)}$ (uM)	$B(OH)_{3(aq)}$ (mM)	Alk. (meq/L)	DIC (meq/L)	Log PCO_2	SI_{cal} (log Q/K)	SI_{arag} (log Q/K)	SI_{dol} (log Q/K)	% Charge Error
Majors Cave										
MC-0-2005	21.46	18.45	0.272	2.395		-2.801	0.163	0.019	2.216	-0.25
MC-1-2005	21.40	18.45	0.279	2.415		-2.799	0.166	0.021	2.223	0.28
MC-2-2005	21.48	18.17	0.289	2.436		-2.785	0.168	0.023	2.220	0.24
MC-3-2005	21.47	18.45	0.293	2.498		-2.775	0.165	0.021	2.230	0.78
MC-4-2005	21.76	19.37	0.298	2.482		-2.696	0.106	-0.039	2.094	0.81
MC-5-2005	22.13	19.10	0.295	2.557		-2.645	0.085	-0.059	2.061	1.37
BN-0-2005	19.31	20.13	0.220	2.433		-2.735	0.105	-0.039	2.091	0.34
BN-1-2005	20.79	19.01	0.286	2.461		-2.655	0.034	-0.111	1.976	1.63
BN-2-2005	21.35	18.73	0.261	2.4		-2.708	0.065	-0.080	2.035	0.56
Watling's Blue Hole										
WBH-2005	21.30	0.00	0.276	2.218		-3.734	0.963	0.819	3.838	1.59
Ink Well Blue Hole										
IW-2005	3.71	21.82		2.848		-2.589	0.223	0.079	1.976	0.39
Crescent Top Cave										
CT-2005	28.28		0.437	2.091		-2.687	-0.045	-0.190	1.859	1.92
Crescent Pond										
CP-2005	30.41		0.460	2.079		-3.727	0.895	0.715	3.665	-0.40
Over Bridge Wells										
OBW-1-2005	0.31	73.75	0.159	4.015		-2.514	0.442	0.297	2.259	10.73
OBW-2-2005	0.37	23.50	0.169	5.048		-2.415	0.658	0.514	2.668	10.79
North Point Well										
NP-2005	0.20	60.56	0.159	1.799		-2.633	0.293	0.149	1.439	1.08
Six Pack Pond										
SPP-2005	38.72	0.00	0.590	2.523		-3.629	0.902	0.757	3.738	1.21

Appendix 4. Water chemistry of samples collected in June 2006.

Samples	Depth (m)	pH	Cond. (mS/cm)	Temp. (C)	Salinity (psu)	Na^+ (mM)	K^+ (mM)	Mg^{2+} (mM)	Ca^{2+} (mM)	Cl^- (mM)	Br^- (mM)
Majors Cave											
MC-0-2006	0.1	8.00	3.17	24.3	1.80	22.97	0.71	2.16	1.17	23.06	0.032
MC-1-2006	0.1	7.84	11.75	24.2	7.60	93.16	2.32	9.54	2.77	104.22	0.152
MC-2-2006	0.3	7.78	29.40	24.1	20.30	242.81	4.94	27.65	6.21	269.42	0.393
MC-3-2006	0.4	7.76	38.70	24.1	27.80	330.26	6.99	38.62	8.19	390.44	0.584
MC-4-2006	0.5	7.78	41.40	24.1	30.00	347.54	7.09	40.81	8.52	420.86	0.614
MC-5-2006	1.0	7.72	42.70	24.1	31.00	355.73	7.48	41.31	8.48	424.49	0.637
MC-6-2006	1.5	7.59	43.00	24.1	31.10	356.60	7.54	41.65	8.60	414.36	0.633
BN-0-2006	0.1	7.64	38.30	24.1	27.40	323.68	6.79	37.85	7.96	366.00	0.533
BN-1-2006	0.3	7.65	40.60	24.1	29.20	336.82	7.26	39.51	8.11	387.44	0.599
BN-2-2006	0.5	7.61	42.00	24.1	30.30	354.67	7.46	41.15	8.39	402.66	0.598
BN-3-2006	1.0	7.57	43.00	24.2	31.10	362.22	7.50	41.91	8.62	411.63	0.616
BN-4-2006	2.0	7.54	43.40	24.2	31.50	367.88	7.77	42.69	8.71	415.70	0.609
Crescent Top Cave											
CT-2006	0.1	7.55	53.40	26.6	40.10	456.32	9.87	53.80	10.28	541.72	0.841
Crescent Pond											
CP-2006	0.1		50.30	32.4	37.50	437.97	9.54	51.13	9.73	499.55	0.772
GRC Wells											
GRC-1-2006	0.1	7.39	1.43	27.4	0.50	4.54	0.14	2.07	2.01	7.46	
GRC-1PT-2006	0.1	7.40	1.40	27.3	0.50	4.59	0.15	2.14	1.98	7.38	
GRC-2PT-2006	0.1	7.27	1.55	26.7	0.60	5.75	0.16	2.35	2.03	9.18	
Museum Well											
MW-2006	0.1	7.37	2.12	27.3	0.90	10.58	0.26	1.59	1.76	15.84	
North Victoria Well											
NVH-2006	0.1	7.48	15.15	26.5	10.00	112.75	1.97	13.00	3.85	128.18	0.191
GRC Catchment											
Catchment-2006	0.1	9.18	0.07	30	0.00	0.12	0.01	0.03	0.03	0.09	

Appendix 4. cont.

Samples	SO_4^{2-} (mM)	$SiO_{2(aq)}$ (uM)	$B(OH)_{3(aq)}$ (mM)	Alk. (meq/L)	DIC (meq/L)	Log PCO_2	SI_{cal} (log Q/K)	SI_{arag} (log Q/K)	SI_{dol} (log Q/K)	% Charge Error
Majors Cave										
MC-0-2006	0.91		0.060	3.030	2.31	-2.82	0.27	0.13	2.00	4.27
MC-1-2006	4.81		0.121	2.712	2.67	-2.78	0.19	0.05	2.12	1.56
MC-2-2006	12.64		0.187	2.775	2.87	-2.79	0.28	0.13	2.41	3.10
MC-3-2006	19.81		0.283	2.823	2.88	-2.80	0.30	0.16	2.49	-0.25
MC-4-2006	21.50		0.309	2.804	2.83	-2.83	0.32	0.18	2.54	-1.55
MC-5-2006	21.62		0.310	2.808	2.84	-2.77	0.26	0.11	2.42	-0.89
MC-6-2006	20.90		0.316	2.877		-2.63	0.15	0.01	2.20	0.65
BN-0-2006	18.34		0.267	2.940	3.09	-2.66	0.20	0.06	2.29	2.12
BN-1-2006	19.33		0.243	2.925		-2.67	0.21	0.06	2.31	1.26
BN-2-2006	20.17		0.263	2.809		-2.66	0.15	0.01	2.21	1.81
BN-3-2006	20.65		0.263	2.881		-2.60	0.13	-0.01	2.17	1.73
BN-4-2006	20.90		0.266	2.857	3.83	-2.58	0.10	-0.04	2.11	2.06
Crescent Top Cave										
CT-2006	28.43		0.407	2.569	2.62	-2.65	0.12	-0.03	2.18	-0.62
Crescent Pond										
CP-2006	25.59		0.373	2.351	1.84					
GRC Wells										
GRC-1-2006	0.43			4.316	4.88	-2.01	0.19	0.05	1.60	0.91
GRC-1PT-2006	0.43		0.058	4.841	5.30	-1.96	0.26	0.11	1.75	-0.41
GRC-2PT-2006	0.47		0.054	4.787	5.06	-1.84	0.11	-0.03	1.48	-0.83
Museum Well										
MW-2006	0.63		0.049	4.365	4.33	-1.98	0.10	-0.05	1.35	-10.28
North Victoria Well										
NVH-2006	6.35		0.120	3.465	4.34	-2.30	0.09	-0.06	1.92	1.45
GRC Catchment										
Catchment-2006	0.01		0.043	4.999	0.44	-4.741	-0.675	-0.819	-0.033	-43.56

FAUNAL AND GEOCHEMICAL VARIABILITY OF OSTRACODE FAUNAS FROM SALINE PONDS ON SAN SALVADOR ISLAND, BAHAMAS

Lisa E. Park and Kenton J. Trubee
University of Akron
Department of Geology and Environmental Science
Akron, OH 44325
lepark@uakron.edu

ABSTRACT

We examined ostracode faunas from eleven lakes ranging from normal marine to hypersaline conditions on San Salvador Island, Bahamas to determine: 1) if lakes of higher salinity have different diversities than less saline lakes, 2) if there is a correlation between species distribution and water chemistry, 3) if genders of the same species have the same or different partitioning ratios, and 4) if species within the same lake have similar Mg and Sr partitioning ratios.

Water and ostracode samples were collected from all eleven lakes. Water temperature, pH, alkalinity, conductivity, and salinity were measured in the field with hand held meters. Over 600 right valves were counted from each lake and statistically analyzed to determine faunal distribution. Three species--*Cyprideis americana, Hemicyprideis setipunctata* and *Perissocytheridea bicelliforma* were geochemically analyzed for major trace elements, including Mg and Sr, using ICP-MS.

Species distribution and alpha diversity appears to be correlated to lake chemistry, primarily salinity, with peak diversity occurring at the calcite branchpoint. Surprisingly, dissimilar faunas occur in adjacent lakes with similar chemistries. Lakes that were similar in chemistry were sometimes geographically separated by distance or by a significant barrier. This similarity indicates that dispersal of ostracodes may not necessarily be as frequent and widespread as previously thought.

While species distribution appears to correlate with lake water chemistry, the partitioning ratios for Mg and Sr show different trends with respect to lake water salinity. For all valves measured, K_d [Mg] increases with salinity while K_d [Sr] shows a strong negative correlation. In addition, *P. bicelliforma* appears to have a wider variance of Mg and Sr partitioning ratios indicating a possible 'species effect.' There are also slight differences seen between males and females of *C. americana*. These minor differences in trace element uptake may be due to differences in average valve mass, as *P. bicelliforma*'s relatively small size as well as the smaller size of the female *C. americana*, suggest that these valves might have weaker calcification that might contribute to these differences. Whatever the cause, the differences, although slight, reinforce the necessity of using a single species for trace element and isotope analyses when analyzing cores or comparing water bodies.

INTRODUCTION

San Salvador Island (SSI)

San Salvador Island (SSI), Bahamas is a small island (~153 km^2) with multiple inland lakes having varying water chemistries (Davis and Johnson, 1989) and depositional histories (Figure 1). During Pleistocene sea-level high stands, deposits of dune, beach and sub-tidal carbonates accumulated across the San Salvador platform (Carew and Mylroie, 1995).

Many of the inland lakes occur between these ancient dune deposits or as karst features in the Pleistocene-Holocene carbonate bedrock (Bain, 1991; Teeter, 1985). These lakes vary dramatically in size, chemistry, and faunal composition (Table 1); most are not closed systems but are connected via conduits to each other and the ocean realm.

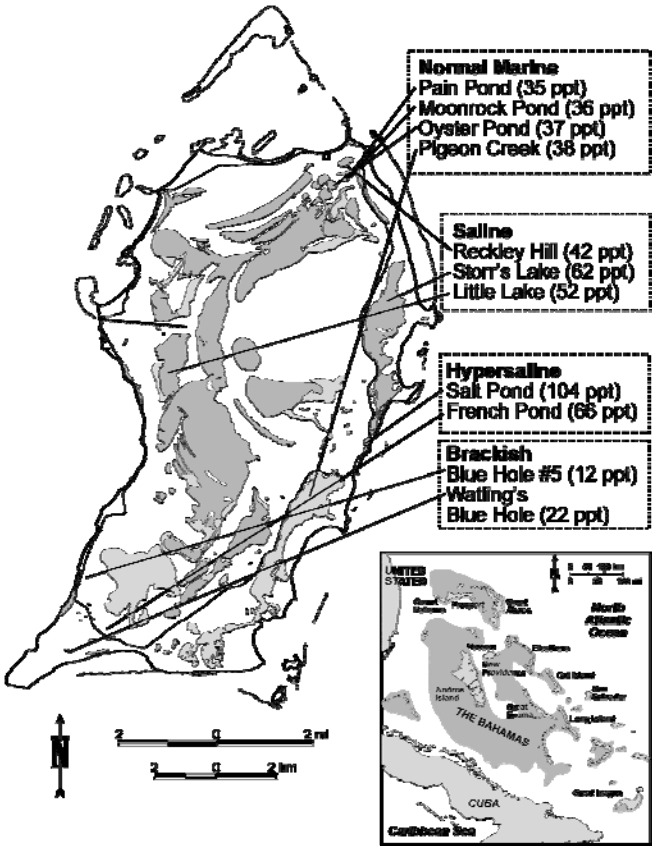

Figure 1. Location map of ponds under study on San Salvador Island. Average salinity noted.

Prior studies have focused on reconstructing the depositional histories of some of these lakes including, Salt Pond, Little Lake, Watling's Blue Hole and Storr's Lake (Crotty, 1982; Sanger and Teeter, 1982; Sanger, 1983; Thalman, 1983; Corwin, 1985; Florentino, 1985; Nutt, 1985; Teeter, 1985; Zaleha, 1987; Teeter and Quick, 1990; Beltz, 1992; Cronin, 1994; and Shamberger, 1998). In most cases, the ostracodes from these lakes can be divided into faunal associations based on salinities and can be used as proxies for paleoenvironmental change (Sanger and Teeter, 1982; Teeter, 1985; Teeter and Quick, 1990; and Park and Beltz, 1998).

Modern Salinities and Sedimentation

Modern lakes on SSI vary in salinity due to factors such as the degree of development of the marine conduit system, the presence of local fresh groundwater lenses, the size of the lake and its elevation relative to sea level, as well as rainfall. Ponds and blue holes that have unimpeded connections to the open ocean exhibit normal-marine salinities and tidal change, although the

Pond/Lake	Salinity Range (ppt)	Average Salinity (ppt)	pH	Conductivity (mS/cm)	Mean Water Temp (°C)	Max. Water Depth (m)	Lake Area km^2	Total Alkalinity (meq)	No. Ostracode Species
Blue Hole #5	4-30	12	8.4	22.9	26.9	6	0.0004	3.54	4
French Pond	32-280	66	8.5	97.5	29.6	2	0.05	3.54	2
Little Lake	38-67	52	8.0	82.5	27.9	3	1.7	2.75	9
Moonrock Pond	na	36	8.0	55.7	30.1	1.5	0.06	3.15	9
Oyster Pond	34-38	37	8.0	59.9	27.4	2.5	0.07	3.15	10
Pain Pond	28-37	35	8.1	56.5	31.6	2	0.018	3.08	9
Pigeon Creek	35-45	35	8.1	66.7	23.9	2	4.4	2.36	19
Reckley Hill Pond	36-59	42	8.6	66.6	30.0	0.5	0.12	4.46	5
Salt Pond	59-356	104	8.6	140.3	37.8	0.5	0.05	3.80	3
Storr's Lake	60-76	62	8.4	95.4	26.0	1.1	3.2	3.34	3
Watling's Blue Hole	10-32	22	8.2	38.0	28.0	7	0.003	3.34	3

Table 1. Pond and lake salinity, pH, conductivity, mean water temperature, area, alkalinity and number of ostracode species found.

range is diminished and timing lags behind ocean tides. Water in ponds having poor interchange with the ocean have long residence times and higher salinities. Salt Pond, for example, can range in salinity from 60 to 300 ppt and has had gypsum and halite precipitating during its history (Furman et al., 1992; Shamberger, 1998). Cores taken from Salt Pond indicate that the pond went from a marine sub-tidal environment, to fresh-water conditions, followed by periods of saline intrusion and increasing salinity. These sediments also record several marked zones of presumed storm wash-over events that can be used to better understand frequency and intensity of tropical storms in the past 2,000 years (Park et al. this volume).

SSI Ostracoda

Ostracodes as Paleoenvironmental Indicators. Ostracodes are bivalved microcrustaceans that range in size from 500 μm to 2 mm. They are common in all aquatic environments and their low-Mg calcite carapaces are readily preserved in the geologic record. Biogenic fractionation of ostracode calcite with respect to the host waters makes them important indicators of salinity and temperature (Chivas et al., 1983; De Deckker et al., 1988; Holmes et al., 1992; Xia et al., 1997; De Deckker et al., 1998; Wansard et al., 1998; and Curry, 1999).

Prior studies on the relationship between water chemistry and ostracode diversity and distribution have been conducted on various lakes on the island, including Salt Pond and Little Lake (Sanger and Teeter, 1982; Teeter, 1985; Teeter and Quick, 1990). These studies indicate that each lake has a different associated fauna that most likely reflects water chemistry.

In this study, we examined the variability of the ostracode faunas in eleven lakes on the island, documenting and determining their chemical affinities as well as faunal distribution and ecology. Specifically, we addressed several questions: 1) do lakes of higher salinity have significantly different species richness than less saline lakes? 2) is there a correlation between ostracode species distribution and lake water chemistry? 3) do different species within the same lake have the same uptake ratios? 4) do males and females of the same species have different uptake ratios of Sr and Mg?

METHODS

Field Sampling

Water and sediment samples were collected from each of the eleven lakes in this study. Measurements of pH, alkalinity, salinity, and temperature were done in the field using hand held meters. Alkalinity was measured using standard titration techniques (0.01639 N H_2SO_4 added to 25 ml H_2O to pH 4.5).

One liter of water was collected in each lake 10 cm above the sediment-water interface, in two sterile, acid-washed and MilliQ® water-rinsed 500 ml plastic bottles and capped underwater. The samples were refrigerated until analyzed.

Approximately 500 ml of sediment was collected as grab samples from the upper two centimeters of the lake-bottom sediment. These were wet-sieved in -2 Ø (2000 μm), 2.0 Ø (250 μm, and 3.0 Ø (125 μm) sieves within twenty-four hours of collection and allowed to air dry. Only live individuals at the time of collection were chosen for geochemical analysis.

Six hundred right valves were picked from each lake. Whether they were recently alive was not necessarily considered for this part of the analysis; the specimens used for geochemical analysis were included in diversity counts. In several samples (French Pond, Oyster Pond, Pain Pond, Reckley Hill Pond, and Salt Pond), there were not 600 adult right valves present in the volume of sediment collected, so all adult right ostracode valves were picked that were available. However, rarefaction analyses indicate that all rare species in these samples were adequately sampled with the number of valves counted, and a statistically robust sample was obtained.

Geochemical Analyses

The three species most commonly found, *C. americana*, *H. setipunctata*, and *P. bicelliforma*, were analyzed by Inductively Coupled Plasma-Source Mass Spectrometer (ICP-MS) for trace elements. Male and female *C. americana* were analyzed separately to determine if gender affects the ostracode's uptake of trace elements. In many organisms, male and female physiology tends to be significantly different. *Cyprideis americana* specimens were chosen to address this question because they are easily differentiated by gender. Thus, for all geochemical analyses, two *C. americana* valves were used, one valve per analysis for *H. setipunctata*, and two to three valves for *P. bicelliforma* (*sensu* Chivas et al., 1983). The number of valves varied, so that the mass of each sample analyzed was greater than 0.001 mg. Masses were measured on a Mettler Toledo® MX5 microbalance. Valves were cleaned with a 000 camel's hair brush and visually inspected with a binocular microscope. Cleaned ostracodes were placed in a bath of 100% reagent grade bleach for twenty-four hours for optimal cleaning without degradation. Samples were removed and rinsed three times with triple distilled (i.e. MilliQ®) water. To ensure cleanliness, a final visual inspection of the cleaned ostracodes was made with a binocular microscope at 40 x magnification.

Analyses of both the dissolved ostracode valves and water samples were performed on a Perkin-Elmer® Elan 6000 ICP-MS using a nickel sampler and skimmer cones. New Tygon or Teflon tubing was used. All plasticware was cold acid leached and soaked in MilliQ® water (18.2 megaOhm) prior to use. Standards were prepared fresh from certified standards from SPEX Corp. All standards and blanks were matrix-matched to the samples using the control acid blank prepared at the time of the dissolution. The external standards were prepared so as to bracket the approximate known concentrations of the given analytes. For calcium ratio samples, the standard cross-flow nebulizer paired with a Scott® double-pass spray chamber was used. Operating conditions were optimized to minimize oxide production. Dwell times were set at 10 ms with each analysis consisting of 350 sweeps per reading, one reading per replicate and ten replicates per analysis. Individual isotopes of the elements of interest were chosen to minimize isobaric overlap and maximize natural abundance. Data files were reprocessed using the Elan software and imported into a Microsoft Excel spreadsheet.

Quantitative Analyses

Alpha diversity was measured by rarefaction and Shannon Diversity Indices. Cluster analyses were also conducted to quantify the similarity according to distance and similarity measures. K_d values for Mg and Sr for the three species analyzed for each lake were calculated using the method outlined by Holmes and Chivas (2002). The data from Pigeon Creek were not used to calculate the K_d values because Pigeon Creek is a tidal estuary, and unlike all the other lakes, is connected by a major channel to the ocean. It was expected that the chemistry of Pigeon Creek would be too greatly influenced by oceanic waters to be a useful comparison.

RESULTS

Chemical Analyses

Lakes were sampled July. They varied significantly with respect to water chemistry. Average salinities in these lakes range from 23.5 to 225.5 ppt (Table 1). Measured pH values ranged from 8.0 to 8.6. Field measurements of salinity ranged from 12 ppt to 104 ppt. Mean temperatures varied between 23.9 to 31.6 ^{o}C. Mg/Ca ratios of the water ranged from 3.44 to 6.02; and water Sr/Ca ratios ranged from 0.01 to 0.07. Chloride concentrations in the water varied from 381 to 1963 mM with major cations being dominated by Na (1270-9870 mM), Mg (68-308 mM), Ca (8-62 mM) and K (1-20 mM). The Mg and Sr content of the water was used to determine ostracode K_d values.

Faunal Analyses

Alpha diversity (i.e. species richness for individual lakes) (N=11) plotted versus measured salinity (ppt) indicates that hypersaline lakes (e.g. Salt Pond, French Pond, Storr's Lake and Reckley Hill Pond) contain fewer species than lakes that are less saline (Figure 2). The lakes with lower salinities had a greater variance in species richness than the hypersaline lakes (Figure 2). Lakes with measured salinities from 35-52 ppt had species richness values that ranged from 5 to 19. However, lakes with salinities greater than 100 ppt had species richness values of 4 or lower (Figure 2). This is similar to Smith (1993), who found that at 350-450 µS/cm there was the maximum species richness, which declined after 750 µS/cm.

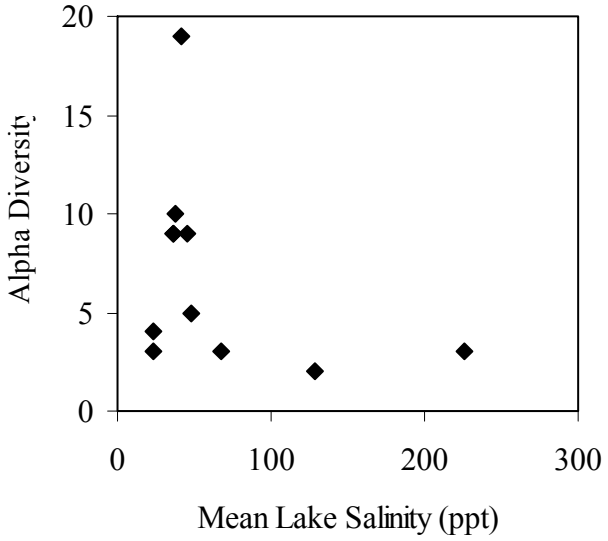

Figure 2. Scatter plot of mean host water salinity versus alpha diversity of all lakes in study. Mean lake water salinity (ppt) on x-axis; alpha diversity of each lake on y-axis. $R^2 = 0.14$.

There is a peak in alpha diversity at thirty-eight ppt (Figure 2). The apex in alpha diversity in a specific salinity range suggests that ostracodes live most effectively in that range of salinities. The highest alpha diversity is from Pigeon Creek, which is a tidal estuary and not an enclosed lake as are the other lakes in this study and may have higher alpha diversity for reasons other than optimal salinity. However, other lakes with relatively similar salinities also showed higher alpha diversities, suggesting that salinity may play a significant role.

A rarefaction plot for all lakes shows that for all lakes except Pigeon Creek, the slope levels off at thirty to forty individuals (Figure 3). The alpha diversity of Pigeon Creek, which has the greatest diversity of all lakes sampled in this study, begins to level off at one hundred individuals. Since our sample counts were one hundred

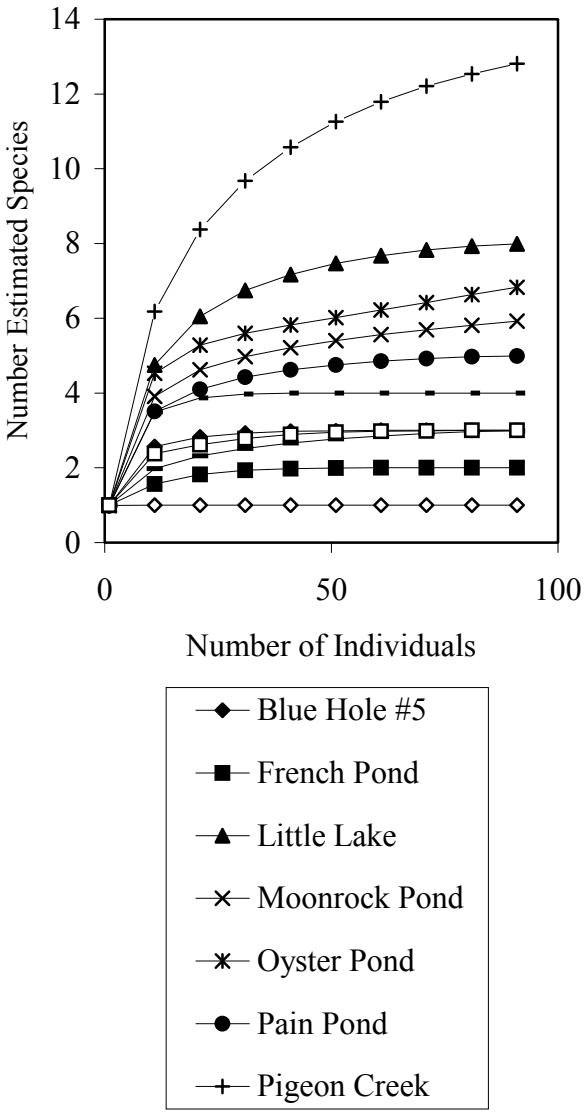

Figure 3. Rarefaction plot of number of individuals sampled versus number of estimated species for each lake in study. Number of individuals sampled on x-axis; estimated number of species on y-axis.

fifty per sample and approximately six hundred valves per lake, except for Salt Pond, French Pond, Pain Pond and Reckley Hill, which had 29, 239, 316 and 471 individuals counted respectively, our sampling method was effective in all cases since the rarefaction plot leveled off at a lower number of individuals than was collected.

Shannon Diversity Indices were calculated based on Shannon H' Log base 10, Shannon Hmax Log base 10, and Shannon J'. Pigeon Creek has the highest diversity index at 0.991, while Storr's Lake has the lowest at 0.027. Salt and French Pond have low indices at 0.111 and 0.213, respectively. Little Lake, and Moonrock, Oyster, Pain, and Reckley Hill Pond all have values between 0.55 and 0.73. The two "blue holes" have indices of approximately 0.4.

Detrended Correspondence Analyses of the fauna show similarity between lakes with similar salinities (Figure 4). For example, French and Salt Pond are plotted very close together and have similar species and water chemistries. Blue Hole #5 and Watling's Blue Hole also plot near one another as does Pain and Reckley Hill Ponds. Pigeon Creek and Storr's Lake are the least similar, despite being extremely close geographically. Little Lake and Oyster Pond also plot close to one another, despite having a great geographical distance between them.

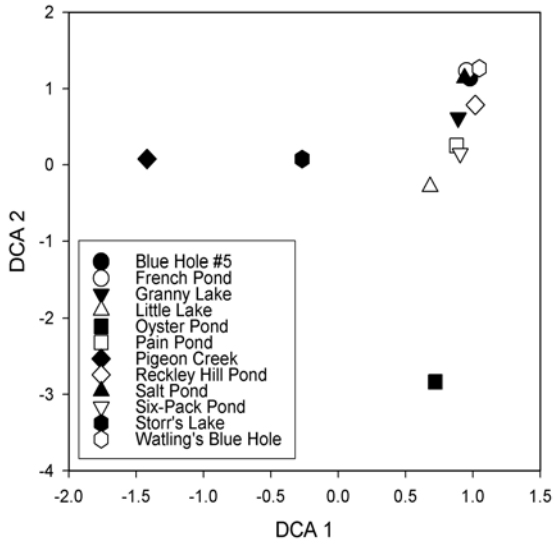

Figure 4. Detrended Correspondence Analyses Plot for lakes in study. Axis 1 plotted versus Axis 2. Axes are functions of faunal populations.

These trends and associations are corroborated by the Bray-Curtis cluster analysis showing the similarity of lake faunas in two-dimensional space (Figure 5). In this diagram, Salt and French Pond are clustered to themselves, with weak linkage to the other ponds or lakes. The two blue holes are also clustered together and linked to Pain and Reckley Hill Ponds. While the blue holes are close in proximity to each another and Pain and Reckley Hill Ponds are close in proximity to one another, neither grouping is in close geographical proximity to the other (Figure 1). Moonrock Pond, which is located in the northern part of the island in a group of karst-formed lakes that includes Oyster, Pain, and Reckley Hill Ponds is only weakly linked to those other ponds' faunas and shares the most faunal similarity with Pigeon Creek and Storr's Lake (Figure 5).

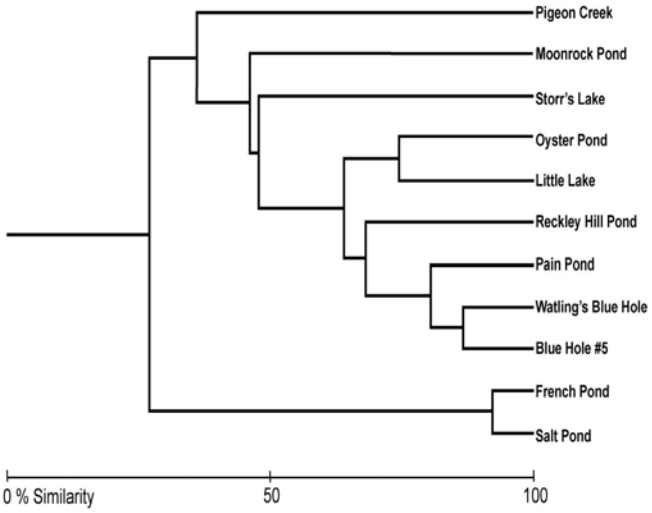

Figure 5. Bray-Curtis Cluster Analysis of lakes in study. Each lake shown on right side of dendrogram. Percent similarity on bottom.

Valve Chemistry

Mg/Ca and Sr/Ca ratios of the three ostracode species (*Cyprideis americana*, *Hemicyprideis setipunctata*, and *Perissocytheridea bicelliforma*) were calculated and plotted as a function of Mg/Ca and Sr/Ca ratios of the host water. Mg/Ca ratios for *C. americana* (male and female) and *H. setipunctata* had similar ranges (0.0131 to

0.0375), while ratios for *P. bicelliforma* were slightly higher from 0.0241 to 0.0397. There is a positive trend in Mg/Ca ratios for *C. americana* and *H. setipunctata* as the Mg/Ca ratios of the water increased. However, there was a slight negative trend between Mg/Ca ratios of the host water and Mg/Ca ratios of the carapace with *P. bicelliforma*.

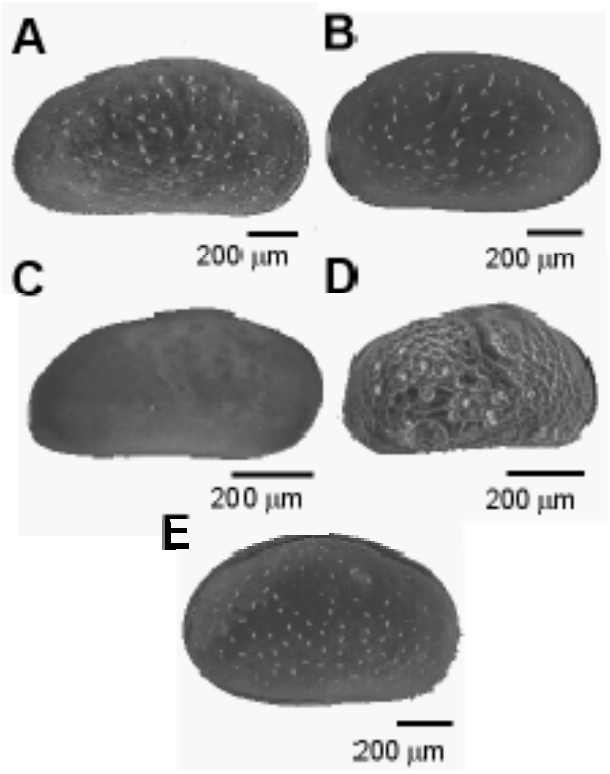

Figure 6. Scanning electron microscope images of the ostracodes used in the geochemical analyses in this study. A) Cyprideis americana *(male); B)* Cyprideis americana *(female); C)* Dolerocypria inopinata*; D)* Perissocytheridea bicelliforma*; E)* Hemicytheridea setipunctata*. All scale bars are 200 microns as indicated.*

The Sr/Ca ratios show a slightly different pattern. While all three species appear to have similar ranges (0.0034 to 0.0087), the lighter of the three, *P. bicelliforma* has a much wider range (0.0039 to 0.0085) than does *H. setipunctata* (0.0034 to 0.0059). This could be due to the fact that the latter species can be analyzed with a single valve, while the lighter species requires two to three valves per sample. Like the Mg/Ca ratios, there is a positive trend between the Sr/Ca of the valves and water for *C. americana* and *H. setipunctata* but a slight negative trend for *P. bicelliforma*.

Mean ostracode valve mass was determined for the three species and plotted versus the K_d[Mg] and K_d[Sr] of those species, as calculated using the following equation:

$$K_D[M]_T = \frac{M/Ca_{valve}}{M/Ca_{water}}$$

Where M=Mg or Sr, T=temperature (˚C), and M/Ca are molar ratios. K_d is the trace element uptake coefficient for a given element at a given temperature (Chivas et al., 2002).

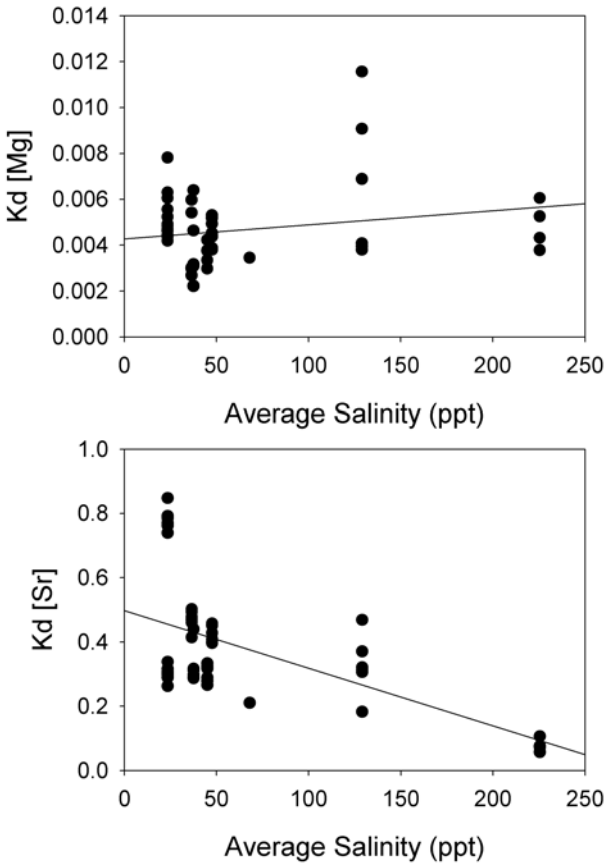

Figure 7. Scatter plots of mean water salinity versus K_d[Mg] and K_d[Sr] for ostracode valves of male and female Cyprideis americana*, as well as* Hemicyprideis setipunctata *and* Perissocytheridea bicelliforma*.*

Perissocytheridea bicelliforma is the lightest species (mean mass 0.004 mg); *H. setipunctata* is the heaviest (mean mass 0.110 mg). *Cyprideis americana* (both male and female) had a total mean value of 0.051 mg. There is a difference in mass between the males and females of *C. americana* of 0.002 mg. The 0.002 mg difference measured within the valves is within the resolution of the microbalance (+/- 0.001 mg). While there is a slight but not statistically significant overall negative trend (R^2= 0.018) between ostracode sample mass and K_d ratios for Mg, *P. bicelliforma* is statistically different (p=0.95) than either *C. americana* or *H. setipunctata*. This could be the case because *P. bicelliforma* is significantly lighter than the other two species. The K_d values for *C. americana* and *H. setipunctata* are most similar, yet their masses are very different, with *H. setipunctata* being more than twice as heavy as *C. americana*.

Mean ostracode valve mass was plotted versus K_d[Sr] as calculated by the same equation as above. There appears to be a slight difference in K_d[Sr] in *C. americana* with respect to gender (Figure 3B). In both the K_d[Mg] and K_d[Sr], the male *C. americana* has a smaller variance than the females, even though they are the lighter of the two. Interestingly, in some lakes, there were no males of *C. americana*. The lack of male *C. americana* could be explained by parthenogenic reproduction, which is not uncommon in ostracodes but has not been reported for *Cyprideis* sp. (Smith and Horne, 2002). The males have a narrower K_d[Sr] range (0.21-0.77), while the females have a wider range (0.11-0.79). *H. setipunctata* (0.18-0.79) has a similar wide range, but *P. bicelliforma* has a much narrower range and overall lower value than the other two species (0.06-0.43). There is a weak positive correlation between mass and K_d[Sr] values.

Ostracode K_d[Mg] were plotted as a function of salinity for all three species (Figure 6). There is no significant trend, positive or negative, between K_d[Mg] and salinity. While Teeter and Quick (1990) reported a negative trend and De Deckker et al. (1999), on a different species of *Cyprideis* from Australian lakes, reported a positive correlation, our data do not suggest any relationship between K_d[Mg] and salinity. In some of these lakes, dolomite may be forming and has been shown to form, which may account for this trend, as the Mg gets taken up in this process (Bain, 1991).

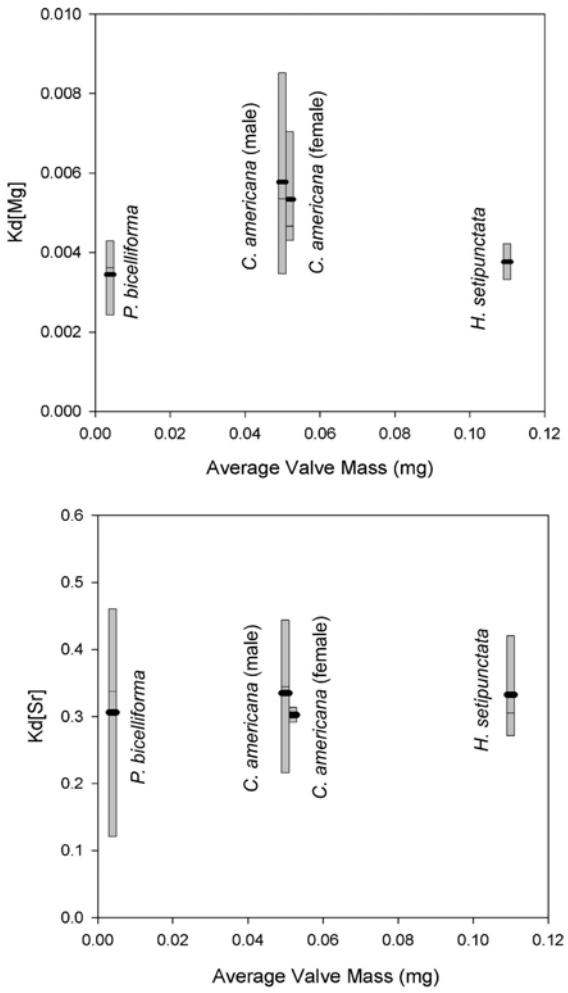

Figure 8. K_d[Mg] and K_d[Sr] vs average mass.

Examining K_d[Sr] versus salinity, there is a strong negative correlation between them (Figure 6). All three species have wider ranges at lower salinities (0.26 to 0.85), while in K_d[Mg], the higher values were found only in the *P. bicelliforma*.

Examining the male versus female Sr/Ca uptake ratios of *C. americana* suggests that male *C. americana* metabolize Sr differently than fe-

males (Figure 7). Statistically, the Sr/Ca ratios of *C. americana* are not the same between genders, as evidenced by t-test results (p=0.95), further suggesting that at least in some cases, the gender of the ostracode affects the calculated K_d[Sr] for a given species. Despite this possible gender effect for Sr uptake, results of a t-test (p=0.95) on Mg/Ca ratios indicate that there is no significant difference between male and female *C. americana* for this ion. In both instances, more data would be useful to further test this relationship.

DISCUSSION

Results of this study indicate several important relationships regarding ostracode valve chemistry and host water as well as faunal affinities and distributions.

The lakes and ponds on San Salvador vary dramatically in size, chemistry, and faunal composition. Interestingly, some lakes that are the closest in geographic proximity have the greatest difference in fauna or in chemistry. This is similar to other invertebrates on the island and suggests that much of this distribution is based on chance. Other biotic factors, such as competing meiofauna or macrophytes may play a minor role, but similar biogeographic patterns also exist in ostracode faunas from the Great Plains of North America (A. Smith, personal communication) with little explanation other than random dispersal processes. Likewise, the lakes that are most similar in chemistry have differences in fauna. In general, lake formation and history on San Salvador is controlled by karst and geomorphic processes. The island's bedrock is dominated by marine and aeolian lithified carbonates, of both marine and aeolian origin. In addition, these lakes are not closed systems, but are connected via lake drains to each other and the ocean realm. The connection of the lakes to the ocean realm and to each other has an influence on ostracode shell chemistry as well as faunal distribution.

Faunal Distribution and Ecology

Alpha diversity is affected by lake salinity. Hypersaline lakes are less diverse than lakes with normal or average salinity. Less saline lakes have a greater variability with respect to species richness than hypersaline lakes. Data suggest that there is a "preferred" salinity for high alpha diversity, near marine salinities and the calcite branchpoint, even if the faunal populations are not similar for similar salinities. Lakes with extreme salinity ranges tend to be populated by a few cosmopolitan species that tolerate a wide range of salinities, while the faunal composition and distribution in lakes with lower salinities is most likely controlled by other factors, such as size, depth, substrate, longevity, basin history and biotic factors.

Rarefaction analyses indicate that species sampling was adequate to capture the diversity of each lake. In all cases, the sampling threshold was exceeded. This indicates that the underlying sampling was reflective of the ostracodes present in the lakes. The Shannon Diversity Indices calculated indicate that Pigeon Creek, which is a tidal estuary, was different from the rest of the lakes or ponds. This is not surprising because it is a well-documented bestiary for fish and mollusks (Godfrey et al., 1994).

Finally, the correspondence and cluster analyses were highly significant because not only did they corroborate one another, they indicated that 1) adjacent lakes are not necessarily similar in fauna, while lakes geographically separated by distance or barriers may be similar, and 2) lakes of similar chemistries did not always have similar faunas, yet the lakes with the most extreme salinities were the most similar in faunal composition. Interestingly, Salt Pond and French Pond, are not geographically close, therefore, their extreme conditions must be influencing the faunas. Cosmopolitan, euryhaline species (*P. bicelliforma* and *C. americana*) that can tolerate such hypersaline conditions populate these two lakes. The lack of clinal distribution of ostracodes within these lakes and ponds on such a small island (~153 km^2) suggests that ostracode dispersal mechanisms remain enigmatic. The lake drains that connect these ponds and lakes to the marine cannot necessarily have that great an influence on species' presence or absence because then all lake and ponds would have similar or the same fauna. Likewise, the tra-

ditional explanation of dispersal via bird's feet may or may not have a role here. With such a small island and so many lakes and ponds, it would appear highly probable that they would have more similar faunas if birds were the predominant mechanism of dispersal. However, if birds were one of the primary mechanisms, then it would suggest that this type of dispersal event is rare in the ecological and evolutionary history of these organisms. Core studies have indicated presence of certain species and their disappearance due to environmental change (Sanger and Teeter, 1982). Whether or not this could explain the entire extant biogeographical distribution of these ostracodes is still not known. Further work, particularly with the fossil record via cores, is required to sufficiently address this question.

Geochemistry

The weak positive correlation between the Mg/Ca and Sr/Ca ratios of the host water and the resulting Mg/Ca and Sr/Ca ratios of the ostracodes that live in the water is consistent with other studies (Chivas et al., 1983; De Deckker et al., 1988; Holmes et al., 1992; Xia et al., 1997; De Deckker et al., 1998; Wansard et al., 1998). This is because the organism precipitates its valve from the contents of the host water, therefore relative concentrations of trace elements present in the host water will be reflected in the shell as it is being precipitated (Turpen and Angell, 1971).

The K_d uptake ratios for both Mg and Sr indicates that K_d is not necessarily dependent on ostracode valve mass (which is a function of valve thickness and density). However, *P. bicelliforma* may have a wider variance or higher K_d[Mg] and K_d[Sr] due to either its low mass or the fact that the measurements were made on more than one valve and thus averaged. These results are consistent with De Deckker et al. (1999) in that the partition coefficient appears to be species-dependent and K_d is most likely controlled by species and not mass. However, there are some concerns that *P. bicelliforma* is so weakly calcified as compared to the other two species in the geochemical analysis, that mass may still play a role, but only as a function of varying physiological conditions of different species.

Perhaps most surprising are the apparent differences in male versus female Sr/Ca uptake ratios of *C. americana* (p=0.95). However, these results are understandable because most organisms in the animal kingdom have significant physiological differences between males and females. This is a potentially significant concern for future applications of trace element geochemistry for palaeoenvironmental reconstruction, as it makes it necessary to discriminate between a species' gender. It is also significant that there is no difference between male and female *C. americana* uptake of Mg (p=0.95). In both instances, additional studies need to be done to determine if this trend is present in other species and in *C. americana* in other locations.

The lack of any significant trend in Mg/Ca (valve)/Mg/Ca (water) as salinity increases for all species, is not consistent with De Deckker et al. (1999) or Teeter and Quick (1990). De Deckker and others (1999) noted this discrepancy between their findings and Teeter and Quick (1990), suggesting that the differences between these two previous studies was because Teeter and Quick did not measure the Mg/Ca of the waters in which they collected their ostracodes. In addition, it was also suggested that Teeter and Quick's samples might have been time averaged due to molting at different times of the year or transport due to strong tides or affected by formalin treatment after collection. Finally, De Deckker et al. (1999) suggested that the differences could be due to certain ostracodes being collected from high salinities and therefore were poorly calcified.

While these are conceivable explanations, data presented in this study indicate that none of the reasons given by De Deckker et al. (1999) are necessarily valid for the San Salvador system and the discrepancy between their results and that of Teeter and Quick (1990) may be due to the fundamental differences in the systems under study. Specifically, our data were collected and analyzed similar to De Deckker et al. (1999), measuring the Mg/Ca of the host waters and not preserving the valves in formalin. Time-averaging due to the differences in molting times was negligible be-

cause the overall trends are consistent with one another and therefore all species would have to have the same time-averaging problem in every lake, which is highly improbable due to differences in lake-basin size and sedimentation patterns. In addition, geochemical analyses were performed on ostracodes collected while still living in the water. Tidal influence for ostracode transport is also considered to be negligible because lakes adjacent to one another do not share similar faunal assemblages. If tidal influence was prominent, then lakes linked closely via karsted conduits would be more likely to share similar faunas, especially if they shared similar salinities. This is clearly not the case on SSI. Indeed, ostracodes are not the only species that show this disjointed distributional pattern on the island; bivalves, gastropods and crustaceans all show similar disconnectedness (Godfrey et al., 1994).

In addition, the fact that *P. bicelliforma* is so light in mass and poorly calcified, and that *H. setipunctata* is so heavy, yet their K_d values overlap, indicates that stress due to high salinity causing poor calcification in the carapace is not the case in this carbonate-dominated, open lake system. Because the SSI lakes are perched upon limestone carbonate bedrock and connected to the marine realm via lake drains, carbonate availability is not a problem, nor is availability of Mg or Sr as trace elements. Therefore, the differences in these trends may simply be due to the differences in the systems under study. The lakes on San Salvador are being continuously "refreshed" and carbonate is always available from both the host waters and underlying bedrock. These findings in no way invalidate the findings of De Deckker et al., (1999), but instead, help further support their findings by explaining, as they indicate, the only documented case where their relationships did not hold.

The wider range of Sr/Ca (valve)/Sr/Ca (water) values at lower salinity values for *C. americana, H. setipunctata* and *P. bicelliforma* indicates that valves from higher salinities have lower Sr/Ca (valve)/Sr/Ca (water) values and lower salinity valves can have higher or lower values. It is not a linear relationship and is consistent with De Deckker et al. (1999). This is also important to note, because it is consistent with the Mg/Ca (valve)/Mg/Ca (water) trends. This suggests that Mg and Sr are correlated in this environment.

CONCLUSIONS

The ostracodes from the lakes sampled for geochemistry on SSI indicate that there may be a slight difference between uptake ratios between different species. However, this is not necessarily related to individual species mass, but to some other vital effect. Likewise there appears to be a difference in the male and female uptake ratios of Sr for *C. americana* but not for Mg. In addition, it appears that lakes with higher salinity have less alpha diversity and those species present are most likely cosmopolitan and adapted to wide environmental tolerances. Interestingly, some of these hypersaline lakes lack males in some species, suggesting parthenogenesis under these extreme conditions. Finally, there is not necessarily a correlation between ostracode species distribution and lake-water chemistry. In some cases, such as the hypersaline lakes, there is. However, in the less saline lakes, species distribution appears to be influenced and controlled by other factors. Thus, faunal analyses alone may not be enough to reconstruct palaeoenvironments. Corroborative geochemical data should also be used, when and where possible.

Thus, our study yields significant implications for palaeoclimatological, palaeoecological and palaeogeographical investigations. First, before choosing to use ostracodes as geochemical proxy indicators for palaeoclimatological reconstructions, one needs to choose the species that not only is the most abundant, but has a well-calcified carapace to limit the amount of variability that exists in the lighter species, such as *P. bicelliforma*. Second, looking at the palaeoecological changes within a single lake system may not give you a complete picture of the ostracode fauna within that region. Since ostracode faunas can differ dramatically from adjacent lakes with similar chemistries, examining more than one lake, in this geographical context, is essential for under-

standing the entire ostracode fauna on this island. In addition, the presence or absence of a specific species does not always correlate to geochemical conditions. It is clear from our analysis that *C. americana* would be the best species for palaeoclimatological and palaeoecological studies in the future.

ACKNOWLEDGMENTS

The authors wish to thank the following people: J. Peck, A. Smith and D. Black for early reviews of the manuscript. A special thanks to Vince Voegeli, Director of the Gerace Research Centre on San Salvador Island, Bahamas for field and lab support as well as E. Brown and J. Agnich, Large Lakes Observatory, Duluth, Minnesota, for ICP-MS support. We are particularly grateful to Doug Ricketts (LLO), J. Beltz, J. Teeter and G. Kunze (UAkron) for providing insights on this project. Many thanks to T. Quick and E. Sinkovich for logistical support. This project was generously supported by the Geological Society of America, the Paleontological Society, Sigma Xi, and a University of Akron Faculty Research Grant (UA-FRG#1526) to Park and was conducted under permit #01/31 from the Bahamas Department of Agriculture.

REFERENCES

Bain, R.J., 1991, Distribution of Pleistocene lithofacies in the interior of San Salvador, Bahamas, and possible genetic models, *in* Bain, R.J., ed., Proceedings of the Fifth Symposium on the Geology of the Bahamas: Bahamian Field Station, San Salvador, Bahamas, p. 11-21.

Beltz, J.F., 1992, Holocene salinity history of Oyster Pond, San Salvador Island, Bahamas, [M.S. Thesis]: University of Akron, Akron, Ohio.

Chivas, A.R., De Deckker, P., and Shelley, J.M.G., 1983, Magnesium, strontium and barium partitioning in non-marine ostracode shells and their uses in paleoenvironmental reconstructions – a preliminary study, *in* Maddocks, R.F. ed., Applications of Ostracoda: University of Houston Press, Houston, TX, p. 238-349.

Carew, J.L., and Mylroie, J.E., 1995, A stratigraphic and depositional model for the Bahama Islands, *in* Curran, H.A. and White, B., eds, Geological Society of America Special Paper 300: Terrestrial and Shallow Marine Geology of the Bahamas andBermuda, p. 5-31.

Chivas, A.R., De Deckker, P., Wang, S.X., and Cali, J., 2002, Oxygen-isotope systematics of the nektic ostracod Australis robusta, *in* Holmes, J.A., and Chivas, A.R., eds., The Ostracoda: Applications in Quaternary Research: Geophysical Monograph Series v. 131, p. 301-313.

Corwin, B.N., 1985, Paleoenvironmental history of Holocene Ostracoda, Storr's Lake, San Salvador, Bahamas, [M.S. Thesis]: University of Akron, Akron, Ohio.

Cronin, M.S., 1994, Holocene salinity history of selected karst pits, eastern Granny Lake, San Salvador Island, Bahamas, [M.S. Thesis]: University of Akron, Akron, Ohio.

Crotty, K.J., 1982, Paleoenvironmental interpretation of ostracod assemblages from Watling's Blue Hole, San Salvador Island, Bahamas, [M.S. Thesis]: University of Akron, Akron, Ohio.

Curry, B., 1999, An environmental tolerance index for ostracodes as indicators of physical and chemical factors in aquatic habitats: Palaeogeography, Palaeoclimatology, Palaeoecology, v. 148, p. 51-63.

Davis, R.L., and Johnson, C.R.J., 1989, Karst Hydrology of San Salvador, *in* Mylroie, J.E. ed., Proceedings of the Fourth Symposium on the Geology of the Bahamas: Bahamian Field Station, San Salvador, Bahamas, p. 118-135.

De Deckker, P., Colin, J.-P., and Peypouquet, J.-P. eds., 1988, Ostracoda in the Earth Sciences: Elsevier, Amsterdam, 302 p.

De Deckker, P., Chivas, A., Shelley, J.M.G., and Torgersen, T., 1998, Ostracod shell chemistry: a new palaeoenvironmental indicator applied to a regressive/transgressive record from the Gulf of Carpentia Australia: Palaeogeography, Palaeoclimatology, Palaeoecology, v. 66, p. 231-241.

De Deckker, P., Chivas, A., and Shelley, J.M.G., 1999, Uptake of Mg and Sr in the euryhaline ostracod *Cyprideis* determined from in vitro experiments: Palaeogeography, Palaeoclimatology, Palaeoecology, v. 148, p. 105-116.

Florentino, E., 1985. Distribution, petrographic analysis, and origin of the Granny Lake oolite, San Salvador, Bahamas, [M.S. Thesis]: University of Akron, Akron, Ohio.

Furman, F.C., Woody, R.E., Rasberry, M.A., Keller, D.J., Gregg, J.M., 1992, Carbonate and evaporite mineralogy of Holocene (<1900 RCYBP) sediments at Salt Pond, San Salvador Island, Bahamas, preliminary study, *in* White, B., ed., Proceedings of the Sixth Symposium on the Geology of the Bahamas, Bahamian Field Station, San Salvador, Bahamas, p. 47-54.

Godfrey, P.J., Davis, R.L., Smith, R.R., and Wells, J.A., 1994, Natural history of northeastern San Salvador Island: a "New World" where the new world began: Bahamian Field Station, San Salvador, Bahamas, 47 p.

Holmes, J.A., Hales, P.E., and Street-Perrott, F.A., 1992, Trace-element chemistry of non-marine ostracods as a means of palaeolimnological reconstruction: an example from the Quaternary of Kashmir, northern India: Chemical Geology, v. 95, p. 177-186.

Holmes, J.A., and Chivas, A.R., 2002, Ostracod shell chemistry-Overview, *in* Holmes, J.A., and Chivas, A.R., eds., The Ostracoda: Applications in Quaternary Research: Geophysical Monograph Series v. 131, p. 185-204.

Nutt, W.H., 1985, Post Pleistocene depositional history of Pigeon Creek, San Salvador Island, Bahamas, using Ostracoda in selected cores, [M.S. Thesis]: University of Akron, Akron, Ohio.

Park, L.E., and Beltz, J.F., 1998, Biogeography of Neogene tropical non-marine Caribbean ostracod faunas: GSA Abstracts with Programs, v. 30(7), p. 287.

Robinson, M.C., and Davis, R.L., 1999, Downloadable GIS topographic map: University of New Haven and Bahamian Field Station.

Sanger, D.B., 1983, Determination of post-Pleistocene depositional environments of Little Lake, San Salvador Island, Bahamas, using ostracode microfauna: M.S. thesis, University of Akron, Akron, Ohio.

Sanger, D.B., and Teeter, J.W., 1982, The distribution of living and fossil Ostracoda and their use in the interpretation of the post-Pleistocene history of Little Lake, San Salvador Island, Bahamas: CCFL Bahamian Field Station, Occasional Papers 1. San Salvador, Bahamas.

Shamberger, E.A., 1998, Depositional history of a coastal evaporite salina-- Salt Pond, San Salvador Island, Bahamas, [M.S. Thesis]: University of Akron, Akron, Ohio.

Smith, A.J., 1993, Lacustrine ostracode diversity and hydrochemistry in lakes of the northern Midwest of the United States, *in* McKenzie, K.G. and Jones, P.J., eds., Proceedings of the Eleventh International Symposium on Ostracoda: Rotterdam: Balkema Publishers, p. 493-502.

Smith, A.J., and Horne, D.J., 2002, Ecology of marine, marginal marine and nonmarine ostracodes, *in* Holmes, J.A., and Chivas, A.R., eds., The Ostracoda: Applications in Quaternary Research: Geophysical Monograph Series, v. 131, p. 37-64.

Teeter, J.W., 1985, Holocene lacustrine depositional history, *in* Curran, H.A., ed., Pleistocene and Holocene carbonate environments on San Salvador Island, Bahamas, p. 133-145.

Teeter, J., and Quick, T., 1990, Magnesium-salinity relation in the saline lake ostracode *Cyprideis Americana*: Geology, v. 18, p. 220-222.

Thalman, K.L., 1983, A Pleistocene lagoon and its modern analogue, San Salvador, Bahamas, [M.S. Thesis]: University of Akron, Akron, Ohio.

Turpen, J.B., and Angell, R.W., 1971, Aspects of molting and calcification of the ostracode *Heterocypris*: Biological Bulletin of the Marine Biology Laboratory, Woods Hole, Massachusetts, v. 140, p. 331-338.

Wansard, G., De Deckker, P., and Julià, R., 1998, Variability in ostracod partition coefficients D(Sr) and D(Mg) Implications for lacustrine palaeoenvironmental reconstructions: Chemical Geology, v. 146, p. 39-54.

Xia J., Engstrom, D.R., and Ito, E., 1997, Geochemistry of ostracode calcite: Part 2. The effects of water chemistry and seasonal temperature variation on *Candona rawsoni*: Geochimica et Cosmochimica Acta, v. 61, p. 383-391.

Zaleha, R.D., 1987, Holocene paleoenvironmental history of Six-pack Pond, San Salvador Island, Bahamas, [M.S. Thesis]: University of Akron, Akron, Ohio.

THE 2004 HURRICANE FRANCES OVERWASH DEPOSITION IN SALT POND, SAN SALVADOR, THE BAHAMAS

Janice M. McCabe and Tina M. Niemi
Department of Geosciences
University of Missouri-Kansas City
Kansas City, MO 64110
NiemiT@umkc.edu

ABSTRACT

The island of San Salvador experienced the direct hit of the Hurricane Frances on 2 September 2004 as a Category 4 hurricane. The high storm surge from the hurricane breached the sand dunes east of Salt Pond causing an overwash into the basin. Our leveling transect across the dunes and into Salt Pond show that the height of the eroded dune crest is 2.15 m across the main washover. Comparison of this transect to the elevation of the dune crest to the south suggests that as much as 62 cm of sand may have been eroded from the dune. Some of this sand was deposited westward as an overwash fan into the Salt Pond basin. Four shallow trenches were dug at Salt Pond on the mudflat exposed in March 2005 in order to document the sediment and sedimentary structure of the storm surge washover deposits from the 2004 Hurricane Frances. In addition, four cores were collected adjacent to the trenches and were analyzed for grain size and organic content. In all four trenches, the Hurricane Frances overwash fan can be divided into a lower coarse-grained sand with cross bedding and grading that contains shells and shell fragments capped by an upper, medium-grained sand. Parallel asymmetrical ripples are preserved across the upper sand layer near Trench 5. These data indicate that the lower sand formed by migrating sand waves from higher velocity waves compared to the upper sand. The maximum overwash sediment thickness from our study was 12 cm. Capping all of the overwash sand was a 0.5- to 1-cm-thick layer of desiccated cyanobacterial mat. The surface of the exposed lake bed was reddish brown from the mat. The mats draped over the ripple beds. At the base of the crust was a dark brown layer. Our cores penetrated older sediment that underlies the Hurricane Frances overwash sand. Layers of coarse-grained sand with shells and shell fragments that grade up section into finer-grained sand are likely to be the record of previous storm deposits. The data from the four cores suggest that there have been at least two other times that Salt Pond has received storm surge deposits. However, the basal scour of the Hurricane Frances overwash deposits indicates that the record of past hurricanes is likely to be incomplete due to the erosion of sediment in the location where we studied the deposits. Cores from the deeper more distal part of the lake are likely to have a more complete record of storm overwash sedimentation.

INTRODUCTION

The 2004 Atlantic Hurricane season was an active season with an above average six major hurricanes including Hurricanes Charley, Frances, Jeanne, and Ivan that wreaked havoc on islands in the Caribbean, the Bahamas, and making landfall in the United States (NCDC, 2004). The 2004 season was followed by the devastating 2005 hurricane season that spawned an unprecedented 27 named storms and four Category 5 hurricanes including Hurricanes Katrina and Rita (NCDC, 2006). The recent increase in the number and ferocity of hurricanes (Emanuel, 2005) has led to a debate as to whether global warming and the concomitant rise in sea surface temperatures (Mann and Emanuel, 2006) or natural climatic variability (Goldenberg et al., 2001) is the cause for the increased intense hurricanes. Clearly, longer re-

cords of past hurricanes are needed to help resolve this debate.

The emerging field of paleotempestology (Liu, 2004; Donnelly and Webb, 2004) has become a powerful tool for assessing the long-term cycles of hurricane activity beyond the period of historical records. Major intense hurricanes, those of Category 3 to 5 on the Saffir-Simpson scale that pass within 50 km to a coastal lagoon or lake, can produce a storm surge large enough to overtop a coastal barrier. The storm surge transports coastal and nearshore sand into the lake where it is deposited as an overwash (or washover) sediment fan. This so-called tempestite is thicker near the coastal barrier and thins toward the center of the lake. In this way, cores recovered from a coastal lake record past intense hurricane landfalls.

This study focuses on hurricane deposition on the Bahamian island of San Salvador. The islands of the Bahamian archipelago are approximately located between latitudes 21°N and 26°N along the Atlantic hurricane track east of Florida and north of Cuba. Most hurricanes cross the region along a track from southeast to northwest, or along a track the moves over the islands from south to north from the Caribbean (Shaklee, 1996). Between the period of 1899 and 1995, Shaklee (1996) reports that thirteen hurricanes have directly tracked over the island of San Salvador. Historical records show a distinct low level of hurricane activity during the three decades of the 1960s through the 1980s (Shaklee, 1996), which corresponds to a general low Atlantic hurricane activity (Nyberg et al., 2007). More recently, San Salvador has been struck by Hurricane Lili in 1996 (Garver, 1996), Hurricane Floyd in 1999 (Curran et al., 2001), and Hurricane Frances in 2004 (Beven, 2004).

Hurricane Frances made initial landfall on the southeast side of the island of San Salvador (Figure 1) with a direct hit of the eyewall on September 2, 2004 at 3 p.m. EDT (Parnell et al., 2004). Just prior to making landfall, Frances was a Category 4 hurricane with sustained maximum winds of 233 kilometers per hour (145 miles per hour). The hurricane stalled over the island and dropped to a Category 3 hurricane. Barometric pressure readings recorded on the island at the Gerace Research Centre at 3 p.m. reached a low of 954 millibars before the instrument failed (Parnell et al., 2004). The heaviest damage to structures was reported in the United Estates settlement on the northeast side of the island, although structures on the west side of the island in the town of Cockburn and near the airport were also damaged (Parnell et al., 2004).

Hurricane Frances storm surge heights of 3.11 m along the east shore, 2.65 m at the seawall in Fernandez Bay, and 3.75 to 5 m at Sandy Point were reported by Parnell et al. (2004). The maximum storm surge from Hurricane Frances recorded from the highest elevation of flotsam and jetsam along the southeast shore of the island was 4.8 to 5.5 m (Niemi et al., 2008; this volume). These data and other evidence of coastal damage from Hurricane Frances are presented in a company paper in this volume.

Our study investigates the back-barrier lake know as Salt Pond on the east side of San Salvador (Figure 2). This lake is separated from the ocean by a road and a low coastal dune that acts as a coastal barrier to storms. During Hurricane Frances, the storm surge overtopped and breached the dune and deposited a blanket of sand into the Salt Pond. Our goals were to document the sediment composition and sedimentary structures of the Hurricane Frances overwash deposits in order to provide a modern analog for investigating the frequency of past episodic storm deposition within this and other lake basins. Salt Pond also provides a unique opportunity to monitor the recovery of the coastal sand dune barrier by repeat leveling and visual surveys.

SALT POND

Salt Pond, a small, shallow coastal lake, is ideally situated to preserve a sedimentary record of ancient hurricane deposits. The lake is located along the eastern (windward) side of the island San Salvador (Figure 2) and is separated from the Atlantic Ocean by a narrow coastal sand dune barrier to the east. Bedrock exposed along the northeast shore of the Salt Pond separates it from the

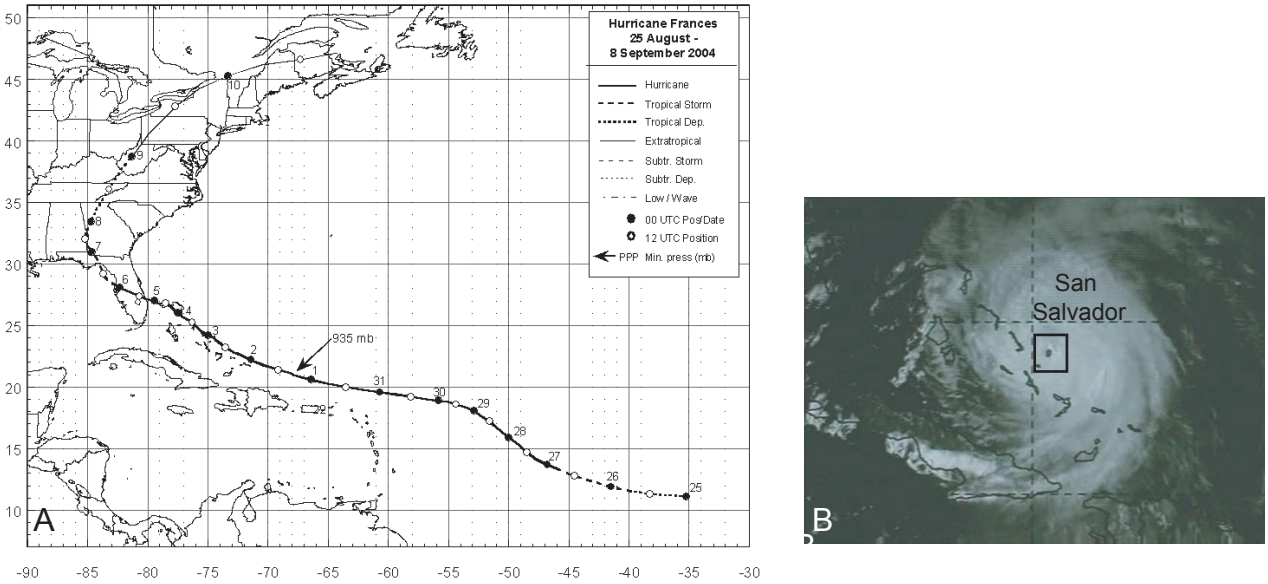

Figure 1. A) Storm track of Hurricane Frances from 25 August to 8 September, 2004. The numbers along the track mark the days. The storm reached its lowest barometric pressure and Category 4 hurricane status on September 1, 2004. Hurricane Frances struck most of the Bahamian Islands as a Category 3 hurricane and Florida as a Category 2 hurricane. (Source of image: Beven, 2004). B) Satellite image showing the eye of the Hurricane Frances passing directly over the island of San Salvador (outlined in the box) (NOAA-16 satellite Advanced Very High Resolution Radiometer (AVHRR) three channel color composite daytime image of Hurricane Frances from 2 Sept. 2004, 18:42 UT).

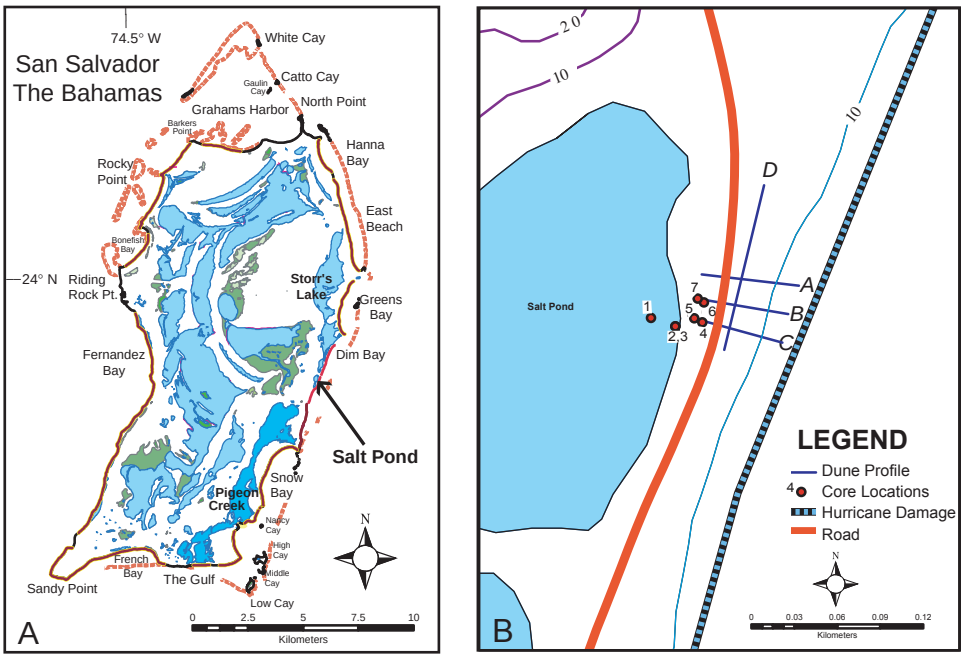

Figure 2. A) Salt Pond is located on the east side of San Salvador. Images are plotted from the GIS database of R. Laurence Davis and Matthew C. Robinson (1999, University of New Haven and the Gerace Research Centre). B) Location of profiles and cores SP05 1-7 collected from Salt Pond during March 2005. Four pits (4-7) were hand dug into the storm surge overwash fan adjacent to cores 4-7. The map also shows the location of three topographic profiles perpendicular to the eroded coastal dunes, labeled A-C, and one topographic profile along the dune crest, labeled D (Profiles shown in Figure 5). Contour interval on map is 10 feet.

Storr's Lake basin to the north. The water depth of the lake in general does not exceed 2 m (Shamberger, 1998).

The hypersaline lake gets its name from halite depositional crusts that form by evaporation and periodic complete desiccations (Teeter et al., 1987). The salinity of the lake is highly variable. In general during the rainy months in the Bahamas between May and October (Shaklee, 1996), freshwater input causes the lake level to rise and reduces the water salinity. These months roughly correspond to the Atlantic basin hurricane season from June to November. During the drier months, evaporation exceeds freshwater inflow and Salt Pond lake levels fall and salinity rises. Teeter et al. (1987) suggest that seawater is also supplied to Salt Pond through subsurface seepage along the eastern margin of the basin.

High lake level water lines are marked across the bare bedrock that is exposed along the northeast shore of Salt Pond. When we conducted our field research during March 4-11, 2005, the level of Salt Pond was low (Figure 3). This is in marked contrast to photographs published by Yannarell et al. (2007) from October 14, 2004 that show a dramatic rise in the lake level after Hurricane Frances. Water levels of the lake rose immediately after the hurricane due to the combined rainfall (~5.5 inches or 140 mm; Beven, 2004) and the marine water inundated inland.

The most extensive monitoring of microbial activity in Salt Pond has been carried out recently by the University of North Carolina research group (Paerl et al., 2003; Yannarell et al., 2007). Measurements of the Salt Pond salinity and photographs before and after Hurricane Frances provide key observations on environmental changes in the lake basin. Figure 3 (A-F) published in Yannarell et al. (2007) show photographs of Salt Pond on 30 August 2004 and on 14 October 2004. These data closely bracket the effects of Hurricane Frances that struck the island on 2 September 2004. The salinity of the lake on 30 August 2004, reported as 280 PSU (practical salinity units; 35 is normal sea water), was reduced on 9 September 2004, just one week after Hurricane Frances impacted the island, to a salinity of 87 PSU (Yannarell et al., 2007). Cores of the outwash sand (Figure 3) showed variations in sand thickness from a few millimeters to 10 cm. Other notable observations from the study include the rapid development of cyanobacterial mats on the outwash sediment just six weeks after the hurricane. A dominant shift in the cyanobacteria community was documented. Furthermore, Yannarell et al. (2007) found that the nitrogen fixation of the organisms appeared to be higher on the overwash sand deposition sites compared to areas with a mud substrate.

The depositional history of Salt Pond has previously been studied from the analyses of sediment cores (Teeter et al., 1987; Furman et al. 1992; Shamberger, 1998). All previous studies of cores indicate that the sedimentary cover overlying bedrock is quite thin. The longest core recovered from the lake is 84 cm in length. These studies show that Salt Pond sediment is composed of organic-rich carbonate mud interbedded with sand layers and evaporites (namely gypsum and halite) representing alternating periods of low lake salinity and hypersalinity. The sand layers were interpreted as sporadic storm events or possible aeolian deposition (Teeter et al., 1987). Twelve sand horizons found in a core extracted from approximately 30 m from the eastern edge of the Salt Pond were interpreted by Shamberger (1998) to represent washover storm events. Recent multiproxy analyses of two 60-cm-long sediment cores by Park et al. (2008; this volume) found considerably more than twelve storm event horizons. In addition, hurricane-induced lake freshening events were found to increase faunal diversity and provide a potential signature for interpreting past hurricanes from the stratigraphic record.

COASTAL DUNE PROFILES

East of Salt Pond are low-lying coastal sand dunes that are stabilized at their base by bedrock (Shamberger, 1998). The dunes were eroded and overtopped by the Hurricane Frances storm surge (Figure 4). Some of the imbricated

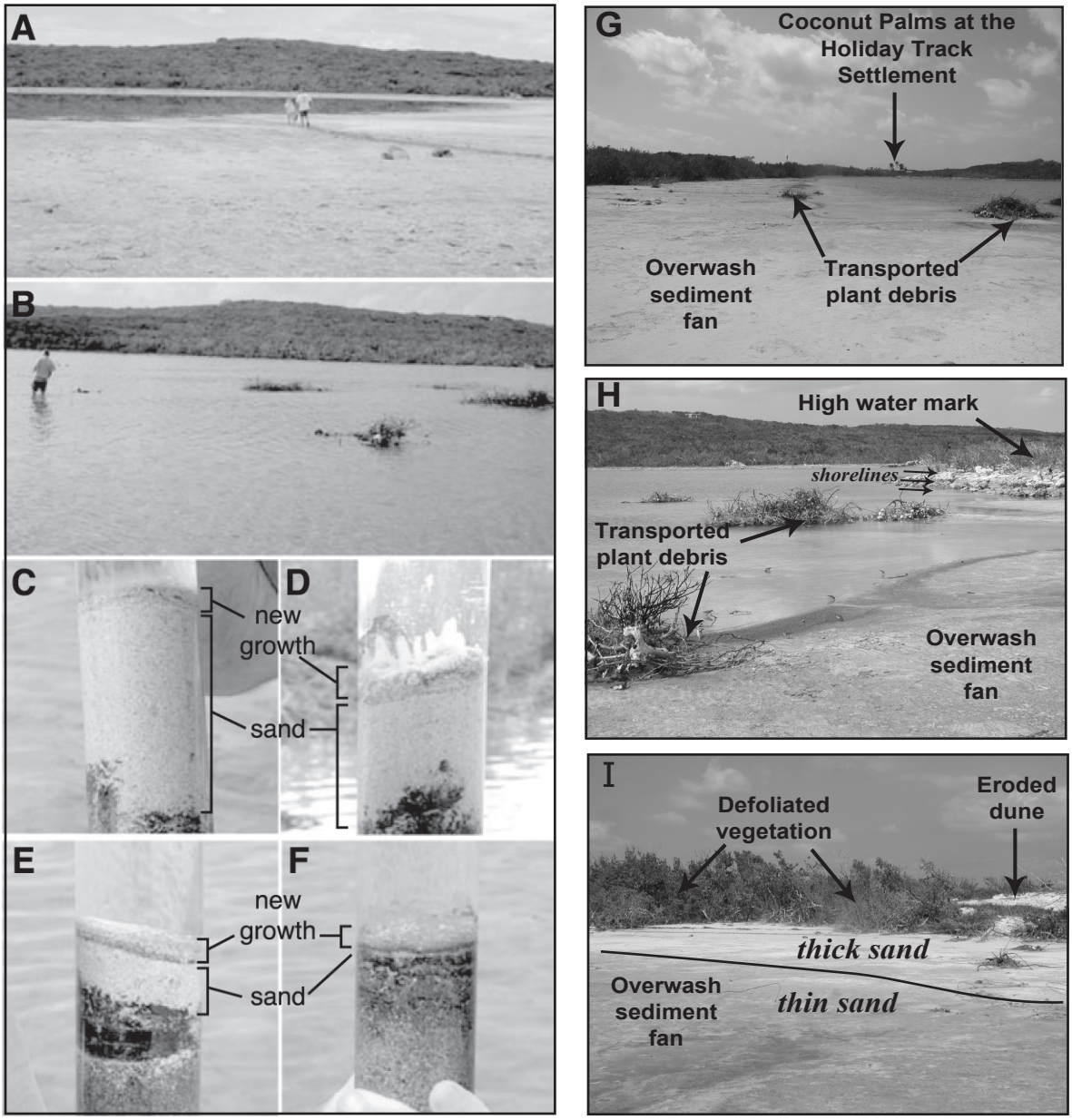

Figure 3. Photographs of Salt Pond from from August 2004, October 2004, and March 2005. Photographs A-F were published in Yannarell et al. (2007). A) View toward the west across Salt Pond from 30 August 2004 before Hurricane Frances (Yannarell et al., 2007). B) View toward the west across Salt Pond from 14 October 2004 after Hurricane Frances (Yannarell et al., 2007). C-F) Cores taken of the Hurricane Frances storm surge sand showing the buried microbial mats and the new growth of cyanobacteria on 14 October 2004 (Yannarell et al., 2007). G) View south across the Hurricane Frances overwash sand deposited as a fan into the northeastern edge of Salt Pond in March 2005. H) View northwest across Salt Pond in March 2005. Bushes transported into the lake by the storm surge are shown. Shorelines shown as water marks on bedrock (arrows). I) Photograph showing the overwash sediment fan in Salt Pond viewed toward the northeast and the Atlantic Ocean in March 2005. The vegetation along this shoreline has been defoliated by the storm surge. The low sand dune that acted as a barrier between Salt Pond and the Atlantic Ocean was extensively eroded and is shown in the background of the photograph.

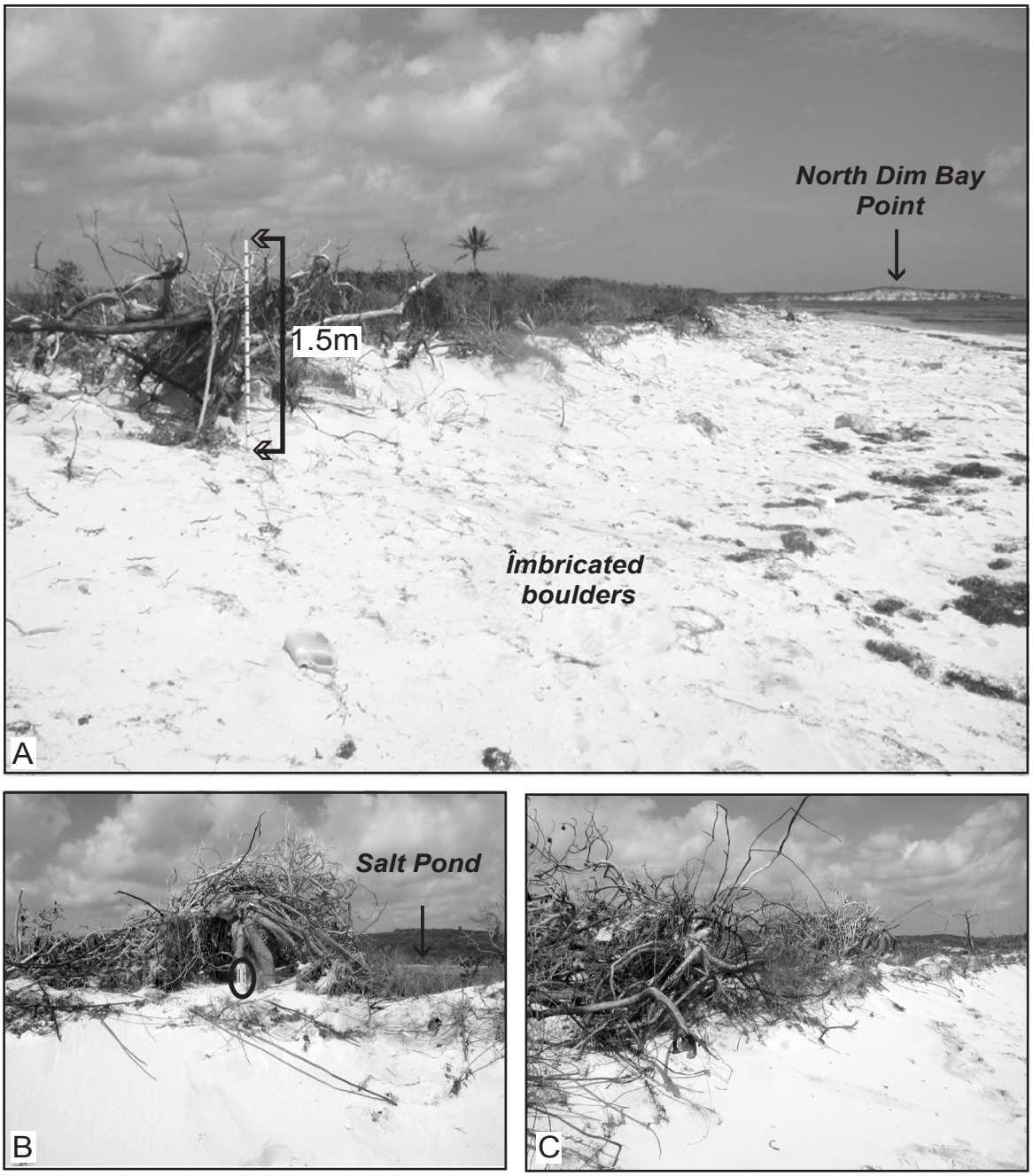

Figure 4. Photographs of the coastal dune barrier between Salt Pond to the west and the Atlantic Ocean to the east from March 2005. A) The low coastal dunes east of Salt Pond were eroded and overtopped by the Hurricane Frances storm surge. View northward along the dunes with the point at the north end of Dim Bay shown. In the foreground are imbricated beachrock boulders dipping seaward that were transported inland by the hurricane storm surge and previous storms. B) The coastal vegetation was uprooted, removed, and defoliated on the sand dunes adjacent to Salt Pond. View toward the west and Salt Pond. Oval circle marks a 15-cm photo scale. C) The 70-m-long sand dunes east of Salt Pond were eroded and overtopped. Some of the debris was deposited inland into the Salt Pond basin. View toward the northwest.

beachrock slabs that dip seaward were likely transported landward to the base of the eroded sand dune by the Frances storm surge (Figure 4). The coastal vegetation was uprooted, overturned, removed, and defoliated. Vegetation where the washover occurred was scarce and consisted largedly of new growth in March 2005. Shrubs from the eroded sand dune were also transported into the lake (Figure 3). Bioclastic carbonate sand eroded from the dunes, beach, and subtidal environment by the storm surge was transported inland and deposited in the Salt Pond basin. The median grain size of the beach sand adjacent to Salt Pond as determined by Park et al. (2008, this volume) is 300 microns (medium-grained sand).

Topographic profiles were constructed in March 2005 along three transects from the low tide to Salt Pond and one along the dune crest (Figure 5). The profiles were measured by using a hand level and a 1.5 m stadia rod divided into 10 cm increments. We recorded the elevation variations along the profile at each major inflection point. Transects were measured across the north (Profile A) and south (Profile C) limits of the major washover. The middle profile B was placed at the point of maximum erosion. The washed out dune was measured longitudinally between points of heavy vegetation from the north and south along the dune crest and across the eroded vegetation in Profile D.

The profiles shown in Figure 5 represent the state of the beach and dunes six months after Hurricane Frances. We do not have data for this location prior to the tropical cyclone. Our data show that the height of the dunes was lowest (2.15 m) along profile B and was slightly higher along the north and south profiles (2.55 m and 2.77 m, respectively). The topographic contour map of this coastal location (Figure 2) indicates that the dunes may have been as high as the 10-foot contour (3.0 m) prior to the storm.

The width of the sand dunes east of Salt Pond was narrowest (11 m) along the southern profile. Also along the south profile, a steep eastward-facing scarp was formed by erosion of the sand dune. This type of erosion was prevalent along the eastern coast of San Salvador in locations where the dunes were not overtopped by the storm surge but eroded at their base. The longitudinal profile (D) shows the location of the 30-m-long washover into Salt Pond between Profile C in the south and Profile A in the north. South of profile C, storm surge washover was minimal as the coastal dune is here higher. North of profile A, the Hurricane Frances storm surge overwashed the coastal dunes and defoliated the vegetation along an additional 250 m length of this shoreline (Niemi et al., 2008, this volume).

Our profile data show that the distance from the low tide mark to the shore of Salt Pond is between 43 m and 53 m. The Salt Pond basin floor was lower than our starting point on the beach. At the time of our observations in March 2005, flotsam and jetsam brought into the Salt Pond basin by the storm surge was still visibly caught in the coastal shrubs along the northeast shore of the lake. Washover into Salt Pond deposited debris 1.5 m above the shore of the high water line of the lake. The highstand lake level appeared to be about 0.35 m above the March 2005 levels.

HURRICANE DEPOSITION IN SALT POND

In order to investigate the thickness, depositional style, and sedimentary structures of the overwash sediment, we collected and described the deposits in cores and in shallow trenches. We used a 5-cm-diameter, clear plastic, piston corer from the Gerace Research Centre to collect cores. Three cores (SP05 1-3 in Figure 2) were taken within the shallow water of Salt Pond on the distal portion of the overwash fan. The recovery of these cores was low (measuring only between 10 cm to 13 cm) and disturbed within a slurry of water. This paper describes the analyses of the four cores (SP05 4-7 in Figure 2) that were collected on the exposed mudflat and overwash fan. Cores SP05-4 and SP05-5 were located about 2 m and 10 m (respectively) from the eastern margin of the Salt Pond basin along the south profile C (Figure 5). Cores SP05-6 and SP05-7 were the same distance from the basin edge as cores SP05-4 and SP05-5 but along the middle profile B (Figure 5). In the

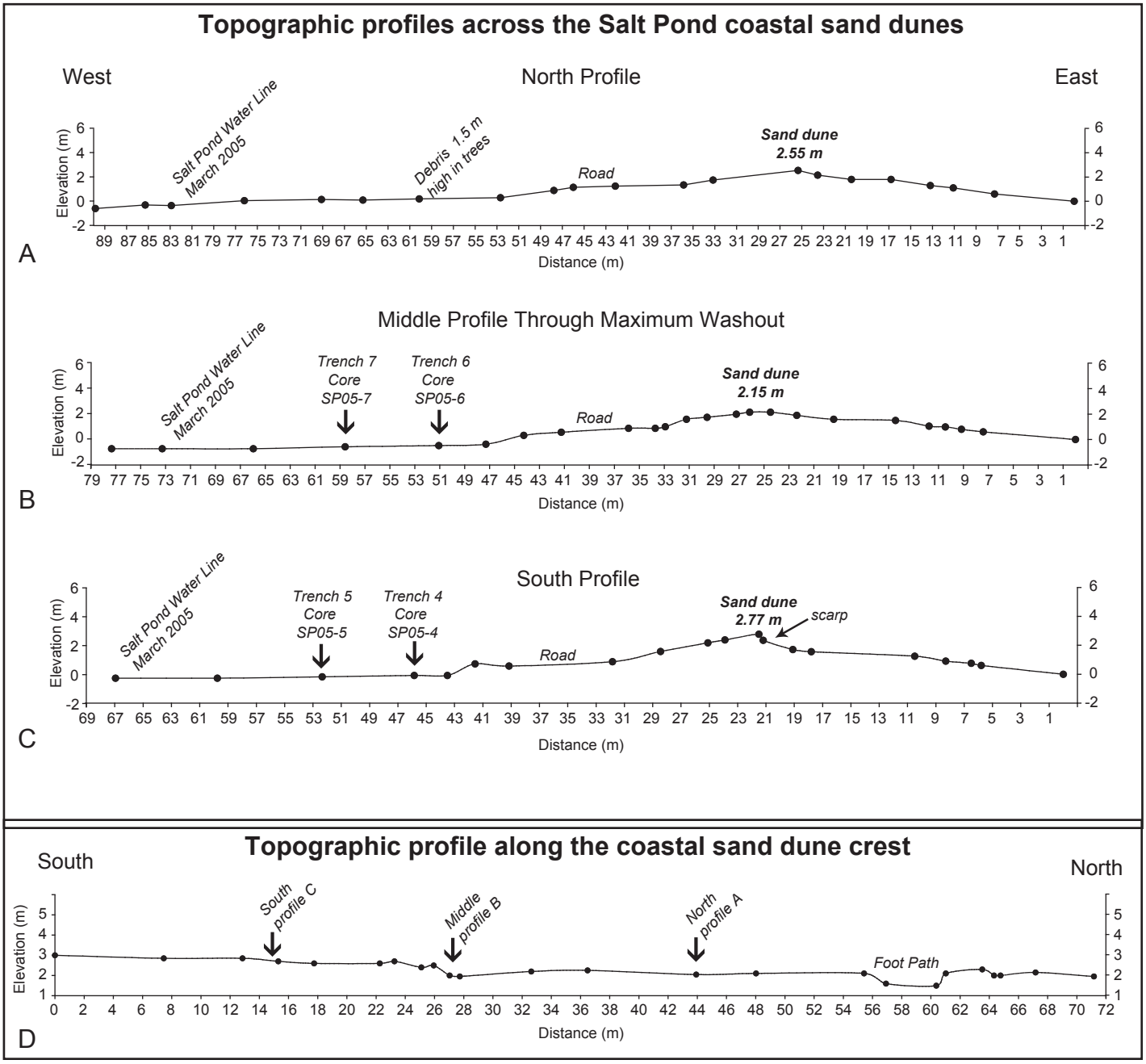

Figure 5. Topographic profiles of the coastal sand dunes east of Salt Pond constructed by leveling in March 2005. A) The northernmost topographic profile from the low tide beachface into the Salt Pond basin to the west. B) Topographic profile through the lowest washout in the sand dunes adjacent to Salt Pond. The location of Trenches 6 and 7 and Cores SP05-6 and SP05-7 are shown. C) The southernmost topographic profile across a partially eroded sand dune. A steep eastward-facing scarp was formed by erosion of the sand dune (see photographs in Figure 4). The location of Trenches 4 and 5 and Cores SP05-4 and SP05-5 are shown. D) Topographic profile along the crest of the sand dune east of Salt Pond. The location of the cross profiles are shown. The 30-m length of sand dune between the south and north profiles was heavily eroded with large tracts of coastal vegetation completely removed. A second zone of erosion is seen north of the northermost topographic profile. This low-lying area appears to be an area of little vegetation and enhanced erosion due to a foot path for beach access and boat launch. Extensive storm surge overwash occurred northward to the south end of Storr's Lake.

field, the cores were described while they were still in the clear acrylic core barrel. The cores were then extruded, wrapped, and shipped to UMKC for further study.

Adjacent to cores SP05 4-7, we hand excavated shallow trenches to expose the sedimentary structures and the lateral variations of the sand sheet. The trench dimensions were about 30 cm by 50 cm. Trenches 4-7 were about 12 cm in depth, while Trench 7 was excavated to a depth of 17 cm. Because of water infiltration, only the upper 7-9 cm of sediment was clearly exposed. Field sketches, descriptions, and photographs were made of the trench exposures.

Additional analyses on the core sediment were conducted in the UMKC laboratory. Cores were sampled every 4 cm. Grain-size analyses were determined using the sieve method of Folk (1974). Samples were first oven dried for 12 hours. The dried sand was reweighed and sieved using U.S. Standard Sieve Series mesh sizes 40 (0.42 mm) for coarse-grained sand, 60 (0.25 mm) for medium-grained sand, 120 (0.125 mm) for fine-grained sand, and 220 (0.074 mm) for very fine-grained sand. Sand trapped on each sieve was weighed. The weight percentage for each of the grain-size categories was calculated and plotted on a graph verse depth of sample. The percent organic matter of approximate 0.1 grams of each sample was determined using the loss-on-ignition method (Dean, 1974). The following section describes the results of both the field and laboratory analyses of each of the trench exposures and core samples.

Description of Trench Exposures and Cores

Trench and Core 4 The exposure of Hurricane Frances overwash sand in Trench 4 and in Core SP05-4 is shown in Figure 6. The upper layer of Trench 4 and Core SP05-4 is a post-Hurricane Frances cyanobacterial mat layer and surface crust. This layer is composed of a 3 mm dark, organic mat buried at a depth of 1 cm below a thin, surface sand and crust. The surface sand is organic rich and appears red in color similar to the exposed mudflat crust. Below the cyanobacterial mat layer and surface crust (designated unit 1), approximately 11 cm of sand were deposited from the Hurricane Frances storm surge. The deposit can be divided into two distinct sand layers with an apparent erosional lower contact. The upper 4- to 6-cm-thick unit 2 is a medium- to fine-grained sand. The lower unit 3 is a coarse- to medium-grained sand that contains organic debris, shells, and shell fragments. Unit 3 appears to contain cross laminations and several cycles of graded bedding.

Grain-size analyses of sediment from Core SP05-4 clearly show that the sand is predominantly medium grained (0.5 to 0.25 mm) in size throughout the entire 36 cm length of the core. Grading of the lower Hurricane Frances sand (unit 3) is evident in the data. The core also provides data for pre-Hurricane Frances storm deposition. At least two lower cycles of beds with fining upwards (graded) sequences with a higher percentage of coarse-grained sand at the base and fine-grained sand at the top are seen in unit 6 and units 4-5 in the core stratigraphy. At the present resolution, the organic matter data do not show a significant change with depth in this core.

Trench and Core 5 Trench 5 and Core SP05-5 (Figures 2, 5, and 7) were located farther into the Salt Pond basin than the location 4. One of the most unique features of this area is the surface bedforms exposed across the lake bottom. The exposed lake floor shows parallel ripples draped with red-colored cyanobacterial mats. The ripple bed migration is toward the southwest (Figure 5A). The stratigraphic section in Trench 5 shows an upper post-Hurricane Frances surface organic mat similar to Trench 4. The Hurricane Frances storm surge deposit at this location was 3 cm thick and consisted of three faint layers (units 2a, 2b, and 2c). These layers show a slight change in color that may reflect a slight compositional change. The base of unit 2 is flat and appears to be aggradational, and resting conformably on the underlying organic-rich unit 3. This is in contrast to other

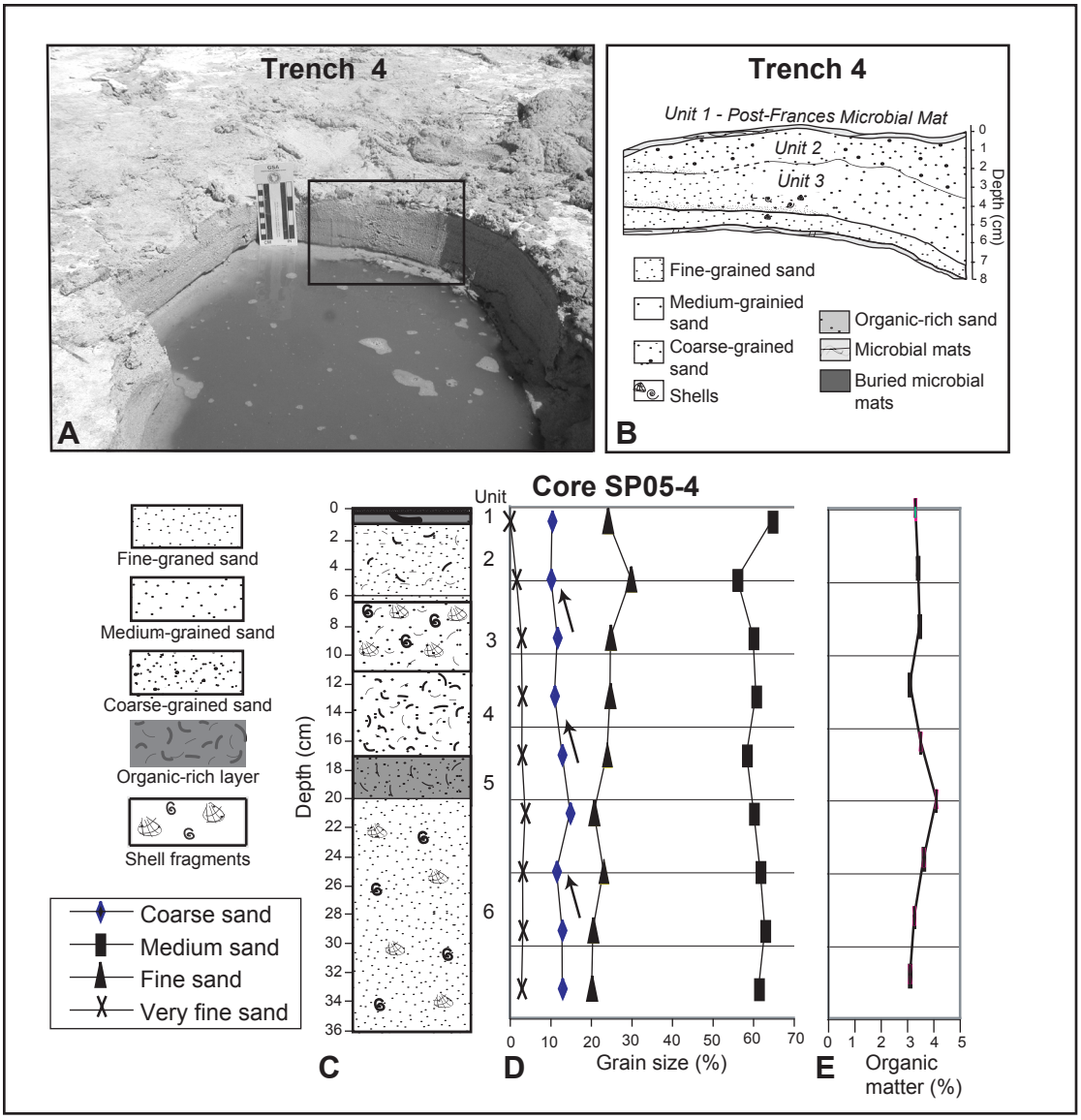

Figure 6. Exposure of Hurricane Frances overwash sand in Trench 4 and in Core SP05-4. A) Photograph of Trench 4 viewed toward the southeast. Approximately 11 cm of sand were deposited from the Hurricane Frances storm surge in two distinct sand layers. The box outlines the area drawn in Figure 6B. B) The base of the storm surge is defined by an erosional lower contact. The11-cm-thick storm surge sand appears to be divided into a lower coarse- to medium-grained sand that contains organic debris and shell fragments (unit 3), and an upper medium- to fine-grained sand (unit 2). Faint indications of graded bedding and cross laminae are present. C) Lithologic section through Core SP05-4. D) Grain-size analyses of sediment from Core SP05-4 clearly show that the sand is predominantly medium grained in size throughout the entire 36 cm length of the core. The arrows show beds with fining upwards (graded) sequences. E) The percentage of organic matter in the core showing a layer at 20 cm depth with a slight increase.

locations where the base of the Hurricane Frances storm surge sand is erosional.

Beneath the Hurricane Frances storm surge overwash fan is a 5-cm-thick, organic-rich sand (unit 3) with 14% organic matter (Figure 7F). The upper 1 cm of unit 3 is a buried, dark-colored organic mat. This buried mat was also observed in cores of Yannerell et al. (2007; Figs. 3 A-F). A thin white-colored, sand layer below this buried mat may represent overwash deposition from the 1999 Hurricane Floyd (Figure 7). The exposed sediment in Trench 5 appears similar to photographs published in Paerl et al. (2003) of the microbial mats taken after that Floyd.

A detailed drawing of a portion of this unit (Figures 7B and 7C) shows that it is composed of several horizontally bedded layers of coarse- to medium-grained sand with shells interbedded with black organic mats. Along one portion of unit 3, an angular contact between sand and the underlying organic mats indicates an erosional event. The organic-rich layers and sand layers appear predominately as interbedded sheets indicating that episodic overwash deposition of sand has buried the microbial mats at this location. An adjacent portion of the Trench 5 wall shows bioturbation and is homogenized possibly indicating previous storm remobilization or disturbance by people walking on the mudflat.

Several layers of shell-rich, coarse- to medium-grained sand layers (units 4-6) are found to a depth of 20 cm in core SP05-5. Grain-size analyses of sediment from core SP05-5 indicate that between 40-60% of the sand is medium grained in size. Several coarse-grained sand layers with shell fragments probably represent previous storm deposits in Salt Pond.

Trench and Core 6 Approximately 12 m north of cores 4 and 5, Trench 6 and Core SP05-6 were located in the Salt Pond basin along the path of the maximum washout of the coastal dune (Profile B, Figure 5). The sandy surface of the overwash storm surge fan is here, as in the other locations, composed of a crust with a cyanobacterial mat within medium-grained sand to a depth of 0.5 cm. The storm surge sand has a lower erosional contact that scours the underlying sand (Figure 8). The wavelength of the scour appears to be approximately 15 cm. The cross lamination in the lower coarse-grained sand shows sedimentary migration toward the southwest. The upper fine- to medium-grained sand (unit 2a) is an even 1 cm-thick deposit that is lighter in color from the deposits above and below it. It may represent a post-storm surge deposit.

Underlying the Hurricane Frances sand in Core SP05-6, unit 3 is a 5- to 7-cm-thick mixed organic-rich sand. It is coarse to medium grained and contains wood and other debris at its base. It is likely to present an amalgamation of previous storm surge deposits. The mixed nature of the deposit also suggests that it may be bioturbated, perhaps from people walking over the surface.

Between a depth 10 cm and the base of the core at 36 cm, two depositional events are evident that may be interpreted as storm related. The first event occurs at about 17 cm depth (unit 4), and the second at 230 cm (unit 5). These events are identified based on an increase in the coarse- and medium-grained sands and a decrease in fine-grained sand and organic material (Figure 8).

Trench and Core 7 Located just 8 m west of Trench 6, Trench 7 contains the thickest overwash sediment from our study. The 12 cm-thick Hurricane Frances storm surge deposits (Figure 8) contained a lower, cross-bedded sand (unit 2b). Unit 2b is coarse grained at its base and grades upward to medium- and fine-grained sand. The storm surge layer did not extend evenly across the trench. The base of the sand was marked by a deep (>7 cm), erosional scour. The scour trough trends northwest-southeast across the trench. The erosion truncated a 2 cm-thick microbial mat and underlying 5 cm-thick mixed organic-rich sand with wood debris. Unit 2b truncates and buries the cyanobacterial mat. The upper 2-3 cm of the storm surge deposit

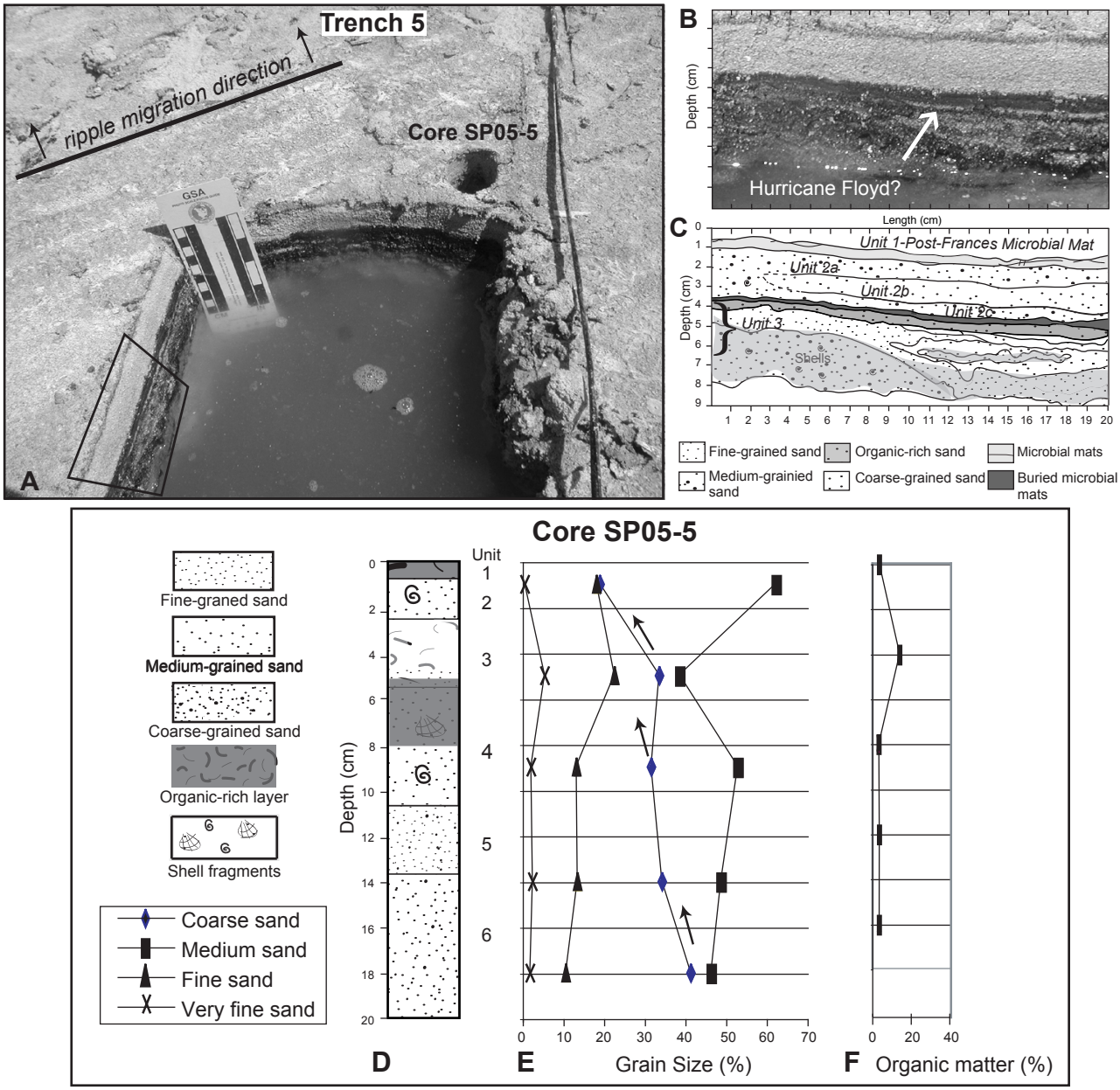

Figure 7. Stratigraphic sections from Salt Pond Trench 5 and Core SP05-5. A) Photograph of Trench 5 showing the locations of Core SP05-5 and area of close-up detail (Figs. 7 B and C). The surface of the exposed lake basin floor shows parallel ripples draped with red-colored microbial mats. The ripple bed migration is toward the southwest. B) Detailed photograph of the south wall of Trench 5. C) Sketch of the stratigraphic layers. The upper layer consists of the post-Hurricane Frances microbial mat. The Hurricane Frances storm surge deposit is 3 cm thick and buries layers of microbial mats and thin sand sheets. D) Lithologic section of core SP05-5 showing division into 6 units. The Hurricane Frances storm surge overwash fan (unit 2) overlies an organic-rich sand (unit 3) and several layers of shell-rich coarse- to medium-grained sand layers. E) Grain-size analyses of sediment from core SP05-5 indicate that between 40-60% of the sand is medium grained in size. The arrows show beds with fining upwards (graded) sequences. F) The percentage of organic matter was measured using the loss-on-ignition method (Dean, 1974). Unit 3 was shown to have nearly 14% organic matter.

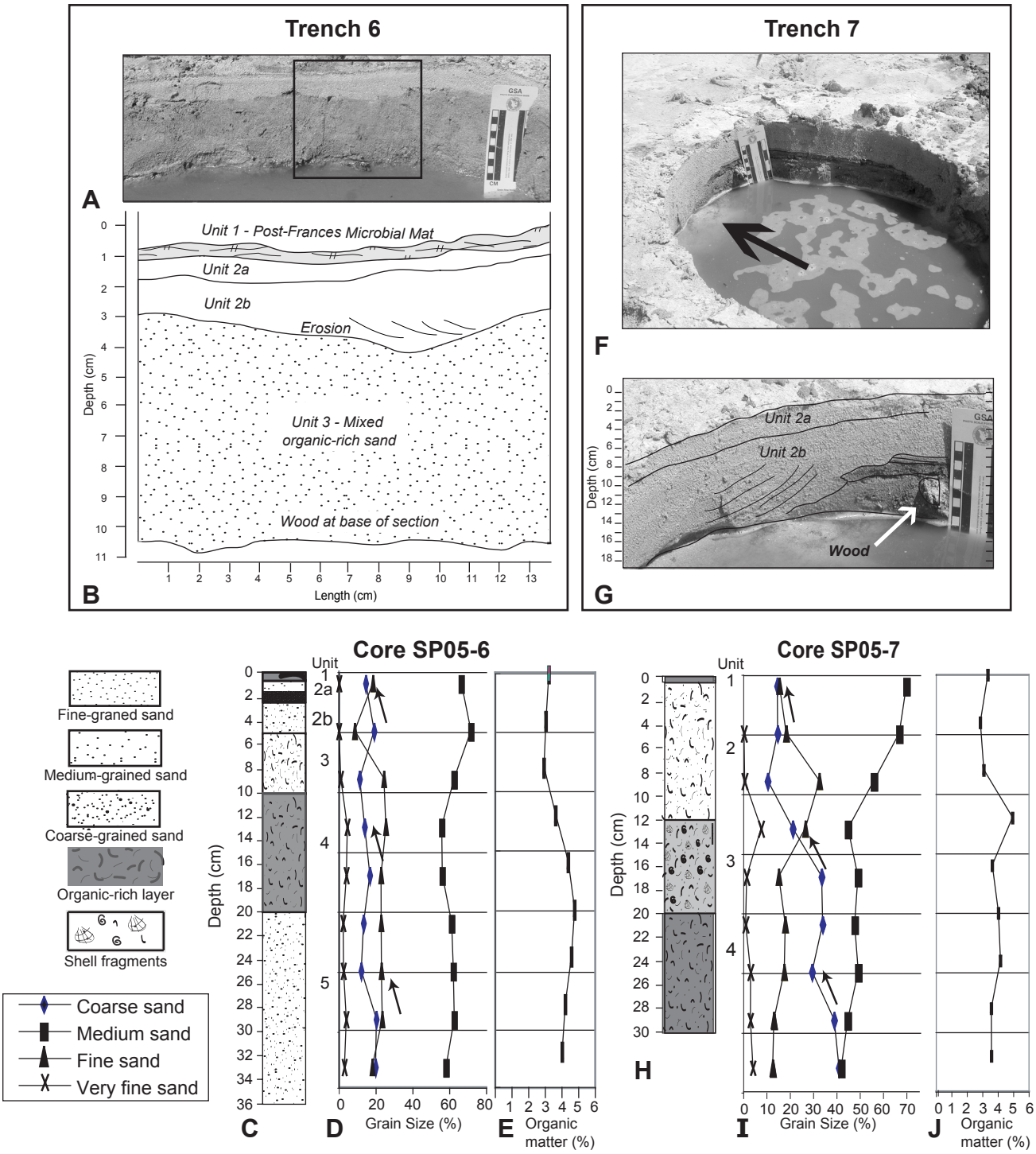

Figure 8. Subsurface exposures of Trenches 6 and 7 and stratigraphic data for Salt Pond core SP05-6 and core SP05-7. A and B) View of Trench 6 showing the irregular erosional base of the Hurricane Frances storm surge sand. Top layer consists of a microbial mat. C) Lithologic section of Core SP05-6. D and E) Grain-size and organic content data for Core SP05-6. See text for discussion. F) Photograph of Trench 7 viewed toward the north. The arrow points to the pit wall that is detailed in Figure 8G. G) Detailed view of the basal scour of the Hurricane Frances storm surge. The overwash sediment apron here consists of a lower cross-bedded sand (Unit 2b) and and upper ripple-bedded sand (Unit 2a). H) Lithologic section of core SP05-7. I and J) Grain-size and organic matter data for core SP05-7 . See text for discussion.

(unit 2a) is a medium-grained sand with shell fragments. Unit 2a lies just below a 0.5 cm-thick, desiccated cyanobacterial mat that was present across the surface of the exposed lake bed.

Two lower storm events can be interpreted from Core SP05-7 at about 17 cm and 28 cm depth where the coarse-grained sand grades into finer sand. Most of the core from 12 cm to 30 cm depths is composed of mixed organic material and sand. Very little evidence of bedding is preserved.

DISCUSSION AND CONCLUSIONS

The island of San Salvador experienced the direct hit of the Hurricane Frances on 2 September 2004. The category 4 wind speeds and forward motion of the storm as it approached the island from the southeast caused a high storm surge. The maximum Hurricane Frances storm surge was measured as 4.8 and 5.5 m based on the upper elevation limit of flotsam and jetsam deposited along the southeastern shores of the island both north and south of Salt Pond (Niemi et al., 2008; this volume).

East of Salt Pond, the low-lying sand dunes were easily overtopped by the storm surge. Although we do not have any dune profile data prior to the storm, published topographic maps suggest that the sand dunes are not likely to have been higher than the 10-foot contour (3 m). Our leveling transect (Profile B) across the dunes and into Salt Pond show that the height of the eroded dune crest is 2.15 m across the main washover. The vegetation was largely stripped from the coastal barrier at this point. Bushes and shrubs from the dunes were transported westward and deposited in the Salt Pond basin. A comparison of profile B with a transect to the south with a dune crest of 2.77 m and considerably less removal of dune vegetation suggests that perhaps as much as 62 cm of sand was removed from the coastal barrier. Some of this sand from the dunes was deposited westward as an overwash fan into the Salt Pond basin.

The storm surge caused scouring in Salt Pond. This erosion is evident in trenches located more proximal to the coastal barrier (Trench 4 and 6) at the eastern edge of the Salt Pond basin. The trough of the deep scour in Trench 7 trends northwest-southeast and only erodes sediment across half the trench. The basal sand in the other part of Trench 7 and in Trench 5, located 10 m farther into the lake basin, is flat and conformably buries the pre-Hurricane Frances dark organic mat.

In all four trenches, the Hurricane Frances overwash fan can be divided into a lower coarse-grained sand with cross bedding and grading that contains shells and shell fragments capped by an upper, medium-grained sand. Parallel asymmetrical ripples are preserved across the upper sand layer near Trench 5. These data indicate that the lower sand formed by migrating sand waves from higher velocity waves compared to the upper sand. The maximum overwash sediment thickness from our study was 12 cm. The sand deposit is thicker along the northeast shore of the lake adjacent to the eroded and overtopped coastal sand dunes.

Capping all of the overwash sand was a 0.5- to 1-cm-thick layer of desiccated cyanobacterial mat. The surface of the exposed lake bed was reddish brown from the mat. The mats draped over the ripple beds. At the base of the crust was a thin dark brown to black layer.

Our observations were made six months after the 2 September 2004 Hurricane Frances storm. Other storms, including Hurricane Jeanne that passed approximately 100 km east and northeast of the island during 19-25 October 2004 (Lawrence and Cobb, 2005) may have produced enhanced storm surge and wave action that could have overtopped the lowered coastal barrier. It is not possible from our study to definitely ascribe all of the sedimentary structures observed in the trenches and upper layers of the cores to Hurricane Frances.

However, the study and photographs published by Yannarell et al. (2007) provide support to the interpretation that cyanobacterial mats were already growing on 14 October 2004.

The Yannarell et al. (2007) study documented microbial mat activity after Hurricane Frances and before Hurricane Jeanne. Since the cyanobacterial mats drape the ripple beds it suggests that both the lower and upper sand seen in the trenches are Hurricane Frances storm surge deposits.

The Yannarell et al. (2007) study also showed both a surface growth of a microbial mat, and modification of the sediment to a depth of about 1 cm. The study clearly demonstrates that microbial activity is not limited to the sediment-water interface.

Hurricane Floyd (1999) overwash deposition was documented by Paerl et al. (2003). These authors note that a thin layer of carbonate sand was deposited on top of the microbial mats and provided a clear marker bed for the study. The Floyd overwash appeared as a white sand layer overlying a black organic mat. In the Paerl et al. (2003) study, the surface microbial mats were shown to be horizontally stratified in three layers: 1) the upper brown-colored cyanobacterial mat, 2) a lighter-colored subsurface photosynthetic bacterial layer, and 3) a deeper, balck anerobic sufide layer. We observed similar layering in Trench 5 where horizontally interbedded sand and black organic-rich layer was buried by the Hurricane Frances overwash deposit. The upper thin sand sheet in this buried unit (3) may possible represent the Hurricane Floyd overwash sand.

Our cores penetrated older sediment that underlies the Hurricane Frances overwash sand. Layers of coarse-grained sand with shells and shell fragments that grade up section into finer-grained sand are likely to be the record of previous storm deposits. The data from the four cores suggest that there have been at least two other times that Salt Pond has received storm surge deposits. However, the basal scour of the Hurricane Frances overwash deposits indicates that the record of past hurricanes is likely to be incomplete due to the erosion of sediment in the location where we studied the deposits. Cores from the deeper more distal part of the lake are likely to have a more complete record of storm overwash sedimentation.

ACKNOWLEDGMENTS

We thank Vincent Voegeli, past Executive Director of the Gerace Research Centre, for discussions and guidance in locating Hurricane Frances storm deposits on San Salvador. Funding for this project was made available through the UMKC Students Engaged in Artistic and Academic Research (SEARCH) and through funds from the UMKC Department of Geosciences. We thank Alexander Daehne, Jennifer Goucher, and Ta'ni Sutherland for assistance in the field. We would also like to thank Dr. Donald T. Gerace, Chief Executive Officer, and Dr. Thomas A. Rothfus, present Executive Director of the Gerace Research Centre, San Salvador, Bahamas for assistance and use of the field station on San Salvador. This study was conducted under permit number 07-05 and earlier permits from the Department of Agriculture, The Bahamas.

REFERENCES

Beven II, J.L., 2004, Tropical cyclone report: Hurricane Frances 25 August-8 September 2004: NOAA National Weather Service, National Hurricane Center, http://www.nhc.noaa.gov/2004frances.shtml, posted 17 December 2004.

Curran, H.A., Delano, P., White, B., and Barrett, M., 2001, Coastal effects of Hurricane Floyd on San Salvador Island, Bahamas, *in* Greenstein, B.J., and Carney, C.K., eds., Proceedings of the 10th Symposium on the Geology of the Bahamas and Other Carbonate Regions: San Salvador, Bahamas, Gerace Research Centre, p. 1-12.

Dean, W.E. Jr., 1974, Determination of carbonate and organic matter in calcareous sediments and sedimentary rocks by loss on ignition: Comparison with other methods: Journal of Sedimentary Petrology, v. 44, p. 242–248

Donnelly, J.P., and Webb III, T., 2004, Back-barrier sedimentary records of intense hurricane landfalls in he Northeastern United States, *in* Murnane, R.J., and Liu, K.-B., eds., Hurricanes and Typhoons: Past, present, and future: Columbia University Press, New York, p. 58-95.

Emanuel, K.A., 2005, Increasing destructiveness of tropical cyclones over the past 30 years: Nature, v. 436, p. 686-688.

Folk, R.L., 1974, Petrology of Sedimentary Rocks: Hemphill Publishing Company, Austin, TX.

Furman, F.C., Woody, R.E., Rasberry, M.A., Keller, D.J., and Gregg, J.M., 1992, Carbonate and evaporite mineralogy of Holocene (<1900 RCYBP) sediments at Salt Pond, San Salvador Island, Bahamas, preliminary study, *in* White, B., ed., Proceedings of the Sixth Symposium on the Geology of the Bahamas: Bahamian Field Station, San Salvador, Bahamas, p. 47-54.

Garver, J.I., 1996, Some Effects of Hurricane Lili on San Salvador Island, Bahamas. http://minerva.union.edu/garverj/geo35/hurricane/Damage.htm, Geology Department, Union College, Posted 15 December 1996.

Goldenberg, S.S., Landsea, C.W., Mestas-Nuñez, A.M., and Gray, W.M., 2001, The recent increase in Atlantic hurricane activity: causes and implications, p. 474-479.

Lawrence, M.B. and Cobb, H.D., 2005, Tropical Cyclone Report: Hurricane Jeanne 13 - 28 September 2004: NOAA National Weather Service, National Hurricane Center. http://www.nhc.noaa.gov/2004jeanne.shtml, posted 22 November 2004. Revised: 7 January 2005.

Liu, K.-B., 2004, Paleotempestology: Principles, methods, and examples from Gulf Coast lake sediments, *in* Murnane, R.J., and Liu, K.-B., eds., Hurricanes and Typhoons: Past, present, and future: Columbia University Press, New York, p. 13-57.

Mann, M.E., and Emanuel, K.A., 2006, Atlantic hurricane trends linked to climate change: Eos, v. 87, p. 233-241.

NCDC (National Climatic Data Center), 2004, Climate of 2004 Atlantic Hurricane season: National Climatic Data Center, NOAA: http://www.ncdc.noaa.gov/oa/climate/research/2004/hurricanes04.html, last updated - 13 December 2004.

NCDC (National Climatic Data Center), 2006, Climate of 2005 Atlantic Hurricane Season: NOAA http://www.ncdc.noaa.gov/oa/climate/research/2005/hurricanes05.html, last updated 21 August 2006.

Niemi, T.M., Thomason, J.C., McCabe, J.M., and Daehne, A., 2008, Impact of the September 2, 2004 Hurricane Frances on the coastal environment of San Salvador, The Bahamas, *in* Park, L.E. and Freile, D., eds., Proceedings of the Thirteenth Conference on the Geology of the Bahamas and Other Carbonate Islands, This Volume, p. 42-62.

Nyberg, J., Malmgren, B.A., Winter, A., Jury, M.R., Kilbourne, K.H., and Quinn, T.M., 2007, Low Atlantic hurricane activity in the 1970s and 1980s compared to the past 270 years: Nature, v. 447, p. 698-701.

Paerl, H.W., Steppe, T.F., Buchan, K.C., and Potts, M., 2003, Hypersaline cyanobacterial mats as indicators of elevated tropical hurricane activity and associated climate change: Ambio, v. 32, p. 87-90.

Parnell, D.B., Brommer, D., Dixon, P.G., Brown, M.E., and Gamble, D.W., 2004, A survey of Hurricane Frances damage on San Salvador: Bahamas Journal of Science, p. 2-6.

Park, L.E., Metzger, T.J., Sipahioglu, S.M., Siewers, F.D., and Leonard, K., 2008, After the hurricane hits: recovery and response to large storm events in a saline lake, San Salvador Island, Bahamas, *in* Park, L.E. and Freile, D., eds., Proceedings of the Thirteenth Conference on the Geology of the Bahamas and Other Carbonate Islands, This Volume, p. 63-75.

Shaklee, R.V., 1996, Weather and Climate: San Salvador Island, Bahamas: San Salvador, Bahamas The Bahmaian Field Station limited, 67 p.

Shamberger, E.A., 1998, Depositional history of a coastal evaporite salina Salt Pond, San Salvador Island, Bahamas, [M.S. Thesis]: University of Akron, Akron, Ohio, 144 p.

Teeter, J.W., Beyke, R.J., Bray, T.F., Brocculeri, T.F., Bruno, P.W., Dremenn, J.J., and Kendall, R.L., 1987, Holocene depositional history of Salt Pond, San Salvador, Bahamas, *in* Proceedings of the Third Symposium on the Geology of the Bahamas: San Salvador, Bahamas, Bahamas Field Station, p. 145-150.

Yannarell, A.C., Steppe, T.F., and Paerl, H.W., 2007, Disturbance and recovery of microbial community structure and function following Hurricane Frances: Environmental Microbiology, v. 9, no. 3, p. 576-583.

IMPACT OF THE SEPTEMBER 2, 2004 HURRICANE FRANCES ON THE COASTAL ENVIRONMENT OF SAN SALVADOR ISLAND, THE BAHAMAS

Tina M. Niemi, Jamie C. Thomason, Janice M. McCabe, and Alexander Daehne
Department of Geosciences
University of Missouri-Kansas City
Kansas City, MO 64110
NiemiT@umkc.edu

ABSTRACT

The impact of Hurricane Frances that directly hit San Salvador, Bahamas as a Category 3 hurricane on September 2, 2004 was investigated from satellite imagery and field mapping in March 2005. Landsat 7 Enhanced Thematic Mapper images of San Salvador from before and after the storm were analyzed to determine the storm surge impact and identify areas for field research. Our main focus was documenting storm surge deposits and beach accretion and erosion processes on the southeastern coast of the island from Dim Bay to Sandy Hook. These areas clearly show a significant reworking of sand and loss of vegetation. Other areas of the island also showed significant changes in beaches, but were not studied at this time. The storm surge from Hurricane Frances ripped up large slabs of beachrock (up to 1 m^2) along the southeast beaches, Sandy Hook, and the Gulf, transported them inland, and deposited them in seaward-dipping, imbricated piles. The mangrove vegetation line retreat on Sandy Hook was measured as approximately 40 m. The adjacent beach to the south showed signs of a 30 m accretion. A maximum height of the storm surge of 4.8 m, 4.9 m, and 5.5 m was measured by leveling to the upward limit of flotsam and jetsam deposited by Hurricane Frances at three localities—the south end of Storr's Lake and two sites near the tombolo called 'The Thumb'—along the eastern shore of San Salvador. Evidence of Frances and other storms were also found in stratified trash deposits south of and around The Thumb. A 1.7-m-thick section was measured that showed 80 cm of aeolian sand burying a 40 cm thick horizon of stratified trash. At this location Hurricane Frances deposits were found at higher elevations and further inland. These data indicate that the Hurricane Frances storm surge was likely more intense than the previous hurricanes that hit the island during the 1990's. The storm surge washed over the coastal barrier, defoliated a large tract of land, and deposited a blanket of sand and other debris into Salt Pond and Storr's Lake from the east and Pigeon Creek from the south. Based on a line of organic debris and defoliated vegetation marking a high water mark, either high winds or the storm surge from Hurricane Frances caused Pigeon Creek tidal estuary to overwash its northwest and north shore. The damage data and storm surge height measurements for Hurricane Frances correspond to a Category 4 hurricane. The enhanced storm surge height measured along the southeast side of San Salvador is likely the combination of the onshore-directed winds with the forward movement of the storm center as the hurricane eyewall made landfall on the island.

INTRODUCTION

The 2004 Atlantic hurricane season was one of the most active on record. Five hurricanes made landfall in the United States with an unprecedented four hurricanes (Charley, Frances, Ivan, Jeanne) hitting Florida (NCDC, 2004). This was the first time since 1886 that a state had been struck by four hurricanes in one season (NCDC, 2004). By its end the 2004 hurricane season was the most costly U.S. hurricane season on record. This record was eclipsed by the devastating and

record-breaking 2005 hurricane season. The 2005 Atlantic hurricane season is noted for the most named storms and the most hurricanes recorded in a single season (NCDC, 2006). Four hurricanes (Emily, Katrina, Rita, and Wilma) were classified as Category 5 hurricanes (NCDC, 2006).

Of the storms that developed in the 2004 and 2005 hurricane seasons, Hurricane Frances was the only storm to make landfall on San Salvador and to cause significant damage (Figure 1). San Salvador is a small outer island of the Bahamas Archipelago located about 640 km southeast of Florida at 24° N, 74.5°W. Hurricane Frances made landfall on the island of San Salvador on September 2, 2004, at 3:00 p.m. (EDT) as a Category 4 hurricane on the Saffir-Simpson Hurricane Scale (Table 1) with sustained maximum winds of 233 kilometers per hour (kmph; 126 knots, kts; 145 miles per hour, mph) (Parnell et al*.,* 2004).

The following information about Hurricane Frances is summarized from the National Hurricane Center's Tropical Cyclone Report (Beven, 2004). Hurricane Frances began as a tropical wave off the coast of Africa on August 21, 2004, and quickly developed on August 24 to a tropical storm status. By August 26, 2004, the storm was named a hurricane. On August 31, 2004, Hurricane Frances reached peak intensity of a Category 4 less 36 hours before making landfall on San Salvador. The air pressure low and wind speed maximum for the storm reached a double peak (Figs. 1C and 1D). The first peak intensity period was during the night of August 31st to September 1st when the lowest central air pressure was estimated by research flights at 934 millibars (mb). The second peak intensity period with low pressure and high winds occurred on September 2nd. Graphs of the best track for the storm's pressure and wind speed show that the hurricane was close to its maximum by midday on September 2, 2004, and then began to lose intensity.

The Gerace Research Centre on the north side of the island at Graham's Harbor recorded the lowest pressure value from a land station of 954 mb before the instrument malfunctioned (Parnell *et al*., 2004). Rainfall from Hurricane Frances on San Salvador was recorded as 5.47 inches (139 mm; Beven, 2004).

The post-Hurricane Frances survey of Parnell et al. (2004) conducted between six and ten days after the storm showed that the heaviest damage to structures was reported in the United Estates settlement on the northeast side of the island. Structures on the west side of the island in the town of Cockburn and near the airport were also damaged (Parnell et al*.,* 2004). Hurricane Frances storm surge heights were reported to be 3.11 m along the east shore, 2.65 m at the seawall in Fernandez Bay, and 3.75 to 5 m at Sandy Point (Parnell et al., 2004).

Most of the rain from Hurricane Frances fell on the mainland of the United States. Hurricane Frances's destruction potential passed almost as quickly as it formed, the storm became a tropical depression in the northeastern United States on September 7, 2004. Hurricane Frances was indirectly related to 42 deaths, and directly related to 7 others (Beven, 2004).

San Salvador has been hit by several hurricanes in the past decade. During the period from 1899-1994, thirteen hurricanes directly tracked over the island (Shaklee, 1996). During the same period, September was the month when the most hurricanes made landfall in the Bahamas (Shaklee, 1996).

Most recently during the summer of 1996, San Salvador was directly hit by two storms, Tropical Storm Bertha and Hurricane Lili (Lawrence, 1996a,b). Coastal damage caused by the 1996 hurricanes was concentrated mainly on the southwestern side of the island of San Salvador. Damage to homes and other buildings was extensive. Damage surveyed by Garver (1996) consisted mainly of scattered coral damage, trash deposition, and major overwash sediment fans around French Bay and the Gulf.

Hurricane Floyd indirectly hit San Salvador in 1999. Floyd passed 30-56 km to the northeast to north of San Salvador (Pasch et al., 1999). Gamble et al. (2000) report that the eye of Hurricane Floyd passed 24 km north of San Salvador. Damage from Hurricane Floyd was most intense on the northern and western shores of San Salvador but less intense than the 1996 Hurricane Lili (Gamble et al. 2000). Significant erosion occurred on Fernandez Bay with significant washout of the

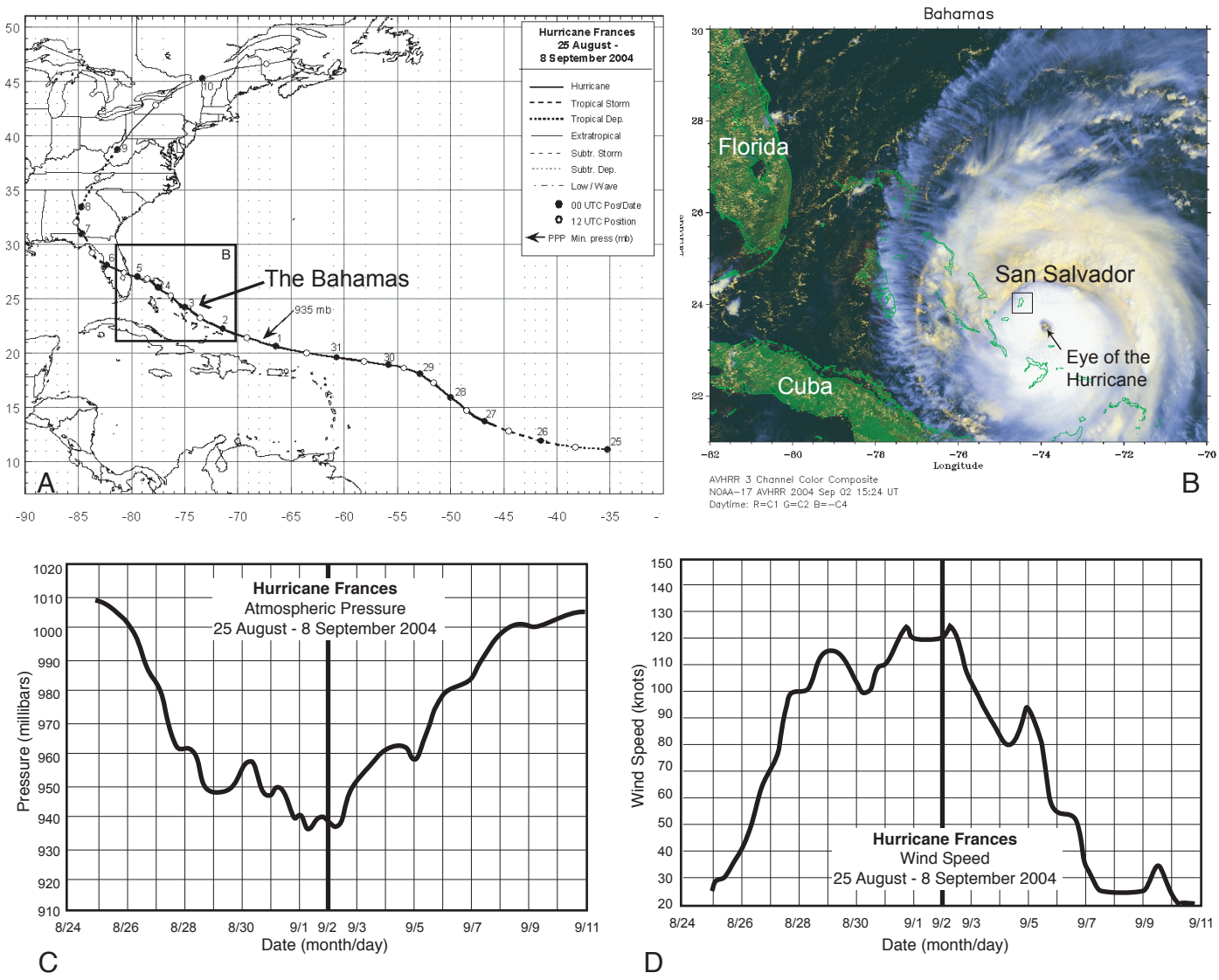

Figure 1. A) Storm track of Hurricane Frances from 25 August to 8 September, 2004. The numbers along the track mark the days. The storm reached its lowest barometric pressure and Category 4 hurricane status on September 1, 2004. Hurricane Frances struck most of the Bahamian Islands as a Category 3 hurricane and Florida as a Category 2 hurricane. The location of Figure 1B is outlined. (Source of image: Beven, 2004). B) NOAA-17 satellite Advanced Very High Resolution Radiometer (AVHRR) three channel color composite daytime image of Hurricane Frances as it approached San Salvador on 2 September 2004 at 15:24 UT. Image used by permission and courtesy of Dr. Steven Babin and Ray Sterner of The Johns Hopkins University Applied Physics Laboratory (http://fermi.jhuapl.edu/hurr/04/frances/index.html). C) The National Weater Service's National Hurricane Center published its best track of the barometric air pressure changes of Hurricane Frances (Beven, 2004). Hurricane Frances struck the island of San Salvador on 2 September 2004 when the storm was near its barometric lowest pressure. D) The National Hurricane Center's best track for the maximum wind speed of Hurricane Frances (Beven, 2004).

road in places (Curran et al., 2001). In Cockburn Town, the dock was heavily damaged and further damage occurred to homes and buildings adjacent to the beach. Walker et al. (2001) documented damage to the Cockburn fossil reef exposure. The town cemetery was also severely damaged. Along most of the western shore and on Coast Guard Beach, severe erosion led to the development of a scarp with a maximum height of 1.8 m (Curran et al., 2001).

In this paper we focus on documenting the height of the storm surge, overwash deposition, and beach accretion and erosion processes caused by Hurricane Frances on the island of San Salvador. We concentrated our field investigations on the southeastern coast of the island from Dim Bay to French Bay where the hurricane made initial landfall (Figures 2 and 3).

ANALYSES OF SATELLITE IMAGERY

Our goals in analyzing satellite images taken before and after Hurricane Frances were to determine the extent of the areas damaged by the hurricane and to identify locations where detailed field investigations could be conducted to measure the storm surge impact. Figure 2 shows panchromatic images (Band 8) of San Salvador acquired by the Landsat 7 Enhanced Thematic Mapper Plus from before the storm on August 30, 2004 and after the storm on October 1, 2004. The spatial resolution of the images is 15 m. Black lines are a result of an instrument failure of the satellite's Scan Line Corrector that occurred on July 14, 2003 and extends to all images acquired to the present date. The lines show the original data gaps which gradually diminish in width toward the center of the scene. The GeoTIFF image files were radiometrically and geometrically corrected by the provider. The scene was plotted using Leica Geosystems' ERDAS Imagine and ESRI's ArcView products. Points for discussion are labeled on Figure 2.

Sandy Point (labeled point "a") is the southwesternmost extension of the island. A visual comparison of the pre- and post-Hurricane Frances images shows a pronounced reduction in the width of the Sandy Point beach. The onshore and offshore movement of sand and its control on beach width is a seasonal phenomenon. The beach narrows during the rainy season months of high intensity storms during September through November when erosion causes removal of sand and a scarp to form in the back beach area. The beach widens during the dry season months of December-August when sand deposition and beach bar accretion dominates the sedimentary processes. This has been previously documented for Sandy Point by repeated beach profiling (*e.g.* Loizeaux et al. 1993; Beavers et al., 1995; Curran et al., 2001). We also observed a very narrow beach and ~2-m-high erosional beach scarp at Sandy Point in March 2005 lasting well into the dry season. This observation indicates that Hurricane Frances and likely Hurricane Jeanne caused extensive erosion on this beach that had not yet recovered six months after the storms. Wide beaches were observed at Sandy Point in March 2007.

The Gulf is located on the southern part of the island where deep water lies close to the shoreline. The location of point "b" on Figure 2 shows the area where storm surge overwash inundated the southern part of Pigeon Creek. Comparison of the satellite images before and after Hurricane Frances shows that the width of the beach (zones of bright reflections) has narrowed. This is largely due to the massive movement of blocks and boulders of bedrock landward caused by the storm surge.

Low Cay is marked as point "c". Comparison of the images in Figure 2 show that the vegetated area of the island was sharply reduced by the hurricane. Large areas of defoliated vegetation and re-deposited sand are noted on the eastern side of the island.

The Pigeon Creek tidal inlet is labeled as point "d". The beach south of the inlet down to the southeastern point is known as Sandy Hook. The satellite data confirm that the east face of Sandy Hook was significantly altered by the Hurricane Frances storm surge. The beach has narrowed by processes of vegetation and removal at

Table 1: Saffir-Simpson Hurricane Scale

Category	Wind Speed	Barometric Pressure	Storm Surge	Damage Potential
Tropical Depression	< 39 mph < 34 kts			Minimal
Tropical Storm	39 - 73 mph 34 - 63 kts			Minimal
Hurricane 1 (Weak)	74 - 95 mph 64 - 82 kts	28.94" or more 980.02 mb or more	4.0' - 5.0' 1.2 m - 1.5 m	Minimal damage to vegetation
Hurricane 2 (Moderate)	96 - 110 mph 83 - 95 kts	28.50" - 28.93" 965.12 mb - 979.68 mb	6.0' - 8.0' 1.8 m - 2.4 m	Moderate damage to houses
Hurricane 3 (Strong)	111 - 130 mph 96 - 112 kts	27.91" - 28.49" 945.14 mb - 964.78 mb	9.0' - 12.0' 2.7 m - 3.7 m	Extensive damage to small buildings
Hurricane 4 (Very strong)	131 - 155 mph 113 - 135 kts	27.17" - 27.90" 920.08 mb - 944.80 mb	13.0' - 18.0' 3.9 m - 5.5 m	Extreme structural damage
Hurricane 5 (Devastating)	> 155 mph > 135 kts	< 27.17" < 920.08 mb	> 18.0' > 5.5m	Catastrophic building failures possible

The Saffir-Simpson Hurricane Scale defining the category of hurricanes based on wind speed in miles per hour (mph) and knots (Kts), barometric pressure in inches (") and millibars (mb), the resultant storm surge height in feet (') and meters (m) and description of damage potential. Source of Table: http://meta1.srcc.lsu.edu/OEP/hurr_scale.html.

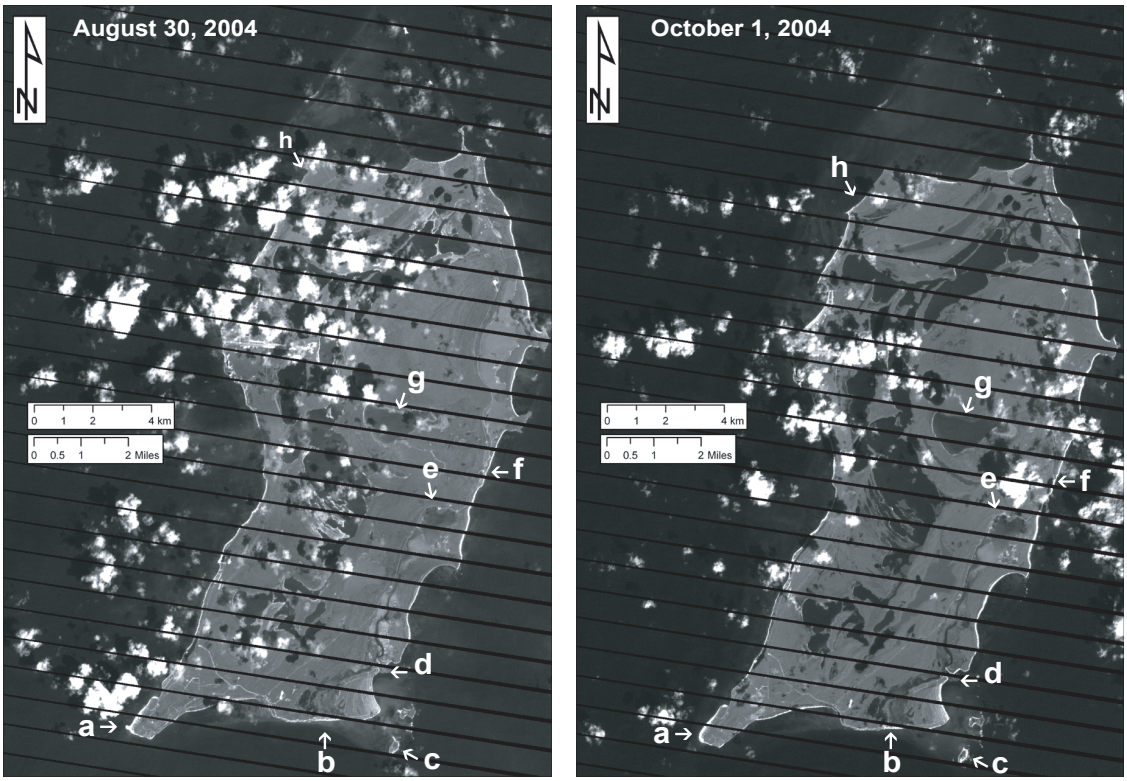

Figure 2. Panchromatic images (Band 8) of San Salvador acquired by the Landsat 7 Enhanced Thematic Mapper Plus from before Hurricane Frances (left; August 30, 2004) and after (right image; October 1, 2004). Cloud cover shown as white spots. Image is annotated for special sites of interest: a=Sandy Point; b= The Gulf; c=Low Cay; d=Pigeon Creek inlet; e=north Pigeon Creek; f=Salt Pond; g=inland lake area; h=north Rocky Point. See text for discussion.

its northern end and slightly widened by sand deposition along the southern end.

The northern end of the Pigeon Creek estuary is marked with the letter "e". The storm caused water to overtop the banks of this water body. The overwash deposition is shown as areas of bright reflections on the October 1, 2004 image (Figure 2).

Point "f" on Figure 2 is the location of Salt Pond. Like the other inland lakes, the levels of Salt Pond rose after the hurricane. The width of the de-vegetated beach also widened north of point "f".

One of the most pronounced differences between the August 30th and October 1st images is in the water level of the interior lakes. Point "g" on Figure 2 highlights only one of the many lakes. This lake is called Granny Lake. On the August image, the bright outlines around the lake mark the lowstand shoreline exposing the un-vegetated lake margins. Lake levels are markedly lower in all the lakes compared to the October 1 image. Hurricane Frances brought 5.47 inches (139 mm) of rain to San Salvador (Beven, 2004).

Other parts of San Salvador experienced impacts from Hurricane Frances. At point "h" on Figure 2, overwash sand deposition was noted in the field. This location is north of Rocky Point. It is likely that other locations along the west and northeast shore of the island were impacted by the hurricane. We, however, did not have an opportunity to study those areas. Data for Hurricane Frances storm surge height along the east, west, and southwest parts of the island, as well as a survey of damage to structures is found in Parnell et al. (2004).

SUMMARY OF FIELD OBSERVATIONS

This research focuses on investigations on the southeastern side of San Salvador, including sites at Salt Pond and south Storr's Lake, the eastern beach area around and south of The Thumb, the north Pigeon Creek area, the Pigeon Creek inlet, Sandy Hook, and the Gulf (Figure 3). These locales were chosen based on analyses of satellite imagery and discussions with Vincent Voegeli who was at the Gerace Research Station at the north end of the island at the time of the hurricane.

Field study of the sites was conducted during March 4-11, 2005. We measured beach profiles at points where the maximum storm surge washover height could be determined using the Emery method (Emery, 1961; Kraus, 2004) with a hand level and a 1.5 m high stadia rod divided into 10 cm and 2 cm increments. The Storr's Lake site profile was measured in March 2005 with the horizontal distance recorded at each major inflection points rather than at every 2 m. The beach profiles at the 'Thumb' and the stratified trash locations were measured in January 2008. The distance from high tide to areas of interest of beach erosion and accretion were measured using the pace method and by tape measure. The following discussion summarizes our observations at each of the field sites.

Salt Pond and Storr's Lake Area

A stretch of low-lying coastal dunes with a height of 3 m or less borders the eastern shore of San Salvador island between the south end of Storr's Lake to the north end of Pigeon Creek. Examination of the 1:10,000 topographic map of this region (Figure 4B) clearly shows two areas of topography lower than the 10-foot contour along this eastern shore. The abandoned Fortune Hill settlement area lies adjacent to these low sand dunes between Storr's Lake and Salt Pond (Figure 3). The Hurricane Frances storm surge overwashed the coastal dunes and defoliated the vegetation along a 300 m length of this shoreline (Figure 4). This is one of the largest areas of washover from the storm that we surveyed. The Sandy Hook area on the southeast section of the island also experienced extensive washover.

Salt Pond. Salt Pond is a small, shallow coastal lake with a highly variable salinity. In general during the rainy months in the Bahamas between May and October (Shaklee, 1996), freshwater input causes the lake level to rise and

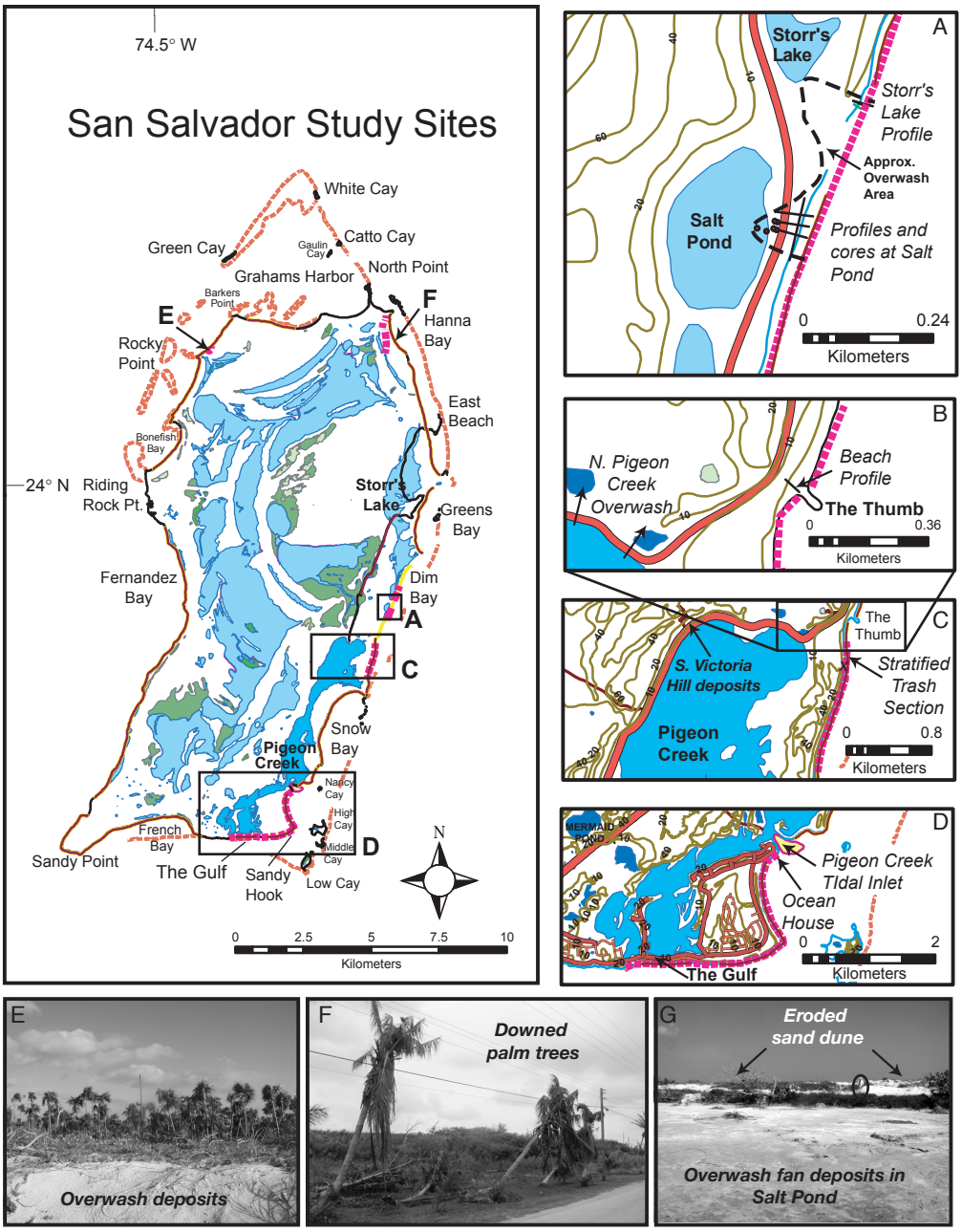

Figure 3: Map showing sites on the island of San Salvador, The Bahamas where damage from Hurricane Frances was documented in this study. Images are plotted from the GIS database of R. Laurence Davis and Matthew C. Robinson (1999, University of New Haven). A) Location of the overwash fan in Salt Pond and Storr's Lake and storm surge profiles and cores. B) Detailed map of 'The Thumb' showing location of beach profile. The overwash from north Pigeon Creek is also labeled. C) Map showing the location of storm surge height profiles at The Thumb and stratified trash section. D) Detail of the southeast section of San Salvador showing the location of Ocean House at the Pigeon Creek tidal inlet and overwash deposits at 'The Gulf'. E) Hurricane Frances also caused overwash deposition along the northwest part of the island. View toward the southeast. F) Four palm trees were blown down onshore of Hanna Bay. View toward the southeast. G) Photograph of the overwash fan deposits in Salt Pond viewed toward the east. The beach barrier sand dune was stripped of vegetation and eroded. Oval outlines a person for scale.

reduces the water salinity. These months roughly correspond to the Atlantic basin hurricane season from June to November. During the drier months, evaporation exceeds freshwater inflow and Salt Pond lake levels fall and salinity rises. Yannarell et al. (2007) report values for the water salinity in Salt Pond before and after Hurricane Frances. The salinity of Salt Pond on August 30, 2004 was hypersaline with a value of 280 PSU (practical salinity units). On September 9, 2004, after the storm, Salt Pond water salinity dropped to 60 PSU—levels that approach the salinity values for Caribbean seawater at 35-40 PSU (Yannarell et al., 2007).

Salt Pond is protected from marine water incursion from the Atlantic Ocean by a coastal sand-dune barrier. The width between Salt Pond and the ocean is narrow; measuring only 50 m wide. The Salt Pond basin is separated from the Storr's Lake basin to the north by bedrock that is exposed along the northeast shore of the lake.

The storm surge of Hurricane Frances eroded the coastal dune and washed sediment and water into Salt Pond. Most of the vegetation along a 70 m length of the coastal dune was stripped off (Figure 3G). Large rooted plants were overturned. Whole shrubs were transported into the Salt Pond basin. In early March 2005, lake levels had retreated and had exposed the overwash fan of sand that was deposited in Salt Pond (Figure 3G). We measured a maximum thickness of 12 cm of overwash sand in Salt Pond from cores and trenches excavated on the exposed fan. The maximum thickness of sand overwash deposition is likely to have been thicker depending on where sampled. Vincent Voegeli (pers. comm., 2005) reported that at least 8 inches (20 cm) of sand was deposited over the road adjacent to Salt Pond. Description of the Hurricane Frances overwash deposits in Salt Pond is the subject of a companion paper in this volume (McCabe and Niemi, 2008). Also in this volume, a paper by Park et al. (2008) presents a longer record of hurricane deposition and faunal changes in Salt Pond based on analyses of sediment cores from the center of the lake.

Storr's Lake. Paralleling nearly 7 km of the eastern shore of San Salvador, Storr's Lake can be divided into three sub-basins (Figure 3). The lake has a small south basin located just north of Salt Pond. This south basin is connected to the central Storr's Lake basin through a narrow channel. The central basin extends from the latitude of Dim Bay to Greens Bay. A channel also connects this central basin to the large north basin of Storr's Lake. Storr's Lake is likely to have once been a tidal creek or estuary directly connected to the ocean through a tidal inlet at its south end that is now closed.

The Hurricane Frances storm surge inundated the area landward along approximately 300 m of the shoreline between Salt Pond in the south to Storr's Lake in the north. Most of the foliage was stripped from the coastal vegetation in the area of the storm surge washover (Figure 4A). Deposition of the storm surge sand, flotsam and jetsam, and organic debris can be traced along this entire area. At the south end of Storr's Lake (Figure 4C), the coastal dune was breached and a blanket of sand was deposited as an overwash fan into the lake basin (Figure 4D). A second overwash into the central basin of Storr's Lake occurred at the north end of Dim Bay (Figure 4E and 4F).

The maximum storm surge was identified by flotsam and jetsam on the sand dune crest that separates Storr's Lake from the Atlantic Ocean. We measured a maximum storm surge height of 4.8 m at this location. The east-facing portion of the dune along Dim Bay to its northern limit has been stripped of vegetation and eroded leaving a steep east-facing scarp. The storm transported boulders inland and deposited them in an imbricated pattern dipping east (seaward). These large imbricated slabs line the base of the sand dunes along this eastern shore (Figure 4F) and likely represent an accumulation of numerous storms in addition to Hurricane Frances.

The Thumb Area

Along the east coast of San Salvador just north of Pigeon Creek there is a southeast-trending tombolo locally known as 'The Thumb' (GPS coordinates: 2655774N, 555390E). The

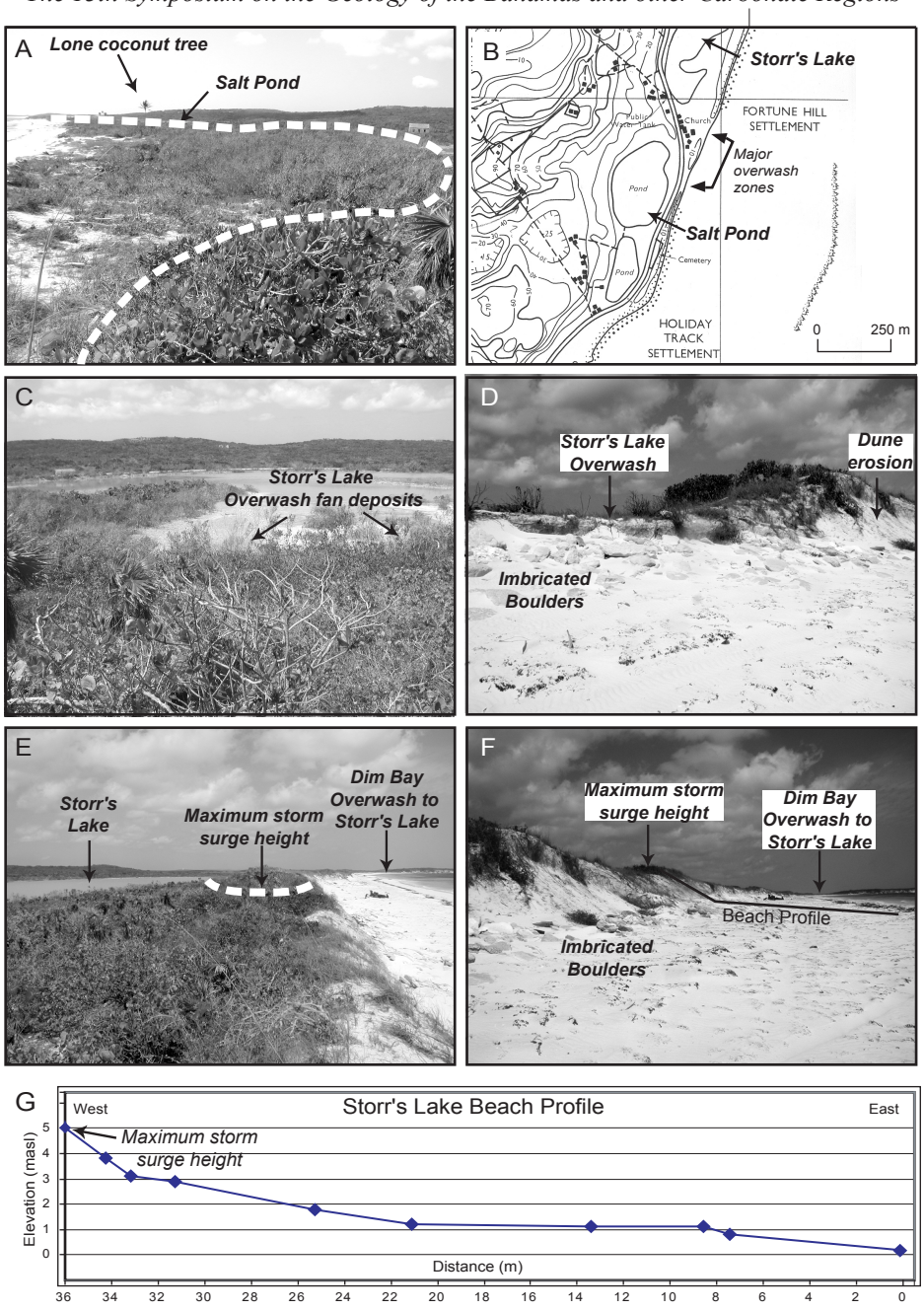

Figure 4:Photographs of Hurricane Frances storm surge damage in the Fortune Hill Settlement area between Storr's Lake and Salt Pond. A) View south from Storr's Lake showing area of extensive washover and defoliated vegetation. B) A portion of the 1:10,000-scale topographic map showing the area around Salt Pond. C) The south end of Storr's Lake showing the overwash fan deposits. Vegetation in the foreground is defoliated. (View west). D) View northwest toward Storr's Lake showing the overwash breach, eroded dunes, and storm deposited imbricated boulders at the base of the sand dune. E) View north along the sand dune crest that separates Storr's Lake from the Atlantic Ocean. The location of the maximum storm surge height is marked. F) The eroded eastern side of the coastal sand dunes viewed north along Dim Bay. The maximum storm surge was identified by the upper limit of flotsam and jettsam deposited on the sand dune. G) Beach profile showing maximum storm surge height (4.8 m). Location of profile in F.

rock outcrop is composed of the Pleistocene-aged Owl's Hole Formation (Carew and Mylroie, 1995) and is connected to the beach by sand. The coastal bluffs are 7-8 m high from the Thumb southward until the point called 'The Bluff' at the north end of Snow Bay where they reach 12 m in height (Figure 3). The offshore fringe reef along this section of coastline is discontinuous. This section of San Salvador appears to have experienced the full force of Hurricane Frances. We studied two sites—the Thumb and a location 540 m to the south.

The Thumb. An areally expansive deposit of flotsam and jetsam has accumulated along the southwestern side of the spit and sand dune connecting the Thumb to the shore (Figures 5A and 5B). The debris includes ropes, buoys, plastics of all types, and what appears to be a portion of a large navigation buoy. A maximum Hurricane Frances storm surge height of 4. 9 m was measured at this location by leveling to the upper limit of the flotsam and jetsam.

The beach profile at this site shows one distinct terrace level (terrace 1; Figure 5F). Hurricane Frances and previous storm debris are concentrated on terrace 1. This terrace is a flat surface covered predominantly by grass that lies at an approximate elevation of 2 to 2.5 m above mean sea level. Below terrace 1 is the active beach berm that is characterized by sparely vegetated dunes and remobilized storm debris.

The bedrock outcrop of the Thumb is marked at its base by a prominent wave-cut notch (Figures 5C and 5D). This notch formed at mean sea level by erosion from wave action during the normal high and low tidal range. The weathered craggy outcrop above the notch is strewn with nets and ropes across the entire exposure indicating complete submergence of the bedrock knob during the hurricane storm surge and in previous storms. Two recognizable terrace levels can be seen in the bedrock profile (Figure 5D). The lower terrace A is a zone of bare rock outcrop formed about 1-2 meters above the notch. The upper flat terrace B is vegetated. This vegetation has been defoliated by the storm surge.

We surveyed the reef in the vicinity of the Thumb by snorkeling. An example of the state of the patch reef located just southeast of the end of the tombolo is seen in the underwater photograph of Figure 5E. The reef shows signs of damage with broken and overturned blocks. There are numerous entangled ropes, nets, and other debris caught in the reef. The entangled debris was likely brought to this and other sites along the eastern shore of San Salvador not just by Hurricane Frances but during numerous storms of lesser intensity that deliver trash entrained in currents of the North Atlantic gyre to this windward side of the island.

Stratified trash site. Approximately 540 m south of the Thumb is a locale we called the 'stratified trash site' (GPS coordinates: 2655236N, 555286E) where the storm surge deposits from the 2004 Hurricane Frances and other hurricanes or storms are visible.

We measured a beach profile at this site (Figure 6E) that shows three terrace levels. The maximum storm surge height of Hurricane Frances at this location based on the upper elevation of flotsam and jetsam was measured at a height of 5.5 m. A heavy accumulation of Frances storm surge debris is also noted across the lower terrace 1. Terrace 1 lies at an elevation of about 3 to 3.5 m above mean sea level. It is broadly equivalent to the low terrace observed at the Thumb but at a slightly higher elevation. The terrace is vegetated predominately with coastal grass. Two upper, higher terraces (labeled terrace 2 and terrace 3) are stablized with thick vegetation and trees. One lower bench in the profile is a storm berm formed after Hurricane Frances.

Erosion of the back beach area exposed a 170-cm-thick stratigraphic section that marks the eastern edge of terrace 1. The section (Figures 6C and 6D) contains a lower 50-cm thick section of aeolian sand overlain by 40-cm-thick layer of trash and storm debris. The section is capped by an 80-cm-thick bed of aeolian sand. The top surface of the section is the grass-vegetated terrace 1 surface. The stratified trash indicates that debris from a previous storm or hurricane was deposited

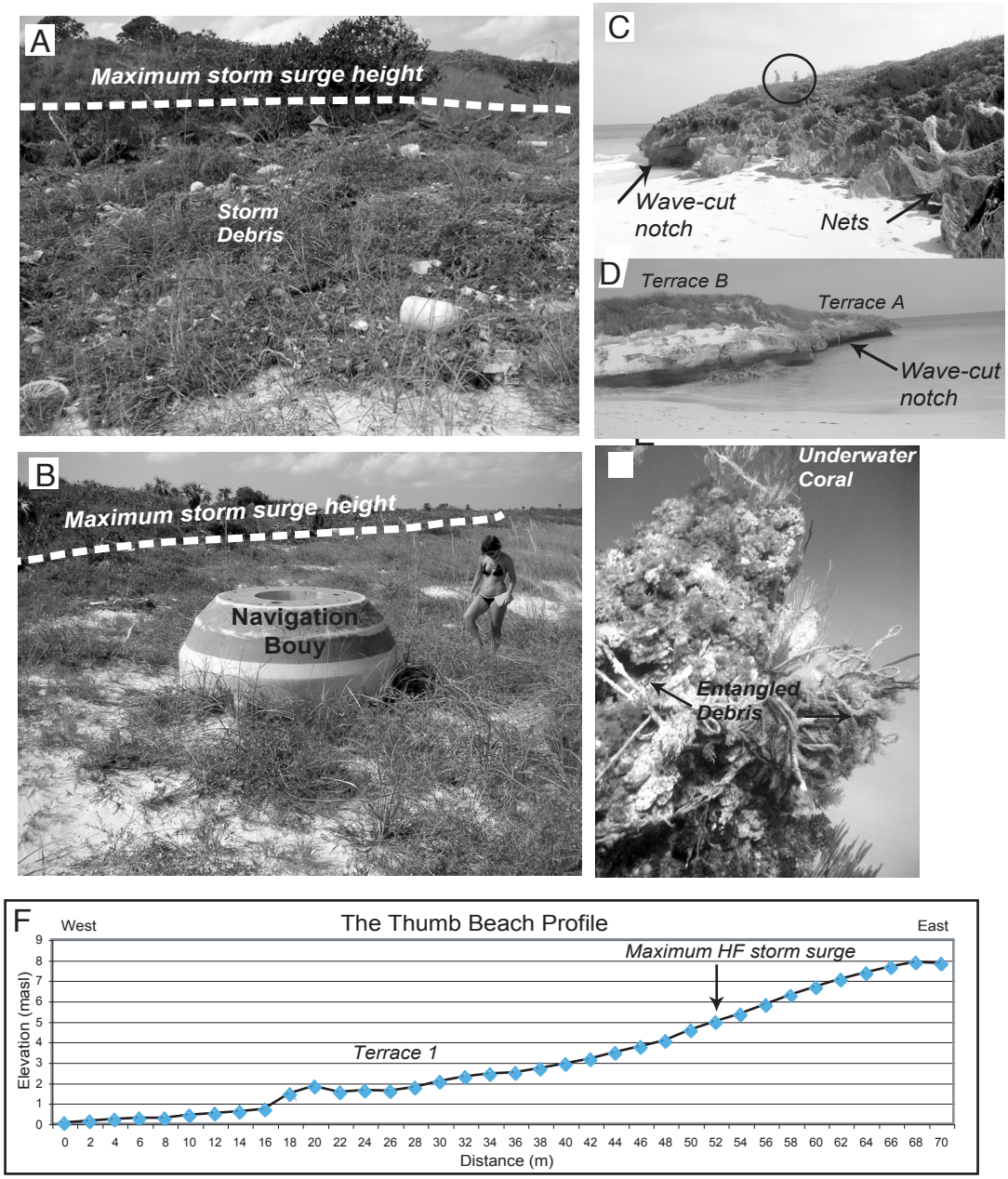

Figure 5: The Thumb is a southeast-trending tombolo located along the east coast of San Salvador (see Figure 3 for map location). A) Photograph of the large amount of flotsam and jetsam accumulated along the southwestern side of the spit and sand dune connecting the Thumb to shore. View to the west with the maximum storm surge height marked. B) View northward of the debris collected on the coastal dunes showing the maximum height of debris marking the storm surge height. C) The bedrock outcrop of the Thumb is marked at its base by a prominent wave-cut notch. The weathered craggy outcrop is strewn with nets and ropes across its height indicating submergence of the bedrock knob during the hurricane. View to the west. Circle marks two persons for scale. D) View of the south side of the Thumb showing the wave-cut notch and two terrace levels. The vegetation has been defoliated by the storm surge. E) Underwater photograph of a patch reef just to the southeast of the end of the tombolo showing damaged reef with numerous entangled ropes, nets, and other debris. F) Beach profile from the base of The Thumb on the west to the top of the coastal ridge on the east. The position of the maximum Hurricane Frances (HF) coastal debris from the storm surge is marked at a height of 4.9 m.

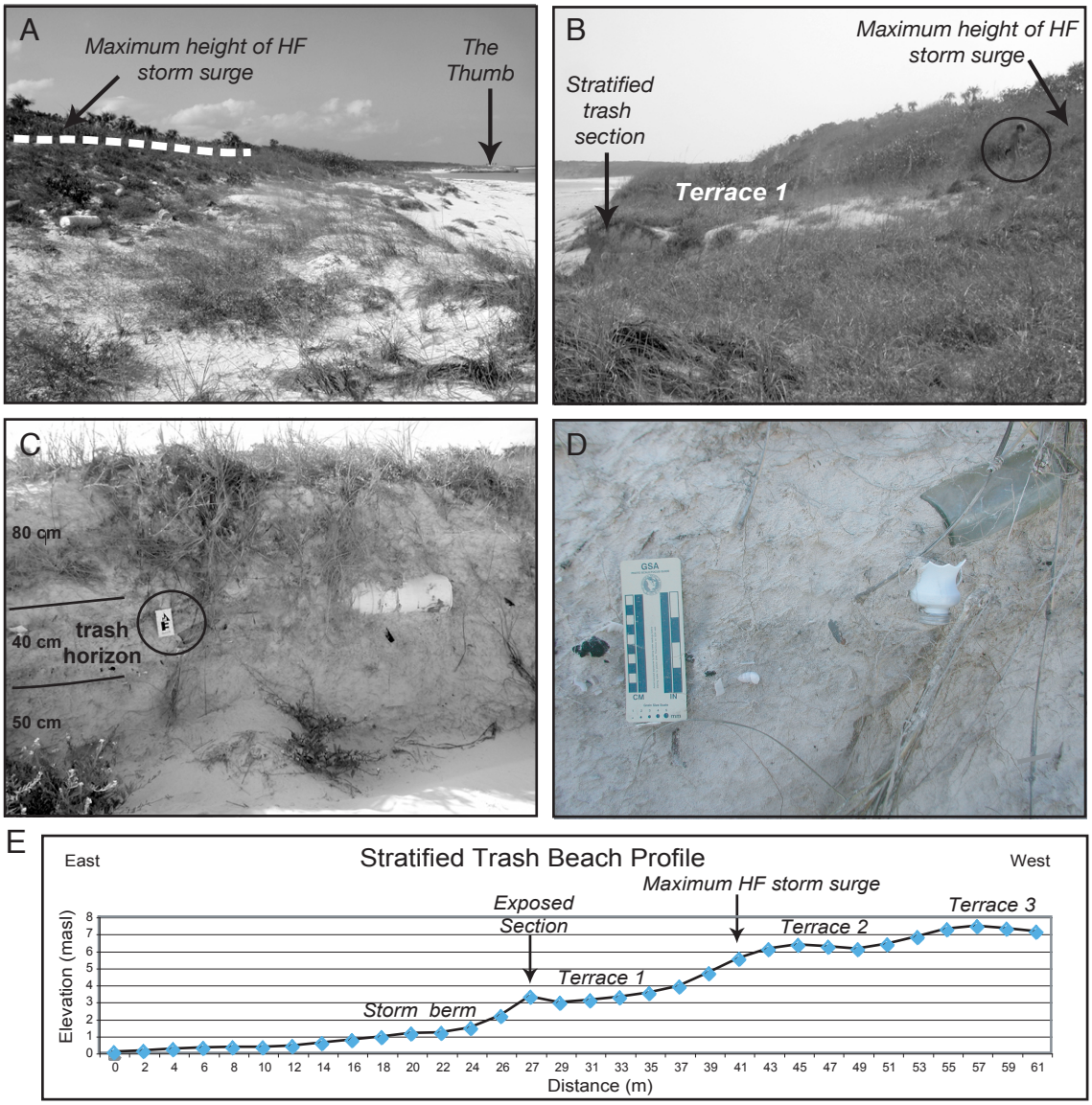

Figure 6. Photographs of storm surge deposits from the 2004 Hurricane Frances and other hurricanes along the beach south of The Thumb. A) View north showing the trash deposited from the storm surge. B) The Hurricane Frances storm surge deposited flotsam and jetsam across terrace 1 to a maximum height of 5.5 m. The circle marks a person for scale. View toward the south. C) Erosion of the backbeach dune exposed a 170-cm-thick stratigrapic section showing storm debris from a previous event interbedded with aeolian sand. Scale within the circle is 15 cm. D) Detailed view of the stratified storm deposit showing plastic fragments and objects, charcoal, a glass bottle, a light bulb and other trash. E) Beach profile showing the maximum storm surge height of Hurricane Frances (HF) based on the upper elevation of flotsam and jetsam. The stratified trash section in photos C and D marks the eastern edge of Terrace 1. One lower bench in the profile is the post-hurricane accumulation of a storm berm. Two upper, higher terraces (labeled terrace 2 and terrace 3) are stablized with thick vegetation and trees. Location of the beach profile is shown in Figure 3D.

in this back-beach berm and then subsequently buried by windblown sand. A close-up photograph of the stratified storm deposit shown in Figure 6D highlights the various objects found in the tempestite including plastic materials of all types, charcoal, a glass bottle, a light bulb, and other trash (Figure 6D). The exposed stratigraphic section indicates that terrace 1 was built from deposition of previous storm events and modified by aeolian deposition. At this location Hurricane Frances deposits were found at higher elevations. These data suggest that the Hurricane Frances storm surge may have been more intense than the previous storms that hit the island in the recent past.

North Pigeon Creek and the Southeast Areas

Along the southeast end of the island generally paralleling the shoreline, there is a northeast-southwest trending water body that is known as Pigeon Creek. This water body is a tidal estuary that contains three shallow basins (south Pigeon Creek, central Pigeon Creek, and north Pigeon Creek) developed around a tidal channel (Figures 2 and 3). The tidal channel leading to the south basin of the Pigeon Creek estuary opens to the Atlantic Ocean through a tidal inlet. Because of the connection to the ocean, Pigeon Creek experiences tides. There is a lag period between the coastal high and low tides and the tides in Pigeon Creek due to the delay in flood and ebb through the inlet. The Pigeon Creek tidal inlet is located about 1.5 km north of the southeast point of the island called Sandy Hook (Figure 3D). Sediment flushing out of Pigeon Creek through the tidal inlet has formed a shallow sandy tidal flat within Snow Bay. The bay is protected from intense wave action by a line of offshore islands—Nancy Cay, High Cay, Cay, Middle Cay, and Low Cay (Figure 3).

Our investigation of Hurricane Frances storm deposits and sites of erosion and damage concentrated on three different regions around Pigeon Creek (Figure 3):

(1) The storm surge caused water to spill out the debris pile have their source in a line of coco- of the north end of Pigeon Creek in the vicinity of the South Victoria Hill Settlement and to the northeast (Figure 7).

(2) At the tidal inlet of Pigeon Creek and south along the shore of Sandy Hook, beach erosion was prevalent (Figure 8).

(3) And along the south end of Pigeon Creek in the area called 'The Gulf', the Hurricane Frances storm surge caused coastal erosion and overwash into the estuary (Figure 9).

North Pigeon Creek. Along the northern end of Pigeon Creek (Figure 3C), water overtopped the normal shoreline leaving a line of debris marking the high water mark. At the northeast corner of the estuary, water surged out of the lake causing defoliation of vegetation and an overwash into two small ponds located north of the road (Figure 3B). In the area of the abandoned South Victoria Hill settlement, the maximum high water level was marked by a 1- to 2-m-wide debris pile that ringed northwest Pigeon Creek about 15-20 m inland of the normal shoreline (Figure 7).

We hand dug a trench through the debris pile at a site (GPS coordinates: 24° 00.726 N, 074° 28.250 W, with an elevation of 3 m) just south of the extant buildings of the settlement and south of the pier (Figure 7). The debris pile is made almost entirely of organic matter. A stratigraphic section drawn through the 33-cm-thick debris pile (Figure 7D) shows four layers. The upper 10 cm was largely leaves, palm fronds, sticks, roots, coconuts, and other vegetative matter overlying a 5- to 7-cm-thick mixed layer of leaves and composted organic debris. These upper layers rest on a moist thin layer of compost and a basal layer composed of medium-grained sand mixed with decayed organic matter.

It is clear that during the six months between deposition of the storm debris and the time of these observations that the material had already heavily decayed. There was a noticeably absence of any material other than sand and organic debris. No plastic debris or other man-made materials were present. The large number of coconuts in nut palm trees that grow along the east side of the

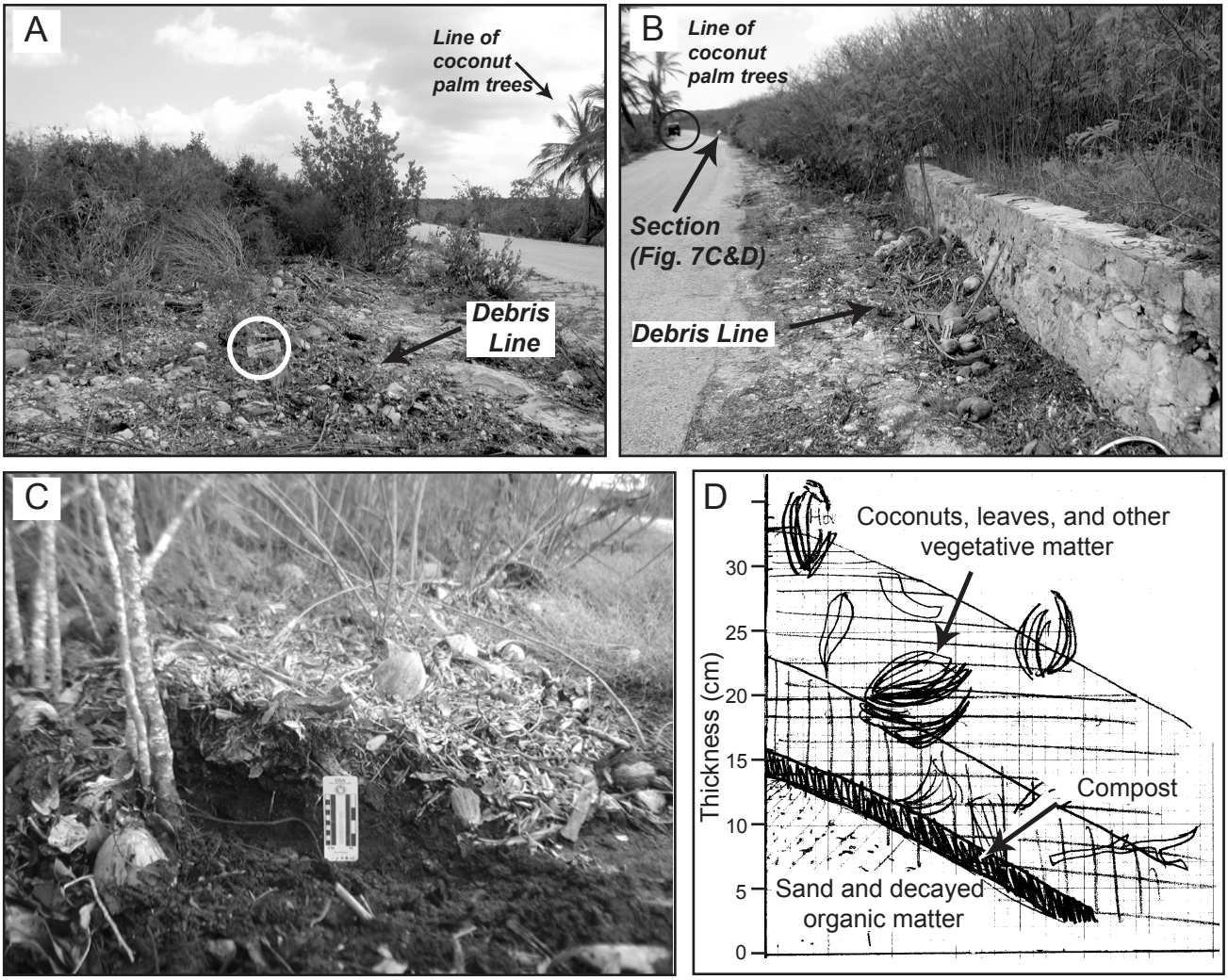

Figure 7. Water overtopped the normal shoreline of the northern end of Pigeon Creek leaving a largely organic debris pile marking the high water mark. (See Figure 3 for location map). A) View north showing the debris line on the west side of the road in the South Victoria Hill Settlement area of north Pigeon Creek. Circle outlines 10 cm photographic scale. B) View south showing the organic debris high water line east of the road and against an old wall of the South Victoria Hill Settlement area. Circle outlines a vehicle for scale. C) Hand-dug section exposure through the debris pile. The large number of coconuts in the debris are derived from a line of palm trees located on the east side of the road. View toward the north. D) Stratigraphic section drawing through the debris pile. The organic material is predominantly palm, mangrove, and other leaves, sticks, coconuts and other organic material that has decayed and composted. Drawing by Tani Sutherland.

road at this location (Figure 7). The other organic matter also has a local source. The mangrove and coastal vegetation surrounding this area of Pigeon Creek has been visibly defoliated. The stripped leaves were deposited in the debris pile.

The appearance of coconuts sitting within a composting debris pile suggests that over time new coconut trees should germinate and take root along the line marking the high water level. Under ideal conditions of moisture and temperature, a coconut should germinate within three to six months (Watson, 1996). As we have observed coconuts among the other flotsam and jetsam marking the Hurricane Frances storm surge deposits as high as 5 m above the shoreline, we hypothesis that coconut palm trees found at higher elevations may mark prior hurricane storm surge deposits. This is particularly true for the lone coconut tree (Figure 4) observed between Salt Pond and Storr's Lake.

Pigeon Creek tidal inlet. The southeast point on the island of San Salvador is called Sandy Hook (Figure 3). Analyses of the Thematic Mapper Satellite image from October 1, 2004 (Figure 2) shows that the east-facing beach of Sandy Hook experienced erosion of coastal vegetation, inland deposition of coastal sediment and accretion of beach sediment. We surveyed the area just south of the mouth of Pigeon Creek at its tidal inlet and at one site about 750 m north of the point to assess the hurricane damage and document the changes in the coastal environment.

The vegetation line at Sandy Hook has retreated about 40 m from its pre-Hurricane Frances position. To the south of the eroded beach, there was accretion. Analysis of satellite images from August and October 2004, we were able to determine this accretion to be about 30 m.

At low tide an area is exposed that measures about 70 m wide that contains remnants of mangrove roots and plants (Figure 8 A-C). Boulders are strewn over the surface. Some areas show signs that they have been newly exposed based on the lack of surface weathering. Examination of the satellite imagery from before (August 30, 2004) and after (October 1, 2004) Hurricane Frances clearly shows that the width of non-vegetated coastline has about doubled (Figure 2). This increase in width of the coastal zone is mostly likely due to the removal of coastal vegetation and deposition of sand and boulders inland.

Large slabs of rock ripped up from the surf zone have been transported inland. The boulders are stacked with a dip toward the east. This imbrication indicates the boulders were transported to the west. The boulders were of local origin. Individual slabs could not be traced back to their original location. Ten large boulders were measured and are recorded in Table 2. The maximum length of the boulders is nearly 1 m (98 cm) and the average length of the boulders measured is 77 cm. If we assume that the classic Hjulstrom diagram that plots relationship between the stream velocity necessary to transport a particle of a given diameter is applicable to wave storm surge velocities, then a particle with an average length of 77 cm would require a water velocity in excess of 600 cm/s.

Table 2: Measurements of large boulders imbricated along the back beach region of Sandy Hook.

Length	Width	Height
65 cm	60 cm	15 cm
75 cm	73 cm	12 cm
68 cm	50 cm	18 cm
43 cm	42 cm	22 cm
91 cm	70 cm	17 cm
95 cm	57 cm	15 cm
72 cm	50 cm	12 cm
98 cm	56 cm	19 cm
90 cm	47 cm	20 cm
72 cm	70 cm	5 cm

There was evidence of past imbrications, aligned in the same orientation as the boulders from Hurricane Frances. These boulders are seen in the background of Figure 8A and 8C and are covered with a black patina from algae, implying that these boulders are part of the supratidal zone (Hinman, 1994), and were transported in previous storm surge events.

One of the structures that sustained significant damage during Hurricane Frances is lo

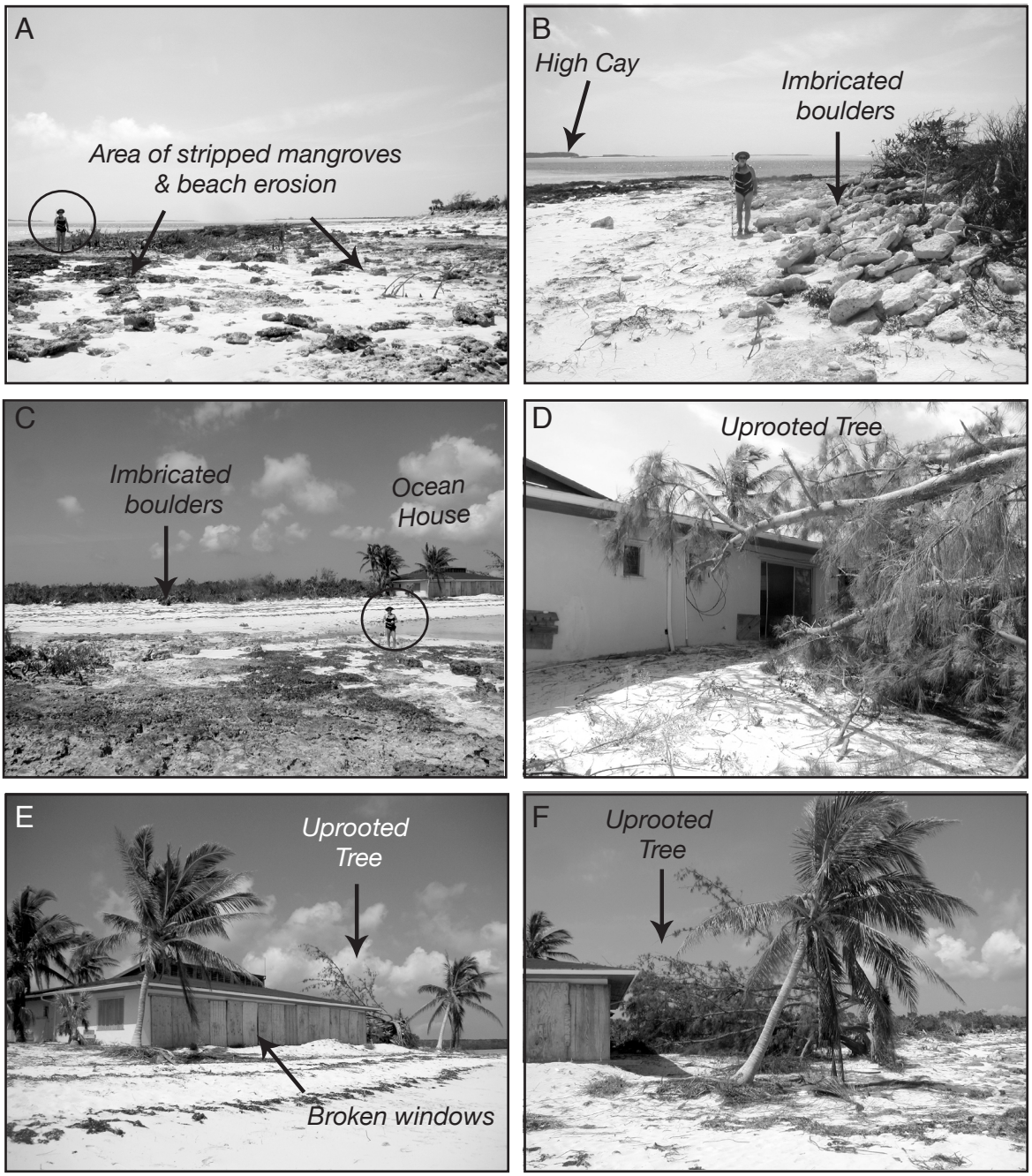

Figure 8: Erosion and hurricane damage to Ocean House located at the tidal inlet of Pigeon Creek on the southeast side of San Salvador Island (See Figure 2 and 3 for map location). A) View south across the area of stripped mangroves and beach erosion. B) Imbricated boulders stacked along the back beach area. View southwest with High Cay island in the background. C) View northwest across the eroded platform that was stripped of mangroves. Ocean House in the background. Person for scale. D) Uprooted Australian pine tree (Casuarina equisetifolia) on the north side of Ocean House. E) View north showing the damaged Ocean House. F) View west of a tilted palm and toppled Australian pine tree.

cated at the Pigeon Creek tidal inlet. This property is known as Ocean House and is shown in Figure 8. The house was built without pilings and just above sea level. The windows throughout the house were knocked out and the storm surge is likely to have swept through the structure. An Australian pine (*Casuarina equisetifolia*) tree on the north side of the house was uprooted and fell toward the house.

The Gulf. The south end of the island of San Salvador extends from a point on the west called Sandy Point that protects French Bay from westerly and northwesterly winds to a point on the east called Sandy Hook. Very deep water and the fringe reef wall are located about 25 m from the shore along the eastern side in an area known as "The Gulf" (Figure 3). Because of the very narrow shelf, wave action is intense and the beach is rocky.

The width of the coast along the Gulf between the Atlantic Ocean on the south and the southern end of Pigeon Creek is very narrow measuring only about 75 - 100 m. We documented several locations with a series of photographs showing the effects of Hurricane Frances along the coastal zone of the Gulf. Large slabs of bedrock are broken and imbricated with slopes toward the south the result of numerous storms that batter the coast (Figure 9A). Some boulders larger than 1 m in length were transported as much as 50 m inland and were deposited along the road (Figure 9B). The storm surge came on shore and stripped the coastal vegetation of foliage. Sand, vegetation, and flotsam and jetsam were deposited on the coastal road (Figure 9C). At two locations, sand and other storm debris washed into the south end of Pigeon Creek forming an overwash fan (Figure 9D).

DISCUSSION AND CONCLUSIONS

Hurricane Frances was a strong Category 4 hurricane that directly struck San Salvador on 2 September 2004. The storm made landfall on the island at 3:00 p.m. (EDT) along the southeast side of the island (Parnell et al., 2004). Hurricane Frances approached San Salvador as a Category 4 hurricane and stalled over the island where it became a Category 3 hurricane. Maximum intensity of Hurricane Frances was reached with a double peak (Figure 1). The lowest barometric pressure and highest wind speeds were first reached on August 31- September 1. A second low pressure and high wind speed peak was reached midday on September 2nd when it made landfall on San Salvador (Figure 1).

Our measurements of the maximum storm surge height of 4.8 to 5.5 m were determined by leveling to the highest evidence of flotsam and jetsam at locations along the east side of the island. These values correspond well with the upper limit of storm surge height for a Category 4 hurricane (Table 1). Tidal chart data for the island for 2 September 2004 indicate low tide at 5:06 p.m. and high tide at 11:11 p.m. (Mobile Geographics online). The tide does not seem to be a factor in the storm surge height. One factor that may have increased the storm surge height in this location to the right of the hurricane eyewall is the combined forward motion of the storm center adding to the onshore-directed winds (Figure 10; Liu, 2004).

We could only measure the maximum storm surge height where the coastal topography provided a high enough barrier marking the upper boundary of debris deposition. Areas with lower topography that were overtopped by the storm surge experienced extensive defoliation of the coastal vegetation. We investigated five sites where overwash sediment entered coastal estuaries, lakes, and the back beach areas. These sites included the south end of Storr's Lake, the central Storr's Lake basin from Dim Bay, Salt Pond, Sandy Hook, and the south island along the Gulf. At each of these sites large boulders of local beachrock were transported landward and deposited in a seaward dipping, imbricated pattern. A 300 m length of coastline between Salt Pond and Storr's Lake was defoliated by the storm surge and overwash.

In areas along the east side of the island where the shoreline is bordered by sand dunes, the beach has been widely eroded. Sand from the east

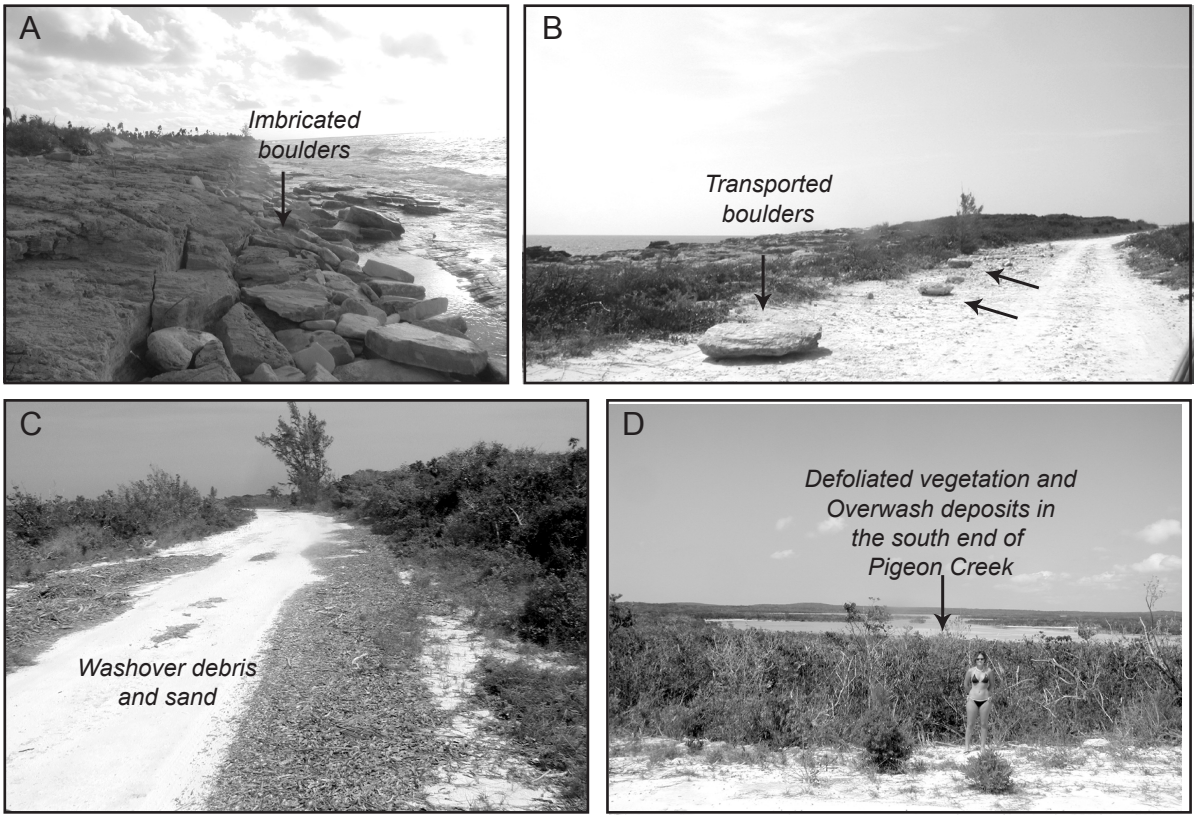

Figure 9. The Gulf is a site located along the south side of San Salvador island where the fringe reef and deep water lie close to the shore line. (See Figure 3 for a location map). A) Photograph along the coast showing imbricated large bedrock slabs and boulders. View to the east. B) Hurricane Frances transported large boulders from the shoreline onto the adjacent road. View to the west. C) In additon to buoys, ropes, plastic and other flotsam and jettsam, the washover debris included large amounts of leaves and organic material stripped from the coastal vegetation and sand. This photograph shows some of the overwash debris. View to the west. D) Overwash sediment was deposited into the southern end of Pigeon Creek. Defoliated vegetation marks the loction of where the storm surge passed.

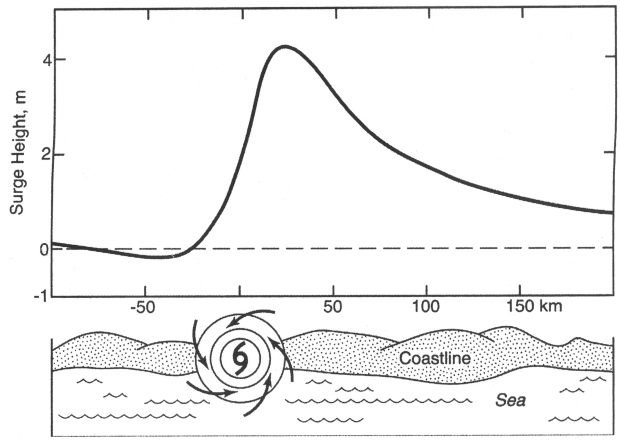

Figure 10. Schematic diagram of the distribution of storm surge heights along a coastline relative to the landfall of the eye of an intense hurricane. The storm surge height is greater on the right side of a hurricane due to the combined forward motion of the storm center and the onshore directed winds. (Figure from Liu, 2004).

face of the sand dunes has been removed as is evident in the development of steep scarps. Adjacent to Salt Pond the coastal sand dune was largely stripped of vegetation and overtopped leaving a blanket of sand in the lake basin. The south side of the island know as 'The Gulf' is composed of lithified Pleistocene reef which is highly resistant to beach erosion. Some blocks in addition to trash and vegetation were washed inland into the south end of Pigeon Creek in the storm surge.

The storm surge from Hurricane Frances or possibly the wind caused Pigeon Creek tidal inlet to overtop its banks along its northwest and north shore. A trench dug in the debris pile west of the road near the abandoned South Victoria Hill settlement exposed a mixture of sand and organic material such as leaves, seeds, and coconuts. Much of the material was decomposed making it an excellent medium for rooting coconut and seeds carried inland by the storm surge. At other locations, lone coconut trees, which are not native to the island, were found at high elevations along these beaches suggesting evidence of past storm surge deposition.

Evidence of Hurricane Frances and other storms were also found in stratified trash deposits south of and around tombolo known as 'The Thumb'. A 1.7-m-thick section was measured that showed 80 cm of aeolian sand burying a 40 cm thick horizon of stratified trash. At this location Hurricane Frances deposits were found at higher elevations and further inland. These data indicate that the Hurricane Frances storm surge was likely more intense than the previous hurricanes that hit the island during the 1990's

ACKNOWLEDGMENTS

We are grateful to Vincent Voegeli, past Executive Director of the Gerace Research Center, for discussions and guidance in locating Hurricane Frances storm deposits on San Salvador. Funding for this project was made available to undergraduate student authors McCabe and Thomason through the UMKC Students Engaged in Artistic and Academic Research (SEARCH) and through funds from the Department of Geosciences. Additional field assistance for this project was provided by UMKC students Amy Ameis. Jenny Goucher, and Ta'ni Sutherland. A special thanks to Al Curran, Doug Gamble, and Lisa E. Park for reviewing this paper and providing constructive comments. We would also like to thank Dr. Donald T. Gerace, Chief Executive Officer, and Dr. Thomas A. Rothfus, present Executive Director of the Gerace Research Center, San Salvador, Bahamas for use of and assistance while at the field station on San Salvador. This study was conducted under permit number 07-05 and earlier permits from the Department of Agriculture, The Bahamas.

REFERENCES

Beavers, R.L., Curran, H.A., and Fox, W.T., 1995, Long-term, storm-dominated sediment dynamics on East Beach and Sandy Point, San Salvador Island, Bahamas, *in* Boardman, M.R., ed., Proceedings of the Seventh Symposium on the Geology of the Bahamas: San Salvador, Bahamian Field Station, p. 1-15.

Beven II, J.L., 2004, Tropical cyclone report: Hurricane Frances 25 August-8 September 2004: NOAA National Weather Service, National Hurricane Center, http://www.nhc.noaa.gov/2004frances.html, posted 17 December 2004.

Carew, J.L., and Mylroie, J.E., 1995, Depositional model and stratigraphy for the Quaternary geology of the Bahama islands, *in* Curran, H.A., and White, B. eds.,Terrestrial and shallow marine geology of the Bahamas and Bermuda: Geological Society of America Special Paper 300, p. 5-31.

Curran, H.A., Delano, P., White, B., and Barrett, M., 2001, Coastal effects of Hurricane Floyd on San Salvador Island, Bahamas,

in Greenstein, B.J., and Carney, C.K., eds., Proceedings of the Tenth Symposium on the Geology of the Bahamas and Other Carbonate Regions: San Salvador, Bahamas, Gerace Research Center, p. 1-12.

Emery, K.O., 1961, A simple method of measuring beach profiles: Limnology and Oceanography, v. 6, p. 90-93.

Gamble, D.W., Brown, M.E., Parnell, D., Brommer, D., and Dixon, P.G., 2000, Lessons learned from Hurricane Floyd damage on San Salvador: Bahamas Journal of Science, v. 8(1), p. 25-31.

Garver, J.I., 1996, Some Effects of Hurricane Lili on San Salvador Island, Bahamas. http://minerva.union.edu/garverj/geo35/hurricane/Damage.html, Geology Department, Union College, Posted 15 December 1996.

Hinman, G., 1994, A teacher's guide to the depositional environments on San Salvador Island, Bahamas: Bahamian Field Station, San Salvador, Bahamas, 18 p.

Kraus, G., 2004, The "Emery-Method" Revisited—Performance of an Inexpensive Method of Measuring Beach Profiles and Modifications: Journal of Coastal Research, v. 20 (1), p. 340–346.

Lawrence, M.B., 1996a, Preliminary Report Hurricane Lili 14-27 Octorber 1996: NOAA National Weather Service, National Hurricane Center, http://www.nhc.noaa.gov/1996lili.html, Posted 18 November 1996.

Lawrence, M.B., 1996b, Preliminary Report: Hurricane Bertha 05-14 July 1996: NOAA National Weather Service, National Hurricane Center, http://www.nhc.noaa.gov/1996bertha.html, Posted 9 November 1996.

Liu, K.-B., 2004, Paleotempestology: Principles, methods, and examples from Gulf Coast lake sediments, *in* Hurricanes and Typhoons: Past, present, and future, Murnane, R.J., and Liu, K.-B., eds., Columbia University Press, New York, p. 13-57.

Loizeaux, N.T., Curran, H.A., and Fox, W.T., 1993, Seasonal sediment migration and sediment dynamics on Sandy Point Beach, San Salvador Island, Bahamas, *in* White, B., ed., Proceedings of the Sixth Symposium on the Geology of the Bahamas: San Salvador, Bahamian Field Station, p. 83-93.

McCabe, J.M., and Niemi, T.M., 2008, The 2004 Hurricane Frances overwash deposition in Salt Pond, San Salvador, The Bahamas, *in* Park, L.E. and Freile, D., eds., Proceedings of the Thirteenth Conference on the Geology of the Bahamas and Other Carbonate Islands, This Volume, p. 25-41.

NCDC (National Climatic Data Center), 2004, Climate of 2004 Atlantic Hurricane Season: NOAA http://www.ncdc.noaa.gov/oa/climate/research/2004/hurricanes04.html, last updated 13 December 2004.

NCDC (National Climatic Data Center), 2006, Climate of 2005 Atlantic Hurricane Season: NOAA http://www.ncdc.noaa.gov/oa/climate/research/2005/hurricanes05.html, last updated 21 August 2006.

Mobile Geographics online, http://www.mobilegeograpics.com:81/locations/5570.html.

Park, L.E., Metzger, T.J., Sipahioglu, S.M., Siewers, F.D., and Leonard, K., 2008, Event Deposition and faunal fluctuations after atorm deposits: A multi-proxy sediment core analysis from Salt Pond, San Salvador Island, Bahamas, *in* Park, L.E. and Freile, D., eds., Proceedings of the Thirteenth Conference on the Geology of the

Bahamas and Other Carbonate Islands, This Volume, p. 25-41.

Parnell, D.B., Brommer, D., Dixon, P.G., Brown, M.E., and Gamble, D.W., 2004, A survey of Hurricane Frances damage on San Salvador: Bahamas Journal of Science, v. 12(4), p. 2-6.

Pasch, R.J., Kimberlain, T.B., and Stewart, S.R., 1999, Preliminary Report: Hurricane Floyd 7-17 September 1999: NOAA National Weather Service, National Hurricane Center, http://www.nhc.noaa.gov/1999floyd.html, Posted 19 November 1999.

Shaklee, R.V., 1996, Weather and Climate: San Salvador Island, Bahamas: San Salvador, Bahamas The Bahmaian Field Station limited, 67 p.

Walker, S.E., Holland, S.M., and Gardiner, L., 2001, Cockburn town fossil reef: A summary of effects from Hurricane Floyd, *in* Greenstein, B.J., and Carney, C.K., eds., Proceedings of the Tenth Symposium on the Geology of the Bahamas and Other Carbonate Regions: San Salvador, Bahamas, Gerace Research Center, p. 13-19.

Watson, D.P., 1996, Coconut palm from seed: CTAHR (College of Tropical Agriculture and Human Resources) Fact Sheet, Ornamentals and Flowers no. 23 University of Hawai'i Manoa.

Yannarell, A.C., Steppe, T.F., and Paerl, H.W., 2007, Disturbance and recovery of microbial community structure and function following Hurricane Frances: Environmental Microbiology, v. 9, no. 3, p. 576-583.

AFTER THE HURRICANE HITS: RECOVERY AND RESPONSE TO LARGE STORM EVENTS IN A SALINE LAKE, SAN SALVADOR ISLAND, BAHAMAS

Lisa E. Park, Thadeus Metzger, and Sara Sipahioglu
Department of Geology and Environmental Science
University of Akron
Akron, OH 44325
lepark@uakron.edu

Frederick D. Siewers
Department of Geography and Geology
Western Kentucky University
Bowling Green, KY 42101

Karl Leonard
Department of Anthropology and Earth Science
University of Minnesota, Moorhead
Moorhead, MN 56563

ABSTRACT

The nature of response of invertebrate faunas to hurricane and other disturbrance events largely has been undocumented. The shallow, saline lakes of San Salvador Island, Bahamas contain important high resolution records of faunal dynamics, hurricane deposition and salinity changes that can be used to examine the effects of storms on these ecosystems. Two cores, measuring approximately 60 cm each, were taken from the depocenter of Salt Pond, a hypersaline lake on the eastern side of the island. Multiproxy analyses of loss on ignition, grain size distribution, sediment fabric, as well as ostracode and mollusk faunal composition were performed. These cores record sedimentation punctuated by hurricane and other large storm events. They also record a salinity history that varies from brackish to hypersaline, with the formation of salts such as halite and gypsum. Four species of ostracodes - *Cyprideis americana*, *Dolerocypria inopinata*, *Hemicyprideis setipunctata* and *Perissocytheridea bicelliforma* - were used to reconstruct the salinity history of the lake. Faunal diversity and abundance appears to increase after storm events due to the freshening of the lake, suggesting that while the system continues to reset itself, it recovers quickly from each major disturbance.

INTRODUCTION

Hurricanes and other major storm events act as large-scale perturbations on many different ecosystems along impacted coastlines. While studies have been done on both the vegetative and coral reef responses to hurricanes (Liu and Fearn, 1999; 2000), few, if any studies have been done on aquatic faunas found within coastal inland ponds in the same areas. How hurricanes impact the sedimentological and faunal dynamics of these inland ponds is not well understood. Preliminary studies on the lakes of San Salvador Island show that there may be a distinct biotic response to those storm events (Park et al., 2006; Metzger, 2007). The high resolution record that can be recovered from lakes in the Bahamas can yield important information on hurricane frequency and intensity as well as the biotic response to these environmental changes. This paper addresses primarily the latter.

Regional Setting

San Salvador Island (SSI), Bahamas (24.0°N/74.4°W), although similar to other Bahamian islands, is somewhat distinct in that it possesses high ridges and a number of inland lakes with varying water chemistries. During Pleistocene sea-level highstands, deposits of dune, beach and sub-tidal carbonates accumulated across the San Salvador platform. The island's shoreline is characterized by low sea cliffs of eroded Holocene and/or Pleistocene beach accretional ridges and eolianite deposits with and beaches of fine-to-medium grained carbonate sands and Holocene beachrock between headlands. Thus, it represents a unique 'natural laboratory' in which to examine questions concerning hurricane activity and the sedimentological and biological response to these storm events.

Modern lakes on SSI vary in salinity, controlled by the degree of development of the lake drain system, the presence of local fresh groundwater lenses, the size of the lake, its elevation relative to sea level, and rainfall (Teeter, 1985; 1995; Park and Trubee, this volume). Ponds and blue holes that have unimpeded connections to the open ocean exhibit normal-marine salinities and tidal change, although the range is diminished and timing lags behind ocean tides. Water in ponds having poor interchange with the ocean has longer residence times and higher salinities (Park, et al., 2003). Some ponds, such as Salt Pond, can range in salinity from 90 to 300 ppt. This pond is marked by the precipitation of gypsum and halite during its history (Shamberger, 1998; Furman et al., 1992). It is thought to have formed during the early Holocene from dunal development that closed off the Granny and Storr's Lake estuaries, creating a closed basin and resulting hypersaline conditions. Thus, the water budget of Salt Pond is reliant primarily on precipitation (ranging from 195 cm/year to 47 cm/year) and less on 'lake drains' or conduits that might connect the pond to the marine realm. Precipitation from large storms or hurricanes can significantly freshen the water column and result in both algal mat growth as well as a change in water chemistry (Shamberger and Foos, 2004; Yannarell, et al., 2007).

Hurricanes on SSI

San Salvador Island is particularly susceptible to hurricane activity because of its location. Hurricanes commonly cross the Bahamian Archipelago as they enter or exit the region, and as a result, the Bahamas experience more hurricanes than any other area in the Caribbean Basin or southwestern Atlantic (Liu and Fearn, 2000). Studies from the Gulf Coast of the Florida panhandle suggest that at least 12 catastrophic 4 or 5 hurricanes struck that area during the past 3400 yrs, with the most occurring between 1000 and 3400 14C yr B.P. (Liu and Fearn, 2000). This period followed one of relative quiescence. Whether or not there was a similar pattern on SSI has not been documented.

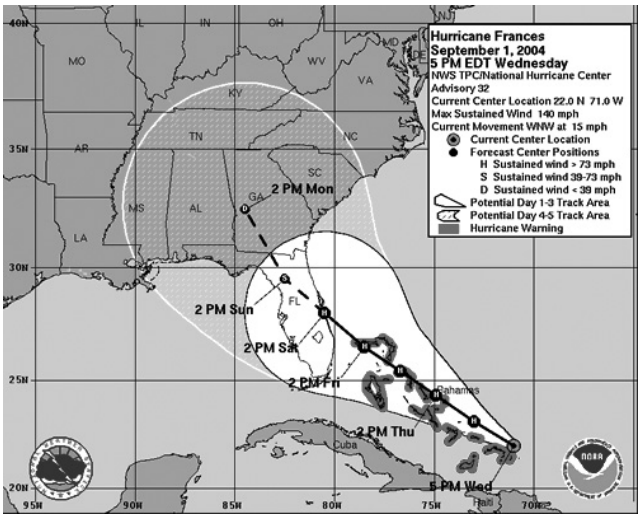

Figure 1. Storm track of Hurricane Frances, September 1, 2004. Source NOAA.

A tropical storm or hurricane of some magnitude has hit the San Salvador Island, on average, every 2.4 years since 1851 (Dijken, 2006). From 1899 until 1996, the Bahamas have experienced 66 hurricanes with 13 crossing directly over SSI (http://stormcarib.com/climatology/) (Figure 1). Recently however, SSI has experienced a decline in hurricane frequency that extends across the entire Archipelago.

In the period from 1960 – 2008, SSI has experienced only 7 hurricanes and 2 tropical storms. This may be due to a shift in regional and global weather patterns as a result of global climate change (Shaklee, 1996; Dijken, 2006; http://stormcarib.com/climatology/). The 1930's had a remarkable number of hurricanes with seven hurricanes crossing the island between 1932 and 1935 (Shaklee, 1996). The hurricanes that are most likely to affect SSI originate in the east-central areas of the North Atlantic and the Caribbean Sea, and occur between the months of June and November.

The last hurricane to hit the island was Hurricane Frances in September, 2004 (Figure 1) that was a Category (CAT) 3 storm as it went over the island. Prior to Frances, Hurricane Floyd hit the island in September, 1999, as a CAT 4. Hurricane Dennis hit that same year as a CAT 1. Salt Pond occurs on the stoss side of the island and is within the wash-over area for hurricanes and therefore can record these events because of the associated allochthonous sediments that get deposited within the basin.

Salt Pond Physical and Faunal Characteristics

The salina Salt Pond is a hypersaline lake with a maximum depth of 2 m, on the eastern side of the island and is within the wash-over area for hurricanes. It is separated from the Atlantic Ocean to the east by a ridge of Pleistocene bedrock, vegetation, and a carbonate sand beach (Shamberger, 1998) (Figure 2). The fauna in Salt Pond has a low diversity due to its extreme salinity. Typically only four species of ostracodes (bivalved microcrustaceans) are present: *Cyprideis americana*, *Hemicyprideis setipunctata*, *Perissocytheridea bicelliforma* and *Dolerocypria inopinata*, all of which are euryhaline (Figure 3). A few (4-5) species of mollusks, bivalves and gastropods, can also be found.

Ostracodes have been important paleoclimate indicators, studied for both marine and non-marine environments. They are common in many aquatic environments, and are easily preserved in the geological record. There are 60 known ostracode species found on San Salvador Island, but only one species has been found in all of the lakes (Park, 2006; 2007; Park et al., 2003; 2006; Park and Trubee, this volume). The lakes with the highest salinities have the lowest species diversity (Trubee, 2002).

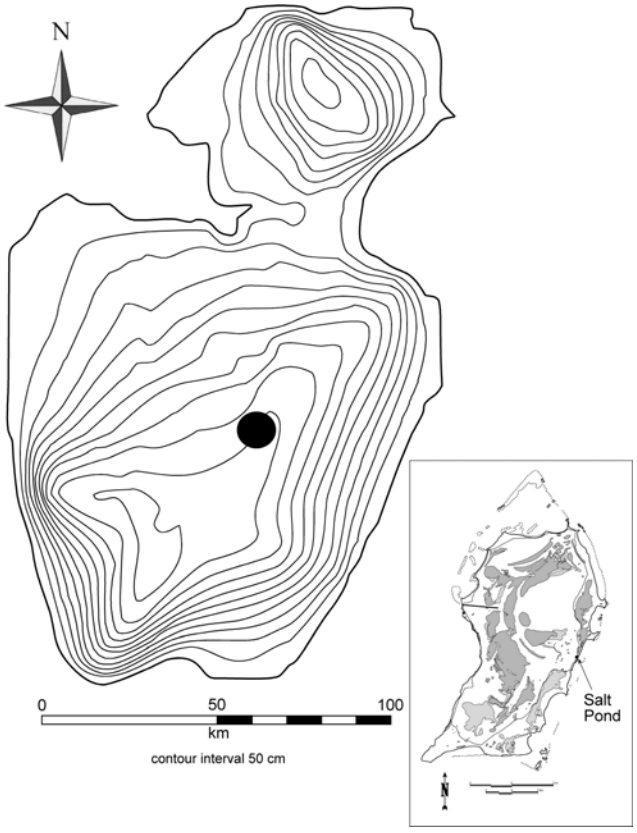

Figure 2. Bathymetric map of Salt Pond on San Salvador Island, Bahamas, showing location of the study site, as well as the core location. Contour interval is 50 cm.

Ostracode Ecology

Ostracodes occur in both stenohaline and euryhaline settings, although those from Salt Pond are all euryhaline forms, with salinity tolerances ranging from about 10 to 100 ppt. The four ostracode species found in Salt Pond have variable salinity tolerances (Figure 4)(Park and Trubee, this volume). *Perissocytheridea bicelliforma* is found in salinities ranging from 8.1 to 27.1 ppt, most commonly between 10 to 20 ppt.

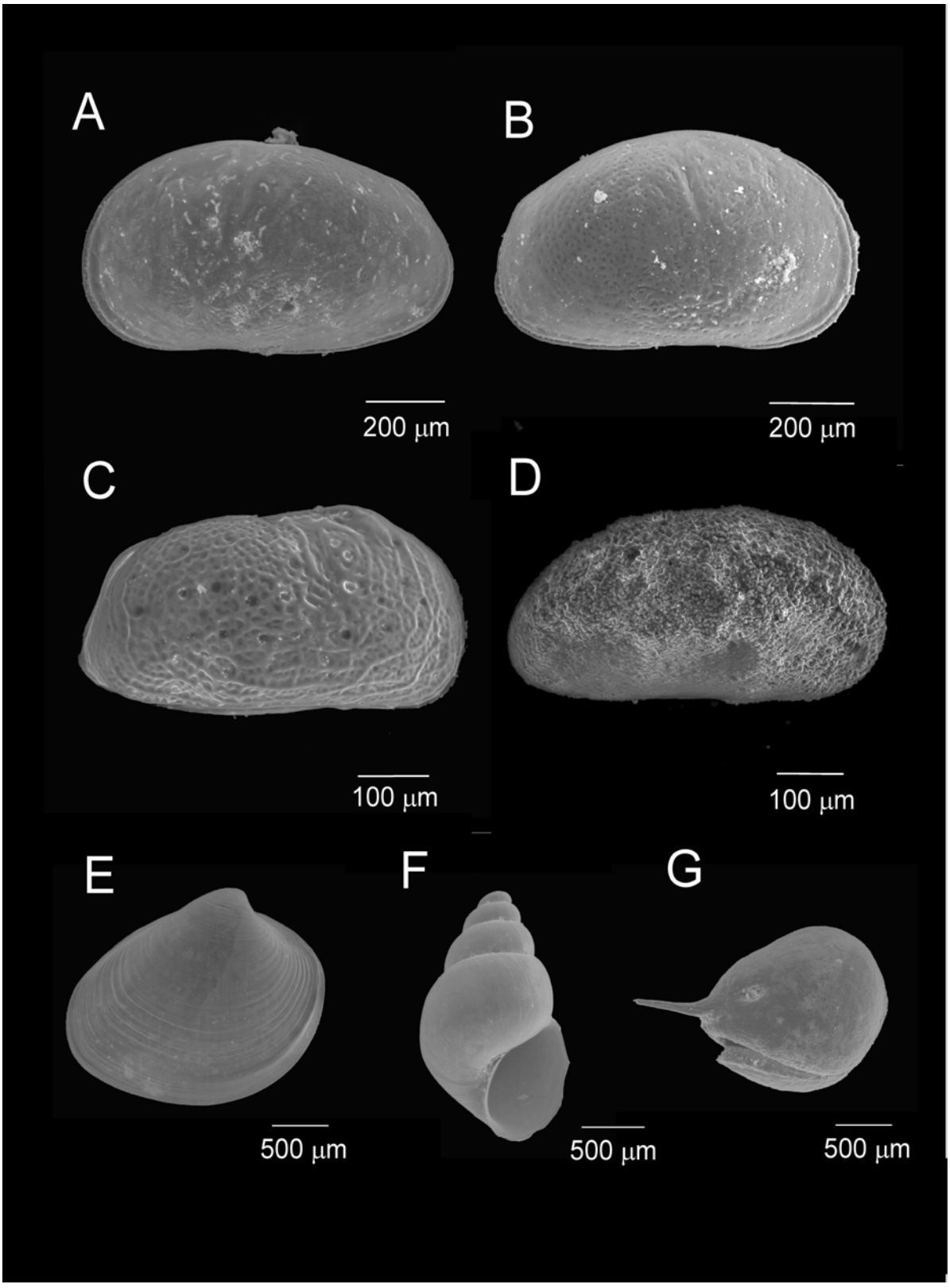

Figure 3. Scanning electron microscope images of A) Hemicytheridea setipunctata*, B)* Cyprideis americana*, C)* Perissocytheridea bicelliforma*, D)* Dolerocypria inopinata*, as well as E) a typical bivalve F) a gastropod shell and G) a seed. Scales are as indicated.*

Cyprideis americana is found in a wide salinity range between 10.8 to 98.5 ppt. It is least abundant in salinities from 30 to 50 ppt. *Hemicyprideis setipunctata* has a salinity tolerance of 11.3 to 60.9 ppt and a peak abundance between 30 to 40 ppt. They morphologically resemble *C. americana*, but are more dorso-ventrally rounded. *Dolerocypria inopinata* occur in salinities from 10.0 to 76.0 ppt and have a slightly elongated carapace. These forms are ideal not only as proxies for overall faunal response to hurricane events, but they can also but used as geochemical tools for obtaining oxygen isotopes as well as Mg/Ca and Sr/Ca trace element ratios (Park and Trubee, this volume).

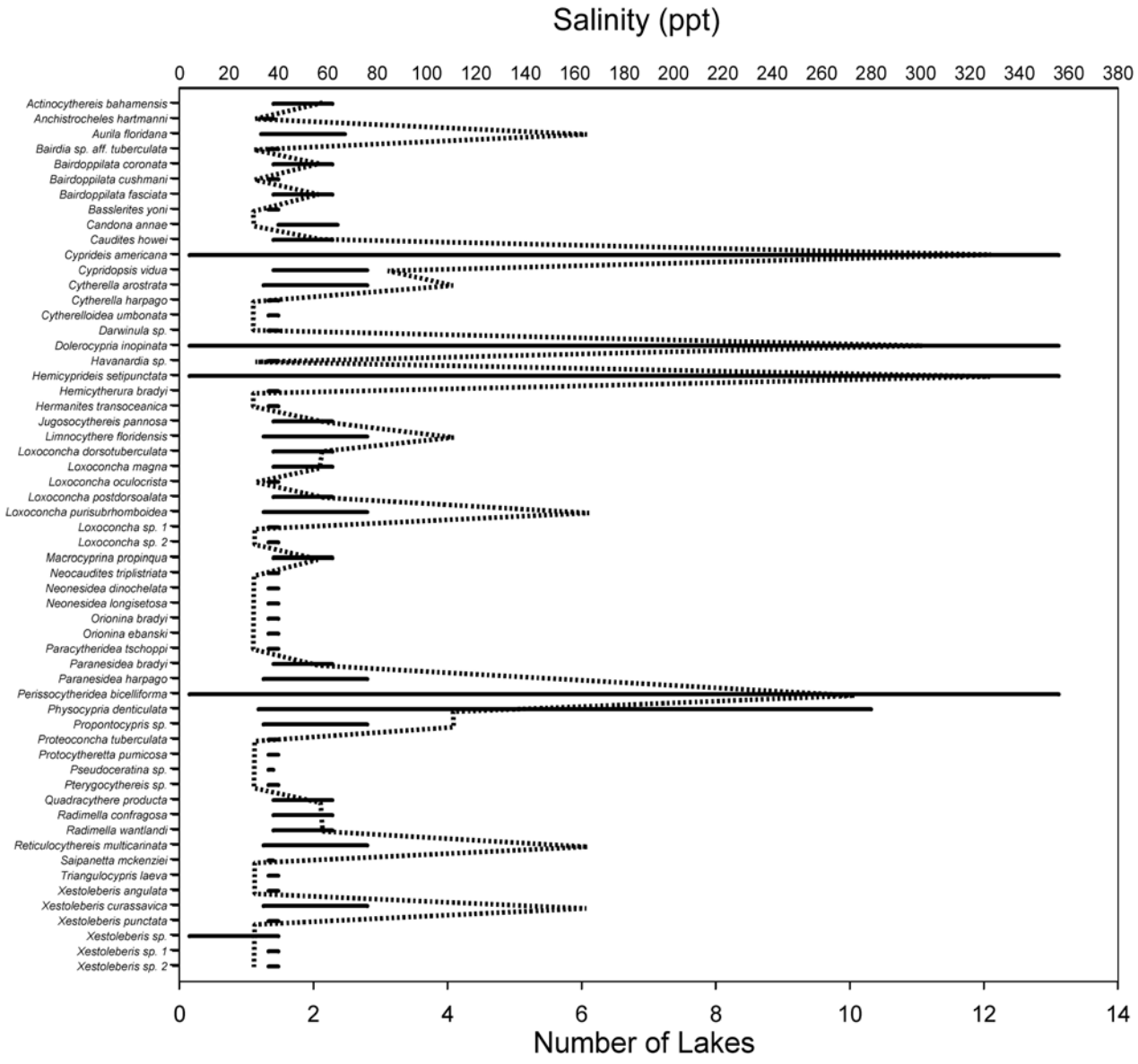

Figure 4. Salinity tolerances based upon species occurrences in the various ponds on San Salvador Island and their salinity ranges.

METHODS

Coring

Two 61 cm Livingstone piston cores were extracted from Salt Pond in January, 2006. The coring site was chosen because it was the depocenter of the lake and correlated with the "40 m" core of Shamberger (1998) (Figures 2 and 5). This area of the lake is constantly submerged. At the time of collection, water depth was approximately 1 meter. Complete recovery of the coring interval was obtained. The cores were refrigerated on the island and were transported to the University of Akron for analysis. The cores were initially described with respect to Munsell colors and any changes in sedimentation style and/or bedding features were noted.

Loss on Ignition and Grain Size Analyses

Loss on ignition (LOI) was done for dry and wet bulk density, water content, organic matter and carbonate content, using standard methods (Boyle, 2001). Dry bulk density may be an indicator of allochthonous sediments, such as carbonate sand that could be washed into Salt Pond during a tropical storm.

Grain size analyses were performed using a Malvern Mastersizer 2000 grain size analyzer (0.3 to 10,000 microns). Sediments were put into a slurry and dissolved before placing them into the Malvern. Five replicated measurements were done and an average was taken for each 1 cm interval of core. In addition to analyzing the core, a sample of beach sand from nearby 'Junk Beach' was also analyzed.

Ostracode Processing and Analysis

Ostracodes were sampled in 1 cm increments using standard freeze-thaw preparatory methods (Forester, 1990). Four species, *Cyprideis americana*, *Hemicyprideis setipunctata*, *Perissocytheridea bicelliforma* and *Dolerocypria inopinata* were identified and counted for alpha and beta diversity. In addition, mollusks, most notably gastropods and bivalves were also picked and counted. The ostracodes and mollusks were used as proxies to examine species composition, diversity, and abundance changes throughout the core. Ostracode diversity counts were done on the entire sample, using only adults. The total count was calculated to find the percentage of total ostracodes for each 1 cm increment. Both right and left valves were initially counted and then the total was divided by 2 for the number of individuals. Photomicroscopy was done on a FEI Quanta 200 , at the University of Akron (Department of Geology and Environmental Science).

Geochemical analyses were performed on ostracode valves from four species--*C. americana*, *D. inopinata*, *H. setipunctata*, and *P. bicelliforma* (*sensu* Chivas et al., 1983). Valves were cleaned and placed in a bath of 100% reagent grade bleach for twenty-four hours. Samples were removed and rinsed three times with triple distilled (i.e. MilliQ®) water. Analyses of both the dissolved ostracode valves were performed on an ICPMS and OES and oxygen and carbone isotopes were analyzed on a KIEL device at the University of Kansas.

Grain size, LOI, and fossil abundance were analyzed by Principal Components Analysis (PCA) using Multi-Variate Statistical Package (MVSP). First axis PCA scores represented 96% of the variance and were plotted against all of the variables to determine which variable was most correlative to storm events.

From these analyses, patterns of sedimentation were constructed to test the influence of climate, anthropogenic and large storm events on the depositional and faunal history of these lakes.

RESULTS

Lithologic and Grain Size Analyses

After careful visual analysis, the core was sudivided into 27 distinct intervals. Some of the intervals repeated with similar intervals later in

the core. Using color, grain size, LOI, and water content, the intervals were divided into four facies with common characteristics (Figures 5 and 6). These facies included: (1) evaporites and flocculated mud, (2) carbonate mud, (3) algal laminated mud, and (4) carbonate sand.

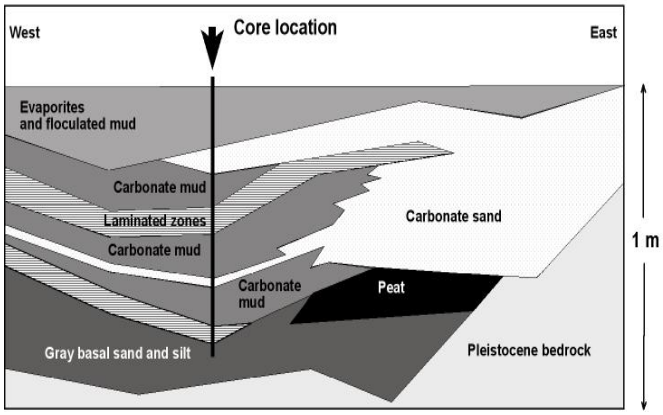

Figure 5. Cross-section of Salt Pond (based on Shamberger, 1998). Core location for this study is at the 40 m from shore mark. Note carbonate sand in eastern portion of lake, denoting storm overwash deposition.

Analyses of grain size show increases in grain size in regular intervals. The interval with the coarsest grain size was interval 4 (10-11 cm) that had a grain size distribution almost identical to that of the beach sand sample. The mean grain size of sediments in interval 4 was very similar to that of the nearby beach sand (Figure 6). The beach sand had a mean size of 300 µm. There were also sediments with more than 40% sand size particles (63 µm to 2 mm) in intervals 10, 14, 21, 25. They also had means slightly less that 300 µm (Figure 6).

Loss on Ignition

Dry bulk density and water content were inversely correlated throughout the core (Figure 7). The dry bulk density peaked in interval 4 at the core depth of 10-11 cm and was high (1.3 g/cm^3) in intervals 13 and 19 at core depths of 26-27 cm and 38-39 cm, respectively. Water content was lower in areas of suspected storm events due to the input of beach sediments. This also corresponds with an increase in percent of sand sized grains (Figure 7). Water content was inversely correlated with dry bulk density, and attained its lowest levels in intervals 4, 13, and 19.

Faunal Diversity

The number of mollusks and forams was highest within or preceding core depths 10-11 cm, 26-27 cm, 37-38 cm, and 51-54 cm downcore. In addition, the only significant number of seeds found were wtihin and preceding the storm interval 4 at 10-11 cm and interval 19 at 37-38 cm (Figure 7).

After the sand-dominated intervals ostracodes showed an increase in diversity. This occurred at 10-11 cm, 26-27 cm, 37-38 cm, and 51-54 cm downcore. These sand layers are overlain by algal-dominated muds having an increase in the number of ostracodes (Figure 7). The four species present in the core that include *Cyprideis americana*, *Hemicyprideis setipunctata*, *Perissocytheridea bicelliforma* and *Dolerocypria inopinata*. These ostracodes have been shown to occur in most of the ponds on San Salvador Island (Park and Trubee, this volume). *C. americana* is the most dominant species, occurring throughout the core, appearing within the most intervals as well as dominating the fauna when present. There appears to be an inverse relationship between *C. americana* and *P. bicelliforma* in many cases (Figures 8 and 9). Faunal abundances tracked the sand deposits in the core.

Mg/Ca and Sr/Ca ratios on species of *C. americana*, *H. setipunctata* and *P. bicelliforma* are inversely correlated. The Sr/Ca ratios are positively correlated with $\delta^{18}O$ isotope values. Principle component analyses on the datasets indicate that sand grain size % is the most accurate proxy for determining storm deposits. This summation of the multi-proxy variables indicates the storm signature that can be used to interpret the rest of the record

.

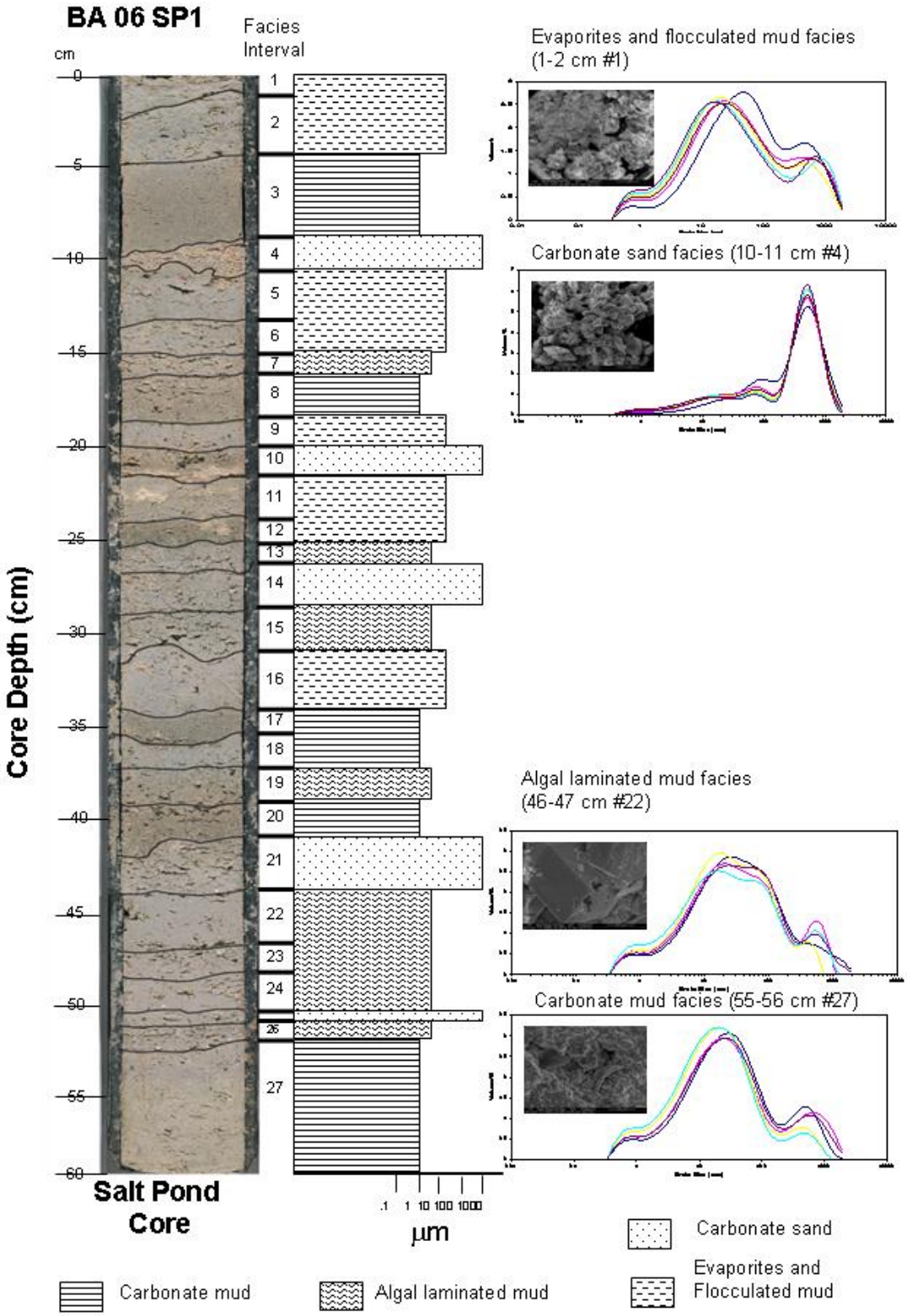

Figure 6. Core with grain size distributions and photos in intervals as indicated.

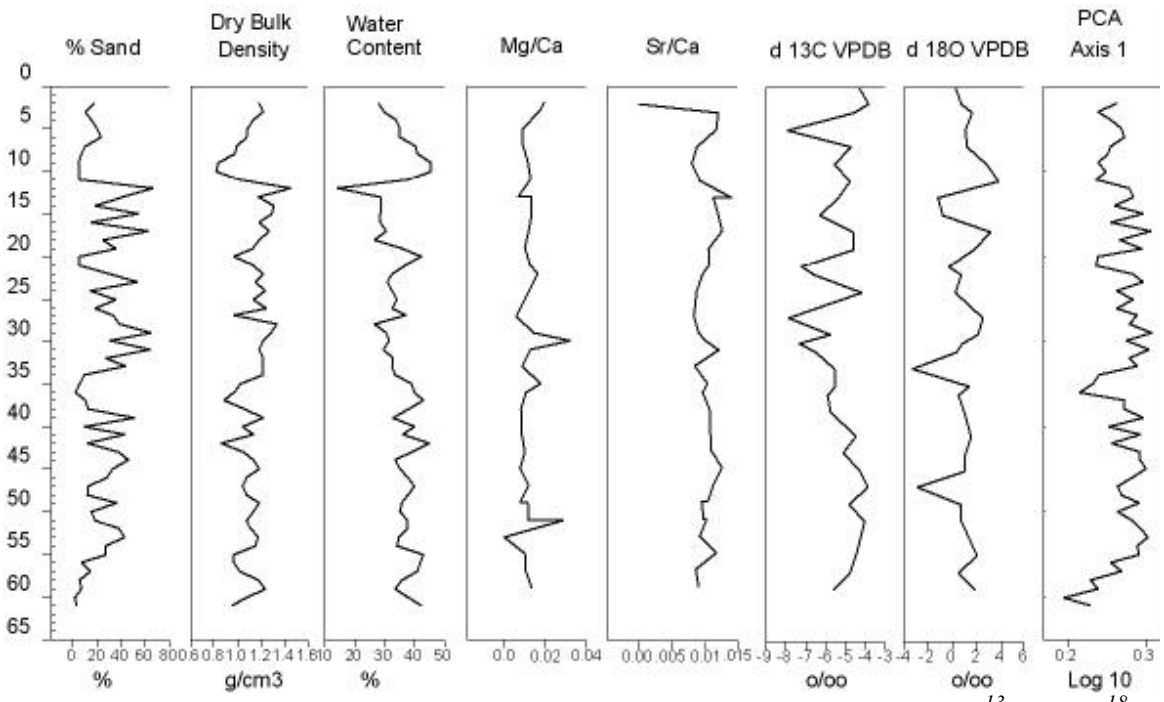

Figure 7. Sand content, dry bulk density, water content, Mg/Ca, Sr/Ca as well as $\delta^{13}C$ and $\delta^{18}O$ from C. americana and P. bicelliforma ostracode shells from Salt Pond core. PCA Axis 1 is on all seven datasets and represents >95% of all the variation within the combined datasets. Scales as indicated.

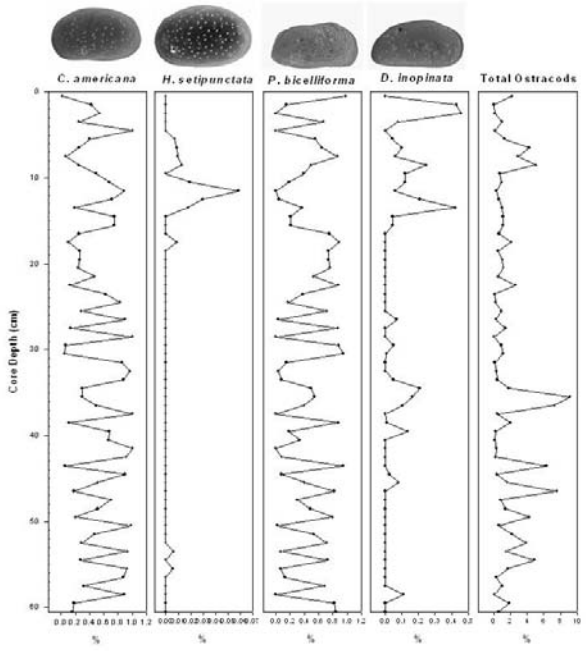

Figure 8. Ostracode % abundances for the four most common species in Salt Pond: Cyprideis americana, Hemicyprideis setipunctata, Perissocytheridea bicelliforma and Dolerocypria inopinata. *Total ostracodes are on the far right.*

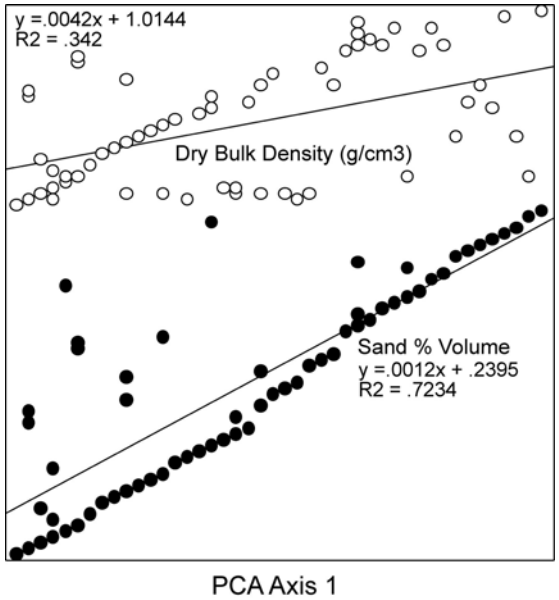

Figure 9. PCA Axis 1 vs. sand% and dry bulk density %; regressions indicate that sand % is the most effective proxy for determining storm deposition.

DISCUSSION

Based on the occurrence and distribution of bivalves, gastropods, forams, and sand particles there appear to be multiple depositional events in Salt Pond that were from large storms, possibly hurricanes. The composition and appearance of the bioclastic sand grains found in these carbonate sand layers appears to be similar to that on the beach to the east. Loss on Ignition (LOI) is an effective method of determining storm events due to wind deposition. The overwash of beach sand during large storms would be the reason for the large increase in carbonate and grain-size present in these layers of Salt Pond sediments.

These storms not only bring in sand from the beach, but also wash in bivalves, gastropods, seeds and forams. This is evidenced by the increase in shells that coincide with the sand deposits and also the fact that these species are not normally found in Salt Pond. Therefore they are most likely to have been washed or blown in by a large storm event. Since Salt Pond is only 50-75 meters from the ocean and separated from the beach by a small dune, the ocean beach is likely the source of the sand and shells. Along with this allogenic material, there is also a large input of freshwater in the form of rainfall into Salt Pond during large storms. In addition, there is an input of ocean water that has a lower salinity than Salt Pond. The increased rainfall causes a "freshening" that is followed by an increase in ostracode abundance and overall diversity.

Thus, the best indicator of a tropical storm in these cores appears to be an increase in sand-sized grains, dry bulk density, gastropods and forams. The sand grains appear to be transported in by overwash and wind. Dry bulk density increases during these times because grain size increases and the carbonate mud and algal layers decrease. Gastropods and forams appear to increase due to the possible freshening of the water to a more normal marine salinity. These sedimentary and paleontological components provide a "storm signature" that can be used to recognize other storm washover deposits in other lakes in the area. In addition, the ostracodes show a marked "recovery" after these large storm events due to the freshening of the lake from increased rainfall. Further studies need to be completed on other lakes to compare these phenomena.

CONCLUSIONS

Cores from Salt Pond can record hurricane and large storm deposits. These storm deposits can be distinguished in the sedimentary record by an increase in sand-sized grains, an increase in dry bulk density, a decrease in water content and an increase in gastropods, forms and seeds. Mollusk and ostracode abundance increased after documented storm deposits. *Cyprideis americana* is the most dominant ostracode species throughout the pond's history and inversely correlates with *Perissocytheridea bicelliforma*.

ACKNOWLEDGMENTS

The authors would like to thank the following people: Tom Quick and John Peck (University of Akron) for help with equipment and logistical support; UA students Daniel Davis, Stephanie Akers, and Quinn Fickey for help in core processing. We also thank Andrew Moore for access to the Malvern equipment at Kent State University. A special thanks to both Vincent Voegeli and Thomas Rothfus from The Gerace Research Centre, San Salvador Island, Bahamas for field and lab support. This manuscript was improved by helpful comments from Tina Niemi and two anonymous reviewers. This project was conducted under permit #01/31 from the Bahamas Department of Agriculture. This is a TREC publication of the University of Akron Department of Geology and Environmental Science.

REFERENCES

Boyle, J.F., 2001, Inorganic geochemical methods in paleolimnology, *in* Last, W.M. and Smol, J.P., eds., Tracking Environmental Change Using Lake Sediments, 2: Kluwer Academic Publishers, London, p. 83-143.

Dijken, G.V., 2006, StormCarib: Caribbean hurricane network. http://storm carib.com/.

Forester, R.M., 1990, Nonmarine calcareous microfossil sample preparation: Ostracods: USGS Technical Procedure, EP-78, R1.

Furman, F.C., Woody, R.E., Rasberry, M.A., Keller, D.J., Gregg, J.M., 1992, Carbonate and evaporite mineralogy of Holocene (<1900 RCYBP) sediments at Salt Pond, San Salvador Island, Bahamas, preliminary study, *in* White, B., ed., Proceedings of the Sixth Symposium on the Geology of the Bahamas, Bahamian Field Station, San Salvador, Bahamas, p. 47-54.

Liu, K-B, and Fearn, M.L., 1993, Lake-sediment record of late Holocene hurricane activities from coastal Alabama: Geology, v. 21, p. 793-796.

Liu, K-B., and Fearn, M.L., 2000, Reconstruction of prehistoric landfall frequencies of catastrophic hurricanes in northwestern Florida from lake sediment records: Quaternary Research, v. 54, p. 238-245.

Metzger, T., 2007, Event deposition and faunal fluctuations after storm deposits: a multiproxy sediment core analysis from Salt Pond, San Salvador Island, Bahamas: Senior Honors Thesis, University of Akron, p. 66.

Park, L.E., 2006, A taxonomic and geochemical atlas of the ostracodes of San Salvador Island, Bahamas. The 13th Symposium on the Geology of the Bahamas and other Carbonate Regions. p. 19.

Park, L.E., 2007. Geochemical and faunal variability of ostracode faunas from saline ponds on San Salvador Island, Bahamas—An integrated taxonomic and geochemical atlas: Joint North and South Central Section of the Geological Society of America,

Park, L.E., Ricketts, R.D., Trubee, K.J., 2003, Are some species better proxy indicators than others? Some case studies from Ostracoda: GSA Abstracts with Programs, v. 34 (7), p. 129.

Park, L.E., Siewers, F., Leonard, K., 2006, Discerning the record of event deposition and paleosalinity fluctuation from saline lakes: insights from sediment cores from Storr's Lake and Salt Pond, San Salvador Island, Bahamas: GSA Abstracts with Programs, v. 38, p. 81.

Park, L.E., and Trubee, K.J., 2008, Faunal and geochemical variability of ostracodes faunas from saline ponds on San Salvador Island, Bahamas, *in* Park, L.E. and Freile, D., eds., Proceedings from the Thirteenth Symposium on the Geology of the Bahamas and Other Carbonate Regions, Gerace Research Center, San Salvador, Bahamas, This Volume, p. 11-24.

Shaklee, R.V., 1996, Weather and Climate San Salvador Island, Bahamas, *in* The Bahamian Field Station Limited, San Salvador Bahamas, p. 67.

Shamberger, E.A., 1998, Depositional history of a coastal evaporite salina- Salt Pond, San Salvador Island, Bahamas, [M.S. Thesis]: University of Akron, Akron, Ohio. p. 144.

Shamberger, E. and Foos. A., 2004, Depositional history of a coastal evaporate salina: Salt Pond, San Salvador Island, Bahamas, *in* Lewis, R.D. and Panuska, B.C., eds., Proceedings of the Eleventh Symposium on the Geology of the Bahamas and Other Carbonate Regions: Gerace Research Centre, San Salvador, Bahamas, p. 179-186.

Teeter, J.W., 1995, Holocene saline lake history, San Salvador Island, Bahamas, *in* Curran, H.A. and White, B., eds., Terrestrial and Shallow Marine Geology of the Bahamas and Bermuda: GSA Special Papers, v. 300, p. 117-124

Teeter, J.W., 1985. Holocene lacustrine depositional history, *in* Curran, H.A., ed., Pleistocene and Holocene carbonate environments on San Salvador Island, Bahamas, p. 133-145.

Trubee, K.J., 2002, Characterizing the variability of non-marine ostracode faunas on San Salvador Island, Bahamas, [Masters Thesis]: University of Akron, Akron, Ohio, 63 p.

Yannarell, A.C., Steppe, T.F., and Paerl, H.W., 2007, Disturbance and recovery of microbial community structure and function following Hurricane Frances: Environmental Microbiology, v. 9, p.576-583.

TESTING THE DEEP FORM OF THE IVORY TREE CORAL, *OCULINA VARICOSA*, AS A PROXY FOR INTERMEDIATE/BOTTOM WATER VARIATION: OCULINA BANKS, FLORIDA, USA

Dorien K. McGee, Gregory S. Herbert, and Peter J. Harries
Department of Geology
University of South Florida
Tampa, FL 33620

ABSTRACT

Deep-water corals grow worldwide and are noted for their ability to grow without the aid of algal symbionts at depths that can exceed 5000 m. Like zooxanthellate shallow-water species, deep-water corals are currently being assessed as potential paleoclimate archives. Because their environmental conditions are thought to be relatively more stable than that of shallow-water corals, and because they lack zooxanthellae, isotopic analyses of deep-water corals are thought to yield "cleaner" signals and serve as intermediate and bottom-water proxies for ocean circulation change, that then may be linked to changes in climate. *Oculina varicosa* is the dominant scleractinian coral on the Oculina Bank and the species responsible for construction of the extensive system of high-relief coral pinnacles and ridges off the east coast of central Florida. These corals grow at depths between 70 and 100 m and are subject to the combined effects of the Florida Current/Gulf Stream and Florida Straits upwelling water masses. This study compared the oxygen and carbon isotopic composition of a specimen of this species with a year-long record of surface temperature, bottom temperature, and bottom current velocity from the area in a pilot study to assess the species' ability to geochemically sense fluctuations in these water masses. Oxygen isotopes ranged between -2.6 and 1.0 ‰ PDB, and carbon isotopes ranged between -6.9 and 2.1 ‰ PDB. Isotopic trends indicate a 2.5 to 3.0 cm per year growth cycle, nearly doubling previous estimates. Mean temperatures of aragonite precipitation calculated from two temperature equations derived for marine carbonates fell within 4.7 °C and 2.7 °C of the observed mean bottom temperature when values of $\delta^{18}O_w$ were estimated as 0‰ and -0.5‰, respectively. Isotopic trends in *O. varicosa* generally reflect bottom temperature trends and periods of nutrient influx triggered by eddies from the Florida Current and upwelling from the Florida Straits. Discrepancies in derived precipitation temperatures might be attributed to isotope fractionation (which may render available temperature equations inapplicable); however, the similarity between the isotope and temperature profiles suggests fractionation might be constant, as seen in other corals. Alternatively, derived temperature discrepancies might be attributed to the expansion of a year-long record of bottom temperature to a 3-year record of coral growth, as well as the lack of seawater oxygen isotope data for the Oculina Banks region. By measuring bottom temperature over a longer time period and building a database of seawater $\delta^{18}O$ from multiple depths in this region, these two issues can be resolved.

INTRODUCTION

Coral Ecosystems and Biology

While corals typically inhabit shallow-marine tropical waters, recent research has explored the presence of deep-water coral ecosystems worldwide ranging from shelf to abyssal depth (Roberts et al., 2006). Although the existence of deep-water corals has been recognized for centuries, only recent technological developments have allowed for the detailed exploration and study of these ecosystems. To date, they have been documented globally, ranging from sparse colonies of individual hard- and soft-coral

species to dense frameworks that support major fisheries.

Deep-water corals are primarily azooxanthellate and rely on nutrients obtained directly from the water column. As a result, colonies are often found in association with pockets of high productivity, such as regions of upwelling, ocean circulation currents, and cold-water seeps (Roberts et al., 2006). However, some species are apozooxanthellate, or facultatively zooxanthellate, and can convert between a zooxanthellate and azooxanthellate growth form based on the existing environmental conditions. These species have been documented at depths ranging from 3 to 100 m in Bermuda and on the eastern Florida Shelf.

Isotope Analyses

In recent years, deep-water corals have been isotopically analyzed to determine their use as paleoclimate archives, with much of the work concentrating on the scleractinians *Lophelia pertusa* and *Desmophyllum dianthus*. The absence of zooxanthellae in these taxa and their position in deeper waters buffered from relatively dynamic surface conditions, were cited as indications that kinetic and vital effects would not be as strong a factor in the interpretation of their isotopes as has been the case with shallow-water corals. However, $\delta^{13}C$ and $\delta^{18}O$ values of the aragonite in deep-water corals have been found to be more depleted relative to their environment (Mikkelsen et al., 1982; Freiwald et al., 1997; Spiro et al., 2000). Wefer and Berger (1991) hypothesized that differences in the $\delta^{13}C$ signature of dissolved inorganic carbon (DIC) between shallow- and deep-water regions could be a potential cause. The same line of reasoning could also be applied to $\delta^{18}O$ from dissolved oxygen (DO). Although sinking organic matter would carry with it $\delta^{13}C$ and $\delta^{18}O$ values from the surface, remineralization and oxidation/reduction reactions occurring at the bottom are hypothesized to alter these values, particularly in areas affected by upwelling and deep-water circulation (Mooers and Feichter, 2005). Aragonite precipitation and feeding would integrate these values within the coral skeleton with metabolic processes, potentially further fractionating the isotopes.

Differences in carbon and oxygen isotope composition, both between individuals of the same species and age, and between samples from the same individual, have been documented in several coral species, further complicating the interpretation of deep-water coral isotopes (Spiro et al., 2000; Smith et al., 2000; Smith et al., 2002). Variations revealed by UV fluorescence in the aragonitic microstructure of individual *Lophelia pertusa* are cited as a possible cause for such isotope differences. These variations are shown to be minimized when using secondary ion mass spectrometry (SIMS) and ion microprobe sampling procedures (Blamart et al., 2005).

Finally, when the $\delta^{13}C$ and $\delta^{18}O$ values of deep-water corals are plotted against one another, they often form a near linear regression (Emiliani et al., 1978; Mikkelsen et al, 1982; Swart, 1983; Spiro et al., 2000; McConnaughey, 2003). Romanek et al. (1992) suggested that $\delta^{13}C$ signals from aragonite should be generated independently of temperature, an idea that was confirmed later by Smith et al. (2000). It was therefore hypothesized by Spiro et al. (2000) that the precipitation of both isotopes must be linked. They further concluded that because salinity and temperature are relatively stable in deep-water environments compared to that of shallow-water environments, and because photosynthesis is not a controlling factor for ahermatypic corals, the elimination of these variables would be expected to stabilize $\delta^{13}C$ and $\delta^{18}O$ signals in the aragonite. Isotopic composition should therefore be affected primarily by coral metabolism and not by independent, external variables.

Despite the apparent difficulties in interpreting the isotope records of deep-water corals, their potential as proxies of bottom water variation warrants further research, with emphasis on studying a wider variety of species. *Oculina varicosa* is an apozooxanthellate coral species common to the eastern Florida Shelf and is the ahermatypic reef builder of the Oculina Bank on the Florida Shelf margin. Little has been done to understand its biology and potential as an envi-

ronmental proxy; however the position of Oculina Banks on the margin of the Florida Shelf, combined with its exposure to the Florida Current above and upwelling from the Florida Straits below make it worthwhile to determine the potential of this species as a proxy for variation in these water masses.

OCULINA BANKS, FLORIDA

Oculina Banks is a north-south trending, deep-water reef structure extending nearly 170 km north to south along the eastern Florida shelf of the United States (Reed, 2002; Figure 1). The region is dominated by high-relief coral pinnacles, mounds, and ridges ranging in elevation from 3-35 m above the surrounding substrate. Substrates underlying the coral framework consist of sand and mud sediments, disarticulated coral debris, and oolitic limestone formed during the Holocene transgression (Macintyre and Milliman, 1970; Reed, 1980).

The high-relief structures are capped by colonies of the apozooxanthellate ivory tree coral, *Oculina varicosa* (sometimes misidentified as *Oculina valenciennesi*). Their distribution varies in depth from 70 to 100 m. At these depths they display their azooxanthellate deep-water morphology (Figure 2-3), with stem and branches generally less than 1 cm in diameter. This differs from their shallow-water zooxanthellate morphology found off the coast of Ft. Pierce and in Bermuda, where stem and branch diameters average 1.5 cm or more. *Oculina varicosa* has been known to expel its zooxanthellae during times of stress, and has been documented converting to its deep-water morphology after being transplanted from the shallows (Reed, 1981).

In this setting, bottom temperatures average 16.2 °C, but can decrease to as low as 7.4 °C during periods of upwelling from the Florida Straits (Reed, 1981; Smith, 1981; and Reed, 1983). Bottom currents average 8.6 cm s^{-1} and can exceed 50 cm s^{-1} when the Florida Current reaches its maximum velocity (Reed, 1981; and Hoskin et al., 1983).

Nutrient-rich water upwells from the

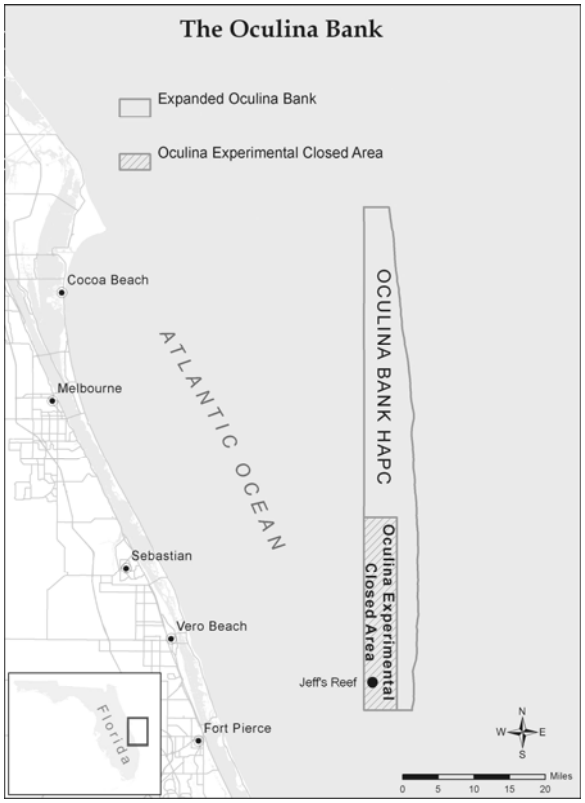

Figure 1. The Oculina Bank, FL (courtesy of A. Shepard, UNC-Wilmington).

Florida Straits periodically throughout the year, with stronger pulses during the winter months (Mooers and Fiechter, 2005; personal comm.). Surface eddies from the Florida Current/Gulf Stream have a 4-7 day frequency, and are more frequent in the winter. Using mesoscale numerical modeling of primary productivity based on physical and biologic observations in the region, Mooers and Fiechter (2005, personal comm.) predicted that while nutrient supplies are relatively constant throughout the year, nutrient loading would occur in the winter, suggesting a strong interaction between the upwelling and eddy water masses.

The combination of nutrient availability and the presence of the corals support a dense macroinvertebrate fauna, that in turn supports a diverse fish population including a number of economically important species (Reed, 2002). However, despite the designation of Oculina Banks as a Habitat of Particular Concern in 1984 (expanding from 315 km^2 to 1029 km^2 in 2000),

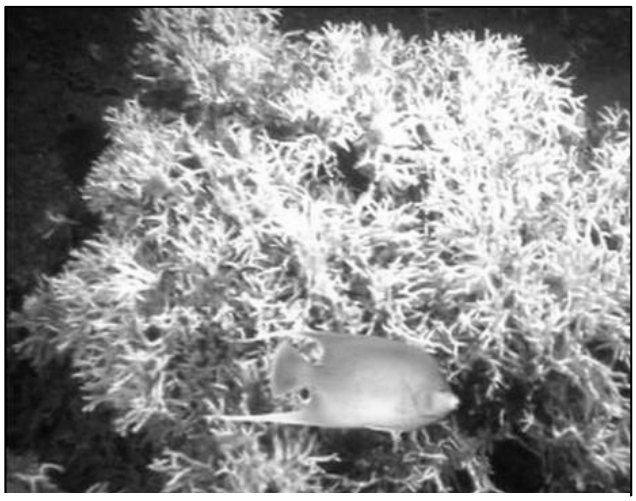

Figure 2. Oculina varicosa *colony. Courtesy of NURC-UNCW.*

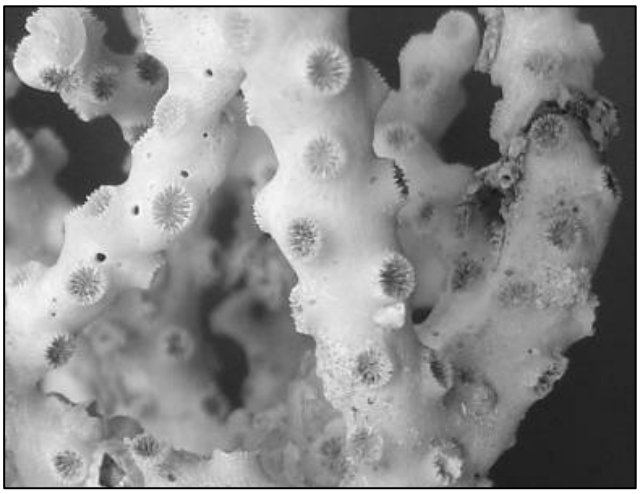

Figure 3. Individual O. varicosa *corallites (average corallite diameter = 1.75 – 2.5 mm).*

illegal bottom fishing and shrimp trawling have continued to damage the coral colonies.

Because few isotopic analyses have been undertaken using the azooxanthellate form of *Oculina varicosa*, this study addresses its potential as a useful proxy for temperature. Since shallow-water corals have yielded effective climatic signatures over time (albeit with some corrections), the ability of *O. varicosa* to exist in both shallow and deep regions (as opposed to *Lophelia pertusa* and *Desmophyllum dianthus*) might suggest that vital effects impacting equilibrium isotope concentrations in solely azooxanthellate species may not be a factor. Alternatively, the ability of *O. varicosa* to convert between growth morphologies may introduce a metabolic effect differing from those affecting azooxanthellate corals. However, because the Oculina Banks are situated in an environment dominated by movement of the Florida Current/Gulf Stream above and the upwelling from the Florida Straits below, the potential of isotopes recorded by *O. varicosa* to serve as a proxy monitoring the flow and interaction of these major water masses over time warrants an investigation of the isotopic composition of the species. By understanding the dynamics of these water masses, we may better understand their flow patterns and associated effects on the region as well as how they may have differed in the past. This paper presents the results of a pilot study using mass spectrometry to assess the capacity of *O. varicosa* as an effective paleoceanographic tool.

METHODS

Sample Collection

Oculina varicosa samples were collected on October 13, 2005 during a multibeam sonar cruise of Oculina Banks aboard the NASA *M/V LIBERTY STAR*. Samples were collected from Station 12 at Chapman's Reef (27° 36.764' N, 79° 58.444' W) at a depth of approximately 82 m using the Phantom S2 remotely operated vehicle (ROV).

Grab samples from this location included live and dead coral specimens, combined with silt and clay. Coral specimens were documented and cataloged for reposit at the Smithsonian Institute. Of these, specimen OB05-12 was shipped to the University of South Florida for the isotope analysis used in this study. This specimen measured 15.1 cm in total length and was composed of six branching stalks of various sizes. Although the specimen was non-living upon collection, it remained relatively free of encrusting organisms except at the base, an indicator of recent mortality in an area where encrusting organisms are common (Winston and Jackson, 1984).

Isotope Analysis

A single stem and associated branches of specimen OB05-12 was selected for isotope analysis based on its relatively straight growth. Powders were spot drilled every 0.25 cm along the length of the stem and along the initial few centimeters of each of the two branches with a Dremel® drill using a 0.8 mm bit. Drilling took place along the coral skeleton away from the septal margins to ensure the samples recorded branch/stem growth and not that of any corallites, which may have varying growth and/or precipitation rates that could influence the isotopic composition. Each drill site was initially prepared by lightly abrading the coral skeleton to remove the site mark and create a fresh drilling surface. Due to the brittle nature of the specimen, drill holes were kept shallow to prevent puncturing the skeleton to hollow voids within the stem. Distances for each drill sample were recorded beginning with 0 cm for the first sample; and sampling at the branches were given equidistant values from the 0 cm starting point as samples along the main stem. Drill powders were weighed on a mass balance to weights between 50 and 100 μg for $\delta^{13}C$ and $\delta^{18}O$ analysis, which was performed using a ThermoQuest® Delta+XL mass spectrometer using NBS-19 as the standard for PDB.

$\delta^{18}O$ values of the skeleton were used in two equations to estimate aragonitic precipitation temperatures:

$$T = 20.6 - 4.34(\delta^{18}O_c - \delta^{18}O_w)$$

Grossman and Ku, 1986

$$T = [(\delta^{18}O_c - \delta^{18}O_w) - 4.97]/-0.25$$

Smith et al., 2000

Although the Grossman and Ku (1986) equation was developed for use with gastropods and foraminifera, it formed the basis of the Smith and others (2000) equation developed for cold-water scleractinian coral species, and was therefore included in this study. Because $\delta^{18}O$ values of depths between 70 and 100 m were not available for this region, a 0 ‰ value was used as a default (Schmidt et al., 1999).

Environmental Data

A record of bottom conditions at 74.68 m was obtained from an instrumental array moored by Oregon Institute of Marine Biology/University of Oregon at Jeff's Reef for 340 days from April 2000 to March 2001. This array included an acoustic Doppler current profiler and temperature profiler that recorded environmental conditions at a frequency of 36 measurements per day (one recording per five minutes for the first fifteen minutes of every other hour). Sea-surface temperatures and meteorologic conditions for the same time period were collected from the National Data Buoy Center online archive of Buoy 41009, located 20 nautical miles east of Cape Canaveral, and the closest data buoy to Oculina Banks. Environmental conditions were recorded hourly, on the hour.

RESULTS

Oxygen and Carbon Isotopes

Isotope values from the coral specimen ranged between -2.6 and 1.0‰ for $\delta^{18}O$ and -6.9 and 2.1‰ PDB for $\delta^{13}C$ (Figures 4, 5). Samples without isotopic values indicate insufficient CO_2 produced from the powders to generate $\delta^{13}C$ and $\delta^{18}O$ values. Isotopic values for $\delta^{13}C$ and $\delta^{18}O$ form a near linear regression when plotted against one another, with an r^2 of 0.92 (Figure 6). Temperatures of precipitation based on $\delta^{18}O_c$ for the Grossman and Ku (1986) equation and assuming a $\delta^{18}O_w$ of 0‰ ranged between 16.1 and 31.7 °C with a mean of 25.9 °C (Figure 7). Temperatures calculated from the Smith and others (2000) equation were slightly lower, ranging between 15.8 and 30.1 °C with a mean of 24.8 °C (Figure 8).

Environmental Temperature

Sea-surface temperatures from April, 2000 to March, 2001 recorded by Buoy 41009 ranged between 18.3 and 30.7 °C, with a mean of 24.0 °C (Figure 9). Bottom temperatures re-

corded at Jeff's Reef ranged from 12.0 to 29.0 °C, with a mean of 20.1 °C. An overall increase in SST occurred between April and August, 2000, followed by a decrease until late January, 2001 before increasing slightly between February and March, 2001.

Bottom temperatures displayed more volatility over the interval, but appear to show an overall increase from May to late October of 2000, before falling in November. Temperatures appeared to rise again between February and March, 2001. Average bottom currents remained between 5 and 20 cm sec^{-1} throughout this interval, with regular, rapid fluctuations between these values (Figure 10). Current velocity peaked at 53.24 cm sec^{-1} for the period studied on March 26, 2001, and was associated with several large bottom temperature fluctuations (varying between 3 and 13 °C) from March 23 to March 26, as well as an overall increase in bottom temperature. Coeval anomalies in sea-surface observations from Buoy 41009 were not apparent.

Tropical Storm Leslie passed approximately 50 km north of Oculina Banks on October 5-6, 2000, however wind speeds remained at 40 kt or less, and air pressures remained at 1007 mb and above (Franklin and Brown, 2000). An increase in current velocity to 12.8 cm sec^{-1} occurs at this time, before quickly falling back to values less than 1 cm sec^{-1}.

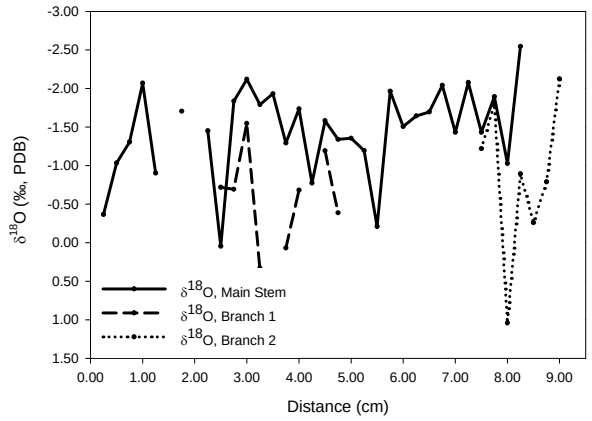

Figure 4. Oxygen isotope profile for main stem and branches of *O. varicosa.*

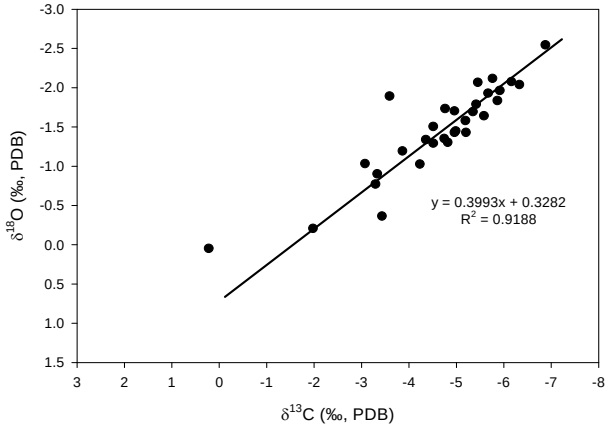

Figure 6. Cross plot of oxygen vs carbon isotopic values.

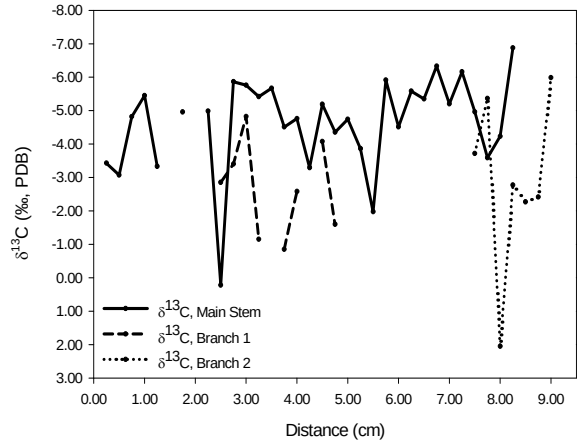

Figure 5. Carbon isotope profile for main stem and branches of *O. varicosa*.

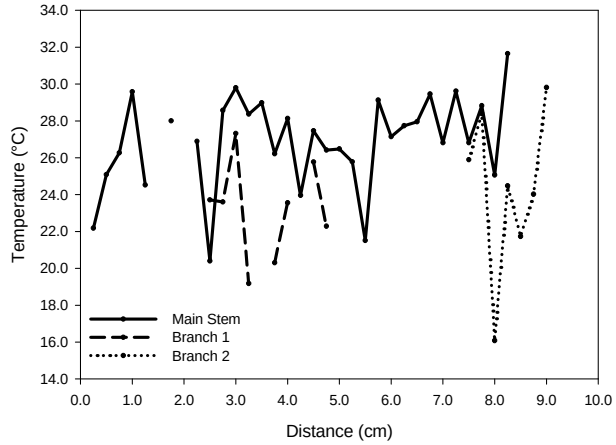

Figure 7. Temperature profile derived from Grossman & Ku, 1986 (assuming 0‰ for $\delta^{18}O_w$).

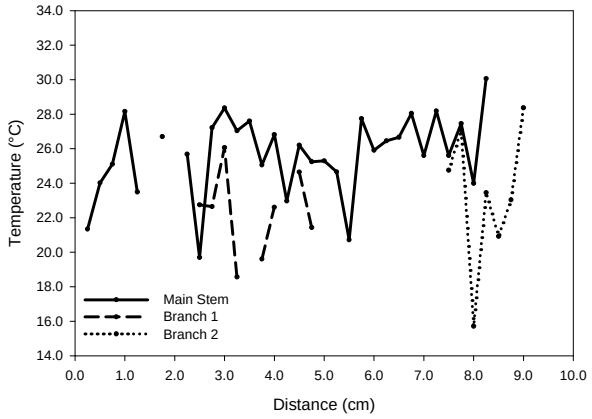

Figure 8. Temperature profile derived from Smith et al., 2000 (assuming 0‰ for $\delta^{18}O_w$).

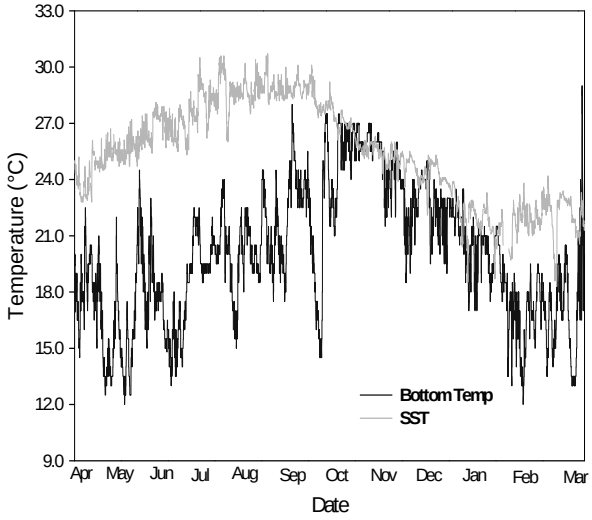

Figure 9. Bottom and surface temperature profiles for Jeff's Reef, Oculina Banks, April 2000 to March 2001.

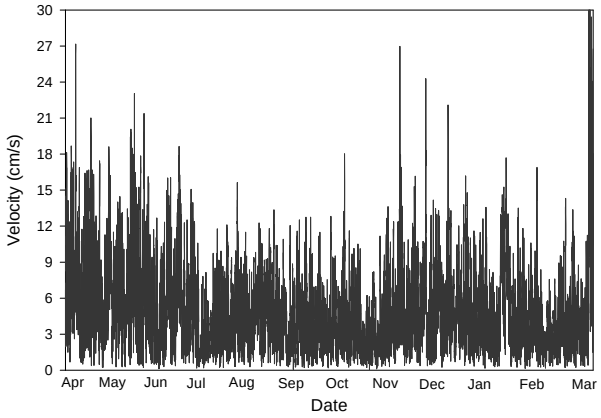

Figure 10. Bottom current profile for Jeff's Reef, Oculina Banks, April 2000 - March 2001.

DISCUSSION

Isotope Sampling

Preliminary analyses suggest the possibility of a 2-3 cm maximum annual growth cycle for *O. varicosa* as opposed to a 1.5 cm cycle observed by Reed (1981). Given that Reed's estimate was based on a transplanted individual, discrepancies in the growth rates should not be unexpected and may reflect stress induced by the relocation of the specimen. Future work that includes microsampling of the specimen used in this study will improve the sampling resolution and may help resolve this issue.

The differing isotopic values between main stem samples and parallel points on the branches of the coral specimen have two primary implications. First, the branches of the coral may grow at a different rate from the main stem, leading to an offset in isotopic values between the two at equal distances. If this is so, finer-scale microsampling should show similar patterns of isotopic fluctuation on different scales, and an estimate of the differences in growth rate can be inferred. However, because the skeletal microstructures of some cold-water scleractinian species have been shown to vary (Blamart et al., 2005), it is possible that fractionation based on these differences yields the isotopic variability seen here. UV fluorescence and SIMS/ion microprobe analysis should determine whether this is the case. Further complications resulting from variable growth rates and skeletal microstructural differences may be acting simultaneously and fine-scaled analysis of the isotopic variation in the microstructures must be resolved prior to establishing differences in growth rates.

Assessing Proxy Potential

The Grossman and Ku (1986) and Smith and others (2000) temperature equations calculated similar temperature results, with means varying by 1.1 °C. Because the Smith and others (2000) equation is essentially a fine-tuned version of the Grossman and Ku (1986) equation, the similarities in temperature results should be ex-

pected. Although the Grossman and Ku (1986) equation is commonly applied in paleotemperature studies, its development for use with foraminiferal and molluscan species suggests it may not be directly applicable for temperature reconstructions using cold-water corals. Its applicability over a number of such equations existing for tropical coral species is another problem to be addressed. Moreover, the Smith and others (2000) equation was established using estimates of $\delta^{18}O_w$ based on salinity averages reported by the World Ocean Atlas 2001 (Boyer et al., 2002) for the coral collection sites rather than observed *in situ* values. As $\delta^{18}O$ values are less commonly recorded and reported relative to other environmental parameters, such as temperature and salinity, particularly at depth, relatively little is known about their localized fluctuation over time in specific locations. In the absence of more tailored equations however, the Smith and others (2000) equation, which is slightly more appropriate to deep-water corals than the Grossman and Ku (1986) equation, must suffice.

Temperature fluctuations observed at Jeff's Reef for the April 2000-March 2001 observation period are much greater than those seen at the surface, likely resulting from Florida Straits upwelling throughout the year. Upwelling pulses may also be interpreted from the current profile, indicating a decrease in average current velocity through the summer followed by a mild increase in the winter, corresponding to upwelling frequency observations (Mooers and Fiechter, 2005; personal comm.). Because the range of temperature fluctuations in bottom waters is larger than that seen at the surface, and because anomalies in the bottom currents do not appear to correlate with surface conditions, it may be inferred that upwelling events do not reach the surface. Thus, the general assumption that increasing depth translates to more regulated environmental conditions is not supported, at least for this dynamic locality. While this assumption may hold for regions not affected by ocean currents, upwelling, and/or seeps, deep-water reefs are generally associated with and influenced by these conditions.

Regardless, these physical and chemical fluctuations in the bottom water should be reflected in the isotopic composition of the corals, and may be more visible with finer resolution sampling. Isotopic fractionation may also play a role in offsetting isotopic values, and may explain why mean temperatures derived from the Smith and others (2000) equation were 4.7 °C higher than the mean calculated from observations at Jeff's Reef (again, assuming the applicability of the Smith and others (2000) equation). Inaccurate $\delta^{18}O_w$ values may also skew temperature yields, as 0‰ was used in the absence of measured values of the ambient water's isotopic composition. NASA's Global Seawater $\delta^{18}O$ Database v1.14 reported a mean global isotopic value of -0.49‰ for depths between 70 and 100 m, based on 1,561 data points. When this average was used in the Smith and others (2000) equation, it lowered the estimated temperature mean to within 2.7 °C of the observed mean at Jeff's Reef (Schmidt et al., 1999). This must be viewed with caution however, for two reasons. First, the range of $\delta^{18}O$ values reported in the database extends from -6.7 to 2.0 ‰, with none of the data points corresponding to the Florida region. Second, the mean bottom temperature reported by Reed in an annual cycle from July 1978 to July 1979 was 16 °C, approximately 4 °C lower than observed in the 2000-2001 profile (Reed, 1981). Because no other long-term bottom temperature profiles exist for Oculina Banks, the variation in bottom temperature from year to year has not been established. Thus, given the current limitations, it may be safest to assume the true $\delta^{18}O_w$ mean for Oculina Banks is close to -0.49‰.

$\delta^{13}C$ values analyzed from *Oculina varicosa* fell within the range of values observed in *Desmophyllum dianthus* by Lutringer et al. (2005) and *Lophelia pertusa* from the northeastern Atlantic, as summarized by Blamart et al. (2005). It is important to note that microsampling performed by Blamart et al. produced values ranging from -0.7 to -15.3‰, and it was determined that microstructural variations in the thickness of the aragonitic skeleton were responsible for this wide divergence in values. The lighter carbon isotopic values measured in this study corresponds to that of marine organisms as discussed by Stahl (1979); however the heavier

values correspond more closely to standard values of marine HCO_3^-. Because marine plankton is isotopically light, ranging from -16 and -27‰, one might expect $\delta^{13}C$ values of *Oculina varicosa* to fall within their isotopic range. This effect, however, may be dampened by heavier DIC values, potentially imported to the region by upwelling events. By obtaining periodic $\delta^{13}C$ values of local DIC, it may be possible to determine how much fractionation is occurring in the coral. From there, culturing the species on a diet of known $\delta^{13}C$ and in a medium of known $\delta^{13}C$ of DIC can help determine whether fractionation is governed by vital or kinetic effects.

CONCLUSIONS

Preliminary analysis of *Oculina varicosa* indicates that it may serve as an effective proxy for intermediate and bottom-water change at Oculina Banks; however, further work must be undertaken to better understand both the environmental parameters and the species' biology in order to better interpret these isotopic data. Higher resolution sampling of the coral will better illustrate any cyclicity in growth patterns and growth rate differences between the branches and main growth axes, if indeed they are reflected in its isotopic composition. Measuring $\delta^{18}O$ values of the bottom water at Oculina Banks is vital to developing a more applicable temperature equation for the coral, particularly if more thorough sampling of bottom temperatures and isotopic composition of multiple specimens can be undertaken. Establishing values of $\delta^{13}C$ values of DIC of the water, as well as coral culturing experiments will aid in the understanding of any carbon isotopic fractionation. Finally, a better understanding of the physical regime at Oculina Banks, including longer-term profiles of bottom temperature, current velocity, and nutrient and/or organic matter concentrations will help provide a more solid foundation for comparison with isotopic data yielded by the corals.

ACKNOWLEDGMENTS

We would like to thank Andy Shepard and Amanda Manness of the National Underwater Research Center at the University of North Carolina at Wilmington, as well as John Reed of the Harbor Branch Oceanographic Institution for providing the coral specimen and sharing their knowledge of the species. We would also like to thank Sandra Brooke of the Oregon Institute of Marine Biology-University of Oregon for providing the data profiles from the moored instrumental array at Jeff's Reef, and Ethan Goddard of the Paleo Lab at the University of South Florida-St. Petersburg for the acquisition of all isotope data. Finally, we wish to thank Jerome Fiechter and Christopher Mooers of the Rosentiel School of Marine and Atmospheric Science at the University of Miami for sharing their insights on the physical and biological oceanography of the Oculina Banks region.

REFERENCES

Blamart, D., Rollion-Bard, C., Cuif, J., Juillet-Leclerc, A., Lutringer, A., van Weering, and T.C.E., Henriet, J., 2005, C and O isotopes in a deep-sea coral (*Lophelia pertusa*) related to skeletal microstructure: *in* Freiwald, A., and Roberts, J.M., eds, Cold-Water Corals and Ecosystems: Erlangen, Springer-Verlag Berlin Heidelberg, p. 1005-1020.

Boyer, T. P., Stephens, C., Antonov, J.I., Conkright, M.E., Locarnini, R.A., O'Brien T.D., and Garcia, H.E., 2002, World Ocean Atlas 2001, Volume 2: Salinity., *in* Levitus, S. ed., NOAA Atlas NESDIS 50: U.S. Government Printing Office, Wash., D.C., 165 pp.

Emiliani, C., Hudson, J.H., Shinn, E.A., and George, R.Y., 1978, Oxygen and carbon isotopic growth record in a reef coral from the Florida Keys and a deep-sea coral from Blake Plateau: Science, v. 202, p. 627-629.

Franklin, J., and Brown, D.P., 2000, Tropical Cyclone Report: Tropical Storm Leslie (Subtropical Depression One), 4-7 October 2000: National Hurricane Center (online access): http://www.nhc.noaa.gov/2000leslie.html.

Freiwald, A., Henrich, R., and Pätzold, J., 1997, Anatomy of a deep-water coral reef mound from Stjernsund, West Finnmark, northern Norway: SEPM Special Publication 56, p. 141-161.

Grossman, E.L., and Ku, T., 1986, Oxygen and carbon isotope fractionation in biogenic aragonite: temperature effects: Chemical Geology, v. 59, p. 59-74.

Hoskin, C.M., Geier, J.C., and Reed, J.K., 1983, Sediment produced from abrasion of the branching stony coral *Oculina varicosa*: Journal of Sedimentary Petrology, v. 53, p. 779-786.

Lutringer, A., Blamart, D., Frank, N., and Labeyrie, L., 2005, Paleotemperatures from deep-sea corals: scale effects, *in* Freiwald, A., and Roberts, J.M., eds., Cold-Water Corals and Ecosystems: Erlangen, Springer-Verlag Berlin Heidelberg, p. 1081-1096.

Macintyre, I.G., and Milliman, J.D., 1970, Physiographic features on the outer shelf and upper continental slope, Atlantic continental margin, southeastern United States: Bulletin of the American Geological Society, v. 81, p. 2577-2598.

McConnaughey, T., 2003, Sub-equilibrium Oxygen-18 and carbon-13 levels in biological carbonates: carbonate and kinetic models: Coral Reefs, v. 22, p. 316-327.

Mikkelsen, N., Erlenkeuser, H., Killingley, J.S., and Berger, W.H., 1982, Norwegian corals: radiocarbon and stable isotopes in *Lophelia pertusa*: Boreas, v. 11, p. 163-171.

Mooers, C.M., and Fiechter, J., 2005, Numerical simulations of mesoscale variability in the Straits of Florida: Ocean Dynamics, v. 55(3-4), p. 309-325.

Reed, J.K., 1980, Distribution and structure of deep-water *Oculina varicosa* coral reefs off central eastern Florida: Bulletin of Marine Science, v. 30, p. 667-677.

Reed, J.K., 1981, *In situ* growth rates of the Scleractinian coral *Oculina varicosa* occurring with zooxanthellae on 6-m reefs and without on 80-m banks *in* Gomez, E.D., Birkeland, C.E., Buddemeier, R.W., Johannes, R.E., Marsh, J.A., and Tsuda, R.T., eds., Proceedings of the Fourth International Coral Reef Symposium: Manila, University of the Philippines, p. 201-206.

Reed, J.K., 1983, Nearshore and shelf-edge *Oculina* coral reefs: the effects of upwelling on coral growth and on the associated faunal communities: National Oceanic and Atmospheric Administration Symposium Series, Undersea Research, v. 1, 119-124.

Reed, J.K., 2002, Deep-water *Oculina* coral reefs of Florida: biology, impacts, and management: Hydrobiologia, v. 471, p. 43-55.

Roberts, J.M., Wheeler, A.J., and Freiwald, A., 2006, Reefs of the deep: the biology and geology of cold-water coral ecosystems: Science, v. 312, p. 543-547.

Romaneck, C.S., Grossman, E.L., and Morse, J.W., 1992, Carbon isotopic fractionation in synthetic aragonite and calcite: Effects of temperature and precipitation rate: Geochimica et Cosmochimica Acta, v. 56, p. 419-430.

Schmidt, G.A., Bigg, G.R., and Rohling, E.J., 1999, "Global Seawater Oxygen-18 Database". (online access): http://data.giss.nasa.gov/o18data/ .

Smith, N.P., 1981, An investigation of seasonal upwelling along the Atlantic coast of Florida, *in* Nihoul, J.C., ed., Ecohydrodynamics, Elseveier, New York, p. 79-98.

Smith, J.E., Schwarcz, H.P., Risk, J.J., McConnaughey, T., and Keller, N., 2000, Paleotemperatures from deep-sea corals: overcoming "vital effects": Palaios, v. 15, p. 25-32.

Smith J.E., Schwarcz, H.P., and Risk, M.J., 2002, Patterns of isotopic disequilibria in azooxanthellic coral skeleton: Hydrobiologia, v. 471, p. 111-115.

Spiro, B., Roberts, M., Gage, J., and Chenery, S., 2000, $^{18}O/^{16}O$ and $^{13}C/^{12}C$ in ahermatypic deep-sea water coral *Lophelia pertusa* from the North Atlantic: a case of disequilibrium isotope fractionation: Rapid Communications in Mass Spectrometry, v. 14, 1332-1336.

Stahl, W., 1979, Carbon isotopes in petroleum geochemistry, *in* Jager, E., and Hunziker, J.C., eds., Lectures in Isotope Geology, Springer, Berlin, p. 274–282

Swart, P.K., 1983, Carbon and oxygen isotope fractionation in scleractinian corals: a review: Earth Science Reviews, v. 19, p. 51-80.

Wefer, G., and Berger, W.H., 1991, Isotope paleontology: growth and composition of extant calcareous species: Marine Geology, v. 100, p. 207-248.

Winston, J.E., and Jackson, J.B.C., 1984, Ecology of cryptic coral reef communities. IV. community development and life histories of encrusting cheilostome bryozoa: Journal of Experimental Marine Biology and Ecology, v. 76, p. 1-21.

A PRELIMINARY GEOLOGICAL RECONNAISSANCE OF ABACO ISLAND, BAHAMAS

Lindsay N. Walker, John E. Mylroie, Adam D. Walker, and Joan R. Mylroie
Department of Geosciences
Mississippi State University
Mississippi State, MS 39762

ABSTRACT

Abaco Island is located on Little Bahama Bank at the northeastern extent of the Bahamian Archipelago. Examples from each of the three major field stratigraphic units—Owl's Hole, Grotto Beach, and Rice Bay formations can be identified on Abaco based on observable field relationships. The Owl's Hole Formation is recognized as a vegemorph-rich eolianite, with foresets truncated by wave energy from a subsequent highstand, covered by a *terra rossa* paleosol. Outcrops of the Grotto Beach Formation show fossil coral rubble (Cockburn Town Member) resting directly on an underlying eolianite with no separation by a *terra rossa* paleosol (French Bay Member). Widespread outcrops containing herringbone cross-bedding also belong to the subtidal Cockburn Town Member. Eolianites lacking a *terra rossa* paleosol are Rice Bay Formation rocks, assigned to the North Point Member as shown by foresets dipping below modern sea level. The Pleistocene/Holocene contact can be seen in outcrop as a *terra rossa* paleosol separating Rice Bay Formation eolianites assigned to the Hanna Bay Member from underlying Pleistocene eolianites.

Karst features on Abaco include large and abundant flank margin caves, pit caves, blue holes, karren, and banana holes--all of which are common features of Bahamian islands. The large positive water budget of Abaco has produced landforms resembling tropical cone karst on Pleistocene eolianites. The first documented tafoni caves in the Bahamas, pseudokarst features formed by wind and salt erosion, demonstrate the need for caution when using caves as sea level indicators.

INTRODUCTION

The Bahamas have long been the focus of much geologic work on modern carbonates (Carew and Mylroie, 1997 and references therein; Tucker and Wright, 1990; Multer, 1977; and Illing, 1954). The Bahama Platform (Figure 1) has particular interest to geologists as it provides a modern analog to the dynamics of ancient carbonate depositional platforms, many of which are major petroleum reservoirs.

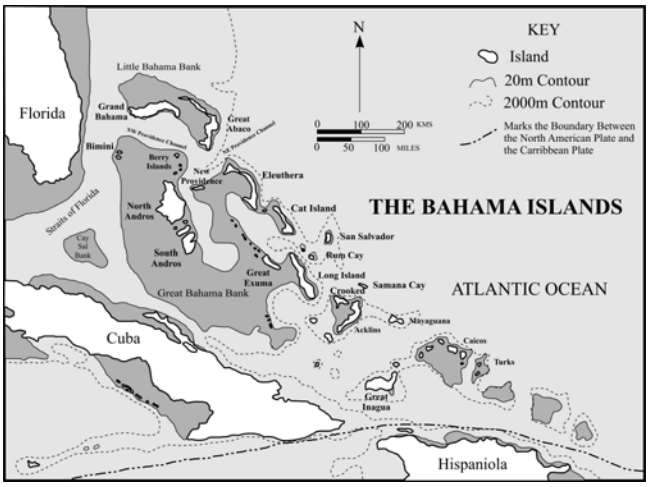

Figure 1. Map of the Bahamian Archipelago (Modified from Carew and Mylroie, 1995a).

The Bahama Platform is composed of a series of thick, shallow-water, carbonate banks along the subsiding margin of North America (Mullins and Lynts, 1977). The current landscape of the Bahamas is largely constructional and is greatly influenced by glacioeustatic sea level fluctuations (Carew and Mylroie, 1997). During sea level lowstands, sea level dropped below the bank

margins. Carbonate sedimentation ceased and karst processes dominated on the exposed bank tops. Lowstands are recorded in the sedimentary record by the development of *terra rossa* paleosols. These fossil soil horizons are the result of the concentration of insoluble materials such as atmospheric dust due to pedogenic processes.

During sea level highstands, the banktops are flooded, allowing for the creation and mobilization of carbonate sediments. The glacioeustatic sea level oscillations that have occurred throughout the Quaternary have allowed for the emplacement of several carbonate depositional sequences capped by *terra rossa* paleosols (Carew and Mylroie, 1997). Due to the known subsidence of the Bahamian archipelago of 1-2 m per 100,000 years, sediments that were originally deposited above current sea level may now be inundated (Carew and Mylroie, 1995a). The only sea level highstand above present to occur recently enough to still be exposed today was the +6 m Oxygen Isotope Substage (OIS) 5e highstand, that occurred approximately 125,000 years ago (Carew and Mylroie, 1995a). Consequently, the only subtidal deposits currently exposed in the Bahamas are the result of that highstand.

Eolianite deposits, however, have been preserved from several past highstands. Eolianites can be deposited at any stage of a sea level highstand, and can thus be described as transgressive-phase, stillstand-phase, or regressive-phase (Carew and Mylroie, 1997). In the field, these eolianites can be differentiated on the basis of known characteristics. Transgressive-phase eolianites, for example, are especially subject to cliffing by wave action because sea level continues to rise during their deposition. They are also characterized by a relative lack of vegemorphs, as the coastal vegetative community has not yet had time to develop at the onset of a sea level rise (Carew and Mylroie, 1997). Regressive dunes, on the other hand, contain abundant vegemorphs, as the coastal vegetative community has fully developed by the time of their deposition (Carew and Mylroie, 1997).

A general stratigraphy of the Bahamas was developed by Carew and Mylroie based on their work on San Salvador Island, Bahamas (Carew and Mylroie, 1995b; 1995c; and 1997). It consists of three major depositional packages separated by *terra rossa* paleosols (Figure 2). The Mid-Pleistocene Owl's Hole Formation, which consists of eolianites from several sea level highstands, comprises the oldest rocks in the Bahamas (Figure 2). The Upper Pleistocene Grotto Beach Formation consists of eolianites, beach deposits, and subtidal carbonates deposited during the OIS 5e highstand (Figure 2). The Holocene Rice Bay Formation contains all deposits, primarily eolianites, associated with the current sea level highstand (Figure 1).

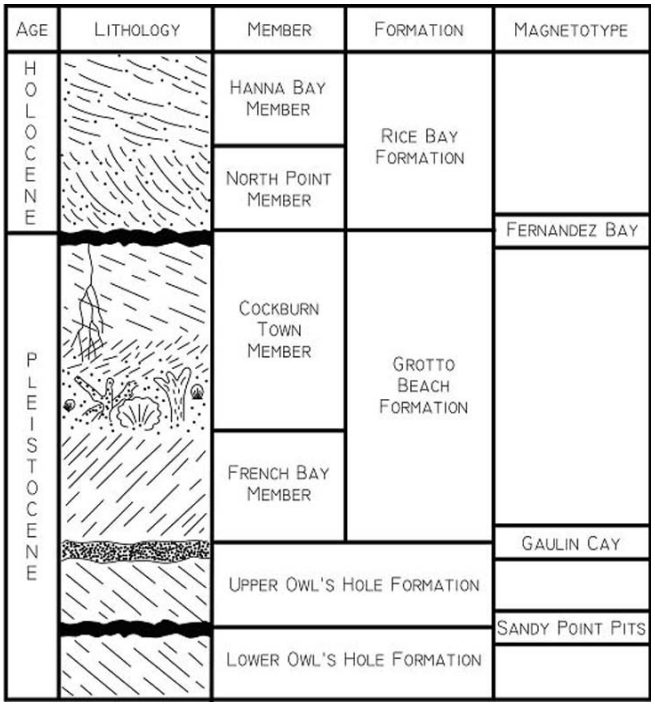

Figure 2. General Stratigraphy of the Bahamas (Modified from Carew and Mylroie, 1997).

Abaco Island is located on Little Bahama Bank and is the most northeastern island in the Bahamian archipelago (Figures 1 and 3). It is bordered on the east by the deep waters of the Atlantic Ocean, on the south by the deep waters of N.W. Providence and N.E. Providence Channels, and on the west by the shallow waters of the Little Bahama Bank (Figure 1). The landmass of Abaco consists of two main islands, Great Abaco Island

and Little Abaco Island, as well as numerous outlying cays (Figure 3).

Figure 3. Map of Abaco Island, Bahamas.

Previous geologic work on Abaco has focused largely on offshore sedimentary processes (Mullins et al., 1984; Mullins, 1983; Mullins and Neumann, 1979; and Neumann and Land, 1975) and coastal geomorphology (Raphael, 1975). Very little work has been conducted on the eolian, beach, and subtidal deposits currently exposed on Abaco. The purpose of this study was to conduct a preliminary reconnaissance of the subaerial geology of Abaco Island in order to determine if the Bahamian field stratigraphy of Carew and Mylroie (1997) is also applicable to Abaco.

METHODS

Preliminary fieldwork, focused mainly on locating important geologic outcrops, was conducted March 11-20, 2005. Initial investigation of the karst and pseudokarst features of Abaco, including flank margin caves, cone karst, karren, blue holes, pit caves, banana holes, and tafoni was also conducted. The remainder of the fieldwork was completed from May 15-June 15, 2005 and consisted of mapping all known flank margin caves, documenting the other karst and pseudokarst features, and classifying the geologic outcrops based on the stratigraphy of Carew and Mylroie (1995b; 1995c; and 1997).

The stratigraphy of Abaco was discerned using parameters that could be identified using field observations. The presence of a *terra rossa* paleosol overlying an eolianite, for example, would demonstrate that deposition of the eolianite was followed by at least one sea level lowstand. Consequently, any eolianite overlain by a *terra rossa* paleosol must be Pleistocene in age. The absence of a *terra rossa* paleosol, however, would indicate a Holocene age. Because the only subtidal deposits currently exposed above modern sea level in the Bahamas must have been deposited during the OIS 5e highstand, any exposed subtidal units must belong to the Grotto Beach Formation.

Internal characteristics of eolianites, such as vegemorph development, are also useful because regressive eolianites have an abundance of vegemorphs while transgressive eolianites do not. The abundance of vegemorphs in regressive eolianites also tends to disrupt fine scale eolianite bedding that is often preserved in transgressive eolianites. Other field observations, such as the presence of wave-cut benches and the relationship of deposits to modern sea level can also be used to help discern the stratigraphic position of an outcrop.

Complex interactions of eolianite deposits, such as onlap of a younger deposit onto an older, can take place and possibly obscure the depositional history (Schwabe et al., 1993; Sparkman-Johnson et al., 2001). In many cases, the exact age and history of a deposit could not be determined with the limited geologic data collected during this study. No interpretation presented here should be considered absolute, as further geologic work on Abaco may result in a better understanding of many of the deposits examined in this study. However, as the interpretations pre-

sented here are based on direct field observations and not subsequent laboratory analyses, they have practical utility for the casual observer. This work should provide a general picture of the geologic history of the island that will aid later, more detailed investigations.

RESULTS

The Owl's Hole Formation

In several locations on Great Abaco Island, including Cherokee, Little Bay, and Little Harbour (Figure 3), an eolianite containing abundant vegemorphs makes up a large portion of the coastline. This eolianite displays truncated foreset beds with a *terra rossa* paleosol draped over the truncations (Figure 4). A similar situation can be observed on several outlying cays including Guana Cay, Elbow Cay, and Man-O-War Cay (Figure 4).

The abundance of vegemorphs preserved in this eolianite show that it was deposited during a sea level regression. The truncated foreset beds show that wave action from a subsequent sea level highstand planed the top surface of the eolianite. The presence of the *terra rossa* paleosol draped over the truncations not only demonstrates that the eolianite is Pleistocene in age, but also that another sea level lowstand followed truncation of the foreset beds.

The sum of these observations allows the stratigraphic position of the eolianite to be determined. The eolianite must be Pleistocene in age, as evidenced by the *terra rossa* paleosol; however, at least two sea level lowstands must have occurred since its deposition. The first lowstand occurred immediately following deposition of the eolianite. Sea level then rose again, causing truncation of the foreset beds by wave energy. During the following lowstand, a *terra rossa* paleosol was developed over the truncations. The eolianite cannot belong to the Grotto Beach Formation, as there has been only one sea level lowstand since its deposition. Thus, the eolianite must belong to the Upper Pleistocene Owl's Hole Formation.

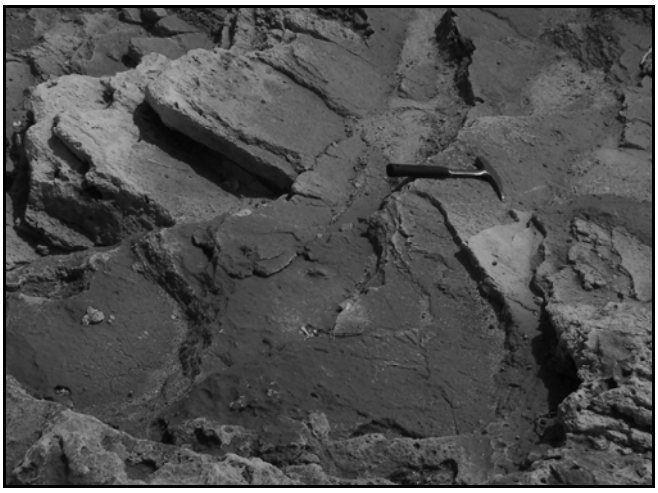

Figure 4. A terra rossa *paleosol (dark grey) deposited over truncated foreset beds on Abaco. Rock hammer for scale.*

The Grotto Beach Formation

At the most southeastern extent of Great Abaco Island there is a long-narrow headland containing a sea arch known as Hole-in-the-Wall. The Hole-in-the-Wall headland is composed of a consolidated eolianite that is covered by a patchy *terra rossa* paleosol. The only vegemorphs present in the eolianite are locally associated with this paleosol. The western side of the headland has a wave-cut bench located a few meters above modern sea level. A boulder coral-rubble outcrop, capped by a *terra rossa* paleosol, is located on this bench (Figure 5). The paleosol on both the eolianite and the coral outcrop indicate both to be Pleistocene in age. However, no paleosol separates the boulder coral outcrop from the underlying eolianite, which implies that they were formed on the same sea level highstand event.

The coral reef rubble outcrop present on the wave-cut bench in these eolianites must belong to the Cockburn Town Member of the Grotto Beach Formation as no other exposed Pleistocene subtidal units are known from the Bahamas. The Cockburn Town corals directly overlie the eolianites making up the headland with no separation by a *terra rossa* paleosol. This is very strong evidence that the eolianites comprising the headland belong to the French Bay Member of the

Grotto Beach Formation. The French Bay Member eolianites were deposited on the initial transgression onto Little Bahama Bank, and were cliffed and notched as sea level continued to rise to the OIS 5e highstand. The coral deposit was then emplaced on this notch during the OIS 5e highstand.

Figure 5. The boulder coral-rubble outcrop. Flashlight for scale.

Exposed subtidal units belonging to the Cockburn Town Member of the Grotto Beach Formation can also be observed along the coast, west of the town of Cedar Harbour (Figure 3). Here, deposits containing oscillation ripples and herringbone crossbedding demonstrate that they were deposited in a subtidal environment. Herringbone crossbedding is also observed in coastal outcrops north and west of Marsh Harbour (Figure 3).

The Rice Bay Formation

One of the most interesting outcrops observed during this study is located on the eastern coast of Great Abaco Island approximately one kilometer north of Lantern Head (Figure 3). It shows a well-consolidated eolianite capped by a thin *terra rossa* paleosol that is overlain by a poorly consolidated eolianite that grades into a modern unconsolidated eolian dune (Figure 6). The upper eolianite is not overlain by a *terra rossa* paleosol.

The lower eolianite is Pleistocene in age as shown by the presence of the *terra rossa* paleosol. However, it is not possible to accurately determine which formation it belongs to (Grotto Beach or Owl's Hole) based on the information available at the outcrop. The upper eoliante must be Holocene in age since it is not capped by a *terra rossa* paleosol. The upper eolianite most likely belongs to the Hanna Bay Member of the Rice Bay Formation because it grades into modern unconsolidated dunes. It also contains vertical structures, possibly related to past vegetation such as palmetto stumps that have been previously described from other outcrops of the Hanna Bay Member (Curran and White, 2001). However, as the outcrop is located several meters above sea level, the definitive evidence for Hanna Bay Member, that of eolian beds grading downward to beach facies at current sea level, cannot be seen. This outcrop is an excellent example of the Pleistocene/Holocene contact on Abaco (Figure 6).

Figure 6. The Pleistocene/Holocene contact on Great Abaco Island. The person is standing on the darker Pleistocene unit. The lighter unit is Holocene in age. A paleosol separates the two units.

Many other examples of the Rice Bay Formation can also be found on Abaco. On Guana Cay, for example, an eolianite is often ob-

served near sea level that is not overlain by a *terra rossa* paleosol. Foreset beds of this eolianite also dip below modern sea level, demonstrating that it was deposited before sea level had reached its current height (Figure 7). This Holocene eolianite belongs to the North Point Member of the Rice Bay Formation and represents rocks deposited on the transgression of the current sea level highstand. Other examples of the Hanna Bay Member, representing the youngest rocks in the Bahamas, include modern beach and eolian dune sands, as well as beach rock. This modern beach rock has bedding planes that are congruent with the present slopes of the beaches on which it is found, showing it was formed under current sea level conditions.

Figure 7. The North Point Member of the Rice Bay Formation, Guana Cay.

Karst and Psuedokarst Features

As a result of this study, 17 flank margin caves were documented and mapped on Abaco Island. Other karst features found on Abaco that are common on other Bahamian islands include pit caves, banana holes, karren and blue holes. The high positive water budget of Abaco has also allowed for intense dissection of Pleistocene eolianite ridges due to karst, fire, and vegetative processes. This dissection has produced landforms bearing a resemblance to tropical cone karst (Figure 8). To date, these eogenetic cone karst landforms have not been described from other Bahamian islands or any other locality worldwide.

Figure 8. Eogenetic cone karst landform on Great Abaco Island.

This study also allowed for the first documentation of tafoni caves in the Bahamas. Tafoni are psuedokarst voids that are typically formed by wind and salt erosion (Huinink et al., 2004). Tafoni form in a variety of rock types and are common on rocky coasts that are exposed to spray, waves, and wind (Sunamura, 1996). The tafoni caves on Abaco (Figure 9) are found in Pleistocene eolianite cliffs between 10 and 23 meters above modern sea level. They form when wave action on eolianite ridges removes the hard, calcrete crust and exposes the soft interior of the ridge to attack by coastal processes. Similar voids have been observed on other Bahamian islands such as San Salvador (Figure 10).

The presence of psuedokarst voids such as tafoni demonstrates the need for caution when using caves as sea level indicators. Flank margin caves currently exposed in the Bahamas are known to form by mixing dissolution in association with sea level highstands (Mylroie and Carew, 1995a). As a result, flank margin caves are found in continuous horizons and show evidence of phreatic dissolution such as large dissolutional cusps and bellholes. The tafoni caves on Abaco are not found in a continuous horizon (Figure 9)

and show surfaces shaped by mechanical rather than chemical processes. It is important not to mistake tafoni and other psuedokarst voids as flank margin caves, especially when using flank margin caves as sea level indicators. While tafoni may form in association with wave action, they do not mark previous sea level positions. Only flank margin caves have implications for past sea levels.

Figure 9. Tafoni voids on Great Abaco Island.

Figure 10. Tafoni void on San Salvador Island.

CONCLUSIONS

The field stratigraphy of Carew and Mylroie (1995b; 1995c; and 1997) is applicable to Abaco Island and each of the three major depositional packages can be observed. Further work on Abaco will lead to a better understanding of the geologic history of the island. Typical karst features that are found on other Bahamian islands, including flank margin caves, blue holes, pit caves, karren, and banana holes, are also common on Abaco.

The wet climate of Abaco as compared to other islands in the Bahamas has allowed for a higher degree of dissection of Pleistocene eolianite ridges than is seen elsewhere. This dissection takes place by a combination of karst, fire, and vegetative processes. The resulting landforms resemble tropical cone karst. Such eogenetic cone karst landforms have not been previously described. Tafoni caves on Abaco are psuedokarst voids that form by mechanical erosion of exposed eolianite ridge interiors. The presence of such features demonstrates the need for caution when using caves as sea level indicators. Tafoni and other psuedokarst voids may be mistaken as flank margin caves by the untrained observer. Only flank margin caves have implications for past sea levels.

ACKNOWLEDGMENTS

The authors would like to thank the Karst Waters Institute, Total SA, and Mississippi State University for providing the funding that made this study possible; the Bahamian government for providing the research permit; Friends of the Environment, Marsh Harbour, Abaco for providing logistical support; all of the residents of Abaco Island that made this study possible, particularly Nancy and Michael Albury, Anita Knowles, Allison Ball, Diane Claridge, and David Knowles; and Brenda Kirkland and Grady Dixon of Mississippi State University for all of their insights and comments during the initial development of this manuscript.

REFERENCES

Carew, J.L., and Mylroie, J.E., 1997, Geology of the Bahamas, *in* Vacher, H.L., and Quinn, T.M., eds., Geology and Hydrogeology of Carbonate Islands: Developments in Sedimentology 54, Elsevier, p. 91-139.

Carew, J.L., and Mylroie, J.E., 1995a, Quaternary Tectonic Stability of the Bahamian Archipelago: Evidence from Fossil Coral Reefs and Flank Margin Caves: Quaternary Science Reviews, v. 14, p. 145-153.

Carew, J.L., and Mylroie, J.E., 1995b, Depositional Model and Stratigraphy for the Quaternary Geology of the Bahama Islands, *in* Curran, H.A., and White, W.B., eds., Terrestrial and Shallow Marine Geology of the Bahamas and Bermuda: Geological Society of America Special Paper 300, p. 5-32.

Carew, J.L., and Mylroie, J.E., 1995c, Geology and Karst Geomorphology of San Salvador Island, Bahamas: Carbonates and Evaporites, v. 10, no. 2, p. 193-206.

Curran, H.A., and White, B., 2001, Ichnology of Holocene carbonate eolianites of the Bahamas, *in* Abegg, F.E., Harris, P. M., and Loope, D.B., eds., Modern and Ancient Carbonate Eolianites: Sequence Stratigraphy and Diagenesis: Tulsa, SEPM (Society for Sedimentary Geology) Special Publication No. 71, p. 47-56.

Huinink, H.P., Pel, L., and Kopinga, K., 2004, Simulating the Growth of Tafoni: Earth Surface Processes and Landforms, v. 29, p. 1225-1233.

Illing, L.V., 1954, Bahamian Calcareous Sands: Bulletin of the American Association of Petroleum Geologists, v. 38, p. 1-95.

Mullins, H.T., 1983, Modern Carbonate Slope and Basins in of the Bahamas, *in* Cook, H.E., Hine, A.C., and Mullins, H.T., eds., Platform Margin and Deepwater Carbonates: Society of Economic Paleontologists and Mineralogists, Short Course no. 12, p. 4.1-4.138.

Mullins, H.T., Heath, K.C., Van Buren, H.M., and Newton, C.R., 1984, Anatomy of Modern Open-Ocean Carbonate Slope: Northern Little Bahama Bank: Sedimentology, v. 31, p. 141-168.

Mullins, H.T., and Lynts, G.W., 1977, Origin of the Northwestern Bahama Platform: Review and Interpretation, Geological Society of America Bulletin, v. 88, p. 1447-1461.

Mullins, H.T., and Neumann, A.C., 1979, Deep Carbonate Bank Margin Structure and Sedimentation in the Northern Bahamas, *in* Doyle, L.J., and Pilkey, O.H., eds., Geology of Continental Slopes: Special Publication of the Society of Economic Paleontologists and Mineralogists no. 27, p. 165-192.

Multer, H.G., 1977, Field Guide to Some Carbonate Rock Environments, Florida Keys and Western Bahamas, Kendall/Hunt, Dubuque, 417 p.

Mylroie, J.E., and Carew, J.L., 1995, Karst Development on Carbonate Islands, *in* Budd, D.A., Saller, A.H., and Harris, P.M., eds., Unconformities and Porosity in Carbonate Strata: AAPG Memoir 63, American Association of Petroleum Geologists, Tulsa, Oklahoma, p. 55-76.

Neumann, A.C., and Land, L.S., 1975, Lime Mud Deposition and Calcareous Algae in the Bight of Abaco, Bahamas: A Budget: Journal of Sedimentary Petrography, v. 45, p. 763-786.

Raphael, C.N., 1975, Coastal Morphology; Southwest Great Abaco Island, Bahamas: Geoforum, v. 6, p. 237-246.

Sparkman-Johnson, S.D., Carew, J.L., and Mylroie, J.E., 2001, The Surficial Geology of the Hard Bargain Area, San Salvador Island, Bahamas, *in* Carney, C.K., and Greenstein, B.J., eds., Proceedings of the Tenth Symposium on the Geology of the Bahamas and other Carbonate Regions: Gerace Research Center, San Salvador Island, Bahamas, p. 67-77.

Schwabe, S.J., Carew, J.L., and Mylroie, J.E., 1993, The Petrology of Bahamian Pleistocene Eolianites and Flank Margin Caves: Implications for Late Quaternary Island Development, *in* White, B., ed., Proceedings of the Sixth Symposium on the Geology of the Bahamas: Port Charlotte, Florida, Bahamian Field Station, p. 149-164.

Sunamura, T., 1996, A Physical Model for the Rate of Coastal Tafoni Development: Journal of Geology, v. 104, p. 741-748.

Tucker, M.E., and Wright, P.W., 1990, Carbonate Sedimentology: Blackwell Scientific Publications, Oxford/London, 482 p.

DISCOVERY OF "THREE ROSES CAVERN," A SUBMERGED HORIZONTAL CAVE SYSTEM ON SAN SALVADOR ISLAND, BAHAMAS

Eric S. Cole, John Campion, Chris Hallgren, and Daniel White
Biology Department
Saint Olaf College
Northfield, MN 55057
colee@stolaf.edu

Sandy Voegeli and Vincent Voegeli
Gerace Research Centre
San Salvador Island, Bahamas

ABSTRACT

A new, underwater cavern system was discovered in a little-known pond on San Salvador Island. The pond was given the name "Merman" Pond because of its proximity to Mermaid Pond. The cavern was named "Three Roses Cavern." This study was undertaken to describe general geologic and biotic characteristics of Three Roses Cavern. In summary, Three Roses may be unique on San Salvador because it harbors fish species that typically inhabit shallow back-reef environments, suggesting that the conduit opens either into neighboring Pigeon Creek, or the more physically remote back-reef environment off the southeastern shore of San Salvador Island.

INTRODUCTION

Merman Pond is an interior pond located on the Montreal Settlement at the southeastern end of San Salvador Island, Bahamas (Figure 1). Landsat infrared images suggest that this pond is "cool" (1985 Landsat Thematic Mapper, Infrared Satellite Image of San Salvador, from the former Gerace Research Center Website). During January, 2006, we cleared a trail to this pond and performed casual snorkel and SCUBA reconnaissance. We returned in March, 2006, and again in January and June, 2007. The pond is generally shallow, less than a meter in most places, deepening to about 1.5 meters towards the center (depending on the tide). Despite being separated from Pigeon Creek by a carbonate dune, and lying 1.4 km from the ocean, Mermaid Pond is clearly tidal, exposing 20-30 meters of carbonate shoreline at low tide.

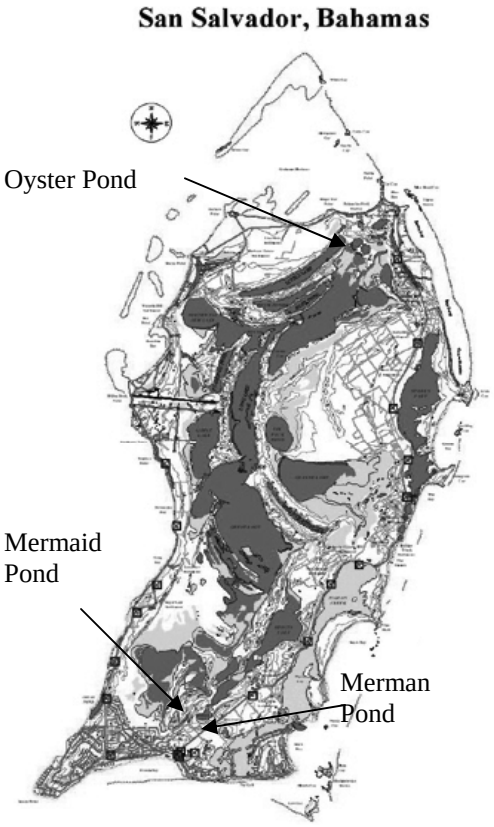

Figure 1. Map of San Salvador Island showing location of Merman Pond. From: Robinson and Davis, 1999, San Salvador Island GIS Database. University of New Haven and Gerace Research Centre.

Figure 2. Google Earth™ close-up of Merman Pond showing location of sinkhole.

The high-tide line is marked by a rich red and black mangrove community whose roots are completely exposed at low tide. In the center of the pond is a sinkhole with a sizable horizontal cave entrance in its eastern wall. The "sink-hole" appears to be the result of a collapse in the carbonate pond bottom (Figure 2). This hole is approximately 30-40 meters across, and exhibits a sloping floor, high in the west, and sloping to a depth of 4.5 meters in the east. Here, the "ramp" encounters a vertical wall; it is at the base of this wall that Three Roses Cavern opens. What is remarkable about this system is that the cavern and the adjoining sink-hole appear to be serving as a refuge for schools of fish that are more typical of a back- reef or tidal creek environment. We explored the cave (within the limits of our non-technical expertise), and the surrounding land and waters to try and account for the source of these reef-fish

within an otherwise shallow, marine-pond environment.

METHODS

To survey the biodiversity within the cavern opening, we employed both snorkel and SCUBA. We also used a Nikonos 35 mm underwater camera, and a Hydrolab Quanta™ water chemistry probe. We deliberately entered the cavern at times between low and high tide (there was very little tidal lag between this pond and the coast) so that the current was pushing against us as we swam into the opening, rather than drawing us into the cavern. This also allowed the tide to flush debris from the cavern, resulting in heightened visibility. Inside the cavern, we used underwater photography and videography techniques supplemented with visual identification to confirm the presence of various species of fish. We also collected a sample of one of three sponge species covering the cavern walls, and a resident goby for identification using a "slurp gun". We measured the dimensions of the first two cavern chambers using a 30 m tape measure. To survey the depth of the drop-off at the back of the second chamber, we lowered the tape measure down until it hit bottom and recorded the distance. We also used an underwater compass to determine the orientation of the cavern. Back at the Gerace Research Centre, we used hydrochloric acid and a light microscope to examine the tissues of living sponge sample.

RESULTS

Physical Characteristics

Merman Pond is probably protected from hurricane events by its small size (wave propagation is minimal), a dense, contiguous mangrove shoreline, and a shallow carbonate ridge separating it from the southern backwaters of Pigeon Creek, 115 meters to the east. The pond is tidal, rising and falling 1-2 meters. Salinity typically ranges from 34.6-35.1 g/Liter (TDS) although following an unusually heavy spring rain in 2007, salinity plunged to 14.1 g/L suggesting that it serves as a rainwater catchment for a large surrounding area, and rainfall can over whelm its tidal turnover. Other physical characteristics (Table 1) suggest that Merman is typical of inland ponds on San Salvador that are served by open conduits to the sea. In short, the water resembles seawater. The pond is located at latitude 23° 57.686' north by, longitude 74°30.560' west. The center of the pond features a large sinkhole that contains the entrance to Three Roses Cavern.

Table 1. Physical Characteristics of Several Inland Ponds on San Salvador Island. Data from Quanta Probe Measurements, January 07.

	Merman	Mermaid	Oyster
TDS (g/L)	35.1	34.5	34.8
Temp (C)	26.9	25.7	25.5
pH	7.9	7.73	7.49
ORP (mV)	283	283	324
dO (%)	98.6	86.1	67.2

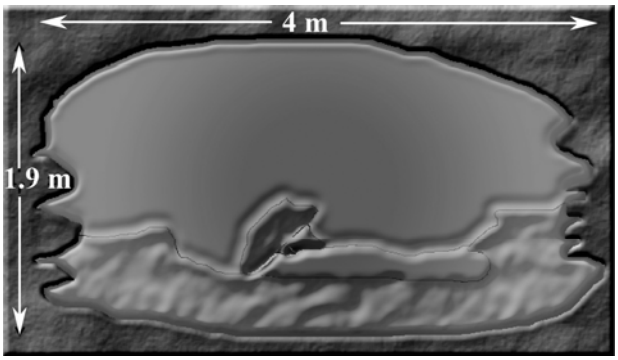

Figure 3. A diagrammatic sketch of the entrance to Three Roses Cavern.

As Figures 3-5 indicate, the sinkhole is approximately 4.3 m deep at its deepest. The sinkhole appears to have formed from a collapsed carbonate platform that slopes gently from west to east. At the eastern end, the sloping floor of the sinkhole intersects a vertical cliff face. At the bottom of the cliff face lies the cavern opening, 4 m wide and 1.9 m tall that faces 230 degrees west by southwest. The first

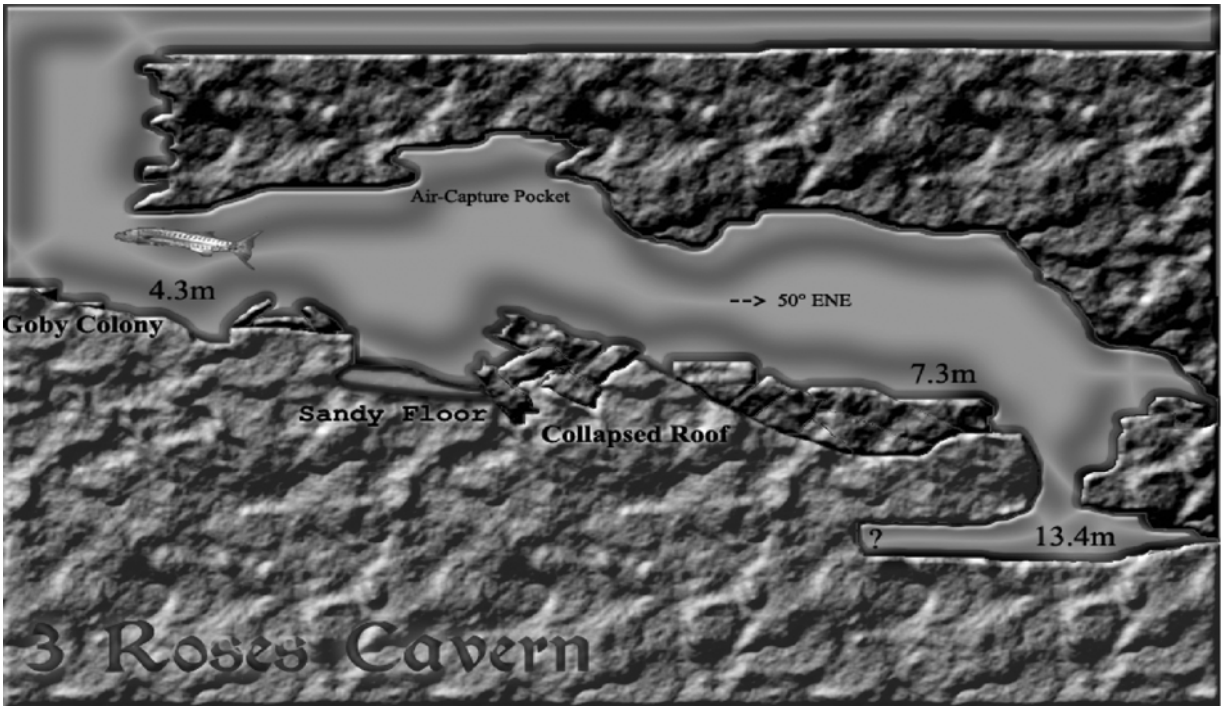

Figure 4. A lateral view sketch of Three Roses Cavern. (Barracuda sighting is indicated).

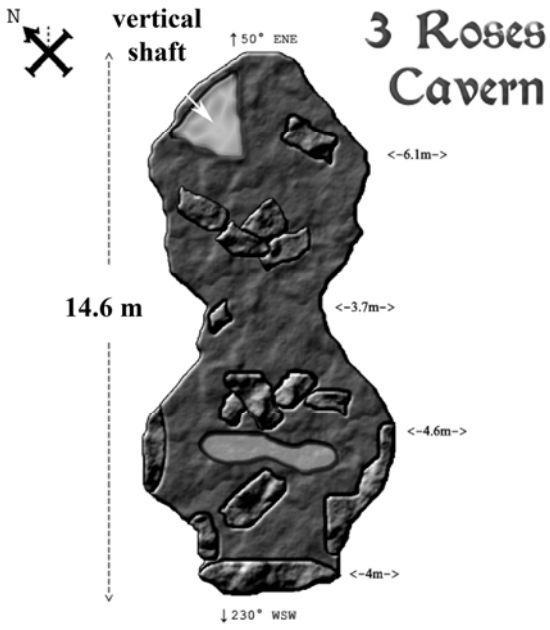

Figure 5. A top-down view of the explored area of Three Roses Cavern.

chamber widens to 4.6 m and features a hard carbonate floor littered with collapsed roof slabs further inside.

We noticed no conspicuous speleothems, although this could be due to the fact that much of the cavern roof has collapsed in sheets, obscuring both original floor features and ceiling features. The cavern narrows to 3.7 m briefly, then opens up to the 6.1 m wide second chamber that descends to a depth of 7.3 m. At the back of the second chamber, a narrow passage drops vertically to 13.4 m and possibly curves back under the main chamber into an unexplored area. The tide was monitored and a slack tide seemed to occur in synchrony with the coastal change in tide.

Biotic Characteristics of Merman Pond

The shoreline of Merman Pond is a rich (though narrow) mangrove composed of both red and black mangroves (*Rhizophora mangle* and *Avicennia germinans*). The *Rhizophora* prop-roots are unusually devoid of epizooitic life. This makes sense when observed at low tide when the prop-roots are completely exposed along with 20-30 meters of carbonate pond bottom.

The pond bottom is a smooth carbonate loosely covered with a mixture of shallow flocculent sediment, and molluscan shell hash. The most common living invertebrates include gastropods (*Battilaria minima* and *Cerithium lutosum*), bivalves (*Tellina*, *Polymesoda maritima*, and *Anomalocardia auberiana*) and occasional lugworms (*Arenicola*) among other polychaete annelids. These organisms are also common to both Oyster Pond, and Mermaid Pond.

In the shallows, the most common vertebrates include two small pond fish the Sheepshead Minnow (*Cyprinodon variegatus*) and the Bahamian Mosquitofish (*Gambusia manni*) species that are commonly found in other inland ponds on the island as well (Godfrey et al., 1994). Near the northeastern end of the pond, the bottom changes to shell hash and an unidentified species of halfbeak (*Hemiremphidae*) may be found swimming in the shallows. Juvenile halfbeaks, less than a centimeter in length, were also sighted in March, 2006, suggesting that these typically coastal fish are breeding in Merman Pond. Halfbeaks have never before been reported in the inland ponds of Sand Salvador Island.

Biotic Characteristics of 3-Roses Cavern

We identified five species of reef fish living in the sinkhole and cavern opening, the Grey Snapper (*Lutjanus griseus*) (a single individual), and schools of Schoolmaster Snappers (*Lutjanus apodus*) and Yellowfin Mojarra (*Gerres cinnereus*) (Figure 6). A colony of Crested Gobies (*Lophobogius cyprinoides*) exist just outside the cavern entrance, making homes in the gravely bottom, and a single Great Barracuda (*Sphyraena barracuda*) was sighted hovering just outside the cavern entrance. Crested Gobies have never before been reported on San Salvador. Within the cave itself, sponge specimens were abundant on floor and ceiling. We observed through a light microscope that our sponge sample contained both proteinaceous spongin and silicaceous spicules (resistant to HCl treatment) suggesting species of the Class Demospongiae.

a.

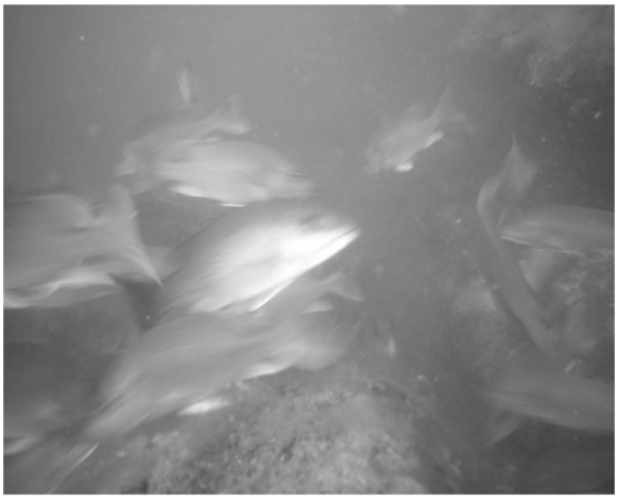

b.

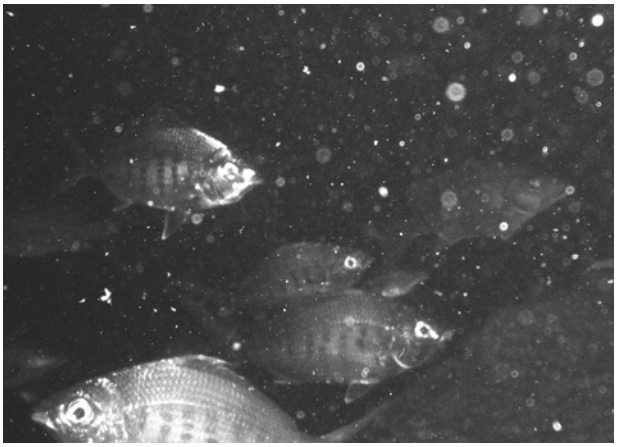

c.

Figure 6. Reef fish found in 3-Roses Cavern. a) Schoolmaster snappers and b) a gray snapper (center) at the mouth of 3 Roses cavern. c) a school of Yellowfin Mojarra just inside 3 Roses Cavern. These rarely came out into the well of the sinkhole.

Most of these fish species have never before been found in other inland ponds on the island. The unique biodiversity in this pond appears to be a byproduct of its extraordinary hydrology.

Source of the Reef Fish

We considered three hypotheses regarding the origins of these fish--1) Storm surge might have carried fish across the ridge from Pigeon Creek during past hurricane activity, 2) the cavern may open onto a point of ingress from some location on Pigeon Creek, or 3) the cavern may open onto the back-reef environment of the outer coast. To test these hypotheses we cleared a trail from the eastern most point on Merman Pond into Pigeon Creek (a distance of 115 meters). We were able to trace storm debris up the east-facing slope of the ridge that separates the two water bodies, but found that debris stopped well short of the ridge top. By no means definitive, this does suggest that, at least recently, storm-surge probably did not populate our pond with fish.

This leaves the cavern as the most likely source of fish migration into Merman Pond. Given the shallow water habits of the cavern's occupants, either an open coast back-reef environment or Pigeon Creek seem likely candidates for the entrance. We canoed most of the Pigeon Creek area closest to Merman Pond and found no evidence of an entrance, in fact the creek bottom is deep with loose carbonate sand marked by callianassid shrimp mounds. However, during our June, 2007 visit, and acting on advice from John Winters, we discovered another large sinkhole in Pigeon Creek (Figure 7) with submerged vertical cave shafts opening onto a horizontal cave system at 12 m depth (See White, et al., 2006). We are still left to contemplate the open coastline (1.4 km away) as a possible outlet for both cavern systems (Figure 7). The Pigeon Creek conduit had been noted earlier by Kenny Buchan, former director of the GRC, in his PhD dissertation (2005).

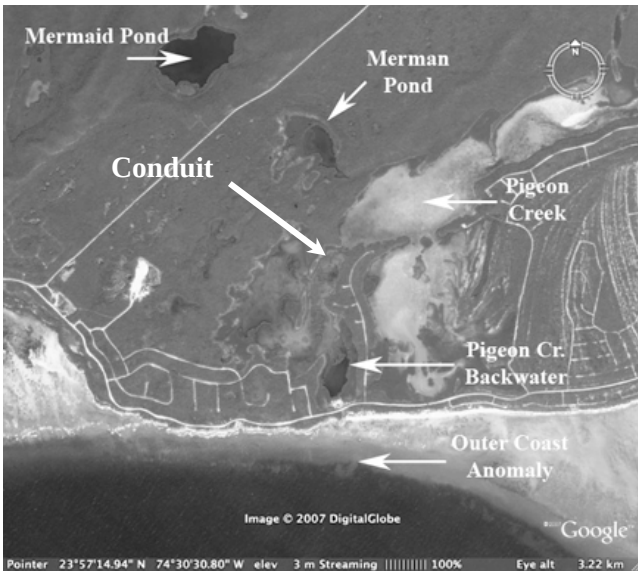

Figure 7. GoogleEarth™ image of Merman Pond, 3-Roses Cave, and adjacent Pigeon Creek with its conduit indicated.

DISCUSSION

Since Merman Pond is tidal and fully marine, and no other openings have been found, the cavern system acts as the sole conduit, exchanging water with the ocean tide. The absence of any notable tidal lag and sizable populations of reef fish (including a well grown barracuda) suggest an unusually large cave passageway. There are several possibilities as to where this cavern opens, either on the oceanic cliff structure known as "the wall," in the back-reef environment, or in the shallow, tidal mangrove habitat of Pigeon Creek. Since manual exploration of the cave is dangerous and impractical, we turned to the fish species sighted inside the cavern (and their habits) to shed light upon the location of the opening.

Since the Bahamian *Gambusia* and *Cyprinodon* are commonly found in marine ponds throughout the Bahamas (Bohlke and Chaplin 1968), they are likely the result of dispersal processes common to all the inland ponds, and unrelated to the cavern.

The Crested Goby, never before sighted on San Salvador, is fairly hardy and inhabits a

range of environments, from tidal creeks and patches of eroded limestone to brackish inland lakes and ponds or mangrove swamps (Bohlke and Chaplin, 1968). In a later reconnaissance of the Pigeon Creek conduit, crested gobies were also found in the surrounding shallows.

The Yellowfin Mojarra and Gray Snapper reveal slightly more. The Gray Snapper, although not generally found in ponds, frequents rocky areas, coral reefs, dock structures (Randall, 1968) and tidal creeks bordered by mangroves (Bohlke and Chaplin, 1968). The Yellowfin Mojarra on the other hand occurs in tidal creeks, rocky surf zones (Bohlke and Chaplin, 1968) and nearby coral reefs (Humann, 1989). The Yellowfin Mojarra prefers depths of 1-12 m (Humann, 1989) while the Gray Snapper frequents depths of 1-18 m (Humann, 1989). This indicates that the conduit entrance is likely within a tidal creek, coral back-reef, or rocky shallow habitats between 1-12 m deep.

The presence of the Great Barracuda inside the cavern does little to tighten this depth range, or indicate a particular habitat, since Barracuda inhabit a wide range of marine environments and are found anywhere between 0-18 m deep (Humann, 1989). However, the presence of the Barracuda does serve as a striking reminder that the cavern must lead to a remarkably different environment, since Barracuda are quite out of place in a shallow inland pond.

The presence of the Schoolmaster and Halfbeaks provide us with our final clues. Schoolmasters frequent coral reefs (Randall, 1968) but are also commonly found in tidal creeks lined with mangroves (Bohlke and Chaplin, 1968) and generally prefer depths between 3 and 24 m (Humann, 1989). Half-beaks on the other hand, are generally inshore surface dwellers, not often found far out to sea (Bohlke and Chaplin, 1968). This narrows the likely depth of the cavern exit to 3-6 m, deep enough for the Schoolmasters, but shallow enough for the Halfbeaks.

Further, the conduit exit must be located near a shoreline with easy access to deeper waters, and may likely be a tidal creek or a back-reef environment, since many of the fish we identified are common in that habitat. This leads us to believe that the conduit leads either to nearby Pigeon Creek, a large, thriving tidal creek environment with nearby coral reefs or a shallow backreef environment on the outer coast. Anecdotal accounts report sightings of most of these fish in Pigeon Creek. Our most recent visit also uncovered a likely candidate for an outlet to Three Roses Cavern, within neighboring Pigeon Creek (White, et al., 2006). It remains possible that fish have entered Merman Pond through multiple paths, both through the conduit and overland from Pigeon Creek during unusually harsh Hurricane storm surges.

The structure of Three Roses Cavern, (and the neighboring Pigeon Creek Conduit) are similar, and invite comparison. Each appears to have been breached by a collapsed carbonate roof, creating a sink-hole exposing what once must have been a broad cave chamber with a floor 4-7 meters below current sea level. In both cases, vertical shafts connect this upper horizontal cave system with a deeper horizontal chamber 12-13 meters below current sea level. Tidal currents at the mouth of each cave suggest that both systems must still open out to the sea (unpublished observations).

Cave morphology has been much studied on San Salvador Island, and two models have been proposed to account for their formation: the “flank margin” model in which carbonate dissolution occurs most aggressively at the edges of freshwater haloclines due predominantly to chemical processes (Pace, et al., 1992; Mylroie, et al., 2004; Roth et al., 2006), and a “bioerosion” model in which haloclines serve to trap organic matter, and microbial respiration acidifies the water increasing its dissolution capacity at this carbon-rich interface (Schwabe et al., this volume). If carbonate dissolution at a halocline was involved, then both Three Roses Cavern and her sister, the Pigeon Creek Conduit, must have been formed during multiple periods of lower interglacial sea-level. It is to be hoped that further study will reveal more of the dynamics of these submarine cave systems, and the geologic history of their formation.

ACKNOWLEDGMENTS

We would like to sincerely thank Dr. Donald T. Gerace, Chief Executive Officer, and Tom Rothfus, Executive Director of the Gerace Research Center, San Salvador, Bahamas for their rich encouragement and support. We had help from St. Olaf students: Megan Bona, Nathan Caple, Brennan Decker, James Morrison, Keisha Sedlacek, Nick Spanel, Chris Torstenson, and Sheryl West. We also wish to acknowledge Karna and Anastasia Campion, for their support both on the home-front and in the field, and a special thanks to Kathleen Rose Stuart, Atia Rose Cole, and Liana Rose Cole (*our 3 Roses*) for supporting these expeditions and adventures.

REFERENCES

Bohlke, J.E. and Chaplin, C.C.G., 1968, Fishes of the Bahamas and adjacent waters: University of Texas Press.

Godfrey, P.J., Edwards, D.C., Smith, R.R., and Davis, R.L., 1994, Natural History of Northeastern San Salvador Island: Bahamian Field Station, p. 17.

Humann, P., 1989, Reef fish identification: New World Publications, p. 46-49.

Mylroie, J.E., Mylroie, J.R., and Jenson, J.W., 2004, Modeling carbonate island karst, *in* Lewis, R.D., and Panuska, B.C., eds., Proceedings of the Eleventh Symposium of the Geology of the Bahamas and Other Carbonate Regions: Gerace Research Center, San Salvador, Bahamas, p. 135-144.

Pace, M.C., Mylroie, J.E., and Carew, J.L., 1992, Investigation and review of dissolution features on San Salvador Island, Bahamas, *in* White, B., ed., Proceedings of the Sixth Symposium of the Geology of the Bahamas: Bahamian Field Station, San Salvador, Bahamas, p. 109-23.

Randall, J.E., 1968, Caribbean reef fishes: T.F.H. Publications, pp. 122-123, 157.

Robinson, M.C., and Davis, R.L., 1999, Downloadable GIS topographic map: University of New Haven and Bahamian Field Station.

Roth, M.J., Mylroie, J.E., Mylroie, J.R., Ersek, V., Ersek, C.C., and Carew, J.L., 2006, Flank margin cave inventory of the Bahamas, *in* Davis, R.L., and Gamble, D., eds., Proceedings of the Twelfth Symposium of the Geology of the Bahamas and Other Carbonate Regions: Gerace Research Center, San Salvador, Bahamas, p. 153-161.

Schwabe, S.J., Herbert, R.A., and Carew, J.L., 2008, A hypothesis for biogenic cave formation: a study conducted in the Bahamas, *in* Park, L.E. and Freile, D., eds., Proceedings of The Thirteenth Symposium on the Geology of the Bahamas and other Carbonate Regions. Gerace Research Center, San Salvador, Bahamas, This Volume, p. 141-152.

White, D.A., Campion, J., and Cole, E.S., 2006, Characterization of three roses cavern and its accompanying conduit system on San Salvador Island, Bahamas: an inland refuge for coastal fish, in Davis, Proceedings of the Twelfth Symposium on the Natural History of the Bahamas: Gerace Research Center, San Salvador, Bahamas.

CAVE AND KARST INVENTORY OF THE PRIMEVAL FOREST, NEW PROVIDENCE ISLAND, BAHAMAS: UNEXPECTED DISCOVERIES

John E. Mylroie, Joan R. Mylroie, Athena M. Owen, and Willapa J. Waterstrat
Department of Geosciences
Mississippi State University
Mississippi State, MS 39762
mylroie@geosci.msstate.edu

ABSTRACT

The Primeval Forest, a new Bahamian national park, is located on the west side of New Providence Island, Bahamas. The small site, 3.5 hectares (8.6 acres), contains a rare high-canopy forest that has escaped development. The park was named for the presence of old forest and plant life. The karst features of the park made the area impossible to use for agriculture, which preserved the older plant life. The relatively unspoiled nature of the site was instrumental in motivating the creation of the park by the Bahamas National Trust to preserve the landscape and its biological contents. The park trends from highest elevation in the northwest, on the side of an eolian ridge, dropping to a low plateau or bench to the southeast, which in turn becomes a flat lowland. The bench portion of the park is riddled with numerous pits, caves, natural bridges, sinkholes, and banana holes. The Trust commissioned a cave and karst inventory to document the extent of the physical resources within the park.

The initial strategy was to survey what was thought to be a series of independent karst features. As such, the survey began in a banana hole, but connections were found to nearby features, and 122 stations subsequently were set in this initial cave. A second team surveyed a surface baseline, from which stations were established at 102 prominent karst features for permanent identification. The karst feature density, one of the highest ever seen in the Bahamas, was unexpected, at approximately 19.4 karst features per acre or 49.7 per hectare. Also unexpected was the degree of connectivity of karst features. These features occurred at a variety of elevations as phreatic tubes, but followed the strike (NE-SW) of the low bench. The bench drops to the SE into a series of low karst valleys that are the result of the coalescing collapse of pits, caves and banana holes. The final unexpected discovery was the herringbone cross bedding, and the trace fossils *Ophiomorpha* sp. and *Conichnus conicus* in pit and cave walls. Based on current understanding, these sub-tidal indicators identify the rocks as the Cockburn Town Member of the Grotto Beach Formation, Late Pleistocene in age. The phreatic passages seen in the caves are syngenetic, as both the rock and the fresh-water lens position were produced by the last interglacial sea-level high-stand, Oxygen Isotope Substage 5e, ~125 ka.

INTRODUCTION

On February 16, 2006, at the request of Mr. Eric Carey of the Bahamas National Trust, an initial reconnaissance of the Primeval Forest property in western New Providence Island (Figure 1) was completed. That investigation indicated that the Primeval Forest has an unusual array of cave and karst features that are unique in The Bahamas. It was recommended that because of the strong interaction between the cave and karst landscape, the flora and fauna, and the bedrock geology, that a full cave and karst resource inventory be undertaken.

SURVEY

The initial cave and karst resource inventory was conducted during March 11-18, 2006. The initial survey placed 125 underground survey stations, 102 karst features stations, and 38

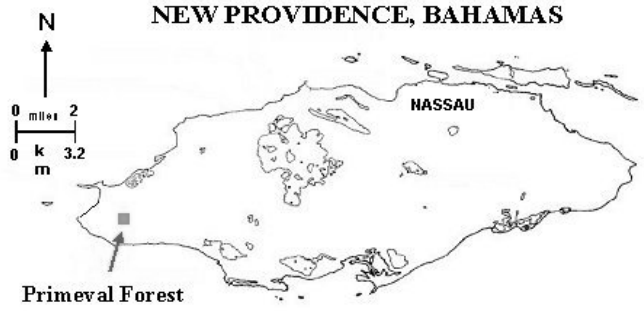

Figure 1. Map of New Providence Island, Bahamas, showing location of the Primeval Forest.

surface survey stations. The survey stations were placed at varying intervals to encompass the individual cave area, as well as facilitate shots into the next cave section (Figure 4). Permanent markers were placed on the karst features resulting from the karst survey, for future identification.

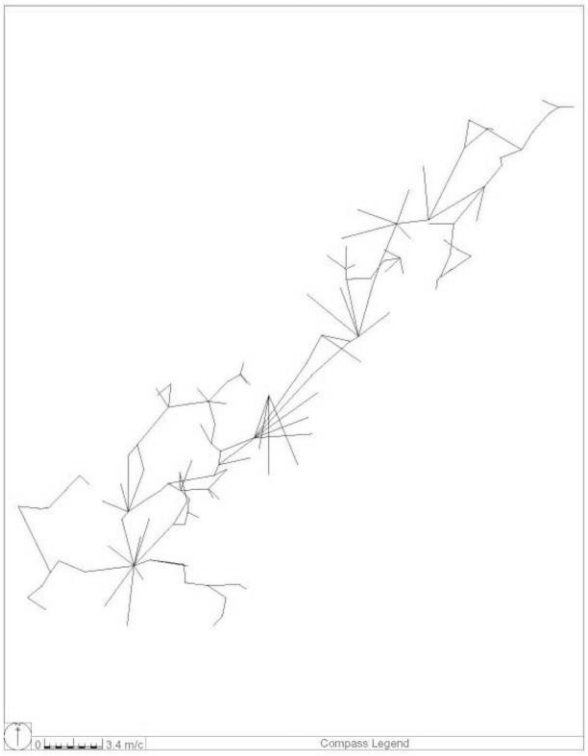

Figure 2. "A" survey showing line plots. North is to the top.

The unexpected result of this effort was the "A" survey--a complex cave system that was originally thought to be two small, interconnected banana holes. This survey was initiated in the first natural bridge cave on the main trail from the parking area into the Primeval Forest. What was originally thought to be the interconnected banana holes ended up being part of a single cave system that continued for 125 stations before all components were finally linked to the survey (Figures 2 and 3). Connectivity of this level is highly unusually and has not been described anywhere else in the Bahamas.

A second survey effort was mounted between May 24-31, 2006, during which an additional 65 surface karst features were linked to the surface survey that was extended by 39 stations (Figure 4). An additional 60 stations were placed in a series of small caves and pits, none of which showed the complex connections found in the "A" survey nor connected to the original "A" survey from March. The results of both surveys were shown in cave maps of the surface openings, the "A" survey cave, and the independent cavelets that were surveyed. A series of these finished maps are shown in Figures 5-9. The most significant of these is Bat Cave (Figure 5), which runs from Karst Station 152 southwest past Karst Station 136 (see Figure 4). A small bat colony of an unknown species exists in the southwest portion of the karst feature. This was the only feature in the park found to contain bats.

The inventory completed on May 31, 2006 is believed to have located and assessed the vast majority of the cave and karst features located in the Primeval Forest (Figure 4). The cave and karst features are concentrated in the northwestern half of the Forest, where the elevation is higher. Isolated features, mostly of small size, approximately a meter or less, were found in the southeastern half of the Forest. They were not surveyed individually or tied into the surface survey grid, due to a lack of time.

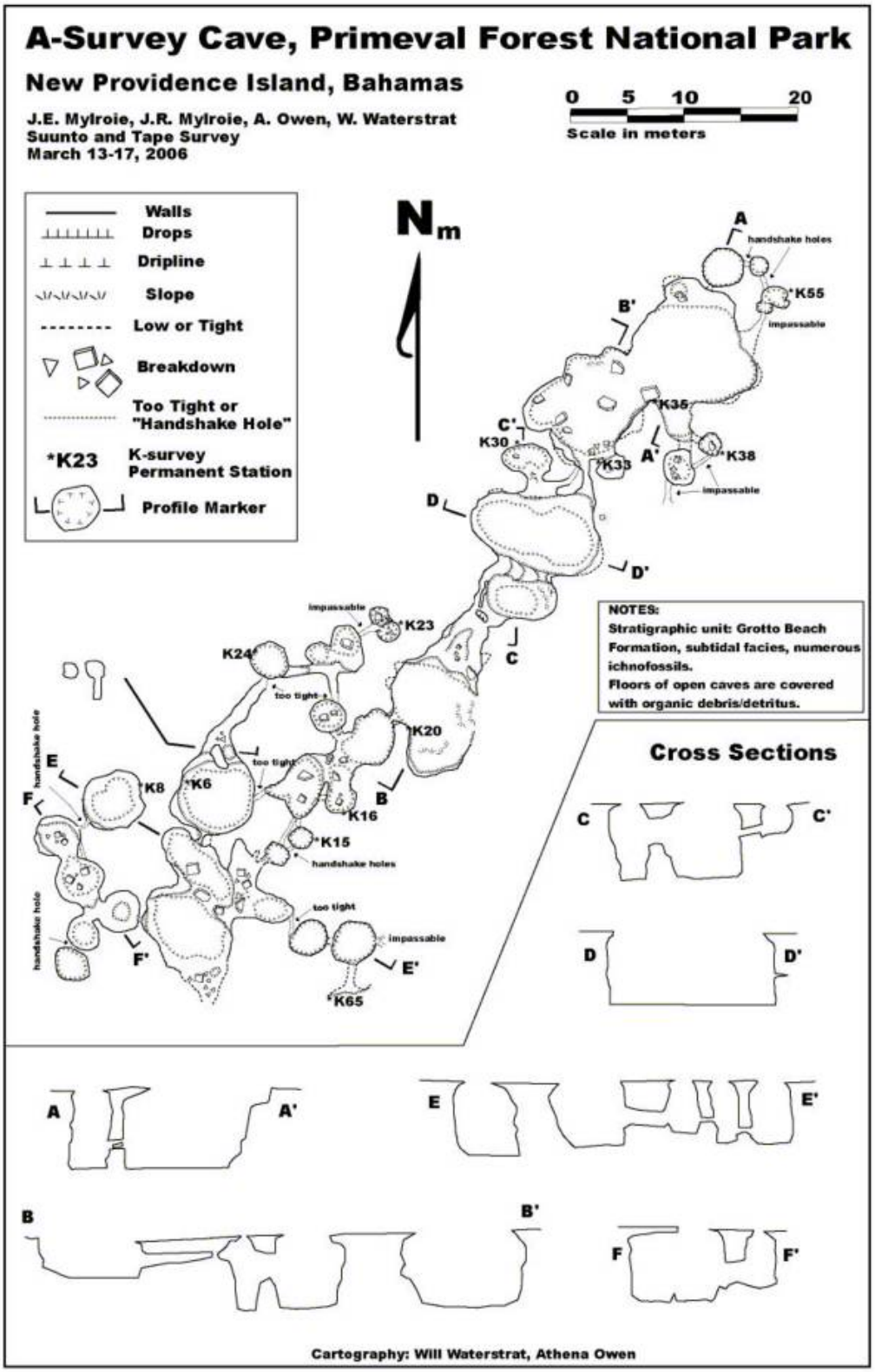

Figure 3. Final Map of the "A" Survey Cave.

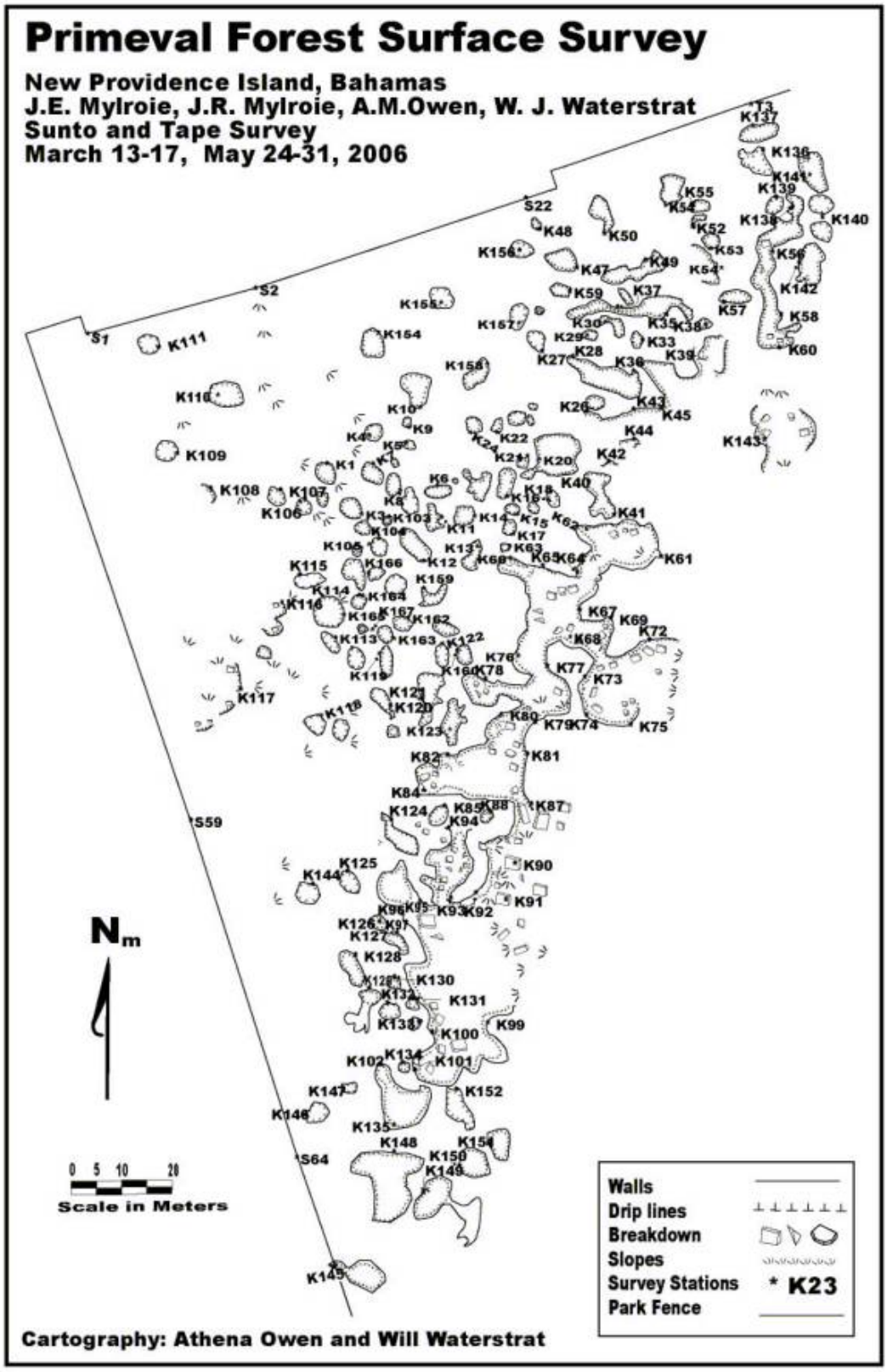

Figure 4. Surface Survey, showing all identified karst features, and portion of the boundary fence.

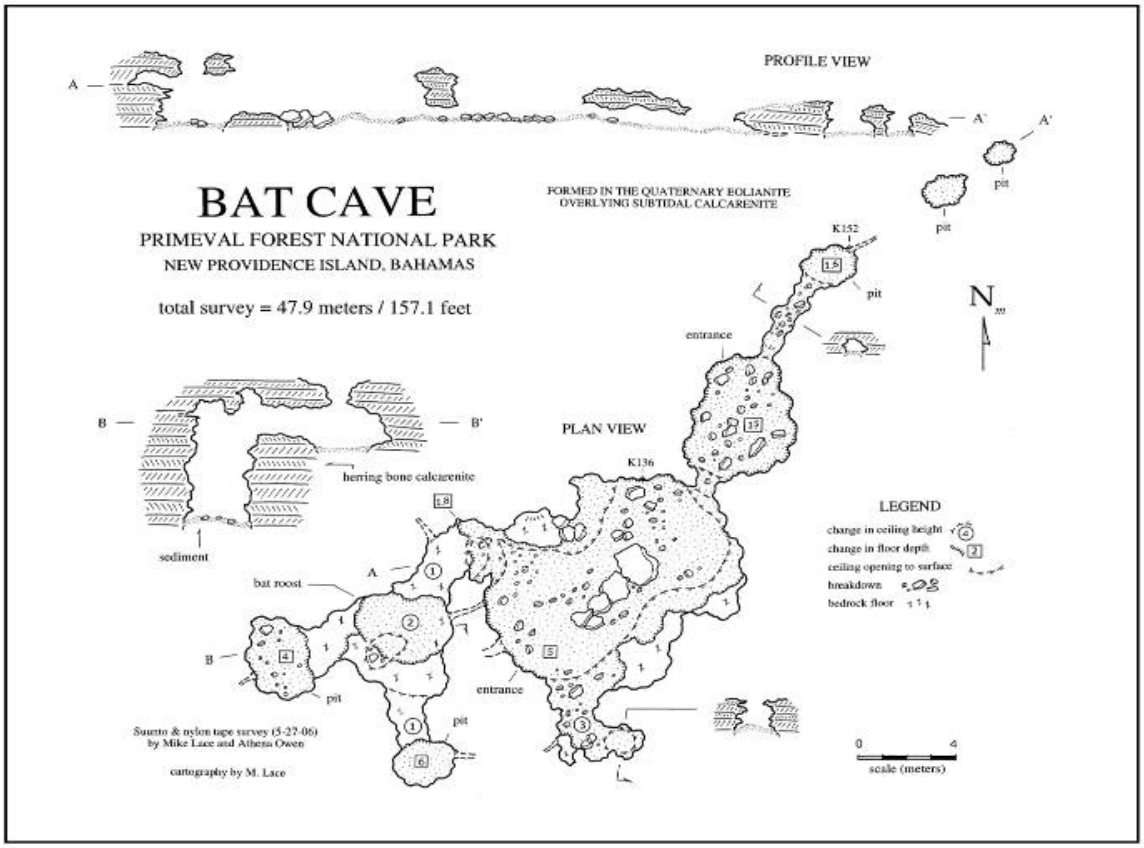

Figure 5. Karst feature 136 and 152 showing the karst location of the only known bat population in the park.

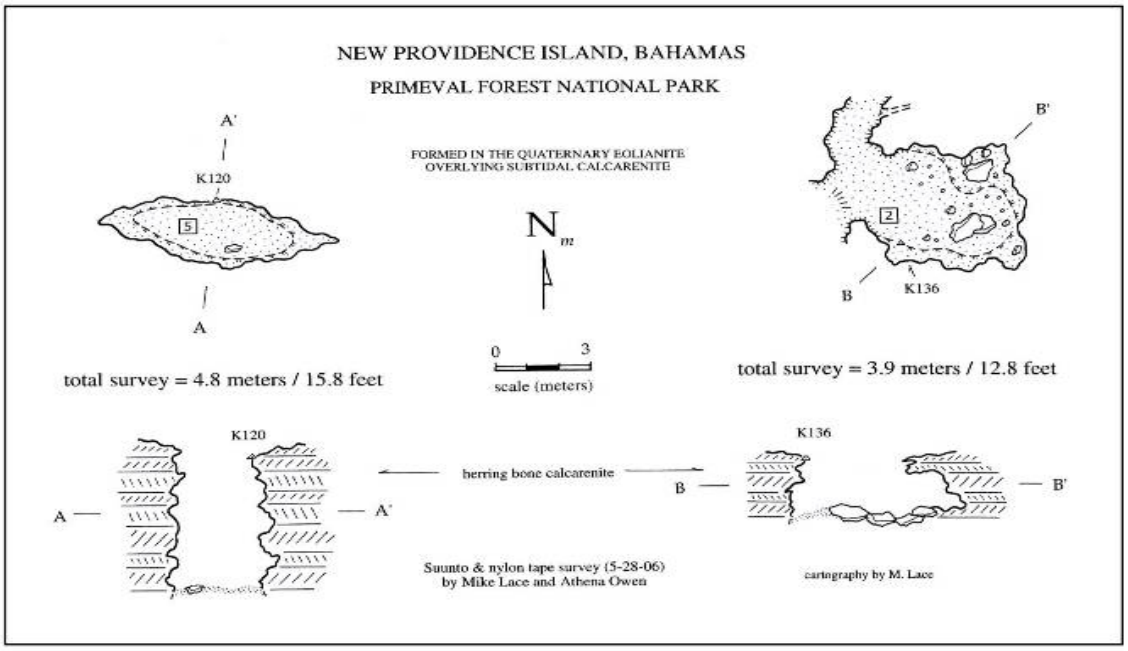

Figure 6. Karst features K120 and K136.

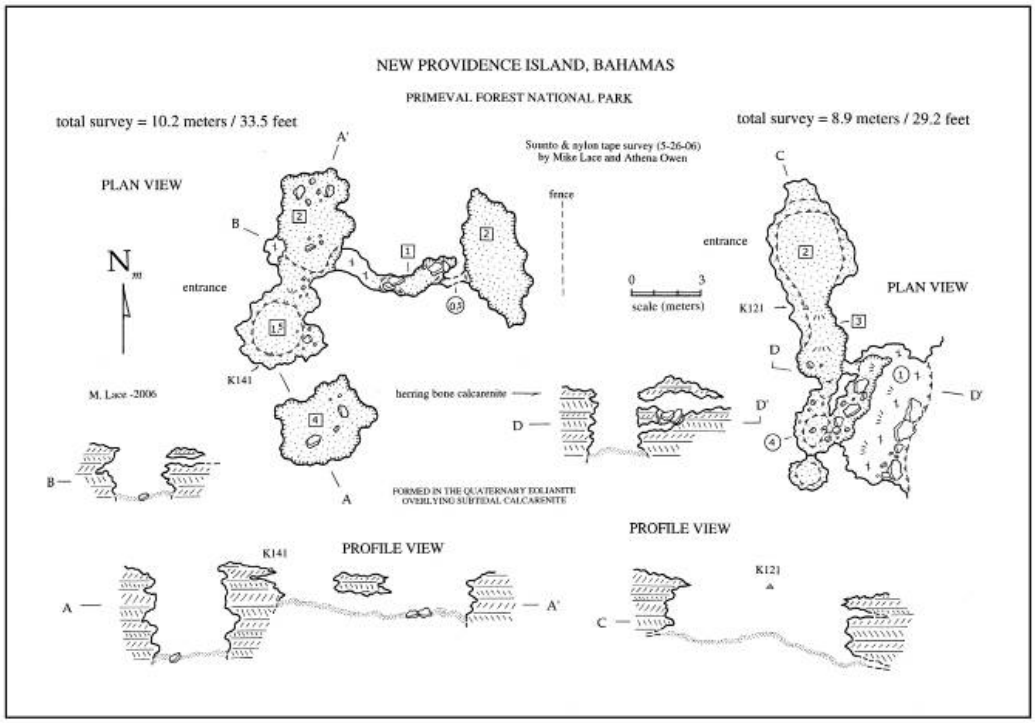

Figure 7. Karst features K141 and K121.

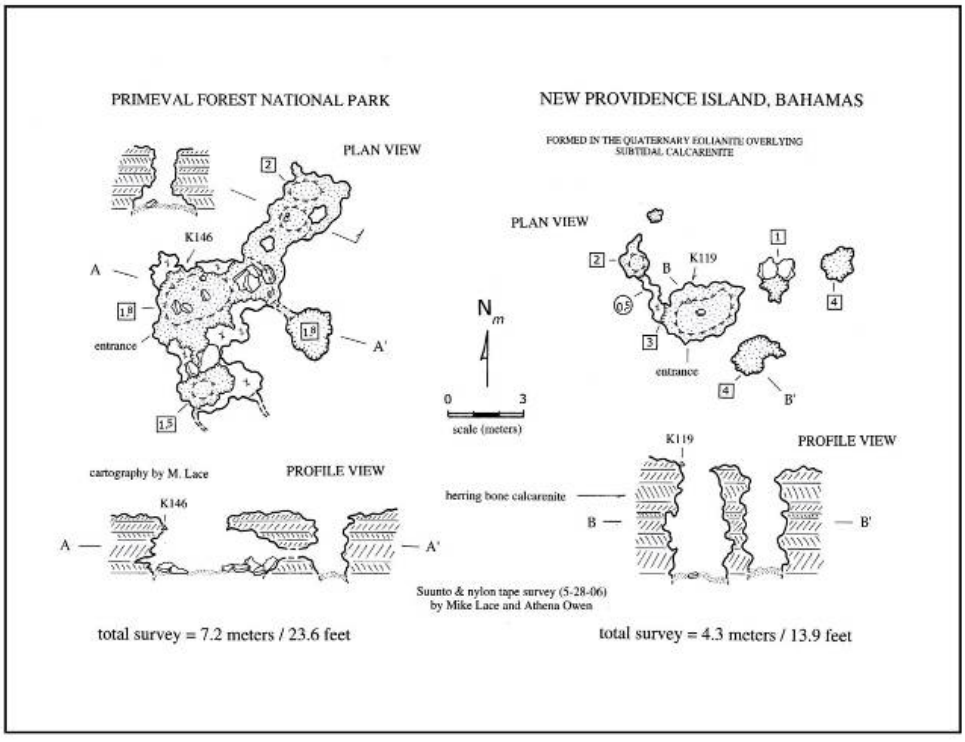

Figure 8. Karst features K146 and 119.

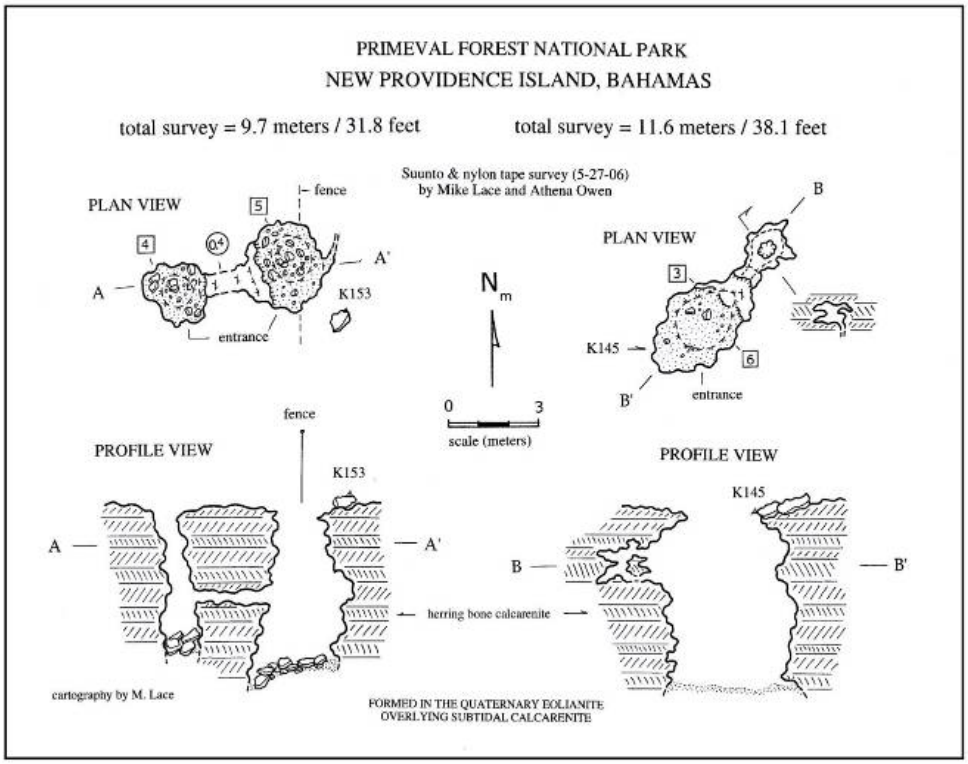

Figure 9. Karst features K153 and K146.

GEOLOGY

A complete review of Bahamian geology can be found in Carew and Mylroie 1995; and 1997 (and references therein) with specific publications relating to New Providence Island in Carew et al., 1992; 1996. The Islands are made of up carbonate rocks that fall into three major stratigraphic units: the Holocene Rice Bay Formation, less than 6,000 years in age; the Upper Pleistocene Grotto Beach Formation, approximately 119,000 to 131,000 years in age; and the Mid-Pleistocene Owls Hole Formation, that consists of numerous units extending from 200,000 years in age to at least 500,000 years in age.

The Rice Bay Formation and Owls Hole Formation are made completely of eolianites (fossilized carbonate sand dunes). The Grotto Beach Formation contains fossil reefs and other sub-tidal units as well as eolianites. The Owls Hole and Grotto Beach formations have well-developed *terra rossa* paleosols, a hard, red to brown crust, on their top surfaces. The Rice Bay Formation, because it is so young, lacks a *terra rossa* paleosol. The Bahamas are tectonically stable, and are slowly subsiding at the rate of 1 to 2 meters per 100,000 years. As a result, the fossil reefs and other sub-tidal units of the Grotto Beach Formation are found above sea level today only because sea level was higher at the time those units were deposited. This past higher sea level was the result of ice sheets melting back a bit more than today. The geologic column for the Bahamas is presented in Figure 10.

The rocks in the Primeval Forest appear to be made entirely of the Grotto Beach Formation, based on the herringbone cross bedding on the cave and pit walls (Figure 11). In addition, there are several ichnofossils from organisms that only live in sub-tidal conditions. Given that these rocks show sub-tidal features above modern sea level, the rocks must be part of the Grotto Beach Formation. Eolianites exist higher up in a smooth transition, indicating that they too are part of the Grotto Beach Formation.

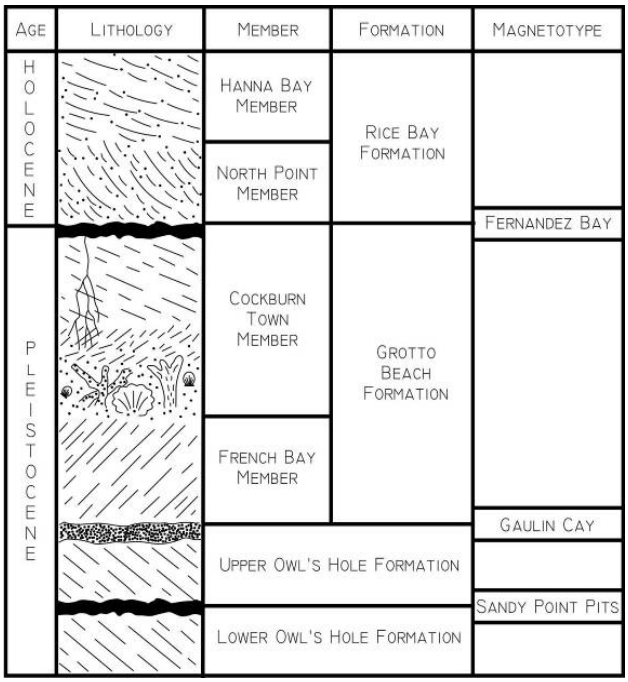

Figure 10. Geologic column for the Bahamas. The Owls Hole Formation contains more units than are shown here.

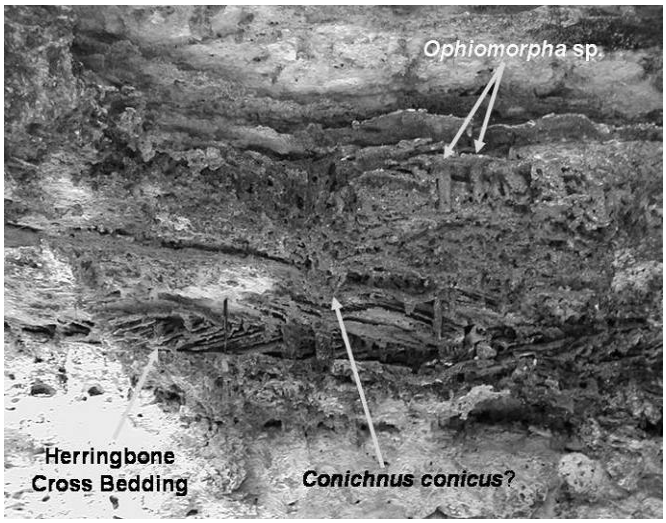

Figure 11. Pit outcrop at the Primeval Forest, at K49 of Figure 4, showing herringbone cross bedding and sub-tidal trace fossils.

CAVE AND KARST DEVELOPMENT

The caves and karst features of the Primeval Forest are similar to what is found throughout the Bahamas, but the high density of the features, their complexity and interconnectivity, are unique. There are three main features present: banana holes, pit caves, and sinkholes. A review of Bahamian karst processes can be found in Mylroie and Carew, 1995, and Mylroie et al., 1995. Sinkholes (Figure 12) are conical depressions found in karst landscapes around the world, produced by dissolution excavating a basin in the rock. This dissolution excavation can be by removal of rock from the surface, or by removal of rock in the subsurface with collapse of surface rock and soil into the underlying void. The sinkholes in the Primeval Forest have formed mostly by collapse. Pit caves are vertical pathways dissolved out of the rock by water descending from the surface into the subsurface (Figure 13). In the Bahamas, they are commonly 2 to 10 m deep (6 to 30 feet). Banana holes are the surface expression of voids dissolved beneath the water table and later expressed at the surface by collapse (Figure 14). In that regard, they are a special case of sinkhole, in that their vertical bedrock walls and overhanging

Figure 12. A simple sinkhole in the Primeval Forest, at K143 of Figure 4, with bedrock ledges and sloping sides.

ledges reveal their origin as an underground void. Banana holes are considered phreatic in origin, that is, they developed below the water table. Pit caves are considered vadose in origin as they develop above the water table. The phreatic voids

Figure 13 a. A pit cave of the Primeval Forest. A view looking down at K16 of Figure 4.

Figure 13 b. A pit cave of the Primeval Forest. A view in the pit cave at K49 of Figure 4.

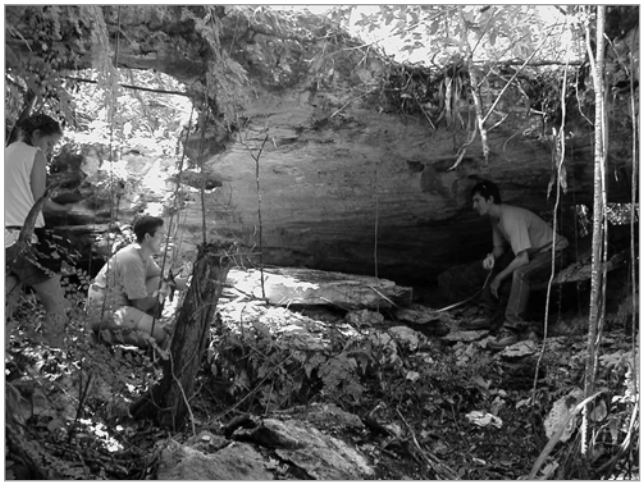

Figure 14. A banana hole in the Primeval Forest, at K8 of Figure 4. Note the natural bridge and low, wide shape of the chamber.

of the banana holes have been revealed by roof collapse, and are dry today because they formed approximately 125,000 years ago, when sea level and the water table was higher.

GEOLOGIC HISTORY

The history of the formation of the rocks and karst features at the Primeval Forest is an example of compression of geologic events, where the karst features formed at or near the same time as the rock formations, instead of long afterwards. The rock units were deposited when sea level was about 6 m (20 feet) higher than present, about 125,000 years ago (Figure 15). A broad shallow lagoon existed at this site, with waves creating the oscillation ripple marks that later became herringbone cross bedding. Organisms living in this shallow lagoon left the trace fossils seen in Figure 11. The lagoon was gradually filled in by beach sands and eolianites that allowed the water table, or fresh-water lens, to invade the entire rock sequence (Figure 16).

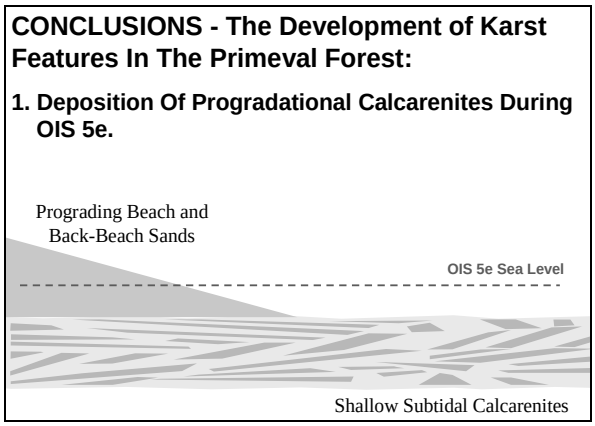

Figure 15. Initial condition of the lagoon at the Primeval Forest, about 125,000 years ago.

Once the fresh-water lens was in place, dissolution could take place in the phreatic zone below the water table. Dissolution is favored at the top of the lens, where vadose and phreatic waters mix (see Mylroie and Carew, 1995, for further discussion). The voids formed near the top of the bedrock body, and the roofs are thin. When sea level fell about 119,000 years ago, the banana holes were drained. They began to undergo collapse due to their thin roofs. Pit caves began to form, and the intersection of these caves helped collapse more of the banana holes (Figure 17).

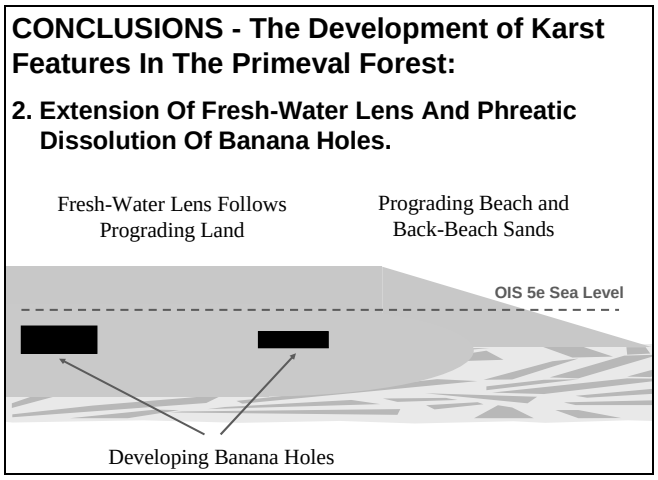

Figure 16. As sands prograde over the lagoon to make new land, the fresh-water lens extends into what was once a lagoon. Dissolution can now take place to make banana holes.

The landscape underwent a progressive erosional evolution. As banana holes began to undergo collapse, pit caves formed and the land surface was degraded. As a result, broad open areas and depressions formed, making large sinkholes, called karst valleys (Figure 18). The karst valleys trend northeast to southwest on Figure 4, with karst features, numbered from the karst survey as, K41, K61, K76, K77, K81, K82, K93 and K101 as point locations (Figure 19). There has been over 100,000 years since the banana hole formation began, and time has allowed an erosional continuum to form, as seen in Figure 18.

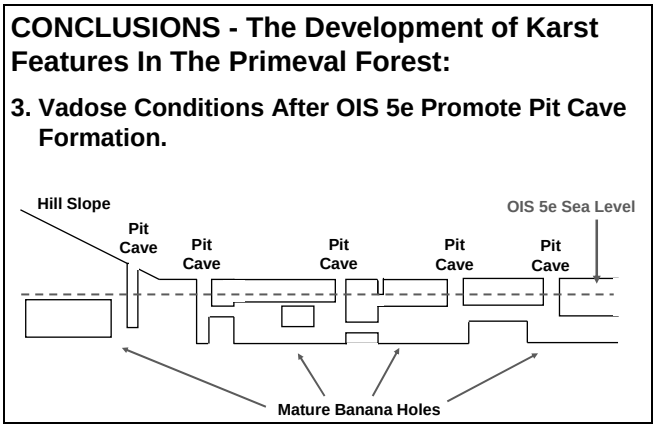

Figure 17. After sea level fell about 119,000 years ago, erosion began to truncate and expose the banana holes, while pit caves penetrated the land surface and opened some of the banana holes.

Few cave or karst features remain to the southeast, where the land is a low, undulating plain. The karst valleys with remnant caves are found toward the northwest. Farther to the northwest, intact and interconnected pit caves and banana holes appear. A few isolated pit caves are found still farther northwest and upslope onto the eolianites. Banana hole voids, if they exist, have not yet collapsed in this area. Two kilometers south (1.25 miles) of the park, at Clifton, the cliffs show the same sequence of herringbone cross bedding and trace fossils seen at the Primeval Forest, but over a greater vertical extent, showing the presence of deeper water in that location.

The caves and karst produced in the Primeval Forest are syngenetic, forming almost concurrently with the host lithology. This is a very rapid geologic process. Once these features formed, they underwent slow erosional decay that degraded them into the landscape we see today at the Forest.

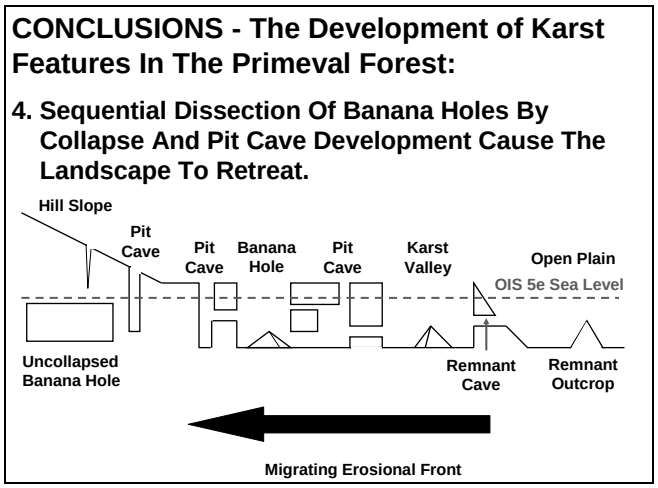

Figure 18. The continued dissection of the Primeval Forest over time by erosion created a sequence of open plain to the southeast, karst valleys in the central areas, banana holes and pit caves to the northwest, to isolated pit caves on the hill slope.

BIOLOGICAL IMPACTS

The flora and fauna of the Primeval Forest are preserved today in part because the chaotic nature of the landscape made the land less desirable for agriculture or development. Other creatures, such as bats, find the caves an ideal location for nesting. The wide variety of pits and banana holes, and the sheltered karst valleys, has created a whole sequence of micro-environments that have helped increase plant and animal diversity. Such karst-specific plant diversity has been reported from San Salvador Island (Lehnert et al., 1997).

CONCLUSIONS

The Primeval Forest is a unique landscape that expresses the full natural history of the Bahamas: the bedrock that forms the archipelago's

a.

b.

c.

Figure 19 a, b, and c. The karst valleys of the Primeval Forest. a) the broad, open expanse of the valleys; b,c) two examples of remnant caves in the karst valley.

foundation, the karst processes that sculpt that foundation, and the biota that make the landscape their home. The property has one of the most unique karst systems in the world. The rapid formation of the karst features and the connectivity of these features are very unusual and should be preserved.

The Bahamas National Trust, by obtaining this property, has made a significant contribution to science and the public. The quick action to fence the property, and to initiate an inventory of the Primeval Forest's contents, will allow the park to become a research, teaching, and recreational tool for The Bahamas. The scenic beauty of the park is outstanding (Figure 19) and will be a great asset to tourism on New Providence.

ACKNOWLEDGMENTS

The authors would like to thank the Bahamas National Trust, and Eric Carey, Department of Geosciences, Mississippi State University, Neil and Ivan Sealey, Pericles Maillius, Mike Lace, and Dr. John Rodgers and Dr. Jamie Dyer, Mississippi State University.

REFERENCES

Carew, J.L., Mylroie, J.E., and Sealey, N.E., 1992, Field guide to sites of geological interest, western New Providence Island, Bahamas, Field Trip Guidebook, The Sixth Symposium on the Geology of the Bahamas, Port Charlotte, Florida, Bahamian Field Station, p. 1-23.

Carew, J.L., and Mylroie, J.E., 1995, A stratigraphic and depositional model for the Bahama Islands, *in* Curran, H.A. and White, B., eds., Geological Society of America Special Paper 300: Terrestrial and Shallow Marine Geology of the Bahamas and Bermuda, p. 5-31.

Carew, J.L., Curran, H.A., Mylroie, J.E., Sealey, N.E., and White, B., 1996, Field guide to sites of geological interest, western New Providence Island, Bahamas: Bahamian Field Station, San Salvador Island, Bahamas, 36 p.

Carew, J.L. and Mylroie, J.E., 1997, Geology of the Bahamas, *in* Vacher, H.L., and Quinn, T.M., eds., Geology and hydrogeology of carbonate islands: Elsevier Science Publishers, p. 91-139.

Lehnert, M.K., Mylroie, J.E., and Arnold, D.L., 1997, An analysis of the relationship between karst features and vegetation type on San Salvador Island, Bahamas, *in* Carew, J.L., ed., Proceedings of the Eighth Symposium on the Geology of the Bahamas: San Salvador Island, Bahamian Field Station, p.122-134.

Mylroie, J.E., and Carew, J.L., 1995, Chapter 3, Karst development on carbonate islands, *in* Budd, D.A., Harris, P.M., and Saller, A., eds., Unconformities and Porosity in Carbonate Strata: American Association of Petroleum Geologists Memoir 63, p. 55-76.

Mylroie, J.E., Carew, J.L., and Vacher, H.L., 1995, Karst development in the Bahamas and Bermuda, *in* Curran, H.A. and White, B., eds., Geological Society of America Special Paper 300: Terrestrial and Shallow Marine Geology of the Bahamas and Bermuda, p. 251-267.

GIS OF THE CAVES AND KARST OF THE MARIANA ISLANDS

Kevin Toepke and John E Mylroie
Department of Geosciences
Mississippi State University
Mississippi State, MS 39762

ABSTRACT

The Mariana Islands are a volcanic island chain in the western Pacific Ocean composed of Eocene volcanic cores with a carbonate mantle. The five islands in this study are Guam, Rota, Aguijan, Tinian, and Saipan. Other workers previously have classified the cave and karst features of these islands into the cave types described in the Carbonate Island Karst Model or CIKM, but no comprehensive GIS has been developed. For this project, a comprehensive GIS of the cave and karst features was produced. The cave and karst features were divided by cave type, physiographic province, and island. The data were then entered into a relational geodatabase for ease of maintenance and analysis. A total of 740 karst features were entered. Layer files were created to retrieve information and to display the feature locations in GIS maps. A total of 82 layers were created for each combination of island, physiographic province, and cave type for a total of 82 distinct layers. A total of 7 GIS maps were produced: one for each island, one with the five islands in the study in a spatially correct orientation, and one with each of the five islands in an individual panel, with each island having its own scale. The karst features in the GIS maps were hyperlinked to a number of HTML pages--one for each feature with additional information, and a set of HTML navigation pages mirroring the organization of the GIS layers. The HTML pages contain textual descriptions, and links to final and working feature maps, and line plot data, and other data not amenable to storage in a relational database. In addition to the karst data, various raster layers were added to the GIS including: LANDSAT images, DRG, DEM, and other layers calculated from the DEM.

INTRODUCTION

Geographic Setting

The Mariana Islands are a volcanic island chain in the western Pacific Ocean located south of Japan (Figure 1), where the Pacific Plate is being subducted beneath the Philippine Plate to the west of the Mariana Trench and the Mariana Islands. The Mariana Islands are composed of fourteen islands divided into two parallel island chains that are the subaerially exposed portion of the Mariana Ridge (Figure 2) (Karig, 1971). The western-most, volcanically active chain is composed entirely of volcanics and is not included in this study. The six islands in the eastern chain are composed of an Eocene volcanic basement with a cover of Cenozoic carbonates. The five islands in this study are Guam, Rota, Aguijan, Tinian, and Saipan. Farallon de Medinilla (located approximately 84 km north of Saipan) was not included in this study because of its remote location and use as a military muni-

tions training area (Jenson et al., 2006). There have been several attempts to characterize cave and karst features in the past, most notably the Carbonate Island Karst Model, or CIKM, but no comprehensive GIS has been developed.

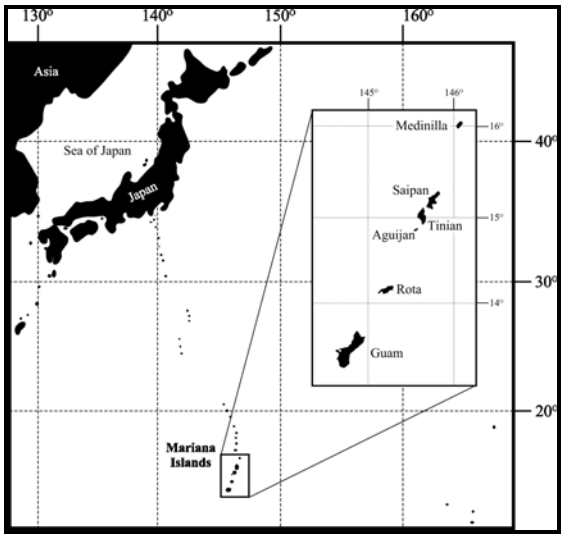

Figure 1. Location map of the Mariana Islands (Jenson et al., 2006).

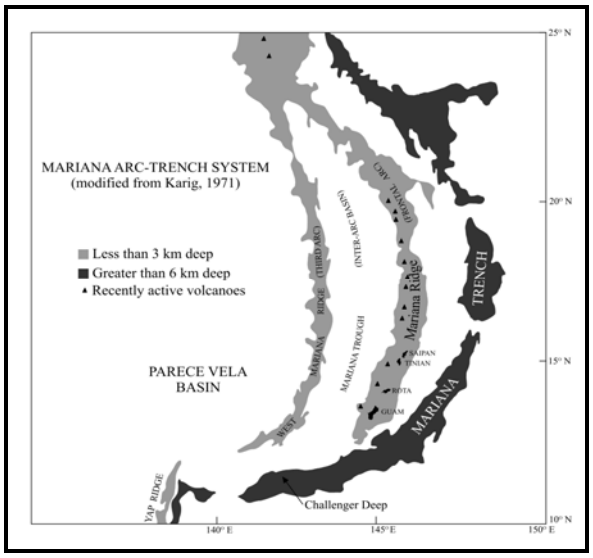

Figure 2. Mariana Arc-Trench System (Keel, 2005).

To construct a comprehensive GIS of the cave and karst features the features first were divided by cave type, physiographic province, and island. The data then were entered into a relational geodatabase for ease of maintenance and analysis. A total of 740 karst features were entered into this database and a total of 5 GIS maps were produced—one for each island. The karst features in the GIS maps were hyperlinked to a number of HTML pages, one for each feature with additional information, and a set of HTML navigation pages mirroring the organization of the GIS layers was also created. The HTML pages contain textual descriptions and links to the final and working feature maps, line plot data, as well as other data not amenable to storage in a relational database. In addition to the karst data various raster layers were added, including: LANDSAT images, DRG, DEM, and other layers calculated from the DEM, such as hillshade, contour lines, and island outline.

Geology

Guam, the southern-most island in the western chain, is located about 2800 km southeast of Tokyo, Japan and 2400 km east-southeast of Manila, Philippines. Guam is the largest of the Mariana Islands with a land surface of about 550 km^2. Guam is divided into two equally-sized physiographic provinces separated by the Pago-Adelup Fault. The Northern Province is an uplifted carbonate plateau with near-vertical cliffs at the coast. The southern province is mostly volcanics and volcanoclastics with isolated limestone bands. The only sizable surface streams on Guam are located on the southern half of the island (Mink and Vacher, 1997).

Jenson et al. (2006) further subdivided the physiographic provinces of Guam into five divisions: Northern Plateau, Basement Outcrops, Southern Coast, South-

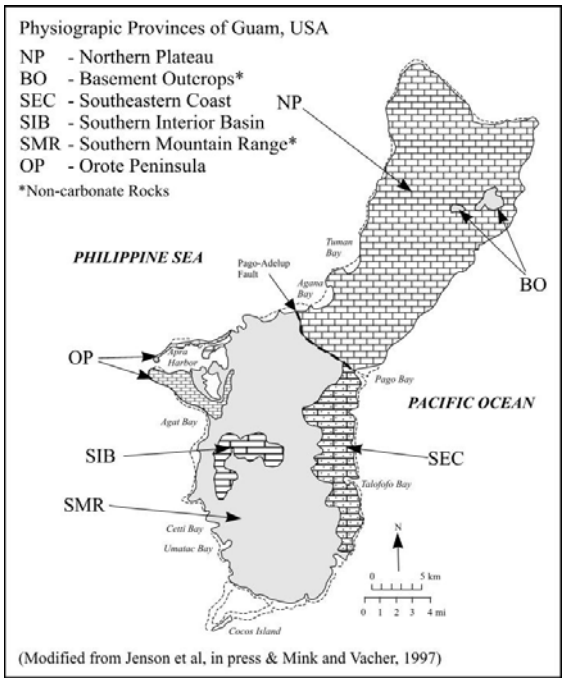

Figure 3. Physiographic map of Guam (Modified from Jenson et al., 2006).

ern Interior Basin, and Southern Mountain Range (Figure 3).

Rota Island.

Rota is located about 80 km north of Guam and has a surface area of about 96 km^2 and a coastal perimeter of about 52 km.

There are six physiographic provinces in three Regions. The regions are: Sinapalo Region, Sabana Region, and the Taipingot Peninsula. Sugawara (1939; and 1949) described the physiographic provinces in terms of their terrace level. The six terrace levels described include Sabana, Aburataruga, Shinaparu, Lugi, Taragaja, and Mirikattan. Keel (2005) divided the island into five regions: Sabana, Talakhya, Sinapolo, Taipingot Peninsula (Wedding Cake) and Songsong Village.

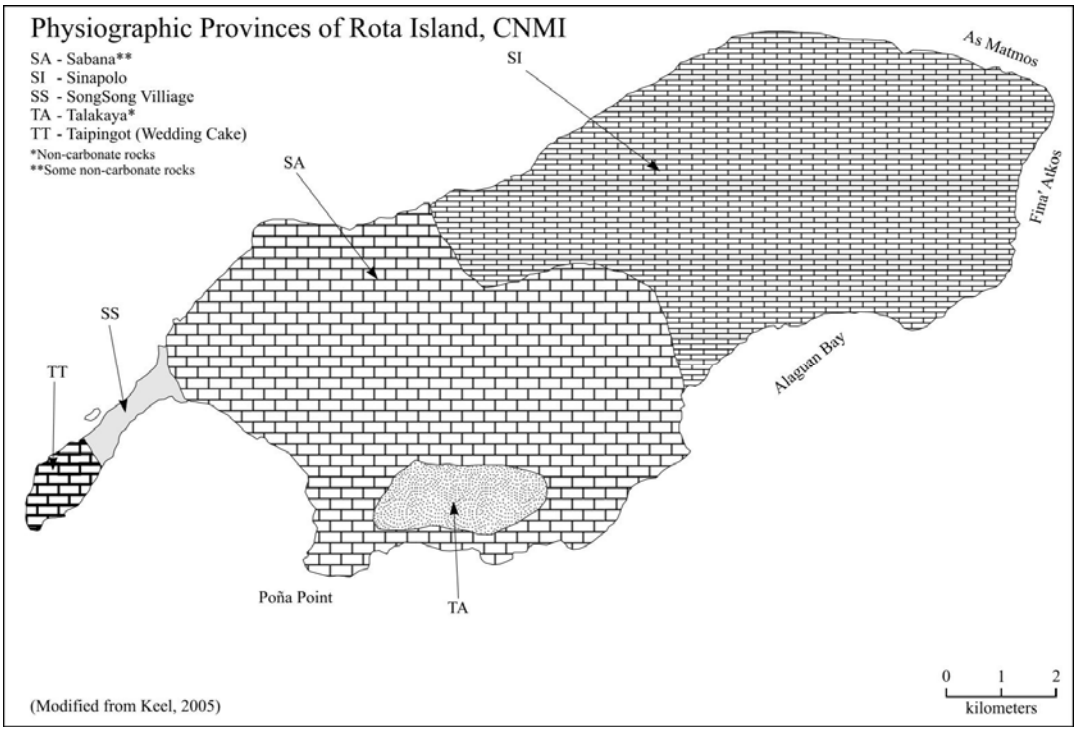

Figure 4. Physiographic map of Rota (Modified from Keel, 2005).

Stafford et al. (2005) reported volcanic outcrops in the Sabana and Talakhaya regions with the only surface streams occurring on the Talakhaya (Keel, 2005).

Aguijan Island

Aguijan has only about 7.2 km^2 of island surface, all of which are exposed Miocene and Pliocene age carbonate rocks, resting on an Eocene volcanic edifice (Tayama, 1936; Stafford, 2003). There are three concentric terraces on Aguijan at elevations 0-50 m, 50 – 100 m, and 100 – 150 m (Figure 5). No surface streams or beaches are present (Jenson et al., 2006).

Tinian Island

Tinian is approximately 102 km^2, and is the third largest of the Mariana Islands (Cloud et al., 1956). The island was divided by Doan et al. (1960) into five provinces separated by high-angle faults: Northern Lowland, North-Central Highland Central Plateau, Median Valley, and Southeastern Ridge (Figure 6). Stafford et al. (2005) reported four volcanic outcrops on Tinian near Sabanettan Mangpang, Bañaderon Lemmai, and Laderan Apaka (Figure 6). Streams flowing overland off of Bañaderon Lemmai provide for point source recharge into the karst system.

Saipan Island

Saipan is the second largest of the Mariana Islands and the largest of the 14 islands in the Commonwealth of the

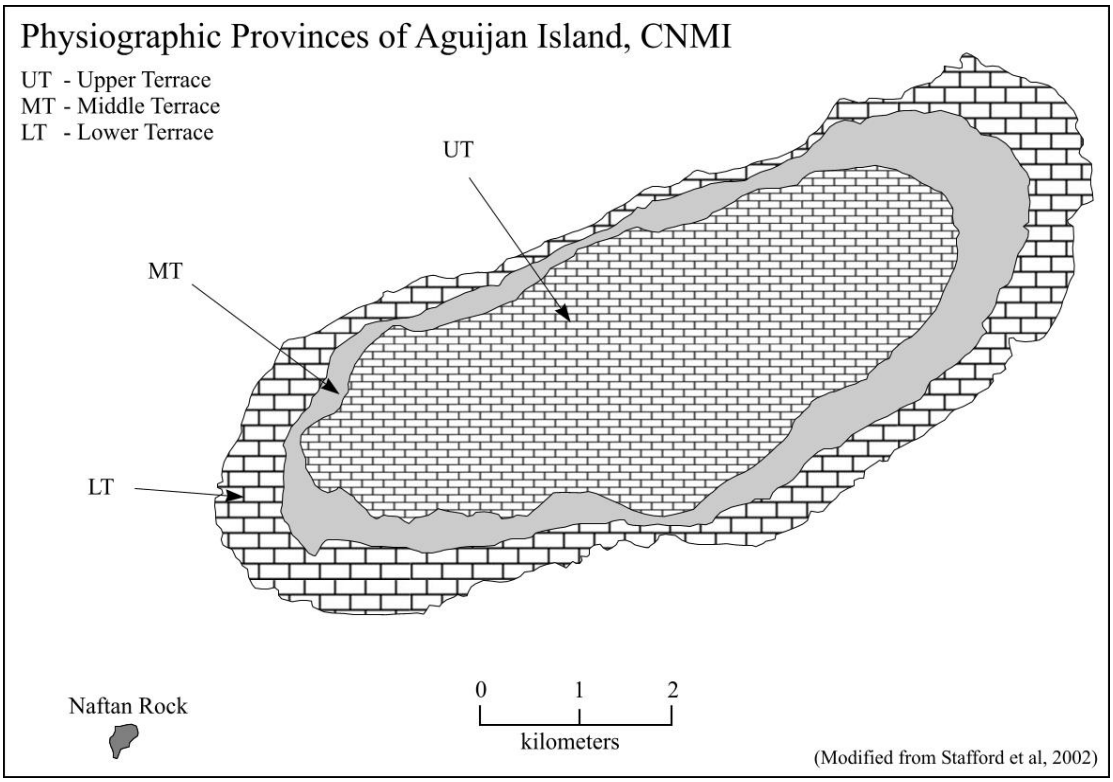

Figure 5. Physiographic map of Aguijan (Modified from Stafford et al., 2005).

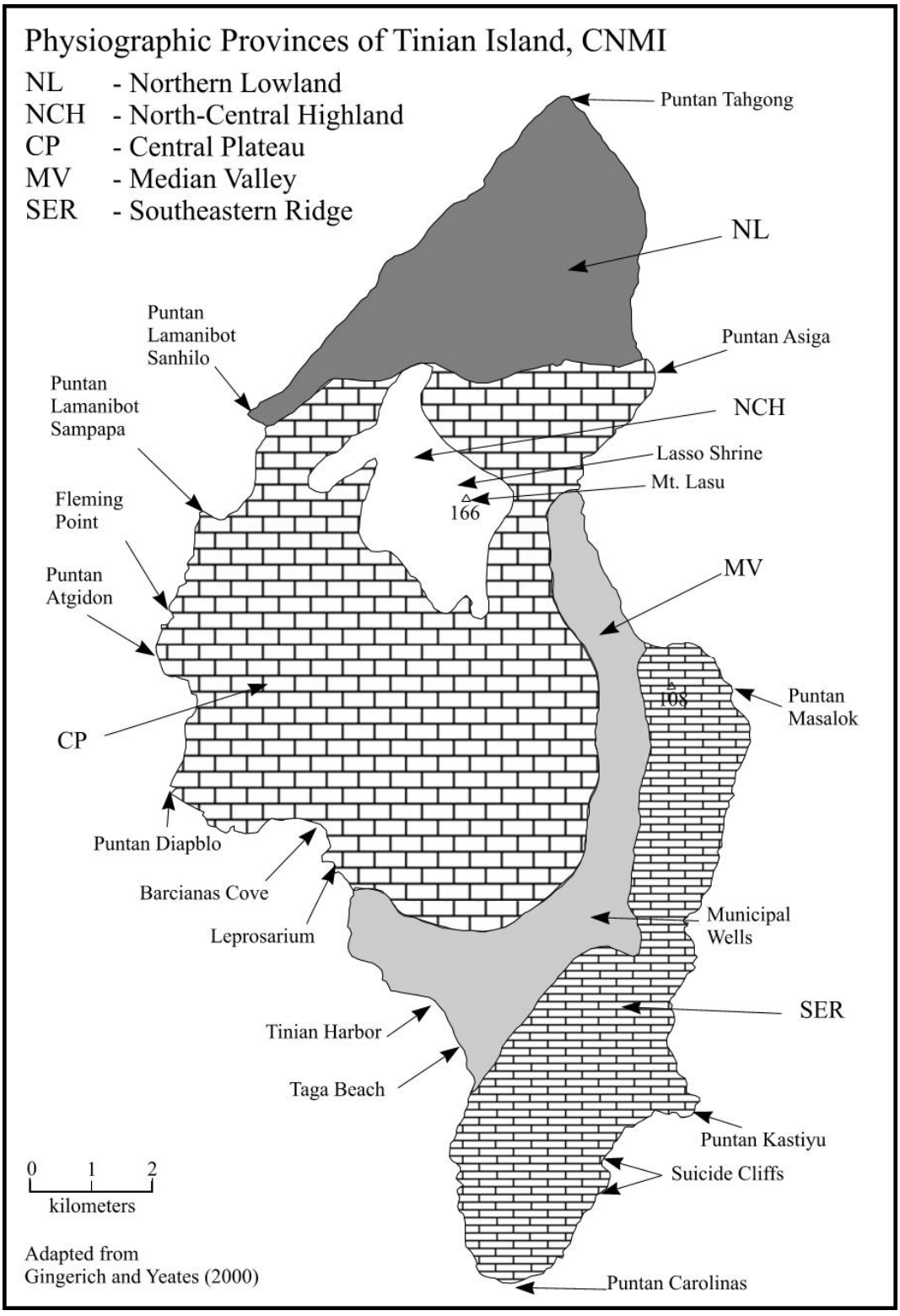

Figure 6. Physiographic map of Tinian (Modified from Stafford, 2003).

Northern Mariana Islands (CNMI) at 124 km^2. The island is divided into five physiographic provinces: Axial Uplands, Coastal Plain, Donni Clay Hills Belt, Coastal Fault Ridges, and Low Platform and Terraces (Figure 7) (Doan et al., 1960). Saipan is the type example for the Complex Island in the Carbonate Island Karst Model (see below) because of its complex and highly variable geology, lithology, and hydrology (Jenson et al., 2006). The faulting and interfingering of lithological units creates a fragmented and sometimes perched water table. In addition the faulting can place carbonates next to non-carbonates and force the phreatic water to take circuitous routes to the sea, create confined (artesian) conditions or even isolate portions of the freshwater lens (Mylroie et al., 2004).

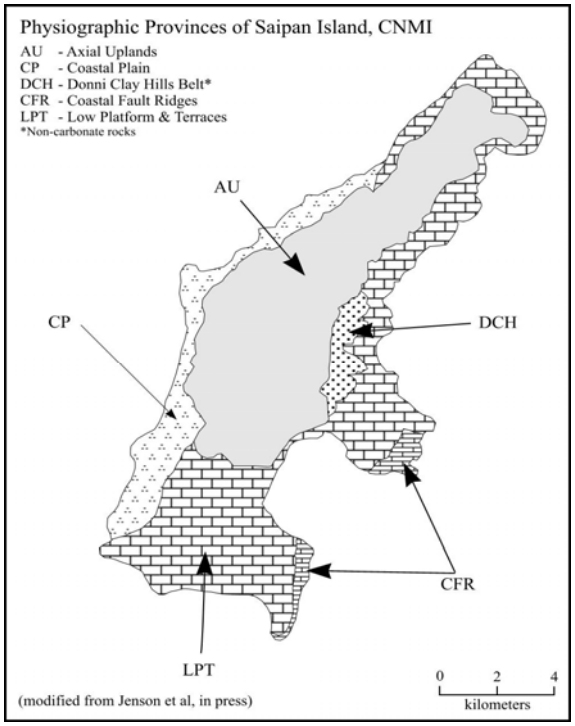

Figure 7. Physiographic map of Saipan (Modified from Jenson et al., 2006).

Karst Feature Classification

The cave and karst features in the database were classified by Keel (2005), Stafford (2003) and Taborosi (2000; 2004) according to the Carbonate Island Karst Model (CIKM) (*sensu* Mylroie et al., 2001; 2004 and modified by Keel, 2005). The CIKM categorizes cave and karst features in young carbonate islands by their position relative to the salt-water lens, and the island type. For a complete description of how the cave and karst features in the CIKM form and their hydrologic functions (see Keel 2005, Stafford, 2003, Taborosi, 2000, and Toepke, 2006).

Previous Karst GIS Work

Very little work has been done with GIS in relation to karst. The most extensive treatment has been done by Gao (2002; 2004), who used a GIS database of known sinkholes along with a model that used the distribution of sinkholes in order to classify the region into one of six relative hazard zones. This model was viewed as a success where the location of sinkholes had been accurately mapped and the density of sinkholes was fairly high. The model used lineament, nearest neighbor, decision tree, and cartographic analysis to delineate the hazard zones.

Typically, GIS has been used simply as a centralized repository of cave and karst data for a specific region. Cave locations and maps, survey data, field observations, lists of unexplored areas of the cave, and other data all have been stored in GIS databases (Addison, 2003; Iliffe, 2003). A GIS can be used to identify gross errors in field notes and to produce better maps (McKenzie and Veni, 2003),

especially when data are entered directly into a GIS system, the use of GIS software can improve cave maps by reducing data errors in the survey.

Alternatively, a descriptive GIS of known caves can be used to identify where a cave resource is likely to be found. If a cave's entrance location is known and the location and size of cave passages is known, overlaying the cave map with the overlying topography can identify where the cave nearly intersects the surface. This information can then be used to identify places where additional field work should be performed in order to potentially find additional cave resources (McKenzie and Veni, 2003). Knowing where to focus exploration can greatly increase an explorer's probability of finding previously unknown caves. One team used GIS to map known cave and karst features in order to identify patterns in and distribution of karst features (Lyew-Ayee et al., 2003). Mylroie et al. (2005) produced a digital karst map of the known cave and karst features of Mississippi. ArcGIS was used to produce maps of counties with known caves as well as all other digital karst maps.

In addition to maps of cave features, GIS has been used for the mapping of karst features including karst-prone geology, and specific karst features such as sinkholes and karst drainage basins. Paylor et al. (2003) used GIS to map the karst prone geology and sinkholes of Kentucky. This statewide map can then be used by the public and both public and private organizations to identify potential environmental and developmental issues. In addition to using GIS to map sub-surface features, GIS has been used to map surficial karst features and sometimes their connection with sub-surface features. One such project is the Florida Cave Database. The National Speleological Society Cave Diving Section and others that map underwater cave passages provided subsurface data for this project. Included in the database are fields such as ownership, entrance locations, conduit size and trend, and direction of water flow. After the data were acquired, an attempt was made to correlate the sub-surface features with known sinkholes and other surficial karst features (Denizman, 2004).

There are significant issues in mapping the flow of water through karst systems because the flow of groundwater in karst aquifers differs from traditional aquifers in speed, direction, and distance that the water travels. Subsurface waters may flow for many kilometers at rates comparable to that of surface streams and may cross under surface divides. Glennon (2003) used GIS to develop a model to better understand and predict the flow of groundwater in karst aquifers.

Lindsay and Smart (2004) used a GIS to map the level of the water table and to identify underground watersheds in terms of quality, quantity, flow directions, divides and conduits. Part of the reason for the mapping of karst groundwater is to map potential contamination risks (Lindsay and Smart, 2004; Singhal and Samuelson, 2004). Other uses for karst aquifer mapping are for governmental planning (Paylor et al., 2003), freeway route selection (Florea and Gulley, 2004; Griffin and Florea, 2004), and creating management zones to redirect urban development (Veni, 2004).

Planning of development in karst regions reduces the environmental impact of human activities and can also be used to help guide development activities. One of the major issues facing planners in karst areas is the high risk of groundwater contamination due to the potential of rapid and unfiltered transport of contaminated

water to unknown destinations. In addition to the work done by Paylor et al. (2003), other workers such as Kostka et al. (2004) have used GIS maps to help governments create development plans and change zoning to better reduce the risk of future groundwater contamination.

METHODS

Database Development

A relational geodatabase (GDB) in 3NF was developed to store spatial and non-spatial information for each of the cave and karst features in the descriptive GIS. The tables in this database are: ACCURACY_INFORMATION, CAVE_TYPES, CAVES, HYDROLOGIC_FUNCTION, ISLANDS, PROVINCES, and SURVEY_GRADE. The ACCURACY_INFORMATION table contains the accuracy of the location information and information as to how the location of the cave or karst feature was obtained; CAVE_TYPES contains information as to the karst feature type (e.g., Flank Margin Cave, Closed Depression, etc.); HYDROLOGIC_FUNCTION stores information on whether the feature serves to recharge the groundwater or if the feature is discharging groundwater, and optionally, at what rate; ISLANDS contains information specific to each island; PROVINCES contains information on the physiographic provinces; SURVEY_GRADE contains information as to the accuracy of the survey performed on the karst feature; and CAVES holds the information on the caves and karst features for the islands including the location information.

Each table has a surrogate (artificial) key as its primary key. Foreign keys to ACCURACY_INFORMATION, CAVE_TYPES, HYDROLOGIC_FUNCTION, PROVINCES, and SURVEY_GRADE were created in the CAVES table and a foreign key to ISLANDS was created in the PROVINCES table.

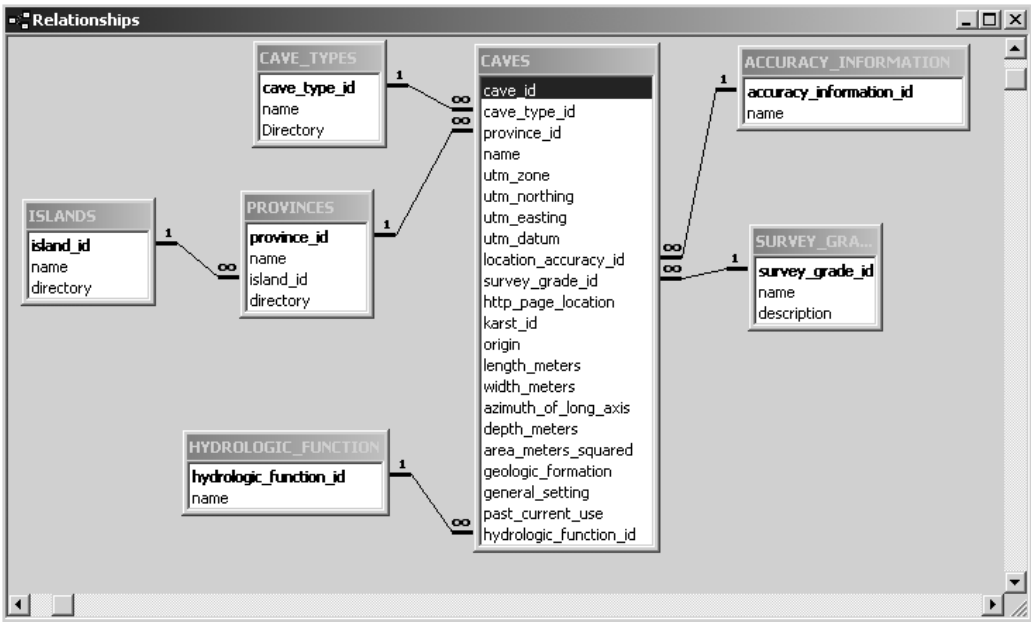

Figure 8. Geodatabase design including tables, columns, and relationships.

To speed retrieval, individual indexes were created on each of the primary and foreign keys as well as each of the name columns. The database design is shown in Figure 8.

To speed retrieval, indexes were created on all of the name columns as well as on the primary and foreign key columns.

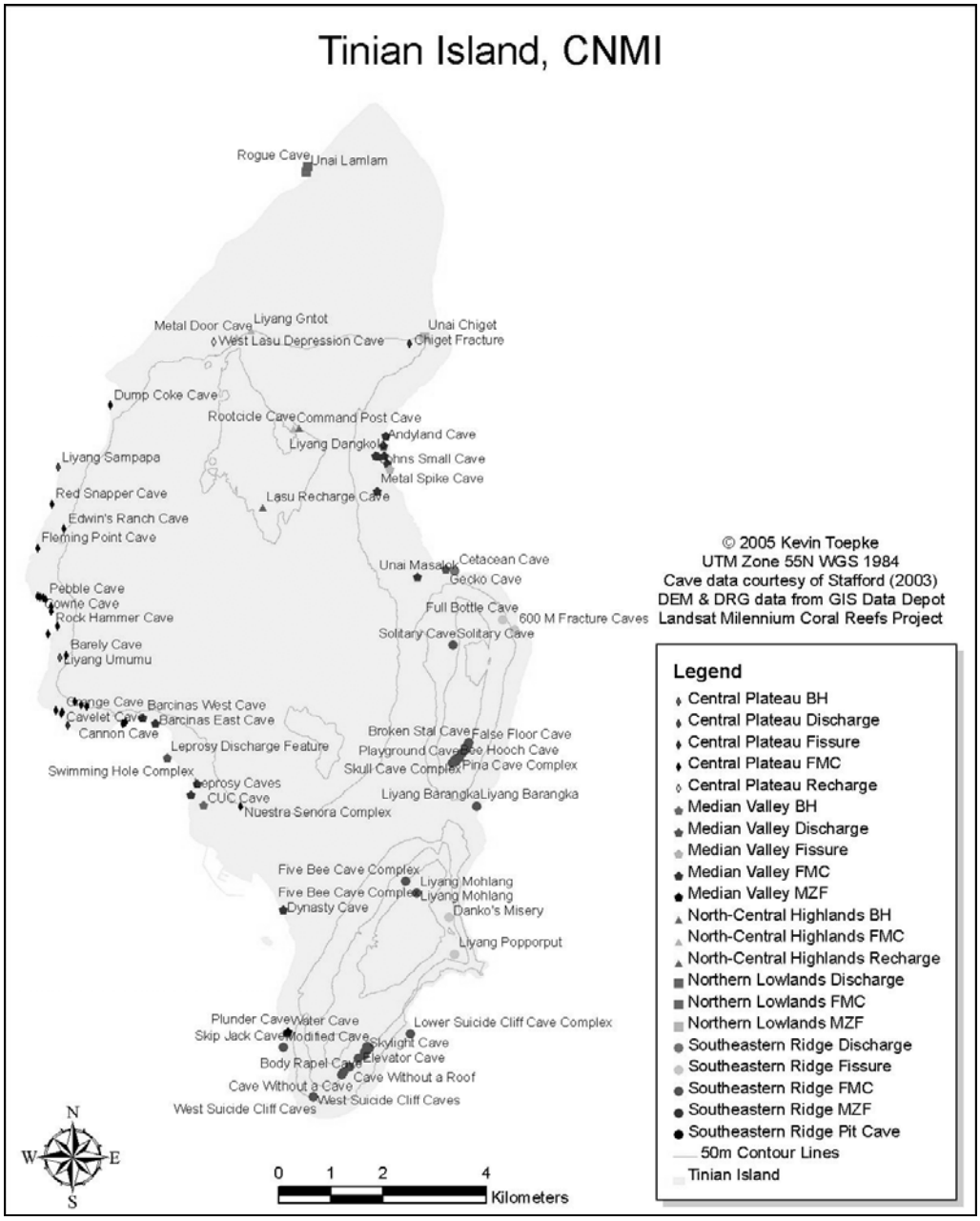

Figure 9. Map of the cave and karst features of Tinian Island, CNMI with island outline and 50 m contour.

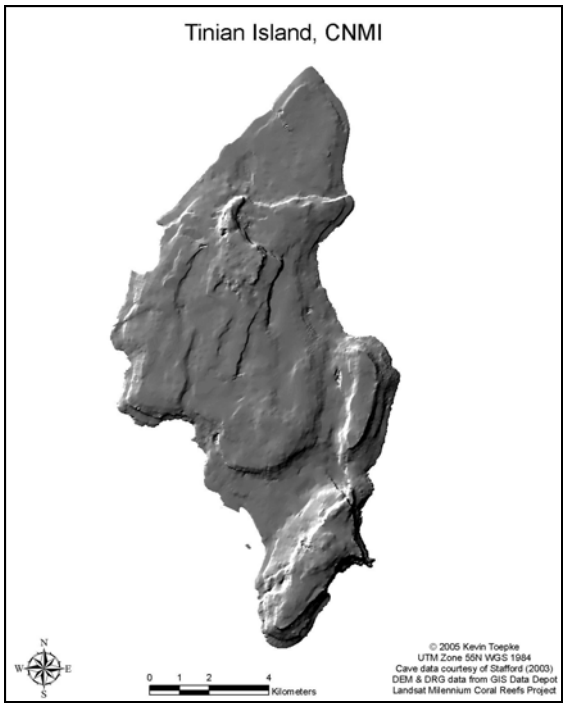

Figure 10. Hillshade of Tinian.

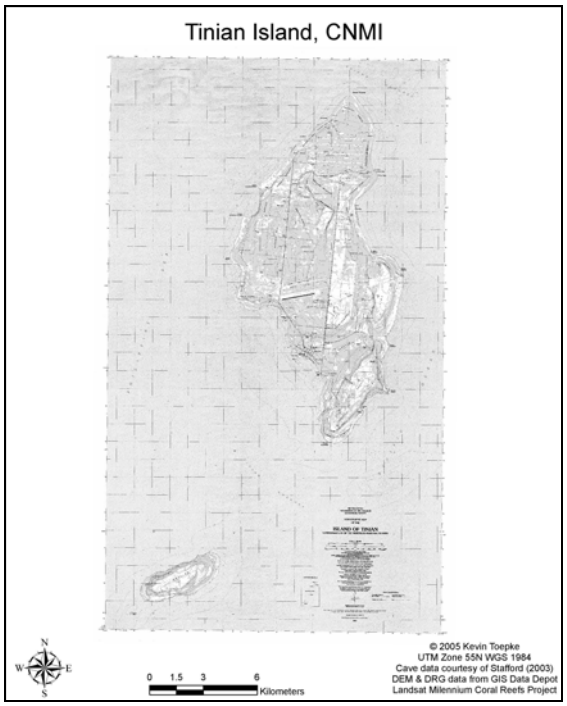

Figure 11. Map of Tinian and Aguijan Islands showing Digital Raster Graphics (DRG) Layer.

The data for this project has already been collected for various projects, including various Masters Theses by Mississippi State University (MSU) and University of Guam (UOG) students. The data for Rota was collected and organized by Keel (2005) for his project at MSU; Tinian and Aguijan by Stafford (2003) for his project at MSU; and Guam from Taborosi (2000, 2004) for his UOG project. Information on most of the caves of Saipan was not available for this project. The data were acquired via personal communication from each author and directly from the theses.

The same process was followed for each of the datasets compiled in this database. The data were validated based on received locations, maps, descriptions and fieldwork. The data then were organized into a series of directories based on island, physiographic province, feature type, and individual feature, as appropriate. The cave data was also loaded into the Geodatabase.

For purposes of this paper, only examples of Tinian will be shown. The same types of figures were created for the other four islands.

Once the cave data were organized, the digital data were organized by island and the DEMs were used to generate hillshades, island outlines, and topographic maps and hillshades at contour intervals (Figure 10). For each island, a map showing the location of each karst feature was created from the data in the Geodatabase. Each feature type was given a distinct symbol/color combination for ease of identification; the generated island outline and 50 m contour lines were added for reference (Figure 9).

Once the maps were produced and the data were organized and vetted, a series of HTML pages was created--a homepage for the entire database, as well as an introduction page for each island, as well as

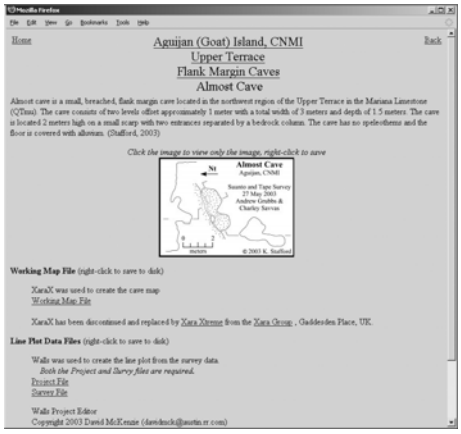

Figure 12. Sample HTML page for a cave.

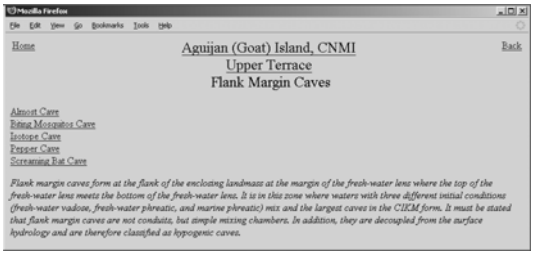

Figure 13. Sample HTML cave type page.

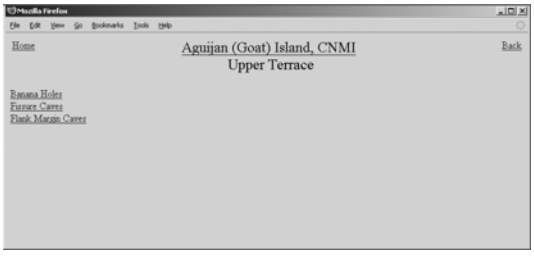

Figure 14. Sample HTML page for a physiographic province.

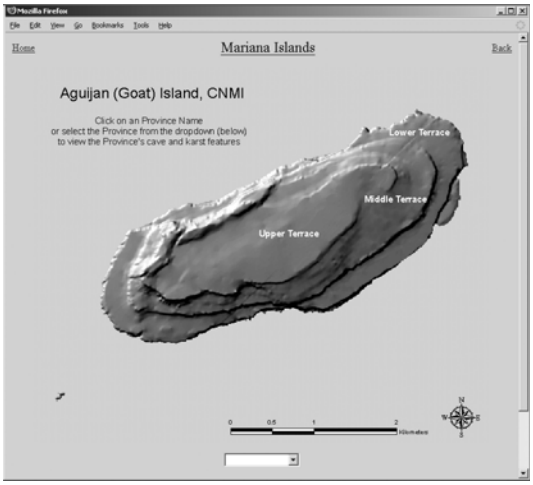

Figure 15. Sample island home page.

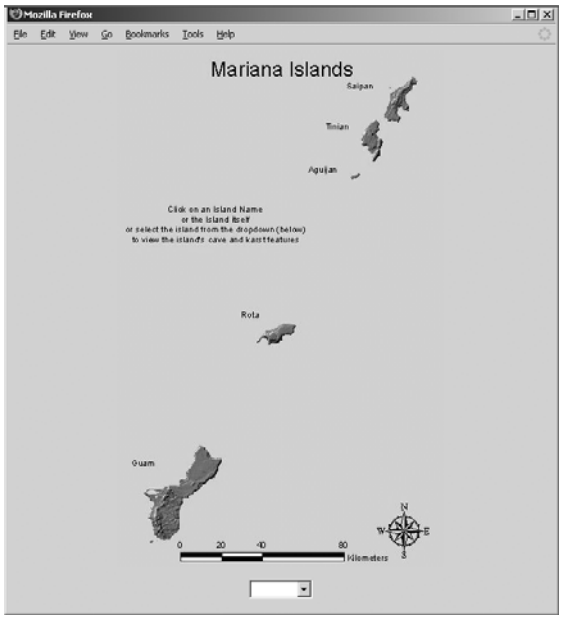

Figure 16. Project homepage.

pages with phyisiographic provice information, cave type within the province, and karst features present. These HTML pages were then linked to the maps via the http_page_location field in the Geodatabase. Samples of the pages created are in Figures 12-16.

CONCLUSIONS

A relational database of cave and karst information, including five comprehensive maps (one for each island), and a series of HTML pages were produced. The geodatabase contains point information for all known cave and karst features in the Marianas, three sets of contour lines (10, 25, and 50 m intervals) for each island stored as polylines, and island outlines stored as polygons. The point information of Saipan is incomplete because the data for only four cave features was received.

The following information is included in each comprehensive map:

- Cave and karst features separated by physiographic province and type
- Three sets of contour lines
- Island outline
- DEM
- Hillshade
- DRG
- True-color LANDSAT image
- False-color IR LANDSAT scenes

The cave and karst features, contour lines, and island outlines are retrieved from the database when the map is loaded. The HTML pages for the cave and karst features contain the feature descriptions, maps, and links to the digital survey project files and the working map documents. Additional web-publishing quality HTML pages were created to allow normal web navigation from the project's root directory.

The five maps and HTML pages along with the geodatabase provide a good start for organizing the cave and karst data of the Mariana Islands. They provide a "one-stop shopping" destination for information on the caves and karst of the Mariana Islands. This consolidation of information will allow researchers to identify future project locations and to more effectively target field activities. Additionally, the data from new projects can be integrated into the database. However, a good deal of extra work could be performed to enhance the geodatabase and maps, such as the addition of tables or fields and the incorporation of these new data into the maps.

Organizing the point, line, and polygon data in a relational geodatabase allows for simplified data management. Future researchers can modify the cave and karst data from a single place. Adding or changing the cave and karst data in the geodatabase immediately propogates the changes in the existing layers used to create the maps.

ACKNOWLEDGEMENTS

We would like to thank Dr. Donald T. Gerace, Chief Executive Officer; Vincent Voegeli, Executive Director of the Gerace Research Center, San Salvador, Bahamas; T. Montgomery Keel, Kevin Stafford, and Danko Taborosi for their generous donation of their data for this project; and the various staff and students at Mississippi State University that assisted in a myriad of ways, small and large, to the completion of this project.

REFERENCES

Addison, A., 2003, ArcPAD GIS mobile software in Cueva del Tecolote, Tamaulipas, Mexico: Journal of Cave and Karst Studies, v. 65, p. 182.

Cloud, P.E., Jr., Schmidt, R.G., and Burke, H.W., 1956, Geology of Saipan, Mariana Islands, Part 1. General Geology. 280-A, U.S. Geological Survey Professional Paper, U.S. Government Printing Office, Washington, D.C., p. 126.

Denizman, C., 2004., Karst Development in Florida: Spacial Analyses Based on Subsurface and Surfical Karst Databases in GIS: Geological Society of America Abstracts with Programs, v. 36, p. 134.

Doan, D.B., Burke, H.W., May, H.G., Stensland, C.H., and Blumenstock, D.I., 1960, Military Geology of Tinian, Mariana Islands: Chief of Engineers, U.S. Army, 149 p.

Dreybrodt, W., 2000, Equilibrium chemistry of karst water in limestone terranes, *in* Dreybrodt, W., Klimchouk, A.B., Ford, D.C., and Palmer, A.N., eds., Speleogenesis, Evolution of Karst Aquifers: United States, National Speleological Society, p. 126 – 135.

Florea, L, and Gulley, J., 2004, Importance of Karst Land Unites in the Assessment of Environmental Impacts: Somerset Bypass Karst GIS [abs.]: Geo^2, v. 30, p. 14.

Gao, Y., 2002, Karst feature distribution in southeastern Minnesota; extending GIS [PhD. Thesis], University of Minnesota, 210 p.

Gao, Y., 2004, Sinkhole Hazard Distribution and Assessment in Minnesota using GIS and Database Management System: Geological Society of America Abstracts with Programs, v. 36, p. 330.

Glennon, A., 2003, Assessing perennial drainage density in the highly karstified Turnhole Bend Basin, Kentucky: Journal of Cave and Karst Studies, v. 65, p. 182 – 183.

Griffin, B., and Florea, L., 2004, GIS Investigation of Potential Karst Impacts Along Proposed I-66 Alignments in Somerset, Kentucky: Program: 2004 NSS National Convention, p. 48 – 49.

Iliffe, T., 2003, The BeCKIS Project – Establishing a GIS for Cave and Karst Conservation in Bermuda [abs.]: The Program of the 2003 NSS Convention, p. 8-31.

Jenson, J. W., Keel, T. M., Mylroie, J. R., Mylroie, J. E., Stafford, K. W., Taborosi, D., and Wexel, C., 2006, Karst of the Mariana Islands: The interaction of tectonics, glacioeustasy, and fresh-water/sea-water mixing in island carbonates, *in* Harmon, R., and Wicks, C., eds., Karst Geomorphology, hydrology, and geochemistry - A tribute volume to Derek C. Ford and William B. White, Geological Society of America Special Paper 404, p. 129-138.

Karig, D. E., 1971, Structural history of the Mariana Island Arc System: Geological Society of America Bulletin, v. 82, p. 323-344.

Keel, T. M., 2005, The Caves and Karst of Rota Island, Commonwealth of the Northern Mariana Islands, [MS Thesis]: Mississippi State University, Mississippi, 221 p.

Kostka, S.J., Mickelson, D.M., and Hinke, H.J., 2004, GIS-Based Quaternary Geology Mapping of St. Croix County, Wisconsin: Geological Society of America Abstracts with Programs, v. 36, p. 581.

Lindsay, J. and Smart, C., 2004, GIS approaches to groundwater and risk analysis: Mammoth Cave National Park, Kentucky: Geo^2, v. 30, p. 40.

Lyew-Ayee, P., Viles, H. A, and Tucker, G., 2003, GIS Techniques for Karst Morphometric Analysis: The case of the Cockpit Country, Jamaica: Geo^2, v. 30, p. 8 – 9.

McKenzie, D. and Veni, G., 2003, Walls 2D: Realistic Drawing and Morphing of Cave Walls and Passage Details and its Application to GIS: The Program of the 2003 NSS Convention, p. 8-31.

Mink, J.F., and Vacher, H.L., 1997. Hydrogeology of northern Guam. *in* Vacher, H.L., and Quinn, T., eds., Geology and Hydrogeology of Carbonate Islands. Developments in Sedimentology 54: Elsevier Science, p. 743-761.

Mylroie, J.E., Moore, C.W., Walker, A.D., and Toepke, K.M., 2005, Digital Karst Map of Mississippi: Digital Submission on CD-ROM to National Park Service.

Mylroie, J.E., Jenson. J.W., Taborosi, D., Jocson, J.M.U., Vann, D.T., and Wexel, C., 2001, Karst features of Guam in terms of a general model of carbonate island karst. Journal of Cave and Karst Studies, v. 63, p. 9-22.

Mylroie, J.E., Mylroie, J.R., Jenson, J.W., 2004, Modeling carbonate island karst, *in* Martin, R., and Panuska, B., eds., Proceedings of the Eleventh Symposium on the geology of the Bahamas and other carbonate regions: Gerace Research Center, San Salvador Island, Bahamas. p. 135-144.

Paylor, R., Florea, L., Caudill, M., and Currens, J., 2003, Karst occurrence and sinkhole GIS coverages for Kentucky: Journal of Cave and Karst Studies, v. 65, p. 183.

Singhal, A. and Samuelson, A.C., 2004, Spacial Variability in the Ground Water Movement in Delaware County, IN: A GIS Based Model [abs]: Geological Society of America Abstracts with Programs, v. 36, p. 6.

Stafford, K.W., 2003, Structural Controls on Megaporosity in Eogenetic Carbonate Rocks: Tinian, CNMI [MS Thesis]. Mississippi State University, Mississippi, 363 p.

Stafford, K.W., Mylroie, J.E., Taborosi, D., Jenson, J., Mylroie, J.R, 2005, Karst development on Tinian, Commonwealth of the Northern Mariana Islands: Controls on dissolution in relation to the carbonate island karst model, Journal of Cave and Karst Studies, v. 67, p. 14 – 27.

Sugawara, S., 1939 [1949], Topography, Geology and Coral Reefs of Rota Island, [MS Thesis]: Tohoku Imperial University, [Translator: Pacific Geological Surveys, Military Geology Branch, US Geological Survey].

Taborosi, D., 2000, Karst features of Guam, [M.S. Thesis]: University of Guam, 324 p.

Taborosi, D, 2004, Field Guide to caves and karst of Guam, Sun Fung Offset Binding Co., Ltd., China.

Tayama, R., 1936, Geomorphology, Geology, and Coral Reefs of Tinian Island Together with Aguijan and Naftan Islands. Institute of Geology and Paleontology, Tohoku University, Japan, 72 p.

Toepke, K.M, 2006, GIS Analysis of the Caves and Karst of the Mariana Islands [MS Thesis]. Mississippi State University, 640 p.

Veni, G., 2004, GIS Applications in Managing Karst Groundwater and Biological Resources: Program: 2004 NSS National Convention, p. 49.

FRESH-WATER LENS ANISOTROPY AND FLANK MARGIN CAVE DEVELOPMENT FAIS ISLAND, FSM

John E. Mylroie and Joan R. Mylroie
Department of Geosciences
Mississippi State University
Mississippi State, MS 39762

John W. Jenson[1] and Robert S. MacCracken
Water and Environmental Research Institute of the Western Pacific
University of Guam
Mangilao, GU 96923
jjenson@uog.edu

ABSTRACT

Fais Island is a small uplifted carbonate platform that lies about 200 km east of Yap, Federated States of Micronesia, in the Caroline Islands of the Western Pacific Ocean. Modern freshwater lens discharge is concentrated where high relief cliffs extend seaward beyond the beach and reef flats. Freshwater flow from the beaches and reef flats is small to insignificant. Flank margin caves are also concentrated in these headlands and are conspicuously absent in the vertical cliffs inland of beach and reef flat areas. The original porosity in the pre-Holocene carbonate rocks of Fais has been rearranged into high permeability flow systems by repeated exposure to the fresh water lens. The older headlands that extend past the lower permeability beaches and reef flats, conduct water from the lens to the sea. At the same time, flank margin cave development between headlands was diminished by the lack of freshwater lens discharge in those areas. A large closed contour depression containing a freshwater pool looks at first sight like a sinkhole, but is in fact, an ancient well dug into terraced Holocene sands that infill a reentrant in a paleo-sea cliff. The low relative permeability of these sands creates a more substantial fresh water lens than is available elsewhere on the island.

INTRODUCTION

The island of Fais is located 220 km east of the island of Yap in the Caroline Islands of the Western Pacific Ocean. It is an uplifted carbonate island, 1.2 km wide and 2.9 km long with a maximum elevation of 28 m (Figure 1). There are no surface streams or water bodies. As with similarly remote islands in the Western Pacific that are vulnerable to frequent typhoons and prolonged drought, especially during El Niño events, ensuring a reliable supply of freshwater for island residents is an ongoing concern. Island residents (~320 people) use rainfall catchment as the primary freshwater source, although their main daily source of bodily fluid replenishment is from co-

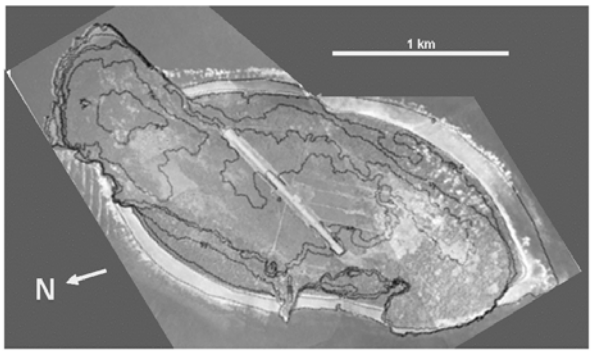

Figure 1. Composite aerial photograph of Fais. Contour interval is 10 ft (3 m).

conuts that grow prolifically on the island (MacCracken, 2006; 2007). Rooftop catchments can be destroyed entirely by the storms and both catchments and associated storage are rendered useless by prolonged drought. Similarly, high winds and prolonged droughts can eliminate the coconut crop. The groundwater resources of the island consist of a few drilled wells and one dug well, that can be brought into service during emergencies. However, water from such wells must be carried in hand containers to the households within the island's three villages. Previous attempts to install additional wells near the villages met with limited success (Zheng, 1996). The purpose of this study was to gain insights into the distribution and potential for groundwater development through a better understanding of the cave and karst features on the island. Such field work has proved useful in the nearby Mariana Islands (Jenson, et al., 2006).

FIELD OBSERVATIONS

Study of the beaches and adjacent terrain in the coastal zone during negative spring tides in May, 2005 showed that modern freshwater lens discharge is concentrated where high relief limestone headlands extend seaward beyond the beach and reef flats (Figure 2). Freshwater flow from the beaches and reef flats, on the other hand, is small to insignificant (Figure 3). Surface surveys show that uplifted flank margin caves are also concentrated in these headlands, but are conspicuously absent in the vertical cliffs inland of beach and reef flat areas. The flank margin cave locations indicate that past mixing zone dissolution occurred preferentially in the headlands, rather than uniformly along the island perimeter. It thus appears that past freshwater discharge was also concentrated in the headlands.

It has been observed in Bermuda and the Bahamas (Vacher and Wallis, 1992) that freshwater discharge is minimized in beaches and related young carbonate rocks, but is enhanced in the older rocks that have experienced the longest contact with the freshwater lens over numerous glacioeustatic sea-level highstands. On Fais, tectonic uplift has combined with glacio-eustasy to produce a more complicated exposure and submersion history for the limestone than has occurred in Bermuda and the Bahamas. The original depositional porosity in the pre-Holocene carbonate rocks of Fais has been re-arranged into high-permeability flow systems by repeated exposure to the freshwater lens. The older headlands extend seaward past the Holocene lower permeability beaches and reef flats and constitute preferred high permeability flow routes to conduct water from the lens to the sea. The outer boundary of the freshwater lens exhibits a high degree of anisotropy. Island morphology suggests that the headlands may lie at the end of faults that dissect the island (Figure 2). The presence of flank margin caves in these headlands, in contrast with their conspicuous absence elsewhere, indicates that the current anisotropic flow regime was also active in the past, promoting mixing-zone dissolution in the distal margin of the freshwater lens under the flank of the enclosing headland rock mass. At the same time, flank margin cave development between headlands was diminished by the lack of fresh water lens discharge in those areas. Uplifted flank margin caves on Fais therefore provide a proxy for freshwater discharge patterns on the island today. It should be noted, however, that cliff retreat from wave erosion is active on the headlands, whereas the inland scarps are somewhat protected. Unexhumed flank margin caves could exist in the interior cliffs where cliff retreat has not advanced far enough to breach the caves. Such retreat has made the caves in the headlands obvious, however.

A large closed-contour depression containing a fresh-water pool exists in an embayment in the cliff on the northwest side of Fais (Figure 2). This feature gives the superficial appearance of a sinkhole or blue hole, but more careful inspection shows it to be a dug well set in terraced Holocene sands that infill this embayment in a paleo-sea cliff (Figure 4). The low relative permeability of these sands creates a more substantial freshwater lens than is available elsewhere on the island, where groundwater dissolution has organized

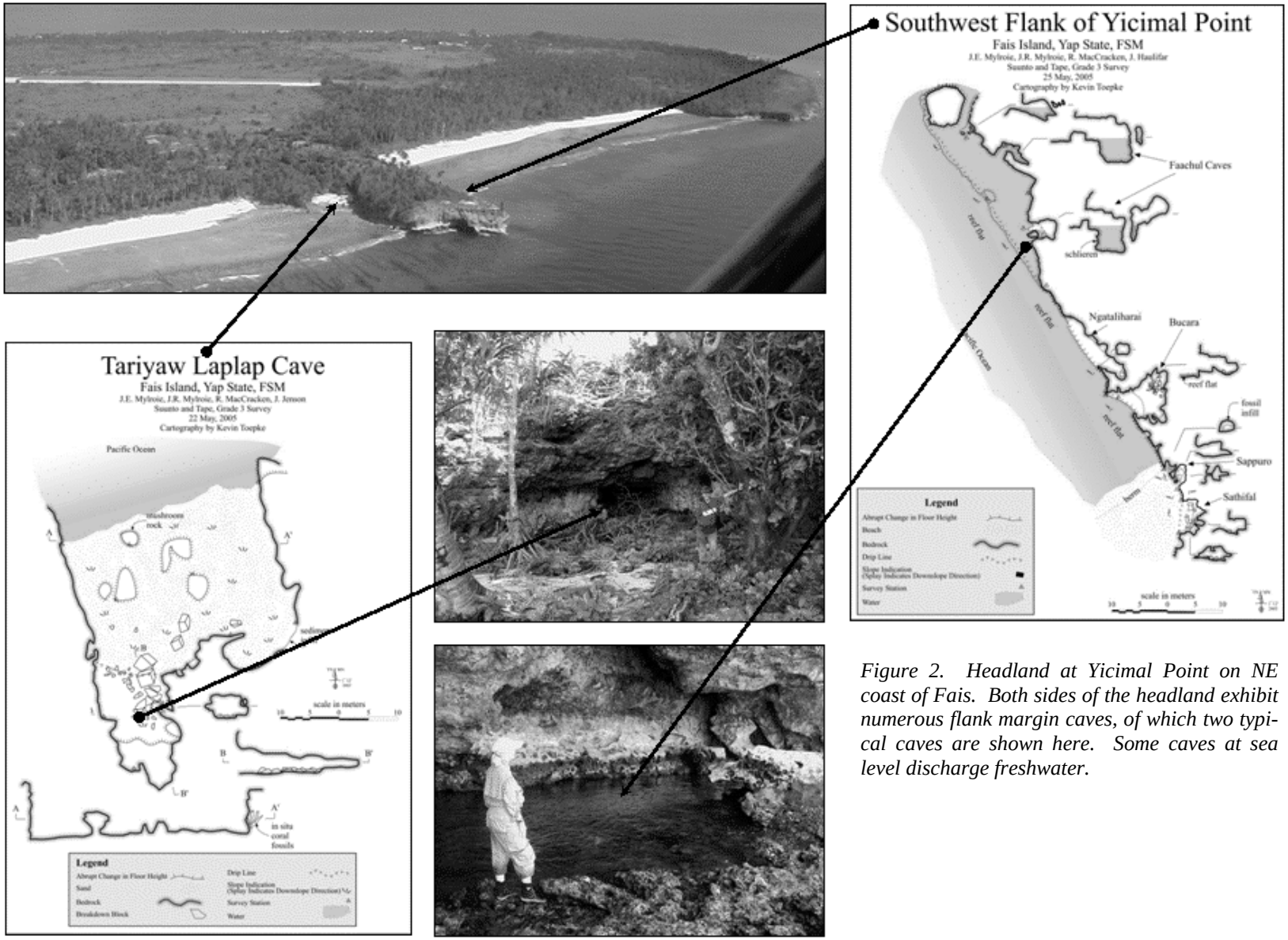

Figure 2. Headland at Yicimal Point on NE coast of Fais. Both sides of the headland exhibit numerous flank margin caves, of which two typical caves are shown here. Some caves at sea level discharge freshwater.

Figure 3. Beach flat at negative tide. No significant discharge is observed.

high permeability pathways in the bedrock. Residents report that the well is ancient, and so was the sole source of freshwater before rooftop rain catchment technology became available.

Figure 4. The Old Well.

Large, deep slots in the limestone that extend from the vegetated region onto the bare rock of the coastal platform at the east end of the island are not karst features. While these slots appear similar to small dissolution corridors, they are fossilized spur and groove features preserved by island uplift (Figure 5). Farther into the interior, isolated rock pinnacles rise up to 4 m above the surrounding land surface (Figure 6). These rock features appear to be dissolutional in origin, based on morphology and the dissection of primary features, especially large coral heads in the rock itself. The island was mined for phosphate by the Japanese from 1914 to1945, and the degree to which these pinnacles represent subaerial features or exhumed subsoil features is not known.

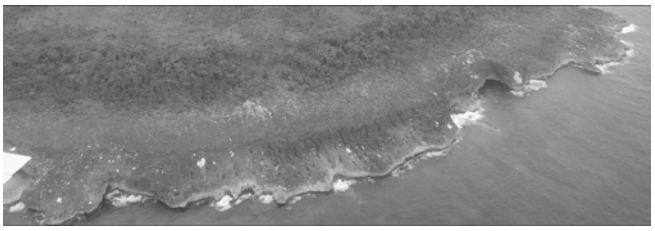

Figure 5. Fossil spur and groove.

Figure 6. Interior karrenfeld.

CONCLUSIONS

Sinkholes, sinking streams, and karst springs typical of continental settings are absent, as would be expected on a small carbonate island. The closed depressions on Fais are either constructional in nature, representing the original depositional morphology, or are artifacts of phosphate mining. The depression containing the dug fresh water well is artificial--the sand walls having been terraced and stabilized by laid stone walls to prevent slumping into the water hole. Pit caves were not identified during the field investigation, and all observed bedrock outcrops were limestone, indicating no allogenic catchment for

meteoric water. All rainfall catchment is autogenic, and rain that is not caught on roof catchments sinks immediately into the epikarst developed on top of the limestone.

The karst inventory of Fais yielded several useful observations:

1) There are no caves in the interior, especially pit caves, so there is no natural access to the water table. To tap groundwater, wells must be drilled, or dug and maintained.

2) The old well dug into relatively low permeability Holocene sands provides easy access to the most voluminous ground water resource on the island and can be brought into service with relatively modest effort. The well is remote from current village locations, and water must be carried in hand containers.

3) Uplifted, relict spur and grooves forming topography along the coast are not eroded stream caves. All documented dissolution caves are flank margin caves that are concentrated along headlands.

4) The uplifted flank margin caves indicate where freshwater discharge occurred in the past, and those areas also proved to be where freshwater discharge occurs today. Flank margin caves are a proxy for fresh water discharge on Fais.

5) The freshwater lens is probably present across the entire island, but lens thickness and water quality (chloride concentration) are likely to be variable, so that the success of any given well cannot be easily predicted in advance. In general, water from the interior most likely flows toward faults or fractures that ultimately intercept the headlands.

6) Fais Island falls into the *simple carbonate island* category of the Carbonate Island Karst Model or CIKM (Jenson et al., 2006), however, the island demonstrates the complexity that can occur even in this single-lithology setting.

ACKNOWLEDGMENTS

Moses Ngirmekur from the Department of Resources and Development on Yap for provided aerial photographs and topographic maps. Jesse Haulifar, Fais' postmaster and travel agent was our our guide, boat operator, and host. Sesario Sigam also assisted us in the field, and Don Rubinstein assisted with spelling and interpretation of place names for the maps. Jesse Raglmar, Chief Clerk of the Yap State Legislature provided knowledge and advice that made the project successful. Finally, we wish to thank all the residents of Fais for their gracious hospitality.

REFERENCES

Jenson, J.W., Keel, T.M., Mylroie, J.R., Mylroie, J.E., Stafford, K.W., Taborosi, D., and Wexel, C., 2006, Karst of the Mariana Islands: The interaction of tectonics, glacio-eustasy, fresh-water/salt-water mixing in island carbonates: Geological Society of America Special Paper, v. 404, p. 129-138.

MacCracken, R.S., 2006, Water Resources Analysis of Fais Island, Yap State, FSM: M.S. thesis, University of Guam, Mangilao, 130 pp.

MacCracken, R.S., 2007, Water Resources Analysis of Fais Island, Yap State, FSM, WERI Technical Report 111: Water & Environmental Research Institute of the Western Pacific, University of Guam, Mangilao, 66 pp.

Vacher, H.L., and Wallis, T.N., 1992, Comparative hydrology of Bermuda and Great Exuma Island: Groundwater, v. 30, p. 15-20.

Zheng, K., 1996, Implementation of Fais Well Drilling Programme and Well Driller's Training, ed, FSM/United Nations Water Resources Assessment and Development Project.

A HYPOTHESIS FOR BIOGENIC CAVE FORMATION: A STUDY CONDUCTED IN THE BAHAMAS

Stephanie J. Schwabe
Department of Geology and Environmental Geosciences
College of Charleston
Charleston, SC 29424
steffi@blueholes.org

and

Rob Palmer Blue Holes Foundation
5 Longitude Lane
Charleston, SC 29401

Rodney A. Herbert
Division of Environmental and Applied Biology, Biological Sciences Institute
University of Dundee
Dundee DD1 4HN, Scotland UK

James L. Carew
Department of Geology and Environmental Geosciences
College of Charleston
Charleston, SC 29424

ABSTRACT

The currently accepted hypothesis for the development of caves in carbonate islands and coastal areas suggests that mixing of $CaCO_3$ supersaturated seawater with $CaCO_3$ saturated groundwater creates undersaturated mixed water that is thought to be responsible for large-scale carbonate dissolution. This hypothesis does not address the dissolution potential of rainwater descending through the vadose zone, or the groundwater. It is known that soon after rainwater has moved through the soil and makes contact with the underlying limestone it becomes buffered by dissolution of $CaCO_3$. We hypothesize that the dissolution capacity of the vadose water is primarily controlled by the assimilation of CO_2 produced by heterotrophic bacteria living in the pores of the host rock.

Rainwater that was collected before it made contact with the ground on San Salvador Island, Bahamas contained 10^3 bacterial cells per milliliter. In contrast, water collected from dripstones in caves contained $>10^4$ to 10^5 colony-forming-units (cfu). Wall-rocks collected from dry caves on the island, contained $>10^6$ cfu, and the dominant heterotrophic bacteria are in Order Actinomycetales, which are known to produce CO_2 and NH_3 as end-products of their metabolism. The presence of these microbial populations, comprising at least 16 different species, provides a significant potential for the production of CO_2 and other microbially generated acids. Surface and 2.5-cm-deep wall-rock samples sealed in sterile vials for 14 days yielded a CO_2 content that ranged from 770 to 410 ppm above the current atmospheric concentration (~380 ppm).

Our observations suggest that bacteria are maintaining and driving the CO_2-related dissolution in the vadose and phreatic zones. It is also likely that secondary porosity and permeability may be enhanced even during periods when the rock is not saturated with water.

Limestone in the phreatic zone, especially where they are exposed to the mobile mixing-zone water, experience the greatest removal of solutes and the greatest concentrations of bacteria. As a result, it is reasonable to suppose that void enlargement reaches the highest rates in association with those environments. Hence, caves develop and enlarge to their greatest extent at or near sea level, which is consistent with the flank margin hypothesis. This can also explain why caves that experienced only relatively short episodes of phreatic conditions can be so large.

INTRODUCTION

In the 1980s, research in the Bahamas revealed that there are many large caves with morphologies that indicate phreatic dissolution that occur in rocks that are only ~330,000 to 120,000 years old. In addition, those rocks have been subjected to phreatic conditions only during one or more of the short (~10,000 years) glacio-eustatic sea-level highstands that occurred in the Mid-Late Pleistocene (Mylroie and Carew, 1988a). Thus, some of these caves must have formed in no more than 10,000 to 12,000 years, and none represent more than 45,000 years of dissolution in the phreatic zone. In an attempt to explain how such large caves could have formed during such short intervals of time, the flank margin hypothesis was proposed by Mylroie and Carew (1990).

The generally accepted view of limestone dissolution is that it is due to the infiltration of low-pH meteoric water and groundwater that results from incorporated atmospheric CO_2 as well as CO_2 from the near-surface (e.g. soil) environment; and it is these initial CO_2 concentrations that dictate the amount of limestone dissolution (White, 1988). It has been assumed that once meteoric water charged with atmospheric and soil CO_2 enters the vadose zone, continuing input of meteoric water keeps this water undersaturated with respect to $CaCO_3$, and thereby maintains its dissolution potential.

It has been noted (Mylroie and Carew, 1990; White, 1988) that there is a large volume of literature linking the formation of caves and the water table. It has also been suggested that the mixing of different water masses that are saturated, or even supersaturated, with respect to $CaCO_3$, can produce undersaturated mixed water capable of significant dissolution of limestone (Plummer, 1975; Mylroie and Carew, 1990; White, 1988; Back et al., 1986; Sanford and Konikow, 1989). It has been further noted (Mylroie and Carew, 1990; White, 1988; Back et al., 1986; Sanford and Konikow, 1989; Stoessell et al., 1989) that dissolution often is most extensive where mixtures of freshwater and seawater are discharging into the sea. However, studies of the hydrogeochemistry of Bermuda (Plummer et al., 1976) demonstrated that calcite saturation in the mixing zone is controlled by CO_2 degassing, and not by the mixing of freshwater with seawater. The source of the CO_2 necessary for driving the dissolution process has not been idenfied.

The flank margin hypothesis of cave formation (Mylroie and Carew, 1990) proposes that the mixing of different water masses saturated with respect to $CaCO_3$ under different conditions is responsible for the rapid cave development seen on these islands. In particular, maximum dissolution is proposed to occur at the discharging margin of the freshwater lens due to the close juxtaposition of the top of the groundwater lens (where vadose water mixes with the fresh to brackish groundwater lens), and at the base of the lens (where fresh to brackish groundwater mixes with underlying seawater).

Currently, the flank margin hypothesis is the only accepted explanation for the development of such caves, and the model has been extended to carbonate islands throughout the world (Frank et al., 1998 ;Mylroie and Carew, 1995; Mylroie et al., 1995; Mylroie et al., 2001). However, we argue that this hypothesis does not address fully the actual dissolution potential of rainwater as it migrates downward through the vadose zone and merges with the groundwater. In addition, it does not correctly identify the actual cause of mixing zone corrosion. We postulate that the dissolutional capacity of the vadose water is enhanced or maintained as the descending meteoric water accumulates microbially-generated CO_2 that is produced by heterotrophic bacteria residing in the pores of the host rock. That is, from the time

rainwater enters the rock to the time it merges with the groundwater at the water table, bacteria living in rock pores (Schwabe et al., 1996) recharge the descending water with CO_2. In addition, bacteria in the fresh, mixed, and marine groundwater also contribute CO_2 and produce other organically generated acids that contribute to the dissolution of carbonate rocks (Schwabe, 1999; Schwabe, 2002). In particular, accumulations of particulate organic carbon (POC), particulate organic matter (POM), dissolved organic carbon (DOC), and bacterial cells at the major density interface at the upper mixing zone boundary and a lesser density interface at the bottom of the mixing zones in currently flooded Bahamian caves, produce optimal conditions where many bacteria thrive on the accumulated POC, POM, and DOC (Schwabe, 1999; Schwabe, 2002). The end-product of carbon metabolism by these microbes produces P_{CO2} levels of at least 3 to 4 times atmospheric concentration (Whitaker and Smart, 1997). We suggest that the resulting microbially-maintained acidic pH at these boundaries is responsible for the observed greater limestone dissolution that seems to have occurred at and around sea level (*sensu* Mylroie and Carew, 1988b), rather than the actual physical mixing of different water masses.

OTHER STUDIES

The role of bacteria in sulfuric acid speleogenesis (SAS) has become an accepted model for some cave development, such as large caves like Carlsbad and Lechuguilla in the Guadalupe Mountains of New Mexico (e.g., Hill, 1990), Lower Kane Cave in Wyoming (Engel et al., 2004), as well as others (e.g., Hose et al., 2000; Angert et al., 1998). Some work in the Bahamas has also indicated a role for sulphur-mediating bacteria (Bottrell et al., 1991; 1993); however, it is our contention that in the Bahamas, and similar carbonate settings, even traditional carbonic acid dissolution is also largely the result of bacterial activity. Whitaker and Smart (2006) suggested that CO_2 must be added to the ground water in the northern Bahamas by oxidation of surface- and soil-derived organics in the lens, but they did not document the presence of abundant populations of bacteria living in the rocks and groundwater as the probable source of CO_2. It is surprising that bacteria have not been recognized as an important aspect of limestone dissolution in the classical karst literature, because research in the 1930s demonstrated the existence of abundant and diverse bacteria on and within rock samples, and also documented CO_2 production associated with bacterial activity and the "decay of stone" (Paine et al., 1933).

Information on the abundance, distribution, and identification of CO_2-producing bacteria in the vadose zone of limestone in other localities is limited. However, information from the Black Creek-Middendorf-Cape Fear (BMC) aquifer system of South Carolina (Chapelle and Lovely, 1990), Patapsco aquifer system of southern Maryland (Chapelle et al., 1987), and the Madison aquifer system of the western United States (Chapelle and Lovely, 1990) indicate that bacterial activity, as measured by rates of CO_2 production, are in the 10^{-4} to 10^{-6} mmole per liter per year range--and all three of those systems are oligotrophic (Plummer et al., 1990). In comparison, the average CO_2 production from Altar Cave rock samples from San Salvador Island, Bahamas, and rock samples from Germany (Ehrlich, 1990) are substantially higher than those recorded from the BMC, Patapsco, and Maryland aquifers. Like the above-mentioned aquifer systems, lack of significant topsoil at the surface, and minor organic matter included within the rock matrix that encloses Altar Cave, San Salvador, also represents an oligotrophic environment. Under such nutrient-poor conditions, the presence of substantial populations of bacteria belonging to Order Actinomycetales is not surprising, as they are well-suited to growing in low-nutrient environments with alkaline pH (Lechevalier and Lechevalier, 1967; Barton et al., 2004).

Other investigators have also reported the dominance of *Actinomycetes* sp. in the rocks of limestone caves (Laiz et al., 1999; Cunningham et al., 1995; Groth et al., 1999). It was reported that in Altamira Cave located on the Cantabrian Cornice, Santillana del Mar, Spain, selective growth of *Actinomycetes* occurred on the cave wall sur-

faces (Laiz et al., 1999; Cunningham et al., 1995). Interestingly, in both the Bahamas and in Spain, analyses of drip waters demonstrated that the microbial communities in the water were different from those of the rocks themselves, and that the *Actinomycetes* remain in the rocks and are not liberated into the drip water.

METHODS

To enumerate bacteria from San Salvador drip water samples, 1 ml aliquots from each dripwater sample were aseptically transferred to 9 ml of sterile 0.9% v/w physiological saline and decimal dilution series were prepared. Tubes were vigorously vortexed between each serial transfer to ensure that the cells remained in suspension. Aliquots (0.1 ml) from each dilution were aseptically transferred to Tryptone Soy agar plates and spread over the plate using a sterile spreader. The plates were incubated at 25^{o} C and inspected daily until no further colonies developed. The colonies on the plates were then counted.

To enumerate bacteria from San Salvador limestone samples, 1 g of limestone was weighed under sterile conditions and transferred to 9 ml sterile 0.9% v/w physiological saline solution. The limestone was crushed using a sterile stainless steel rod (10 mm diameter) until a fine suspension was formed. The limestone suspension was then subjected to 4 x 15 second bursts of sonication using a sterile MSE 150 soniprobe (MSE Instruments Ltd) to detach the bacterial cells. Decimal dilution series were prepared and the dilutions transferred onto half-strength agar plates and incubated in the same way as the drip water samples. The colonies on the plate were counted after no further development occurred.

To enumerate bacteria in formaldehyde-preserved water samples using DAPI staining, the procedure of Porter and Feig (1980) was used. Water samples (10 ml each) were filtered through 0.22 µm pore-size Nucleopore polycarbonate filters pre-stained with Irgalan Black. The bacteria were stained with DAPI (4'6 diamindio-2-phenylindole) at a final concentration of 2 µg ml^{-1} for 10 minutes. After staining, the membranes were mounted on clean microscope slides with a drop of low-fluorescence immersion oil. The slides were examined using an Olympus BH-2 epifluorescence microscope at an excitation wavelength of 350 nm.

To quantify CO_2 production from rock samples, we used 20 ml serum vials that were sterilized along with tweezers, dental tools and rock chisels. Chisels were used to remove the hard surface sample and the soft samples at 2.5 cm deep into the wall were collected using a dental hook. Once in the serum vial, samples were sealed with a sterile butyl stopper and secured with an aluminum crimp. Two of the vials with rock samples were sterilized and the other samples were allowed to incubate for 14 days at 25^{o} C. Using a sterile needle and 5 ml syringe, samples of air were removed from the serum vial and injected into GC carrier vials. The CO_2 analysis was run on a GOW-MAC Series 400 Gas Chromatograph (GC).

RESULTS AND DISCUSSION

Our microbial hypothesis is supported by a variety of data obtained from our recent study of rocks and water in the Bahamas, and from earlier studies (Schwabe et al., 1996; Schwabe 1999; Schwabe, 2002; Schwabe and Herbert, 2004). Rainwater collected under sterile conditions before contact with the ground on San Salvador Island, Bahamas in December 2005 contained ~10^3 bacterial cells per milliliter (Table 1). In contrast, water collected from dripstones in caves contained >10^4 to 10^5 cells/ml (Table 1), and limestone samples collected from Altar Cave on San Salvador Island, Bahamas, contained >10^6 viable cells per half gram of rock sample (Table 1).

The dominantly heterotrophic bacteria present in these limestone samples were aerobic Gram-positive bacteria identified as belonging to Order Actinomycetales (Figure 1; Table 2) that are known to produce CO_2 as an end-product of their carbon-based metabolism. In addition, bacteria recovered from 8-cm-deep rock cores into the wall of a flooded cave in the phreatic zone at 13.9, 14.0 and 15.9 m depths, had cell counts greater than the bacterial cell numbers recovered from the adjacent water column at equivalent

depths (Table 3) (Schwabe, 1999; Schwabe, 2002). In samples from rock cores recovered

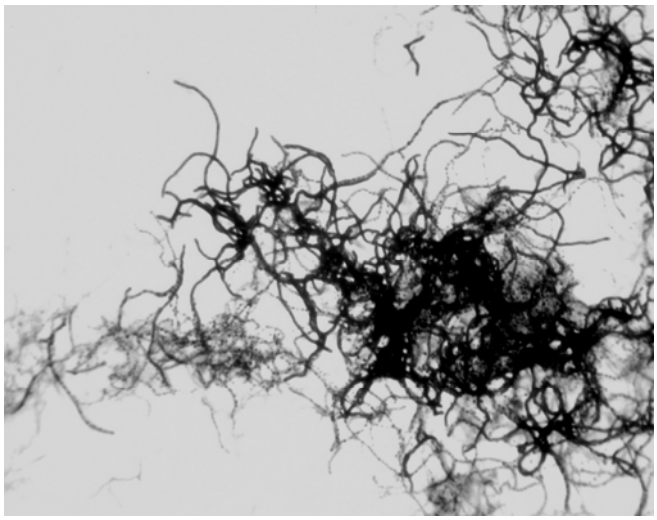

Figure 1. Photograph of bacteria of the Order Actinomycetales. Field of view is approximately 6 µm in width.

from the phreatic zone in Lucayan Caverns on Grand Bahama Island (Schwabe et al., 1996), bacterial counts ranged from 1.321 x 10^6 cells in the outer 2 cm, to 19,756 cells recorded 8 cm deep into the cave wall rock (Table 3). The rock core with the highest bacterial counts was from the top of the mixing zone. The presence of large microbial populations in the rock that comprise a number of different species, provides not only a significant potential for the production of CO_2, but also for other microbially-generated acids.

Furthermore, surface and 2.5-cm-deep cave-wall rock samples from the vadose zone in Altar Cave on San Salvador Island that were sealed in sterile vials for 14 days, yielded CO_2 contents ranging from 770 to 410 ppm above current atmospheric concentration (~380 ppm). In contrast, sterilized rock samples from the site yielded no excess CO_2. These data indicate that the indigenous bacteria present in the rock produce CO_2, and have the potential to sustain and drive CO_2-related dissolution processes in the vadose and phreatic zones (Figure 2). This suggests that the porosity and permeability of the limestone may be enhanced even when the rock is not saturated with water.

Additional evidence of the ability of bacteria to generate large quantities of CO_2 was observed by Schwabe when water samples were collected from the top of the freshwater/saltwater boundary of the water column of a vertical cave on South Andros Island, Bahamas (Schwabe, 1999; Schwabe, 2002). Within 6 hours of their collection, microbial generation of CO_2 (bacteria counts of >10^7 cells/ml) was so great that samples stored in 125 ml vials with ground-glass stoppers had the stoppers explosively expelled, even though the vials were refrigerated.

At other locations in the Bahamas, bacterial counts from water samples collected from the water column within flooded cave systems, reveal that the water column is not homogeneous with respect to numbers of bacteria (Schwabe et al., 1996; Schwabe, 1999; Schwabe, 2002; Schwabe and Herbert, 2004).

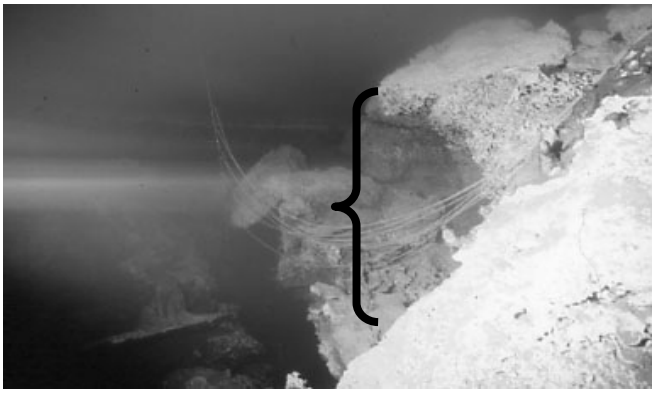

Figure 2. Banding within the water column and the mixing zone (MZ) in a cave on Grand Bahama Island, Bahamas. The bracket marks the MZ. Note the severely-etched rock within the bracket zone. In the water column to the left of the bracket, note the bands within the water column. Density differences support particles, including bacteria, copepods, and carbonate dust knocked off the ceiling by scuba exhaust. The water sampling tubes can be seen leading from the right upper corner of the photograph to where they are secured on a line attached from the ceiling of the cave to the floor.

Instead, bacteria often thrive in centimeter-thick zones (Figure 3) situated throughout the extent of the water column (Schwabe, 1999; Schwabe,

2002). These bands, or layers, are visibly darker than the intervening water (Figure 2), and reveal large populations of microscopic, photophobic, grey-black copepods of a species yet to be identified. Results from ^{3}H thymidine data indicates that there are large numbers of bacterial cells that are unaccounted for in those layers (Schwabe, 1999; Schwabe, 2002). We interpret these data as evidence that the large populations of copepods are grazing on the bacteria, thereby keeping their numbers low; and that both the copepods and the bacteria in such layers must produce abundant CO_2.

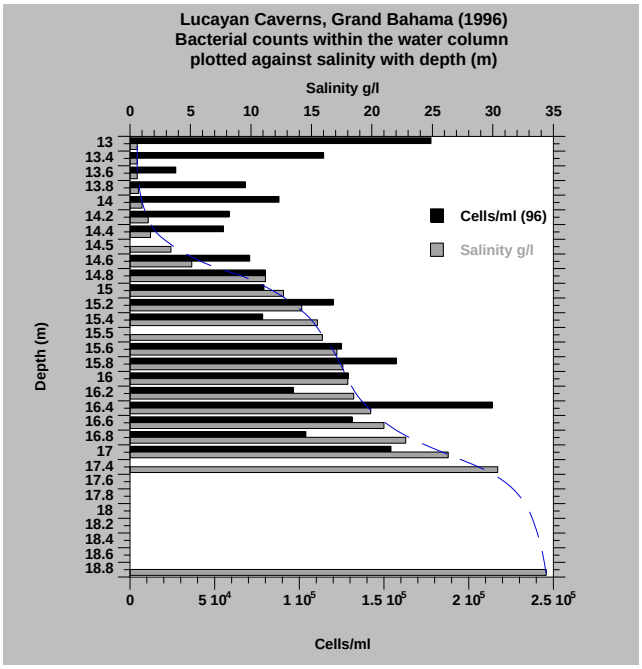

Figure 3. Graph of the salinity and corresponding bacterial counts through a water column in Lucayan Caverns, on Grand Bahama Island, Bahamas. The ceiling in the passage section represented here is at 13 m below sea level. The major density interface at the top of the mixing zone (MZ) begins at 14 m. A salinity step occurs at 16 m. In this particular passage, the water column reaches full marine salinity within the sediments on the floor at (~19.0 m).

The apparent zonation of bacteria in the water column of currently flooded caves in the Bahamas seems to be a result of varying densities within the water column (Figure 3). Geochemical profiles taken throughout the water column show that within a few centimeters, the general geochemical parameters and microbe counts often change significantly. For example, pH levels often vary markedly on the centimeter scale, and it is common to observe pH changes from ~8.5 to 4 over distances of less than 20 centimeters. In addition, bacterial populations within 20 cm vertical distances of one another in the water column (Figure 3) can vary from $<10^3$ to $>10^6$ cells/ml (Schwabe, 1999; Schwabe, 2002). Within most water columns observed in flooded caves in the Bahamas there is a coincidence of high bacterial numbers and acidic pH.

Knowing that bacterial stratification can occur within water columns in flooded caves, it does not seem unreasonable to assume that microbial populations will form microenvironments in the vadose zone of the rocks themselves, based on a discontinuous and variable supply of water, oxygen, and organics (Figure 4). Burial of organic material in the form of reefs, or subtidal grass/algal facies, or buried vegetation in eolianites may act as catalysts for void formation because they provide abundant sources of organic matter for interstitial bacteria. Microbial processes, whether in microenvironments or not, will affect the chemical composition of groundwater and the hydraulic properties of aquifers (Laiz et al., 1999). From the data obtained in our studies, we contend that contrary to the generally accepted model (White, 1988), the pH of rainwater does not play a significant role in carbonate dissolution, because the rainwater experiences significant buffering when it encounters the surface rocks (Figure 4). Evidence to support this conclusion was obtained by analysis of several samples of rainwater. Rainwater caught before contact with the ground had a pH of 5.72 (Table 1). In contrast, rainwater collected from profuse overflow from a building roof during a heavy rainstorm in February 2006 on San Salvador Island had a pH of 8.5, and analysis of the dissolved salts (Table 1) confirm that the pH reflected significant buffering from possible degassing and brief contact with the small quantity of $CaCO_3$ dust and rocks that are on the roof. Still further evidence was provided by analysis of rainwater that accumulated in

the catchment basin of the 18 acre concrete-covered hillside at the Gerace Research Centre during a large storm event in June 2006. The pH of the water collected about 18 hours after the rainstorm, was 9.18 (Jon Martin, pers. comm.). These data show that rainwater is thoroughly buffered within minutes to hours of contact with the surface.

In addition, analyses of water from open wells, cave drip water, brackish water, and sea-water on San Salvador show that they are all supersaturated with respect to calcite, and predominantly at equilibrium with aragonite (Moore and Martin, 2006). Likewise, the calcite Saturation Index of some of our samples of water (Rain06, DR1, and Alt 1 [see Table 1]) indicate that the rainwater (Rain06, SI = +0.42) and drip water Alt1 (SI = +0.51) were supersaturated, and drip water DR1 (SI = -0.07) is saturated.

Table 1. Chemical and microbiological analyses of water and rock.

Sample	pH	T°C	Cl^- mg/l	HCO_3^{--} mg/l	Ca^{2+} mg/l	Mg^{2+} mg/l	Salinity g/l	Microbial counts
*DR0	**	**	**	**	**	**	**	6×10^3 cfu/ml
DR1	7.55	27.7	221	274	96	23	0.7	3.5×10^5 DC
Alt1	7.34	24.7	278	278	211	51	**	4.0×10^4 DC
Alt2	7.89	23.1	761	278	216	53	1.6	**
Rain05	**	**	**	**	**	**	**	1×10^3 DC
Rain06	8.54	24.0	15.6	310	6.9	0.9	0.1	**
Rain07	5.72	27.0	22.3	14	3.2	**	0.25	**
AltRk	**	**	**	**	**	**	**	$> 10^6$ cfu/0.5g

*Possible error on water analysis is ± 5%. *DR0 collected 12/04; DR1& Alt1 collected 12/29/05; Alt2 collected 01/05/06; rainwater collected 12/05, 02/06, and 01/07; AltRk collected 12/05. Under headings **indicates no data, cfu is colony-forming-units, DC is direct counts/ml using DAPI methods, DR is Dripping Rock, Alt, is Altar Cave, AltRk is Altar Cave wall rock samples.*

Table 2. Bacterial genera found in water samples from various sites.

Sample	Gram	Shape	Oxidase	Catalase	Genera
DR	-	Rods	+	+	*Sphingomonas*
DR	+	Cocci	-	+	*Micrococcus*
WBH	-	fat rods	-	+	*Flavobacterium*
WBH	-	short rods	+	+	*Sphingomonas*
WBH	+	short rods	-	+	*Microbacterium*
IW	-	rods	+wk	+	*Flavobacterium*
LHC	+	cocci	-	+	*Micrococcus*

DR-Dripping Rock, WBH-Watling's Blue Hole, IW- Ink Well Blue Hole, LHC - Lighthouse Cave.

Table 3. Bacterial counts within 2 cm sections of digested rock core from cave wall.

Depth m	Water	2.0 cm	4.0 cm	6.0 cm	8.0 cm
-13.9	68,077	737,904	479,843	144,045	32,945
-14.0	88,024	1,321,295	325,611	33,458	19,756
-15.9	157,326	510,504	193,642	75,787	23,291

Bacterial populations at 2 cm depth intervals into the wall rock of a cave show abundant populations at three water depths, and up to 8 cm deep into the rock. The major density interface between fresh and salt water is located at 14.0 m in the second chamber in Lucayan Caverns. The column headed "Water" shows bacteria counts from water samples collected adjacent to the cave wall where each rock core was taken. Note that bacteria are more abundant in the rock than the water up to at least 4 cm deep into the rock.

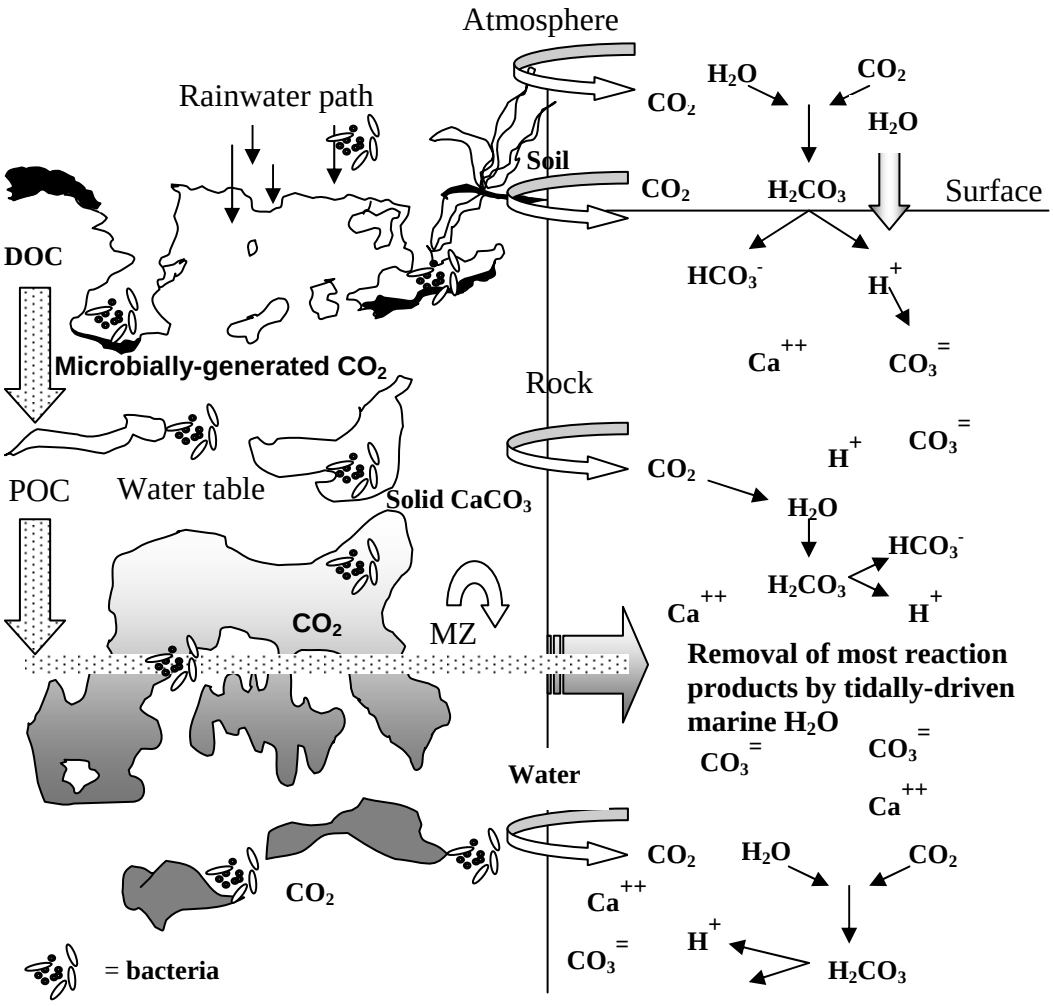

Figure 4. Schematic diagram of some of the chemical activities involved in the dissolution of $CaCO_3$ and the bacterial sources of CO_2 to drive it. Dark shading represents marine salinity, and White represents freshwater. MZ is the mixing zone. The diagram represents a rock column with a vadose and phreatic zone with water, gases, and bacteria.

CONCLUSIONS

It is generally agreed that dissolved carbon dioxide and other acids are the primary cause of the development of secondary porosity and permeability in limestones (White, 1988). However, we suggest that limestone dissolution in the Bahamas is not primarily the result of inorganic physico-chemical reactions and the initial acidic pH of rainwater. Instead, we suggest that rainwater is effectively buffered shortly after it contacts the ground; but as the water descends toward the water table, it is recharged with CO_2 that is produced as an end-product of carbon metabolism by the abundant indigenous bacterial flora living in the rock. As a result, dissolution may take place throughout the vadose zone, and sizable voids may develop in the vadose zone where the organic and moisture content of the rock is sufficient to support indigenous bacteria.

We further suggest that the portions of limestone strata in the phreatic zone, especially in the mixing zone and the upper marine section of the water column, are subjected to the greatest amount of water movement (which enhances solute removal) and the largest concentrations of bacteria (which produce abundant CO_2 and other acids). As a result, the dissolution potential of the water is greatest in those environments (Figure 2). Hence, caves develop to their greatest extent at or near sea level, which is consistent with the earlier-reported usefulness of flank margin caves as indicators of past sea-level position (Mylroie and Carew, 1988b). In addition, the recharging of vadose and phreatic ground water by microbially-derived CO_2 provides a reasonable explanation for how caves in these Bahamian rocks that have experienced only short episodes of exposure to freshwater and mixing zone water can be so large (Mylroie and Carew, 1988a). In addition, we suggest that it is likely that bacteria also control, or substantially contribute to, cave development in the vast majority of settings.

ACKNOWLEDGMENTS

We thank Dr. Larry Davis for geochemical analyses of water samples; Dr. Art Palmer for calculation of saturation indices; Steve Jones for operating the GC; Anton Dumars for assistance with the Altar Cave survey project; and students F. Scott Fitzgerald, Ashley O'Kelly, Majken Schimmel, McKean Smith, Chris Stubbs, Alton Sutter, and Linda Zinnikas for their help in the field. S. Schwabe thanks Dr. John Parkes for his support during her PhD research. We also thank Dr. Donald T. Gerace, CEO, and Vincent Voegeli, Executive Director, of the Gerace Research Centre, San Salvador, Bahamas, for logistical and personal support; and Wings Trust for financial support. Lastly, we thank P.J. Moore and Drs. Tim Callahan, Mitch Colgan, Art Palmer, Jon Martin, and Lisa Park for helpful reviews of earlier versions of our manuscript.

REFERENCES

Angert, E.R., Northup, D.E., and Pace, N.R., 1998, Molecular phylogenetic analysis of a bacterial community in Sulphur River, Parker Cave: Kentucky: American Mineralogist, v. 83, p. 1583-1592.

Back, W., Hanshaw, B.B., Herman, J.S. and Driel, J.N.V., 1986, Differential dissolution of a Pleistocene reef in the ground water mixing zone of coastal Yucatan, Mexico: Geology, v. 4, p. 137-140.

Barton, H., Taylor, M., and Pace, N., 2004, Molecular phylogenetic analysis of a bacterial community in an oligotrophic cave environment: Geomicrobiology Journal, v. 21, p. 11-20.

Bottrell, S.H., Smart, P.L., Whitaker, F., and Raiswell, R., 1991, Geochemistry and isotope systematics of sulphur in the mixing zone of Bahamian blueholes: Applied Geochemistry, v. 5, p. 97-103.

Bottrell, S.H., Carew, J.L., and Mylroie, J.E., 1993, Inorganic and bacteriogenic origins for sulfate crusts in flank margin caves, San Salvador Island, Bahamas, *in* White, B., ed., Proceedings of the Sixth Symposium on the Geology of the Bahamas: San Salvador, Bahamas, Bahamian Field Station, Ltd., p. 17-21.

Chapelle, F.H., Zelibor, J.L., Grimes, D.J. and Knobel, L.L., 1987, Bacteria in deep coastal plain sediments of Maryland: A possible source of CO_2 to ground water: Water Resources Research v. 23, p. 1625-1632.

Chapelle, F.H., and Lovely, D.R., 1990, Rates of microbial metabolism in deep coastal plain aquifers: Applied Environmental Microbiology, v. 56, p. 1865-1874.

Cunningham K.I., Northup, D.E., Pollastro, R.M., Wright, W.G., LaRock, E.J., 1995, Bacteria, fungi and biokarst in Lechuguilla Cave, Carlsbad Caverns National Park, New Mexico: Environmental Geology, v. 25, p. 2-8.

Engel, A.S., Stern, L.A., and Bennett, P.C., 2004, Microbial contributions to cave formation: New insights into sulfuric acid speleogenesis: Geology, v. 32, p. 369-372.

Ehrlich, L.H., 1990, Geomicrobiology Ed. 2: New York, Dekker, Inc., 646p.

Frank, E.F., Mylroie, J.E., Troester, J., Alexander, E. C., and Carew, J. L., 1998, Karst development and speleogenesis, Isla and de Mona, Puerto Rico: Journal of Cave and Karst Studies, v. 60, p. 73-83.

Groth, I., and Saiz-Jimenez, C., 1999, Actinomycetes in hypogean environments: Geomicrobiology Journal, v. 16, p. 1-8.

Hill, C.A., 1990, Sulfuric acid speleogenesis of Carlsbad Cavern and its relationship to hydrocarbons, Delaware Basin, New Mexico and Texas: American Association of Petroleum Geologists Bulletin, v. 74, p. 1685-1694.

Hose, L.D., Palmer, A.N., Palmer, M.V., Northup, D.E., Boston, P.J., and Duchene, H.R., 2000, Microbiology and geochemistry in a hydrogen-sulphide rich karst environment: Chemical Geology, v. 169, p. 399-423.

Laiz, L., Groth, I., Gonzales, I., Siaz-Jimenez, C., 1999, Microbiological study of the dripping waters in Altamira cave (Santillana del Mar, Spain): Journal of Microbiological Methods, v. 36, p. 129-138.

Lechevalier, H.A., and Lechevalier, M.P., 1967, Biology of Actinomycetes: Annual Review of Microbiology, v. 21, p. 71-100.

Moore, P.J., and Martin, J.B., 2006, Can mixing of different water sources generate flank margin caves on small ocean island?: Thirteenth Symposium on the Geology of the Bahamas and Other Carbonate Regions, Abstracts and Program, p. 17.

Mylroie, J.E., and Carew, J.L., 1988a, Field evidence of the minimum time for speleogenesis: National Speleological Society of America Bulletin, v. 49, p. 7-72.

Mylroie, J.E., and Carew, J.L., 1988b, Solution conduits as indicators of Late Quaternary sea level position: Quaternary Science Reviews, v. 7, p. 55-64.

Mylroie, J.E., and Carew, J.L., 1990, The flank margin model for dissolution cave development in carbonate platforms: Earth Surface Processes and Landforms, v. 15, p. 413-424.

Mylroie, J.E., and Carew, J.L., 1995, Karst development on carbonate islands, Chapter 3, *in* Budd, D.A., Harris, P.M., and Saller, A., eds., Unconformities and porosity in carbonate strata: American Association of Petroleum Geologists Memoir 63, p. 55-76.

Mylroie, J.E., Carew, J.L., and Vacher, H.L., 1995, Karst development in the Bahamas and Bermuda: *in* Curran, H.A. and White, B., eds., Terrestrial and Shallow marine Geology of the Bahamas and Bermuda: Geological Society of America Special Paper 300, p. 251-267.

Mylroie, J.E., Jenson, J.W., Taborosi, D., Jocson, J.M.U., Vann, D.T., and Wexel, C., 2001, Karst features of Guam in terms of a general model of carbonate island karst: Journal of Cave and Karst Studies, V. 63, n. 1, p. 9-22.

Paine, S.G., Linggood, F.V., Schimmer, F, and Thrupp, T.C., 1933, The relationship of micro-organisms to the decay of stone: Philosophical Transactions of the Royal Society of London, Series B., v. 222, p. 97-127.

Plummer, L.N., 1975, Mixing of sea water with calcium carbonate ground water, in Whitten, E. H. T. , ed., Quantitative Studies in Geological Sciences: Geological Society of America Memoir 142, p. 219-236.

Plummer, L.N., Vacher, H.L., Mackenzie, F.T., Bricker, O.P. and Land, L.S., 1976, Hydrogeochemistry of Bermuda: A case history of ground-water diagenesis of biocalcarenites: Geological Society American Bulletin, v. 87, p. 1301-1316.

Plummer, L.N., Busby, J.F., Lee, R.W., Hanshaw, B.B., 1990, Geochemical modeling of the Madison aquifer in parts of Montana, Wyoming, and South Dakota: Water Resources Research, v. 26, p. 1981-2014.

Porter, K.G., and Feig, Y.S., 1980, The use of DAPI for identifying and counting aquatic microflora: Limnology and Oceanography, v. 25, p. 943-948.

Sanford, W.E., and Konikow, L.F., 1989, Porosity development in coastal carbonate aquifers: Geology v. 17, p. 249-252.

Schwabe, S.J., Parkes, J., and Smart, P., 1996, Significance of bacterial activity in carbonate diagenesis: *in* Carew, J.L., ed., Proceedings of the Eighth Symposium on the Geology of the Bahamas and other Carbonate Regions: San Salvador, Bahamian Field Station, p. 174-175.

Schwabe, S.J., 1999, Biogeochemical investigation of submerged caves within Bahamian carbonate platforms: [Ph.D. Thesis]: University of Bristol, UK, 235p.

Schwabe, S.J., 2002, Biogeochemical processes that influence cave development within Bahamian carbonate platforms, *in* Martin, J.B., Wicks, C.M., and Sasowsky, I. D., eds., Proceedings of the Symposium Karst Frontiers: Florida and Related Environments: Karst Waters Institute Special Publication 7, p. 103-106.

Schwabe, S.J., and Herbert, R., 2004, Black holes of the Bahamas: what they are and why they are black: Quaternary International, v. 121, p. 3-11.

Stoessell, R.K., Ward, W. C., Ford, B.H., Schuffert, J.D., 1989, Water chemistry and $CaCO_3$ dissolution in the saline part of an open-flow mixing zone, coastal Yucatan peninsula, Mexico: Geological Society of America Bulletin, v. 101, p. 159-169.

Whitaker, F.F., and Smart, P.L., 2006, Geochemistry of meteoric diagenesis in carbonate islands of the northern Bahamas: Evidence from field studies: Hydrological Processes, v. 21, p. 949-966.

Whitaker, F.F., and Smart, P.L., 1997, Groundwater circulation and geochemistry of karstified bank-marginal fracture systems, South Andros Island, Bahamas: Journal of Hydrology, v. 197, p. 293-315.

White, W, B., 1988, Geomorphology and Hydrology of Karst Terrains: New York, Oxford University Press, 464 p.

MAKING CAVES IN THE BAHAMAS: DIFFERENT RECIPES, SAME INGREDIENTS

Stephanie J. Schwabe[1] and James L. Carew
Department of Geology and Environmental Geosciences
College of Charleston
Charleston, SC 29424
steffi@blueholes.org

[1]Rob Palmer Blue Holes Foundation
5 Longitude Lane
Charleston, SC 29401

Rodney A. Herbert
Division of Environmental and Applied Biology, Biological Sciences Institute
University of Dundee
Dundee DD1 4HN, Scotland UK

ABSTRACT

Caves in the Bahamas result from exposure to the same general ingredients, but with variations in the amounts, duration of exposure, and physical location. The ingredients that are known to influence cave development include: waters of differing chemistries, (fresh, brackish, marine), organics (DOC, POC, PIOC), metabolic by-products and end-products of microbial activity, and water flow. Different combinations of these variables generate dissolution at a variety of localities and at all scales. Dissolution occurs throughout the vadose zone, and in the phreatic zone, especially near the upper boundary of the fresh or brackish groundwater lens, and near the base of the fresh or brackish groundwater lens. The types and numbers of bacteria that occur on rock surfaces, within rock pores, and in the water in pores (including flooded dissolution voids) vary depending on the amount and geochemistry of the water, and the amount of organics available.

Data collected from caves currently below and above sea level have been integrated into a single comprehensive model of cave development in the Bahamas. The model recognizes that all dissolution caves result from exposure to a subset of common ingredients, but differ due to variations in the "cave formation recipe".

INTRODUCTION

Caves found on the Bahamian platforms range from small globular air-filled chambers to horizontally extensive flooded caverns, as well as near-vertical shafts that may be dry or flooded. Their openings are found high on eolianite ridges, on low coastal benches, among the mangroves in shallow creeks, in inland lakes, and on the shallow subtidal banks of the Bahamas. Caves within the Bahamian carbonate platforms range from several meters to several kilometers in lateral extent, and depths vary from less than a meter to several hundred meters. Mylroie and Carew (1995, p. 60) state that, "caves on carbonate platforms fall into three main categories: vadose, phreatic, and fracture caves". Recently, Schwabe and Carew (2006) suggested that Bahamian caves, whether currently above or below sea level, should be broadly classified into three general types (horizontal, vertical, and fracture-guided caves) based on their morphologies that result from their modes and locations of origin.

This classification reflects the idea that the horizontal caves currently above sea level, such as flank-margin caves and banana holes, are the re-

sult of the same phreatic dissolutional processes that have also formed or modified the horizontal caves that are currently flooded, many of which are commonly referred to as 'blue holes", a term which is of no scientific use (Schwabe and Carew, 2006). It is likely that the majority of the currently subaerial horizontal caves are younger, or less-developed, versions of the now-flooded caves. Likewise, many currently-flooded vertical caves, many of which are also referred to as "blue holes", likely had an origin that is similar to that of currently subaerial pit caves. Fracture-guided caves, whether exposed on land or currently on the flooded carbonate banks, all have their origins related to fractures that are aligned sub-parallel to steep bank margins adjacent to very deep water. Virtually all these fracture caves also have names that include the term "blue hole".

Regardless of the terms used to describe or classify caves in the Bahamas, it should be recognized that it requires the same basic ingredients to make voids in these carbonate rocks, no matter how big or small the features may be. The reason that these cave types differ from one another is that they result from different amounts of the ingredients needed to make voids, and variations in exposure times in the different dissolutional environments. The ingredients that are needed to make caves are limestone, water, organics, bacteria, and time.

VOID MAKING INGREDIENTS

Water

Obviously, water, is a prime ingredient necessary for cave formation in limestones. The supply of water in the vadose environment is temporally variable, and water movement is primarily downward under the influence of gravity. The generally accepted model for dissolution of limestone suggests that rainwater charged with CO_2 is responsible for dissolving near-surface epikarst features, as well as other voids formed between the land surface and the water table. The rainwater is assumed to be acidic, primarily as a result of incorporated atmospheric CO_2, but other acids (such as nitric acid which is commonly elevated in rain associated with thunderstorms) may also be present. In addition, the meteoric water may be further charged with CO_2 if it infiltrates through soil. That additional CO_2 in soils is generally regarded to be the product of soil microbes and respiration of other soil inhabitants (animals, fungi) (e.g., White, 1988).

We have discovered that rainwater collected in a sterile container before contact with the ground on San Salvador contained 10^3 bacterial cells/ml (Schwabe et al., 2006, 2007). So, the water starts its journey through the soil and rocks already charged with possible CO_2-producing bacteria and organics (bacteria that may be consumed by other bacteria). However, recent studies on San Salvador Island (Schwabe et al., 2006) have shown that rain water is buffered soon after it makes contact with the surface.

Rainwater collected directly into sterile containers in January 2007 had a pH of 5.72 [with salinity = 0.25mg/l, chloride = 22.3mg/l, alkalinity = 14mg/l (all HCO_3^-), and Ca = 3.2mg/l]. In contrast, rainwater collected from profuse overflow from a rooftop at the Gerace Research Centre in 2006 had a pH of 8.5, and the pH of water collected from the 18-acre catchment at the Gerace Research Centre 18 hours after an intense rainstorm in June 2006 had a pH of 9.18 (pers. comm., Dr. Jon Martin, Univ. Florida). The reason that these latter two observations are significant is that they demonstrate that very brief contact with the surface is sufficient to change the pH of the water to non-acidic values. In the case of the rooftop rainwater, a few minutes contact with a thin film of carbonate dust and a few rock fragments on the roof was sufficient to buffer this profuse flow of water to alkaline pH values.

So, it appears that except at the immediate surface and just below soils (epikarst), it is unlikely that significant dissolution could occur in the vadose zone unless there is some other variable affecting the system. We have proposed (Schwabe et al., 2006, 2007) that the previously unidentified ingredient that makes it possible for vadose water to dissolve limestone is abundant populations of interstitial CO_2-producing bacteria living in the rocks of the vadose zone, as well as bacteria populations that live on exposed lime-

stone surfaces, especially in karst voids (e.g., Laiz et al., 1999; Groth and Saiz-Jimenez, 1999). It is also likely that plant roots, with associated fungi and bacteria, which produce CO_2 (and other chemicals that form acids), also play a significant role in some void development.

Because the bacteria are not homogenous in the vadose rock (Ehrlich, 1990), meteoric waters that descend through the vadose zone will not always encounter CO_2 producers. It is reasonable to suppose that in areas where the downward-migrating water in the vadose zone is not acidified by bacteria (and perhaps other taxa), precipitation of cement is likely to occur. It is also likely that other taxa of bacteria may play a role in calcite precipitation. We suggest that bacterial 'hot spots' may explain why macroscopic voids of various sizes are dispersed throughout limestones in the vadose zone. In Holocene rocks in the Bahamas, which have been exposed only to vadose conditions, a wide range of macroscopic voids are already clearly visible.

Water in the phreatic zone comprises freshwater, brackish (mixed) water, and marine water. Study of water from open wells, cave drip water, brackish water in a cave and at a spring, and seawater on San Salvador Island has shown that they are all supersaturated with respect to calcite, and at least at equilibrium with aragonite (Moore and Martin, 2006). As reported by Moore and Martin at the symposium, their study has also shown that, contrary to the currently accepted model, mixing of these various water bodies (both open and closed to CO_2) does not produce sufficient undersaturation to explain the formation of significant sized voids such as flank margin caves and banana holes. Study of phreatic waters in flooded caves on Grand Bahama Island and Andros Island show that they are also saturated or supersaturated, except where there are large bacteria populations, mostly associated with density horizons associated with the zone of mixing between fresh to brackish groundwater and underlying marine groundwater (Schwabe, 1999; Schwabe and Herbert, 2004; Schwabe et al., 2006, 2007). Thus, it also appears likely that bacteria play a significant role in void development in the phreatic zone.

Interestingly, although bacteria occur throughout the water column in the phreatic zone in the Bahamas, they are concentrated in areas at the top of the groundwater lens (a density interface between air and water) and in association with the mixing zone (a density interface between fresh and marine groundwater). This is consistent with the earlier-reported preferential development of banana holes and flank margin caves at those locations (Mylroie and Carew, 1990; 1995)

In most portions of the phreatic zone, water movement as a result of groundwater-lens discharge is crucial for void enlargement (Mylroie and Carew, 1990; 1995). It has also been documented that the marine portion of the water column that flows into and out of the islands as a result of tides, waves, and storms also causes movement of the overlying groundwater (Schwabe, 1999). Water movement due to lens discharge, and entrainment due to oscillations of marine water, is important in the removal of solutes formed by the dissolution of rock. So, the large bacteria populations associated with the mixing zone (Schwabe, 1999; Schwabe et al., 2006, 2007), whose production of CO_2 maintains the dissolutional capacity of these phreatic waters (see further discussion in the Organics section), combined with high water-flow rates are probably responsible for the preferential location of most large karst voids (flank margin caves) in the Bahamas.

In contrast, in a few areas the lack of significant groundwater movement sets up conditions that permit the accumulation of huge bacterial populations which contribute to void development. The prime example of these conditions are the currently flooded vertical caves called "black holes" found on Andros (Figure 1.) and Grand Bahama islands (Schwabe and Herbert, 2004). In these settings there is little to no movement of the marine water beneath the sharp halocline and therefore there is no mixing zone. The lack of water flow allows very thick (>1m) microbial layers to form above the marine water, and vertical migration of such layers via sea level change may explain why these voids are primarily vertical features with no significant horizontal extension (see further discussion in the Organics section).

Organics

The amount of organics (including live bacteria), the type of organic material, and the amount of available moisture will dictate the type and the number of bacteria that will reside and be active within the vadose and phreatic rocks and waters. The organics that bacteria in carbonate rocks, and

Figure 1. Aerial view of the Black Hole of South Andros Island, Bahamas. This nearly circular opening is 300 m in diameter, and is the largest found thus far in the Bahamas. The sparse vegetation surrounding the opening gives the impression that the opening is elevated above the surroundings; however, everything in this field of view is nearly at, or below, current sea level.

in the groundwater, may metabolize comprises a wide variety of materials. The rocks themselves contain an initial organic component in the form of: interstitial bacteria, particulate organic carbon (POC), particulate inorganic carbon (PIOC), dissolved organic carbon (DOC), buried vegetation in eolianites, subtidal grass/algal facies, coral reefs, subtidal hardgrounds, organics in paleosols, etc. Organics are also introduced to the rocks after deposition by infiltration from above (e.g., atmospheric outfall, infiltration of surface organics such as animal wastes and carcasses, dead vegetation, and organics produced by live vegetation and fungi). In addition, the movement of marine water inward into an island via tides and currents delivers organics to the phreatic system, especially when voids are present at the depths where shallow marine water and fresher groundwater are mixing. All these organic materials provide metabolizable material for a variety of bacteria with differing environmental preferences such as aerobic to anaerobic heterothrophs and chemautotrophs. These bacteria in turn produce by-products and end-products of their metabolism that form acids that drive void development and enlargement.

The role of bacteria in sulfuric acid speleogenesis (SAS) has become an accepted model for some cave development (e.g., Engel et al., 2004), and some work in the Bahamas has indicated a role for sulphur-mediating bacteria (Bottrell et al., 1991, 1993); however, it is our contention that in the Bahamas, and similar carbonate settings, even traditional carbonic acid dissolution is also largely the result of bacterial activity. Whitaker and Smart (2006) suggested that CO_2 must be added to the ground water in the northern Bahamas by oxidation of surface- and soil-derived organics in the lens, but they did not document the presence of abundant populations of bacteria living in the rocks and groundwater as the probable source of bacteriogenic CO_2.

Some of the bacteria that have been found within non-SAS cave wall rocks (e.g., Actinomycetales) prefer oligotrophic conditions; that is, they are well suited to live in organic-poor environments (e.g., Chapelle et al., 1987; Chapelle and Lovely, 1990; Plummer et al., 1990; Laiz et al., 1999; Groth and Saiz-Jimenez, 1999). Despite the variety of sources of organics in Bahamian rocks, after the initial depositional organic load is exhausted most of the vadose zone rocks in the Bahamas are oligotrophic environments, so it is not surprising that we have found abundant Actinomycetales in those rocks (Schwabe et al., 2006, 2007). We have also found that some of these bacteria prefer only small amounts of moisture. To culture and isolate these wall-rock bacteria proved to be very difficult, as they were slow growers, and in some cases, unresponsive to many of the media provided. In contrast, we have found that, with only a few exceptions, the bacteria collected from water samples tended to grow rapidly and be easily cultured on a much wider selection of host media.

Although the availability of organics and water in the vadose zone is generally limited, especially compared to the conditions in the phreatic zone, it is possible that some large voids may form in the vadose zone where there were initial large supplies of organics (such as buried vegetation and root masses), or abundant organic input from living vegetation (such as a large tree), and/or a substantial supply of water (such as a perched groundwater lens. In those cases bacterial activity that produced CO_2, or other acids, would result in sizable voids. Such conditions may explain the flank-margin-style cave that occurs at an elevation of about 175 feet asl at Mt. Alvernia on Cat Island (Mylroie et al., 2006), which is well above any possible sea level position that could have placed the freshwater lens there. It is also likely that bacterial populations in the vadose zone play a substantial role in the development of pit caves (such as Owl's Hole on San Salvador Island). In these situations the development may be partly driven by bacterial activity that occurs in the sediment/soil that accumulates in these depressions (Smart and Whitaker, 1989), partly by bacterial and fungal activity associated with vegetation that may be anchored in the features, and partly by bacteria that live on the wall surfaces and within the rock, in a fashion similar to that demonstrated for tombstone and building stone deterioration (Paine et al., 1933; Ehrlich, 1990).

Time and Setting

The remaining ingredients for void development are time and setting. That is, the sizes and shapes of dissolutional voids is also dependent on how long they have been subjected to conditions favorable for void development. For example, due to lesser amounts of water and bacteria, voids formed only in the vadose zone are likely to be of more limited extent than those that have spent a similar time in the freshwater and mixing zone phreatic environments. In addition, rocks exposed for short intervals of time in the vadose or phreatic zone are also likely to be less extensive than those subjected to those conditions for longer intervals of time. However, individual cases of abundant organics, bacteria, and water may result in large voids in either environment even in short intervals of time.

Voids formed in the phreatic environment, particularly in association with the mixing zone, or halocline/pycnocline, where bacteria and organics are most abundant, are more likely to develop to large size than those formed elsewhere in the phreatic zone or in the vadose zone. In addition, voids that have been submerged during multiple episodes of glacio-eustatic highstands of sea level are likely to be larger than those formed during a single episode of submergence. Based on observations in currently flooded caves in the Bahamas, even if the water filling a void consists of marine water, substantial dissolution is likely, because bacteria-rich sediment and biofilm commonly covers the floors, and often drapes the ceilings (Schwabe, 1999). However, again it should be noted that specific conditions that produce abundant supplies of organics and bacteria are likely to produce larger voids than in other settings in rocks of the same age. Although there is no scientific documentation about the effects of organic flushing into the Lucayan Caverns system on Grand Bahama Island, it may not be a coincidence that these largest known horizontal cave systems in the Bahamas have entrances located within mangrove habitats which produce abundant organics that are flushed into the caves (see later discussion).

CAVE-MAKING RECIPES

Exploration of caves in the Bahamas for the past several decades has generated a plethora of data concerning caves currently above sea level and those currently flooded. Researchers studying one or the other of these cave environments have generated separate sets of observations, interpretations, and terminology (e.g., Mylroie and Carew, 1995; Schwabe, 1999; Schwabe and Herbert, 2004). Although it is clear that the currently dry flank margin caves and banana holes have had a submergence history, until now there has been no formal attempt to compare those voids to the currently flooded caves to determine the similarities and differences between them. Of course, over

time, caves may experience a variety of different conditions due to changes in sea level, bank subsidence, and different climatic conditions, and thus can become polygenetic. The following discussion reports some of the significant features and aspects of some of the various cave types in the Bahamas.

Fracture-Guided Caves

Fracture-guided caves vary in the extent of their horizontal versus vertical development, but as the name suggests, they have clearly formed in association with significant fractures along some bank margins. These fractures are thought to result from bank margin failure along steep declivities during times of glacio-eustatic low sea level. Virtually all fracture-guided cave openings have been labeled as blue holes (e.g., Evelyn's Blue Hole, Stargate Blue Hole, etc.). However, aerial views (Figure 2.) of multiple openings in a linear sequence that parallels the coast, easily dispels any question as to their association with a linear

Figure 2. Aerial view of the south end of the fracture system on South Andros Island, Bahamas. Note the linear arrangement of the flooded cave openings.

feature. Fracture-guided caves have thus far been found only on Grand Bahama, New Providence, and Andros islands.

A curiosity concerning these caves is why the openings to caves occur only at isolated locations along the fracture. Although it is only conjectural, one possible explanation is that it has to do with the type of limestone and possible organics 'hot spots'. It has been noticed (by Schwabe) that the rocks that compose many of the explored entrances are composed of fossil reefs commonly also associated with herring bone cross bedding.

Perhaps fossil reefs and associated subtidal deposits that happen to have been intersected by the fracture originally contained abundant organics that 'fed' large bacterial populations that resulted in significant dissolution in those areas, and ultimately collapse into those voids resulted in the development of cave openings at those sites.

The fracture systems extend from land onto the submerged platform, so even in the inland caves, tidal effects are very important. In the marine setting, fracture systems experience very dynamic tidal flux that generates a boil (dome) of out-flowing water at many cave entrances. This outflow is so powerful that entering the cave is nearly impossible and ill-advised. This condition occurs about three to four hours into the ebb tide. The reverse condition, a vortex of descending water that can prevent a diver from exiting from a cave forms at the entrance three to four hours into flood tide (Figure 3). Clear evidence that this phenomenon is related to hydraulic head produced by tidal rise and fall is provided by another phenomenon that has been repeatedly experienced by the researchers that have explored these flooded caves (e.g., Schwabe, R. Palmer). That is, outflow of water can change to inflow in less than a minute when storm waves push water up onto the submerged bank, thereby generating a higher hydrological head on the platform than what the current tide is generating. Once the storm abates and wind-driven water is no longer pushed on to the platform, the water flow returns to outflow.

These tidal and wind-driven water currents have a tremendous effect on many of these flooded caves, because they can pump large quantities of nutrients into the caves (Figure 3). These nutrients also permit encrustation of corals. and other marine life, on cave walls to 60 m depth, even though there may be no available light.

The walls of the flooded voids where this marine life exists, are very pitted and friable and the corrosion extends several centimeters into the wall rock. This bioerosion of the rocks is likely to enhance enlargement of the cave entrances. This phenomenon ceases at 60m depth. This depth limit appears to be associated with the dynamics of water movement within the caves. Observations made by Schwabe while monitoring the water chemistry at the entrance to Fourshark Cave over a 24hr period showed that only the top 60 m of water moves in and out of the cave during the semi diurnal tidal cycles. The water below 60 m in the cave, whose chemistry had been determined earlier, was never identified at the entrance of the cave, which suggests that those deep waters do not leave the cave (Schwabe, 1999). Thus, the water at depth in the caves becomes stagnant. Oxygen and nutrient content is low or non-existent, so the water is not suitable for marine growth (e.g., corals, sponges). This pronounced change in wall morphology at 60 m depth is also observed in the fracture-guided caves with entrances on land. Populations of bacteria that prefer anoxic conditions dominate the waters and cave wall rocks below 60 m depth (Schwabe, 1999). The top 30 to 40 m of cave passage in these settings tend to be the widest portions of the cave systems, and passages at depths > 60 m tend to conform to the shape of the fracture.

Vertical Caves

Vertical caves are generally developed in association with descending water in the vadose zone, by dissolution horizons that migrate up and down in response to sea level changes, or by upward propagation by collapse into a void at depth. Vertical caves may inadvertently intersect horizontal caves, but the horizontal passages are not directly associated with the development of the vertical caves. Vertical caves include subaerial pit caves, and many flooded features called "blue holes" and "black holes". These caves typically have no horizontal passages, or only limited horizontal development. A few known exceptions exist, such as CK1 and John Winter's Cave (Hog Cay Cave), on San Salvador Island, Bahamas. Some of these features have voids that extend along foreset bedding (solution chimneys), and CK1 intersects a large flank margin cave (Major's Cave) (Moore et al., 2004).

At a few places on the flooded Bahama Banks some vertical voids have a deep black color when seen from the air. These 'black holes' (Figure 1) have a dark color because they harbor an unique microbial population that probably plays a significant role in the formation of those voids.

The cause of the black color is a meter-thick layer of dark-pigmented purple sulfur bacteria that occurs about 17.8m below the water surface (Schwabe and Herbert, 2004). These large vertical caves seem to require very specific environments and conditions to form and have to date been found at only a few locations in the Bahamas (Table 1). It appears that the main reason that these black colored microbial layers form in these systems is that there is no significant (measurable) horizontal flow of water at those locations.

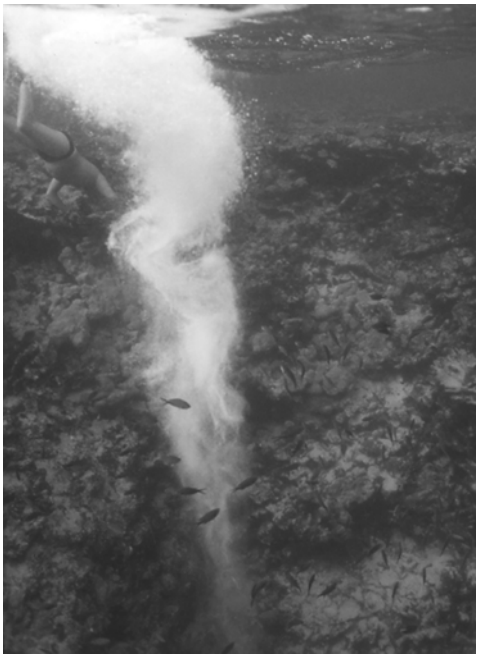

Figure 3. Vortex formed on a flood tide, in the entrance to a cave named 'Luscas Breath'. This is the entrance to a fracture-guided cave located on the eastern bank margin of South Andros near Deep Creek.

Lack of horizontal flow allows these loosely floating populations of mostly purple bacteria to generate dense (bacterial counts $>10^7$ cells/ml), undisturbed, well-defined layers within the water column. These floating bacterial masses are so dense that they appear inky-black, and they have thus far always been found at 17.8 meters depth, and are each about one meter thick. This consistent thickness is most likely due to some light-limited requirement for these bacteria. These bacterial masses are at a consistent depth because they are located on the density interface where brackish water meets the underlying marine water. Any horizontal flow within the marine water beneath the microbial layer would prevent such sharp biological boundaries from forming, and the bacterial masses would be dispersed. Lack of flow and tidal influence appears to dictate where black holes are likely to be found (Table 2).

It has been observed that the walls of these "black holes" are severely undercut where the bacterial layer is located (Schwabe and Herbert,

Table 1. Some geochemical, physical and biological observations of flooded caves.

	Horizontal Caves	Fracture Caves	Vertical Caves
Current	√+++	√	Not detected
Microbial layer	√++	√+	√+++
Fresh Water	√+++	√ to none	√ to none
Brackish Water	Not detected	√+++	√+++
Marine Water	√+++	√+++	√+++
Organics	√+++	√+	√+++
Mixing Zone	√+++	√	none
Pycnocline	√	√	√+++
Measurable tidal changes	√+++	√+++	none

√ very low; √+ low; √++ moderate; √+++ very prevalent

2004). This is likely the result of dissolution enhanced by the end-products and byproducts of the metabolism of these mostly anaerobic bacteria. So, it is possible that movement of this environment vertically with glacio-eustatic changes in sea level may have carved these vertical caves, or it may have enlarged pre-existing pit-cave-type voids.

So, a location deep in the interior of a large platform, where tidal flow is diminished, seems to be a major non-biological ingredient necessary for development of 'black hole' voids. Initiation of these vertical voids may be the result of their insular locations, where large amounts of micrite mud tend to accumulate. It has been noted that this carbonate mud tends to result in ponding of meteoric water (Figure 4).

These ponds of water are colonized by photosynthetic bacteria. However, as such ponds get deeper, less light is available at depth, which may eventually establish an environment better suited

Table 2. Types of flooded caves found to date on different Bahamian Islands

Islands	Horizontal Caves	Fracture Caves	Vertical Caves
Andros	√	√+++	√+++
Grand Bahama	√+++	√+++	√
San Salvador	√	none	√
New Providence	√	√	√
Cat Island	√+	none	√
Long Island	√+	none	√
Eleuthera	√	none	√
Acklins	√+	none	√
Exuma	√	none	√
Abaco	√	none	√

√ very low; √+ low; √++ moderate; √+++ very prevalent

for dark-pigmented bacteria. The larger these populations become, the greater their influence is on the chemistry of the water-column, especially the pH. The water column above and below the bacterial masses is well buffered, with a pH of 8.5; however, in the bacterial layer pH ranges from 4 to 6. Because the walls at these locations are being aggressively dissolved away and there is little or no water movement, one would expect the water to become buffered. However, what we observe (Schwabe and Herbert, 2004) is that the huge bacterial population at these locations is able to maintain an acidic environment, despite lack of water flow.

Energy, to maintain such a large population of bacteria in these vertical caves (i.e., 5 tons dry weight, Schwabe and Herbert, 2004) seems to come from a well-established algal population growing in the water above the toxic water at 17.8 m depth. These algae produce a degradation product of dimethylsulfonium propionate (DMSP), a major osmoregulatory solute in marine algae (Madigan et al., 1997). DMSP can be used as a carbon and energy source by microorganisms and is catabolized to dimethyl sulfide and acrylate. The latter compound, a derivative of the fatty acid propionate, is used to support microbial growth (Madigan et al., 1997). Considering that there is limited vegetation growing outside the holes it seems reasonable that the algae within the hole produce a major energy source for the heterotrophic bacteria.

Figure 4. Ponded meteoric water in the interior west of South Andros Island, Bahamas. These shallow ponds are light green in color suggesting the presence of photosynthesizing bacteria. Note the different sizes of these depressions.

Thus far, only one mature black hole has been found on the partially submerged fringe of the platform on the north side of Grand Bahama Island. One mature flooded vertical cave (Rob's Blue Hole), without the purple microbial layer, has been explored off Nassau's north shore. However, the entrance to this vertical cave is now below sea level, and the languid environment necessary for the purple bacteria mass to develop is absent because the water column is stirred by tides and wave action. The nature of the water column aside, the wall morphology and the growth of abundant algae, is identical to that seen in other black holes. Several such systems on Andros have suffered a fate similar to Rob's Blue Hole, although they still maintain an abundant microbial population (though it is very different from those in the South Andros Black Hole) as well as a significant pycnocline. In those settings, these vertical caves are still relatively sheltered and have only a minor breach open to the sea, thus limiting water column mixing to the top 10 m. It appears that the most important ingredients required for these vertical caves to develop is a large platform, a very stable water column, and a large organic source.

Vertical pit caves are found throughout the Bahamas on high ground in eolianites. All of these vertical voids above 6 meters elevation have never been submerged. So, they are of vadose origin. Development of pit caves may also have have a microbial component. Endolithic cyanobacteria, hetertrophic bacteria, and fungi have been found to cause local dissolution of limestone through production of oxalic and gluconic acids (Ehrlich, 1990). Cyanobacteria and fungi dissolve tubular passages in which they can grow (Golubic et al., 1975).

Because of their need for light cyanobacteria can bore only a short distance into the rock; however, fungi and heterotrophic bacteria are not light limited. In addition, fungi and cyanobacteria can form a symbiotic relationship in the form of lichens (Ehrlich, 1990). In lichens the cyanobacteria share the carbon they fix with the fungi while the fungi share minerals that they mobilize with the cyanobacteria. The lichens and other bacteria that reside in surface depressions, and the rock beneath, produce by- and end-products that form acids that probably contribute to pit cave development. In addition, organics produced by the roots of many plants serve as nutrient sources for

many bacteria; so plant growth in vertical voids may enhance void enlargement. Smart and Whitaker (1989) have proposed an "organic drill" hypothesis for development of banana holes. Although that hypothesis is not valid for the origin of banana holes, which are of phreatic origin, organic-bacterial-mediated dissolution may result in downward enlargement of breached banana holes and pit caves. In addition, bacteria and fungi in the pit walls are also likely to enhance pit development.

In coastal settings lichens and endolithic algae and bacteria provide a food source for snails and other invertebrates that scrape the surface of limestone to feed. This type of bioerosion has been noted on some reef structures in Bermuda (Golubic and Schneider, 1979), as well as in the Negev Desert where this erosion removes 0.7 to 1.1 metric tons of rock per hectare per year (Shachak et al., 1987). In the Bahamas, this mechanism of biological erosion is likely to result in pits in the limestone along the coasts. Formation of such depressions along the coast, which can later become catchments for moisture and organics when sea level falls, can lead to the genesis of pit caves during glacioeustatic sea-level lowstands.

Glacioeustatic sea level changes and island subsidence may eventually flood such pits. In that case, they might become black holes if they are in the right setting; or they may simply become flooded vertical caves, like some of the current marine "blue holes'.

Horizontal Caves

Currently-exposed subaerial horizontal caves, such as the flank margin caves and banana holes, originate from conditions similar to those found in the currently submerged horizontal caves that are found on Grand Bahama and a few other islands (Table 2). The caves, which are currently above sea level, most likely have only been submerged once or twice in their history, whereas the caves that are currently below sea level may have been submerged in the phreatic zone multiple times, and for that reason some are quite large and complex. However, being submerged in the phreatic zone is not by itself enough to make caves larger. There must be water movement, a mixing zone with density interfaces, and numerous active bacteria that generate sufficient chemical byproducts/end-products to keep the water acidified. Lucayan Caverns and Owl's Hole on Grand Bahama Island, Bahamas, are two of the largest known horizontal caves in the Bahamas. At this time there are ~10.5 km of mapped passage in these only partially explored systems. Although these caves are open to the surface, which may not have generally been the case for the development of flank margin caves, they are currently the only locales that provide us with some information about the conditions that might exist in phreatic voids generally.

These currently flooded caves are similar in many ways to subaerial flank margin caves and banana holes. For example, as one enters Lucayan Caverns from the national park side (Figure 5), one passes through the fresh-water lens into a passage with a smooth curvilinear ceiling that rises dramatically over a distance of about 20m then plunges toward the floor at the back of the chamber. The floor of the passage remains relatively level except where there is a pile of collapsed ceiling materials. This room is morphologically similar to the globular outermost chambers characteristic of flank margin caves. At this location in the cave, the top half of the water column is fresh and the lower half is marine. At the back of this chamber the descending smooth ceiling forms a partial wall as it reaches into the marine section of the water column. Once under this wall, the ceiling again rises into the freshwater lens over a distance of about 10m, it remains high until the back of the chamber where the ceiling again descends into the marine section of the water column. This is another globular chamber that is somewhat smaller than the entrance chamber. This morphology is again consistent with what is seen in subaerial flank margin caves, where the chambers behind the entrance chambers are similar in morphology but are typically smaller. Throughout the rest of the explored cave the chambers are within the marine water, and the mixing zone is at the ceiling. Except for the numerous speleothems, this section of the cave pas-

sage looks like a planar section of bedding has been removed. A diver in this passage finds the ceiling and floor a bit close. The passage remains this way for about 2000 m into the cave, where there is a small chamber created where a smooth curvilinear ceiling rises a few meters and then descends again to the depth of the earlier passage.

During a tidal cycle in Lucayan Caverns and Owl's Hole caves, water flows through the passages in the front 300 m of the caves at about two meters per minute (Schwabe, 1999). Approximately 320 m deep into the cave, the flow is greatly diminished and the mixing zone is only pencil-line thin. There is just enough flow to keep the boundary between freshwater and marine water intact. In this environment deep in the caves there are abundant microbial mats. Bacterial mats with morphologies similar to those on the floor in the Black Hole of South Andros cling to the ceilings of the cave. If they become detached they drift downward and form large masses on the cave floors.

At the front of the cave the 2 m/min flow, keeps the water crystal-clear. The cave walls and ceilings that are bathed in freshwater are snow white and only fine carbonate mud is dislodged by scuba exhaust. Within 24 hours dislodged carbonate mud from the ceiling settles out on the density interfaces in the mixing zone and is carried away by flow created by the current in the underlying marine water.

In contrast, the cave walls, ceilings, and floors that are in marine water are covered in orange, brown, and black bacterial biofilm (Schwabe, 1999). As mentioned above, the floors of the caves are buried in some places by several meters of this material giving the impression of a brown fluffy carpet. The bacteria in these microbial curtains and mats produce exopolymeric substances (EPS) that allows them to maintain reducing or dysoxic environments behind them, even though the water within the rest of the chamber or passage is oxidizing. As a result, the ceilings and floors of the caves may be preferred sites of dissolution, including SAS, despite the fact that the water may be marine.

In locations in the caves where there is a mixing zone several meters thick, it is created by dilution of marine water, that results from friction and turbulence created as the relatively denser marine water moves under the less dense freshwater lens. This nearly horizontal body of diluted marine water (mixed water) also harbors a large number of bacteria (Schwabe, 1999), which are caught, along with other organics, in this zone because of the pronounced density interfaces. This environment is very conducive for abundant living heterotrophic bacteria because they are provided ample material that they can metabolize.

The major source of the organic material in Lucayan Caverns comes from the semi-diurnal tidal flow through a 2-mile creek. This water collects large amounts of organic material before entering three known entrances that are located within a mangrove habitat. Large globs of organic material have been observed floating into the entrances during flood tide. Water, darkly stained by tannins and lignins, most likely from the mangrove roots, contain large populations of bacteria and diatoms commonly found in sunlit environments. This organic material is carried into the cave system twice a day, along with a fresh supply of oxygen and organic and inorganic compounds used by the autotrophs, chemolithotrophs, and heterotrophs (Schwabe, 1999).

Not only does the geochemical and microbial environment change vertically through the water column, it changes horizontally as well. At short (~10 m) distances into the cave, dissolved oxygen values are slightly higher than they are at the entrances of the cave. This may be explained by the fact that very large amounts of organics (tree limbs, berries, leaves, etc.) fall into the entrances, and as a result the abundant bacterial populations there consume the oxygen as they metabolize the organics. About 100 m farther into the cave, the environment becomes dysoxic to reducing, and as a result, microbial populations that are better suited for living in low to no oxygen environments prevail there (Schwabe, 1999).

Deep in some of the very extensive horizontal passages, the water is moving so slowly that its movement is nearly impossible to measure. In these settings oxygen concentration is very low, and hydrogen sulfide accumulates. When H_2S is oxidized it produces sulfuric acid.

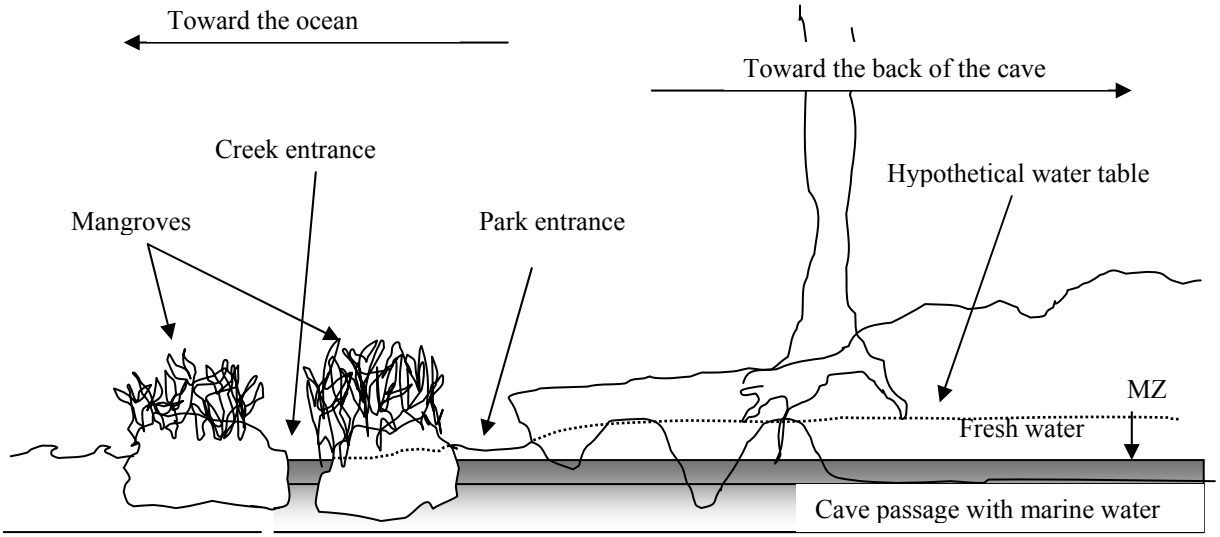

Figure 5. Typical horizontal cave morphology of Lucayan Caverns, Grand Bahama. The mixing zone (MZ) is the darker banding in the water column. The top of the freshwater body is at the dotted line which marks the water table.

While the generation of secondary porosity in the fronts of the caves is mostly driven by heterotrophic CO_2-producing bacteria, especially associated with the mixing zone, toward the back of the caves, in the nearly still environments, the numbers of anaerobic bacteria are higher, as are the concentrations of H_2S and H_2SO_4, so SAS may be the main dissolutional mechanism.

The presence of these various bacterial populations within the currently flooded caves provides us with a probable scenario for the conditions that also created the currently subaerial flank margin caves and banana holes. That once a void has been initiated, whether it is open or sealed, varying bacterial populations will thrive in the different sub-environments that develop based on differences in water movement, densities, and available organics.

CONCLUSIONS

In the Bahamas, horizontal caves, fracture-guided caves and vertical caves are found both above and below current sea level, suggesting that they share similar origins. The currently-flooded caves have probably experienced multiple submergence intervals, whereas the currently subaerial caves may have experienced as few as one (flank margin caves and banana holes) or no (pit caves) episodes of submergence. Study of the flooded caves has provided an opportunity to identify some of the processes that form, enlarge, and reshape caves in the Bahamas.

The variety of cave morphologies and the differences in size are a result of differences in the exposure time and amount of the various ingredients needed to generate secondary porosity. The key components necessary for secondary porosity development in limestones in the Bahamas, and also likely in other regions of the world, are moving or still fresh to marine waters, organics in all forms, various bacterial populations, and time. It appears that moving groundwater tends to result in the development of caves that have greater horizontal extent than their vertical development. The water movement results from groundwater lens discharge, and tidal and wind-driven currents which help generate a mixing zone and entrain the overlying less dense water. However, it is not the mere presence of a mixing zone that is sufficient to form and enlarge caves, as the undersaturation of the mixed water is not sufficient to result in substantial dissolution (Moore and Martin, 2006). Rather, due to density interfaces, the mixing zone physically supports concentrations of organic materials and bacteria which leads to acidification of these waters. In addition, the physical mixing and

groundwater discharge also dilutes carbonate-saturated water, and enhances removal of solutes.

Bacteria in the rock pores of the vadose and phreatic zones, as well as those living in the waters in flooded voids, generate CO_2, H_2S, H_2SO_4, gluconic acid, and oxalic acid depending on the local environmental conditions. These various acids are all likely to cause dissolution.

In phreatic environments open to the surface, where there is little water movement, conditions that favor the accumulation of massive bacterial populations (>10^7/ml water) can develop. Such conditions may result in formation of large vertical caves, as the favored site of dissolution, marked by the pycnocline and the dense bacteria, migrates vertically with sea level changes. On the other hand, in the vadose zone large amounts of organics are not necessary to support abundant heterotrophic bacteria that prefer oligotrophic conditions. Thus pit caves, as well as a variety of other voids, may develop wherever there is sufficient water, perhaps episodically available, to "turn on" interstitial bacterial populations and bacteria on the void walls; and, in open pits, bacteria and other organisms in sediment at the bottoms of the pits may promote downward carving of the void. Some of the dissolution may also be happening from the inside out via interstitial bacterial activity, not just from the void surfaces inward.

A wide variety of bacteria living in the rocks and in the water in flooded caves are able to consume a wide variety of organics, providing opportunities for different bacteria with different environmental requirements to be active when appropriate conditions exist within the voids and rocks. Based on observations in currently flooded caves, the ecology, and therefore the geochemistry, may be very different in the outer portions of caves versus deeper into the caves.

We, and others (e.g., Paine et al., 1933), have documented that limestones harbor a variety of different types of bacteria, some active, and some in limbo at any given time. The appropriate bacteria will become active whenever the proper conditions for them arise. When they are active, they produce byproducts and end-products of their metabolisms that acidify the water they live in. As a result, secondary porosity, including caves, will develop, or be enlarged, where the bacteria are active. Abundant populations of active bacteria will result in the greatest dissolution.

ACKNOWLEDGMENTS

We thank many students and colleagues for numerous discussions that have helped us congeal our ideas. We also thank the College of Charleston Geology Department, and Dr. Donald T. Gerace, CEO, and Vincent Voegeli, Executive Director, of the Gerace Research Centre, for financial and logistical support. Lastly we thank Dr. Lisa Park and two anonymous reviewers for their comments on earlier versions of this manuscript. Their comments helped us improve this paper.

REFERENCES

Bottrell, S.H., Smart, P.L., Whitaker, F., and Raiswell, R., 1991, Geochemistry and isotope systematics of sulphur in the mixing zone of Bahamian blueholes: Applied Geochemistry, v. 5, p. 97-103.

Bottrell, S.H., Carew, J.L., and Mylroie, J.E., 1993, Bacterial sulphate reduction in flank margin environments: evidence from sulphur isotopes, *in* White, B., ed., Proceeding of the Sixth Symposium on the Geology of the Bahamas (1992): Port Charlotte, Florida, Bahamian Field Station, p. 17-21.

Chapelle, F.H., and Lovely, D.R., 1990, Rates of microbial metabolism in deep coastal plain aquifers: Applied Environmental Microbiology, v. 56, p. 1865-1874.

Chapelle, F.H., Zelibor, J.L., Grimes, D.J., and Knobel, L.L., 1987, Bacteria in deep coastal plain sediments of Maryland: A possible source of CO_2 to ground water: Water Resources Research, v. 23, n. 8, p. 1625-1632.

Ehrlich, L.H., 1990, Geomicrobiology 2ed.: New York, Dekker, Inc., 646 p.

Engel, A.S., Stern, L.A., and Bennett, P.C., 2004, Microbial contributions to cave formation: new insights into sulfuric acid speleogenesis: Geology, v. 32, p. 369-372.

Golubic, S., Perkins, R.D., and Lukas, K.J., 1975, Boring microorganisms and microborings in carbonate substrates, *in* Frey, R.W., ed., The Study of True Fossils. New York: Springer-Verlag, p. 229-259.

Golubic, S., Schneider, J., 1979, Carbonate dissolution, *in* Trudinger P.A., and Swaine, D.J., eds., Biogeochemical Cycling of Mineral-Forming Elements: Amsterdam: Elsevier, p. 107-129.

Groth, I., and Saiz-Jimenez, C., 1999, *Actinomycetes* in hypogean environments: Geomicrobiology Journal, v. 16, p. 1-8.

Laiz, L., Groth, I., Gonzales, I., and Siaz-Jimenez, C., 1999, Microbiological study of the dripping waters in Altamira Cave (Santillana del Mar, Spain): Journal of Microbiological Methods, v. 36, p. 129-138.

Madigan, M.T., Martinko, J.M., and Parker, J., 1997, Brock Biology of Microorganisms, Eighth international edition: New York: Prentice-Hall Inc., 982 p.

Moore, P. J., and Martin, J. B., 2006, Can mixing of different water sources generate flank margin caves on small ocean islands?: 13th Symposium on the Geology of the Bahamas and Other Carbonate Regions, Abstracts and Program, p. 17.

Moore, P. J., Seale, D., and Mylroie, J. E., 2004, Pit cave morphology in eolianites: variability in primary structure control, *in* Lewis, R.D. and Panuska, B.C., eds., Proceedings of the Eleventh Symposium on the Geology of the Bahamas and Other Carbonate Regions (2002): San Salvador, Bahamas, Gerace Research Center, p. 145-155.

Mylroie, J. E., and Carew, J. L., 1990, The flank margin model for dissolution cave development in carbonate platforms: Earth Surface Processes and Landforms, v. 15, p. 413-424.

Mylroie, J.E., and Carew, J.L., 1995, Karst development on carbonate islands, Chapter 3, *in* Budd, D. A., Harris, P. M., and Saller, A., eds., Unconformities and Porosity in Carbonate Strata: American Association of Petroleum Geologists Memoir 63, p. 55-76.

Mylroie, J.E., Carew, J.L., Curran, H.A., Freile, D., Sealey, N.E., and Voegeli, V.J., 2006, Geology of Cat Island, Bahamas: A Field Trip Guide, for the Thirteenth Symposium on the Geology of the Bahamas and Other Carbonate Regions: San Salvador, Bahamas, Gerace Research Center, 44 p.

Paine, S.G., Linggood, F.V., Schimmer, F, and Thrupp, T.C., 1933, The relationship of micro-organisms to the decay of stone: Philosophical Transactions of the R. Soc. of London, Series B., v. 222, p. 97-127.

Plummer, L. N., Busby, J. F., Lee, R. W., and Hanshaw, B. B., 1990, Geochemical modelling of the Madison aquifer in parts of Montana, Wyoming, and S. Dakota: Water Resources Research, v. 26, p. 1981-2014.

Schwabe, S.J., 1999, Biogeochemical investigation of caves within Bahamian carbonate platforms, [Ph.D. Dissertation]: University of Bristol, UK, 239 p.

Schwabe, S.J., and Herbert, R., 2004, Black holes of the Bahamas: what they are and why they are black: Quaternary International, v. 121, p. 3-11.

Schwabe, S.J., and Carew, J.L., 2006, Blue holes: an inappropriate moniker for water filled caves in the Bahamas, *in* Gamble, D., and Davis, R.L., eds., Proceedings of the Twelfth Symposium on the Geology of the Bahamas and other Carbonate Regions: San Salvador, Bahamas, Gerace Research Centre, p. 179-187.

Schwabe, S.J., Herbert, R., and Carew, J.L., 2006, A Hypothesis for Biogenic Cave Formation: Thirteenth Symposium on the Geology of the Bahamas and Other Carbonate Regions, Abstracts and Program, p. 22.

Schwabe, S.J., Herbert, R., and Carew, J.L., 2008, A Hypothesis for Biogenic Cave Formation (A Study Conducted in the Bahamas), *in* Park, L.E., and Freile, D., eds., Proceedings of the Thirteenth Symposium on the Geology of the Bahamas and Other Carbonate Regions: San Salvador, Bahamas, Gerace Research Centre, This Volume, p. 137-148.

Shachak, M., Jones, C.G., and Granot, Y., 1987, Herbivory in rocks in the weathering of a desert: Science, v. 236, p. 1098-1099.

Smart, P.L., and Whitaker, F., 1989, Controls on the rate and distribution of carbonate bedrock dissolution in the Bahamas, *in* Mylroie, J.E., ed., Proceedings of the Fourth Symposium on the Geology of the Bahamas: San Salvador, Bahamas, Bahamian Field Station, p. 313-321.

Whitaker, F. and Smart, P.L., 2006, Geochemistry of meteoric diagenesis in carbonate islands of the northern Bahamas: Evidence from field studies: Hydrological Processes, v. 21, p. 949-966.

White, W., 1988, Geomorphology and Hydrology of Karst Terrains: New York, Oxford University Press, 464 p.

MULTIPLE SEDIMENTARY SEQUENCES, BIRD TRACKS AND LAGOON BEACHES IN LAST INTERGLACIAL OOLITES, BOILING HOLE, NORTH ELEUTHERA ISLAND, BAHAMAS

Pascal Kindler
Section of Earth Sciences
University of Geneva
1205 Geneva, Switzerland
Pascal.kindler@terre.unige.ch

H. Allen Curran
Department of Geology
Smith College
Northampton, MA 01063

Daniel Marty
Department of Geosciences
University of Fribourg
1700 Fribourg, Switzerland

Elias Samankassou
Department of Geosciences
University of Fribourg
1700 Fribourg, Switzerland

ABSTRACT

Our review of the last interglacial (Marine Isotope Stage 5e) stratigraphic record from the Boiling Hole exposure in northern Eleuthera Island, Bahamas, revealed the occurrence of two vertically stacked shallowing-upward sequences of oolitic coastal deposits showing beach facies at about 3 and 6 m above mean sea level, respectively. These beach strata dip towards the bank interior and the upper one includes a paleosurface on top of an oolitic grainstone bed with a 2-m-long bird trackway. These fossil beaches correspond to two distinctive sea-level highstands during the last interglacial that could have possibly reached +5 and +8 m above modern datum, respectively, if estimates of regional subsidence are indeed correct. The bird footprints are the first reported occurrence of vertebrate trace fossils from the Bahama Archipelago. The track maker was probably an extant shorebird belonging to the Order Charadriiformes. Track preservation in an oolitic grainstone is remarkable and may be related to an early phase of halite cementation. Finally, the dip of the beach beds indicates that constituent grains were transported onto the island from the bank side by a westerly flux opposite to the modern sediment transport direction in the area.

INTRODUCTION

Northern Eleuthera has some of the most spectacular rock exposures in the Bahamas, owing to the presence of steep cliffs bordering the open North Atlantic Ocean. Moreover, these outcrops have only been studied in a preliminary way. Here, impressive 25 m-high sea cliffs displaying several stratigraphic units await further examination and promise to provide more information on past sea-level stands, ancient climates, and sedimentary processes that are no longer operational. This paper revisits one of the most prominent of these exposures, the Boiling Hole, in order to (1) complement the stratigraphic and sea-level records from the Bahamas for the early part of the

last interglacial period (Marine Isotope Stage 5e); (2) describe the first fossil vertebrate tracks reported from the archipelago; and (3) present an example of a large amount of oolitic sediment that was transported from west to east, contrary to the present-day main sediment transport vector on Great Bahama Bank.

GEOLOGICAL SETTING

Eleuthera is a long and narrow carbonate island (140 x 2-5 km), located on the northeastern and windward margin of the Great Bahama Bank (GBB, Figure 1).

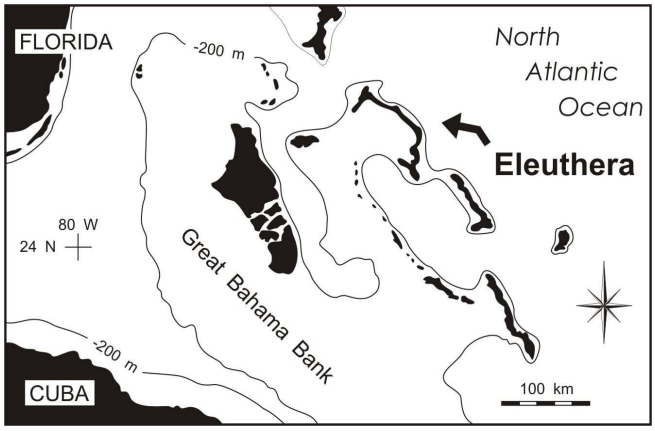

Figure 1. Location of the study area (modified from Kindler and Hearty, 1995).

This area belongs to the tectonically passive northwestern Bahamas (Sheridan et al., 1988) and is only affected by slow (1.6 cm/10^3 years; Lynts, 1970; Mullins and Lynts, 1977; Carew and Mylroie, 1995) subsidence mostly due to thermal decay and sedimentary loading (Pindell, 1985). The main physical parameters controlling sediment distribution on the GBB are wind, wind-induced waves and currents, and tidal currents. The long-term influence of tropical storms and hurricanes is less well constrained (Harris, 1979; Boss and Neumann, 1993). In the Bahamas, prevailing winds are from northeast to southeast during most of the year (Sealey, 1994), with strong northwesterly winds, related to cold fronts, further affecting the area in the winter. Wind further generates waves and currents that determine the subaqueous transport of sediment and the primary generation and distribution of sedimentary bedforms (Purdy, 1963; Swart et al., 2005). Predominant water movement and sediment transport on the GBB is thus towards the west, although some southward and eastward motion can occur during northwesterly gales in the winter (Bathurst, 1975).

The eastern coast of northern Eleuthera displays locally high (>20 m) cliffs, composed of vertically stacked carbonate units and paleosols, that commonly stand less than 1 km from the bank edge. Carbonate units accumulated during interglacial sea-level highstands, whereas the paleosols developed mostly during glacial lowstands (Carew and Mylroie, 2001). Details on the geology and stratigraphy of the area can be found in Kindler and Hearty (1995, 1997), Hearty (1997, 1998), Hearty and Kaufman (2000) and Panuska and others (2002). These carbonate units are dominantly composed of eolian sediments, but marine deposits recording ancient sea stands are present, with some reported to lie up to 18 m above modern sea level (Hearty et al., 1999; Kindler and Hearty, 2000). Eolianite foresets most commonly dip towards the interior of islands, emphasizing further that the source material for these dunes originated from the shore and that only onshore winds are effective in dune buildup (Mackenzie, 1964; Ball, 1967). The widespread occurrence of oolitic deposits in northern Eleuthera, as well as on other windward islands is problematic because no ooids have been reported as presently forming on the narrow outer platforms fronting these islands, which raises the question of the origin of these constituent grains.

The Boiling Hole (lat. 25°25'56"N, long. 76°35'54") is a 75 m-wide cove on the eastward, ocean-facing shoreline of northern Eleuthera, situated about 800 m to the southeast of the Glass Window bridge (Figure 2). The back end of the cove comprises a large sea cave that is only accessible during fair weather and at low tide. The outcrop includes three vertically stacked stratigraphic units (Figure 3) that were first identified by Kindler and Hearty (1995). Unit I forms a chain of deeply karstified eolian dunes of middle Pleistocene age that nonetheless exhibit original topography. The ancient dune crests may reach elevations of up to 25 m above sea level, whereas the

interdune swales, such as the Boiling Hole cove, are partly submerged.

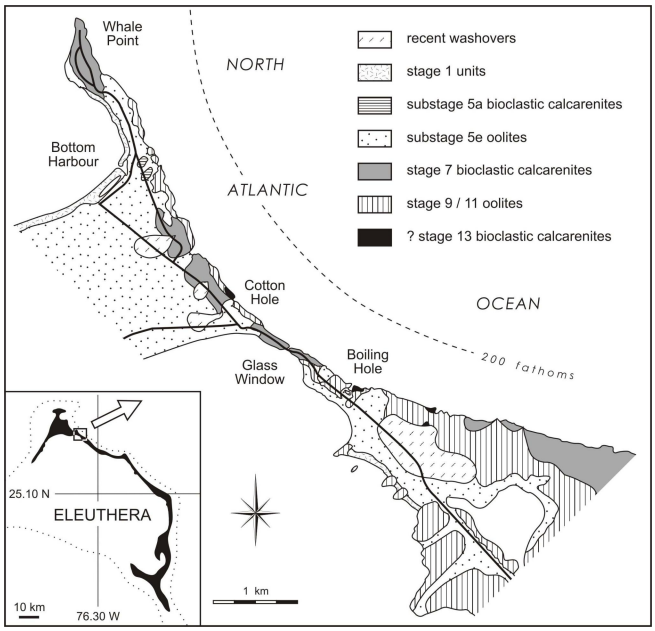

Figure 2. Geologic map of the Boiling Hole area (modified from Kindler and Hearty, 1997).

The northwestern and southeastern flanks of the cove consist of oolitic-peloidal and bioclastic eolianites, respectively (Figure 4) that may correspond to discrete depositional events during separate interglacials (possibly MIS 9/11 and 13, respectively; Hearty, 1998). The upper surface of these limestones is capped by a calcrete and breccia-rich paleosol that commonly has been stripped away by marine erosion particularly at low elevations. Unit II is composed of light-grey beds that partly fill the interdunal depression corresponding to the Boiling Hole cove. Its thickness varies from zero on the sides of the depression, to over six meters in the trough axis. These beds consist of well-cemented, oolitic-peloidal limestone including a small, but remarkable proportion of radial ooids (Kindler and Hearty, 1995; Figures 5a and b). According to previous authors (Kindler and Hearty, 1995; Hearty, 1998; Hearty and Kaufman, 2000), this unit corresponds to one shallowing-upward sequence from lower shoreface to backshore deposits showing fenestrae-rich beach beds at about +5 m above modern sea level. Unit II is

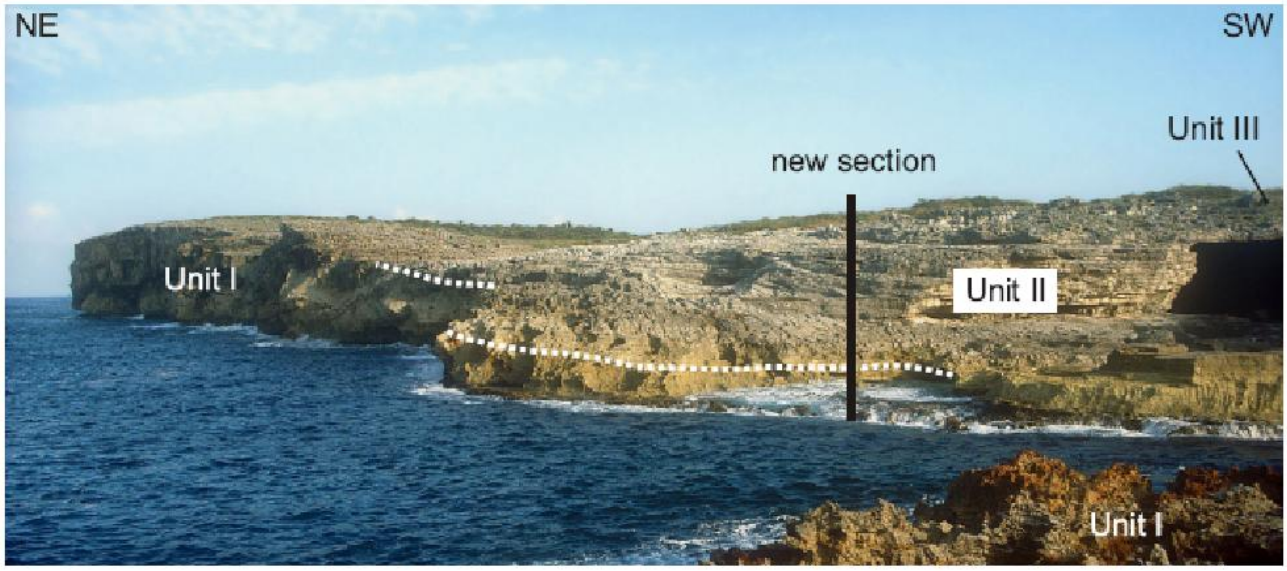

Figure 3. Southeastern end of the Boiling Hole exposure; background cliff height is 20 m. The dotted line emphasizes the boundary between Units I and II which is dipping towards the southwest (modified from Kindler and Hearty, 1995).

attributed to MIS 5e because of its stratigraphic position and the presence of elevated beach facies (Kindler and Hearty, 1995), and also because it yielded whole-rock amino-acid ratios that are consistent with the beginning of the last interglacial period (Hearty, 1998; Hearty and Kaufman, 2000). Unit III overlies Unit II along the back

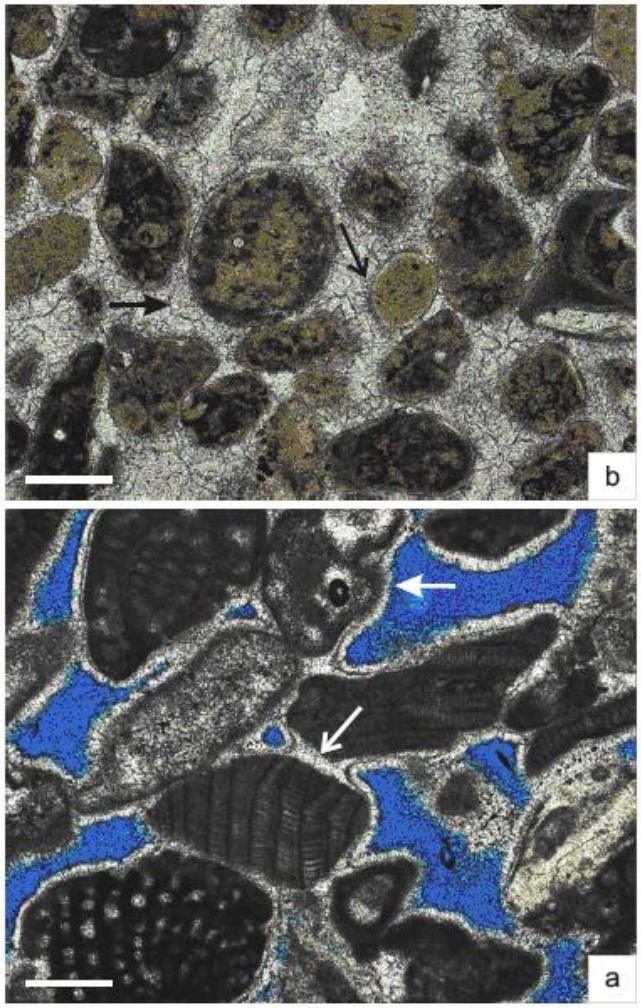

Figure 4. a) Sample EL 169. Microscopic view of the middle Pleistocene (Unit I, MIS 13?) bioclastic eolianite exposed on the southeastern end of the Boiling Hole outcrop. Note the pronounced diagenetic alteration of constituent grains (e.g., peneroplid fragment in lower left corner and Halimeda *clast above center). Note also the early generation of meteoric vadose cement (thin arrow) and the late generation of isopachous fibrous rims (thick arrow) likely precipitated during a later sea-level event. b) Sample EL 64. Microscopic view of the middle Pleistocene (Unit I, MIS 11?) peloidal limestone exposed on the northwestern end of the Boiling Hole outcrop. Note extensive, late meteoric sparry cement. Thin arrow points to remnants of an early isopachous fibrous rim of marine origin. Thick arrow indicates polygonal boundaries suggesting this rock was cemented in a phreatic setting. Scale bars = 200 µm.*

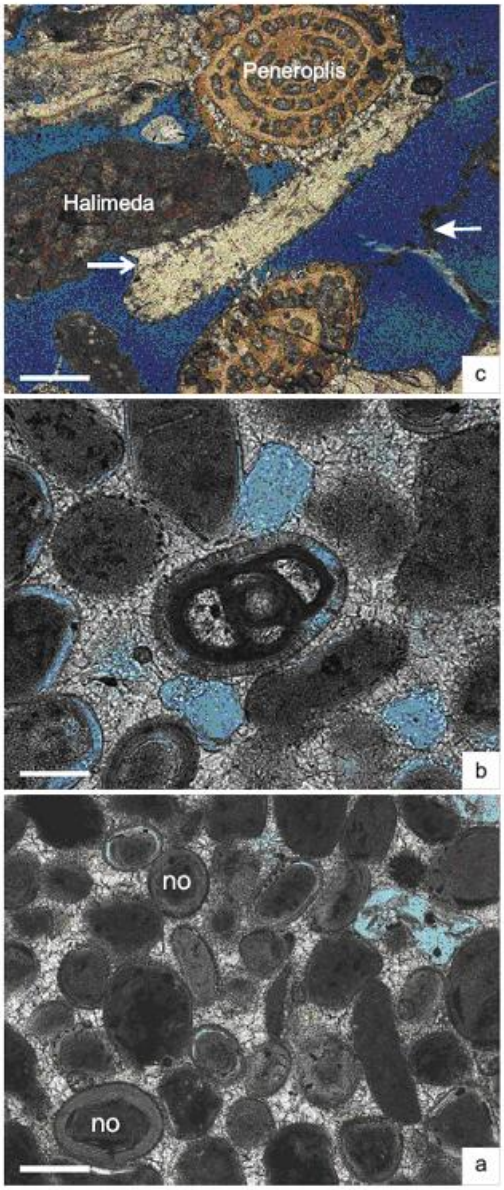

Figure 5. a) Sample EL 205. Microscopic view of last interglacial oolitic deposits (Unit II, MIS 5e) at Boiling Hole. Note the abundance of normal (i.e. thickly coated ooids = no) compared to Fig. 4B; scale bar = 200 µm. b) Sample EL 204. Peculiar radial ooid with a miliolid nucleus. Such ooids are typical of a low energy setting (Land et al., 1979); scale bar = 100 µm. c) Sample EL 69. Microscopic view of the upper Pleistocene bioclastic eolianite (Unit III, MIS 5a). Note the good preservation of bioclasts compared to the middle Pleistocene eolianite (Figure 4a). Note also meteoric meniscus cement (thin arrow) binding the grains and incipient alveolar texture of pedogenic origin (thick arrow); scale bar = 200 µm.

wall of the Boiling Hole cove. In this exposure, a thin calcrete occurs between the two units, whereas at Whale Point, 3.5 km to the NW, they are separated by a 30 cm thick paleosol. Unit III consists of small (up to 3 m high) bioclastic eolianites (Figure 5c) bearing numerous root casts and it is capped by a calcrete. Constituent grains have retained their original mineralogy (aragonite or high-Mg calcite). This difference in petrographic characteristics, the presence of an intervening paleosol, and distinctive whole-rock amino-acid ratios (Hearty, 1998), all indicate that Unit II and Unit III represent separate depositional events and suggest a correlation of the latter unit with MIS 5a.

METHODS

For this study, the geometry, stratigraphy and sedimentology of Unit II were reexamined in detail in the field. Particular attention was given to bounding surfaces and physical sedimentary structures that provide useful information on sediment transport vectors and past depositional environments. A new stratigraphic section was logged at cm-scale on the southeastern flank of the Boiling Hole cove and sedimentological investigations were carried out in the sea cave carved in the back wall of the exposure. The newly discovered footprints were documented and measured according to current vertebrate ichnological standards and methods (e.g., Leonardi, 1987). Track length was measured axially from the tip of digit III along the axis of digit III to the most posterior trace of the heel pad. Width was measured between the tips of digits II and IV. Tracings and a silicon cast of the trackway were made.

RESULTS

The new stratigraphic section logged at the southeastern end of the Boiling Hole cove (Figures 3 and 6) only displays the lowermost two lithological units exposed in the area.

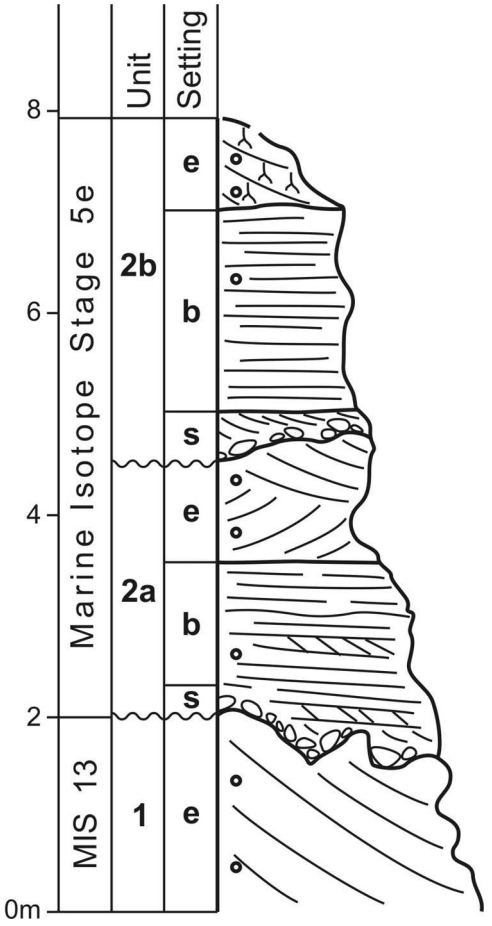

Figure 6. Stratigraphic section logged in the southeastern end of the Boiling Hole exposure. Precise location is indicated on Fig. 3. Setting column: s = subtidal, b = beach, e = eolian. Dots indicate sample locations. Inverted Ys correspond to rhizomorphs (modified from Kindler and Hine, 2008).

Unit I is visible from sea level up to an elevation of 2 m. It consists of a well-cemented, iron-stained, bioclastic eolianite exhibiting large-scale foresets dipping steeply towards the southwest (Figure 7). The upper surface of this rock body is highly irregular and rises towards the

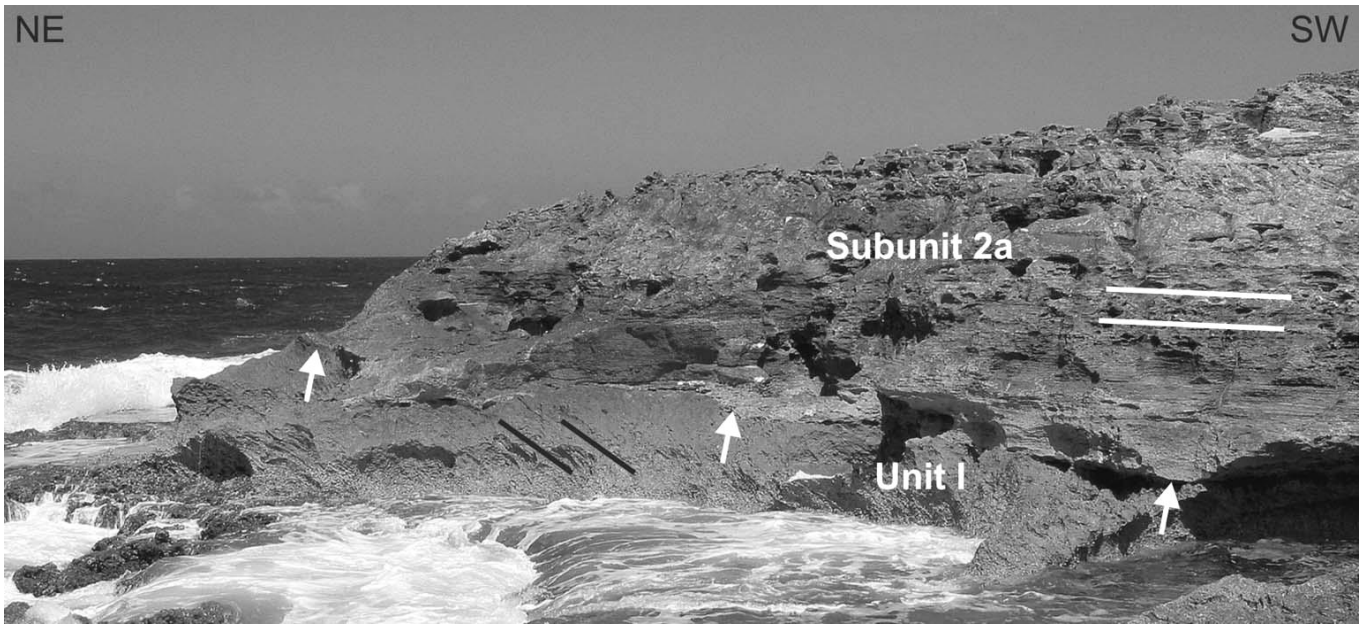

Figure 7. Basal part of studied section. Arrows point to the boundary between Units I and II which rises towards the northeast. Black lines in Unit I correspond to the dip of eolian foresets. White lines in Unit II (subunit 2a) show the dip of beach beds.

northeast (Figure 7). The oolitic-peloidal Unit II is 6 m thick here and includes two shallowing-upward depositional sequences separated, at about 4 m, by a pronounced erosional surface dipping towards the southwest and overlain by a thin conglomerate (Figure 6). Each sequence includes subtidal, beach and eolian facies, identified by sedimentary structures characteristic of these depositional environments (Fig. 6). The subtidal deposits display small-scale cross beds generated by the action of waves and currents. The overlying beach sediments are represented by large-scale, fenestrae-rich, planar cross beds with a low-angle dip towards the southwest (Figure 7) and occur between 2.5 and 3.3 m in the lower sequence and between 5 and 7 m in the upper one. The eolian beds dip mainly towards the southwest and further comprise unusual polygonal structures with a diameter of up to 0.5 m, already observed by Kindler and Hearty (1995), and resembling prism or desiccation cracks (Demicco and Hardie, 1994). The lower sequence disappears towards the back end of the cove (i.e. towards the southwest) where the section described by Kindler and Hearty (1995) was logged. The basal beach beds from the upper sequence form the floor of the large sea cave carved in the back wall of the Boiling Hole cove. Near the southeastern entrance of the cave, the upper surface of one of these beds exhibits bird tracks (Figures 8, 9 and 10).

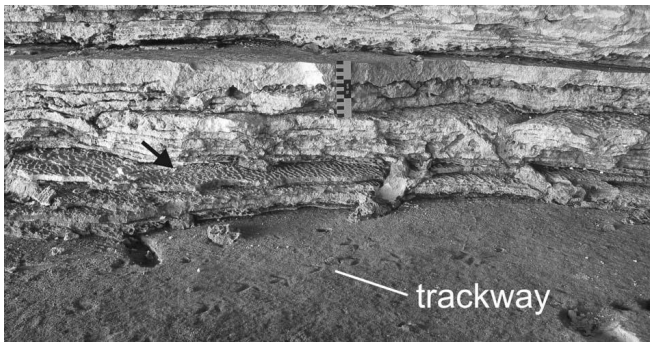

Figure 8. Partial view of the trackway site near the southeastern entrance of the back-wall cave at Boiling Hole. Note the occurrence of small wave ripples in the beds overlying the surface where the tracks are exposed (black arrow). Small wave ripples characterize the lower intertidal and upper subtidal environments.

These tracks are preserved in an oolitic grainstone comprising an early generation of isopachous fibrous cement of marine origin, rare cubic molds that could represent an early halite cement, as des-

Figure 9. Part of the bird trackway showing footprints T2 to T7 (Figure 10). Footprint T7 (far left) is the best preserved track. It has relatively broad digits and a wide divarication, but it shows no evidence for webbing of the foot.

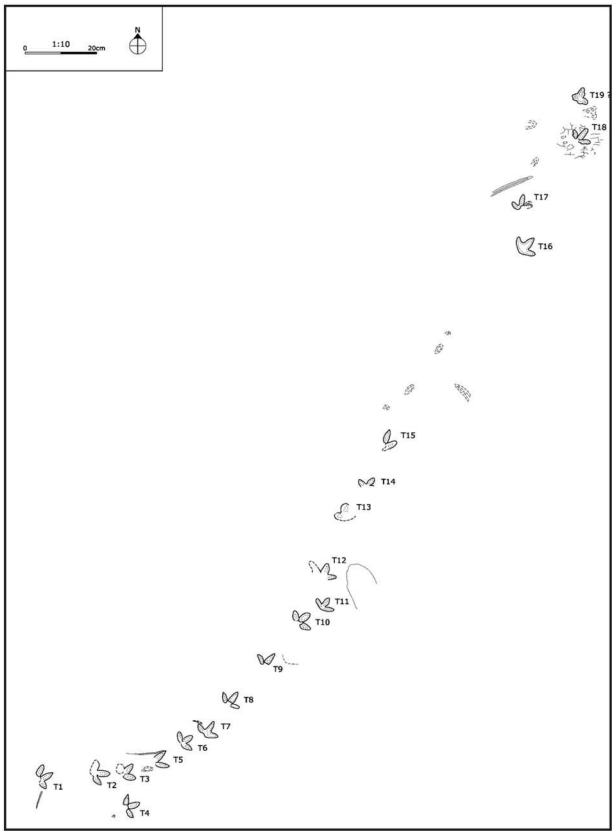

Figure 10. Site map of the bird footprint-bearing paleosurface. Most of the footprints can be attributed to the over 2-m long trackway. Between the footprints T15 and T16, the bird probably walked over a slightly drier substrate. This might explain why only some shallow imprints of the third digit are visible.

cribed by Davaud and Strasser (1984), and late blocky spar precipitated in a meteoric phreatic setting (Figure 11). On the footprint-bearing surface, a total of 19 bird tracks were recognized. Some of the prints are moderately to fairly well preserved, but none show anatomical details such as digital nodes or webbing traces. Nonetheless, all footprints are believed to be true tracks, as it is very unlikely that underprints would form in an unlaminated oolitic grainstone. All but one (footprint T4) can be attributed to the about 2 m long trackway (Figure 10). However, as the left and right footprints could not clearly be identified, pace and stride length have not been measured. Between footprints 15 and 16, several footprints are poorly defined and only some shallow longitudinal grooves that could be the prints of the third digit, were observed. Footprint length varies from 3 to 5.5 cm (average 4.2 cm), and width from 4.5 to 7 cm (average 6 cm). Digit III usually is the most deeply impressed (up to 0.8 cm). The

digits are relatively broad and their tips are U- to V-shaped and without claw impressions. Tracks with three digit prints mostly have a relatively pronounced heel region where the three digits merge together.

Figure 11. Sample EL 220. Thin-section of the oolitic grainstone bed ontop of which the bird tracks are imprinted. Thin arrow points to a square-shaped pore possibly resulting from the dissolution of a halite crystal. Thick arrow indicates partly preserved fibrous rim likely corresponding to an early marine cement. Note partially leached ooids and widespread late sparry cement; scale bar = 200 μm.

DISCUSSION

MIS 5e Sea Level

The recognition of two vertically stacked shallowing-upward sequences in the MIS 5e strata from the Boiling Hole supports earlier reports on the occurrence of two distinctive sea-level highstands in the Bahamas region during the last interglacial period (Chen et al., 1991; Hearty and Kindler, 1993, 1995; Neumann and Hearty, 1996; White et al., 1998; Wilson et al., 1998; Carew and Mylroie, 1999). Due to the lack of suitable material (e.g., *in situ* coral specimens), these sequences could not be precisely dated with the U-series methods. Nonetheless, the intervening erosional surface at 4 m can tentatively be correlated with the sea-level lowstand defined by White et al. (2001) as the Devil's Point Event, and dated at about 125-124 ka. Thus, based on Chen et al.'s (1991) data, the first sequence (sequence 5eII; White et al., 2001) could have been deposited between 130 and 125 ka and the second one (sequence 5eI; White et al., 2001) between 124 and 119 ka. However, the ages of these two depositional/sea-level events ultimately may have to be shifted towards younger values due to recoil-related processes that in most cases, add excess daughter isotopes to the coral framework (Fruijtier et al., 2000; Thompson and Goldstein, 2005). The major point of interest of the MIS 5e record from the Boiling Hole is the occurrence of well-expressed beach facies that, even more than coral reefs, provides a precise estimate of past sea-level stands. Thus, the elevation of beach bedding suggests that mean relative sea level stood at about +3 m (i.e. between 2.5 and 3.3 m) during deposition of sequence 5eII, and at +6 m (i.e. between 5 and 7 m) during accumulation of sequence 5eI. Consideration of the subsidence rates estimated by Lynts (1970) and Carew and Mylroie (1995) places the early eustatic sea-level highstand at +5 m and the later one at +8 m above modern datum. These values are consistent, albeit somehow higher, with those derived from coral data by White et al. (2001), despite the uncertainty related to the depth at which the corals thrived.

Bird Tracks

The bird tracks described here represent the first reported occurrence of fossil vertebrate footprints from the Bahama Archipelago. Moreover, previous reports of Pleistocene bird footprints are few. All footprints are wider than long that is characteristic of shorebird tracks (Abbassi and Lockley, 2004). Among modern birds of the Charadriiformes, only a few have webbed feet. The ichnotaxon *Charadriipeda* bears webbing traces (Sarjeant and Langston, 1994) so we cannot assign the Bahamian footprints to this ichnotaxon, even if webbing might have been present and simply not preserved in the Boiling Hole examples, due to their occurrence in relatively coarse-grained sediment. The Bahamian tracks do match

closely with the ichnotaxon *Avipeda,* that is characterized by three forward directed digits of similar length with a total interdigital spacing of less than 95° (Sarjeant and Langston, 1994). For these reasons, we tentatively assign the Bahamian tracks to this ichnotaxon, using the designation cf. *Avipeda*. Although the tracks are moderately well preserved, we do not elect to erect a new ichnotaxon or ichnospecies at this time.

Figure 12. Shorebird trackway exposed on a modern sand shoal on the leeward side of Long Island, GBB, Bahamas. Note the association of the tracks with small, bifurcating wave ripples. Pen is 15 cm in length.

Observations by one of us (HAC) of similar tracks on a modern sand flat on the bank side of Long Island, Bahamas (Figure 12) indicates that the cm-sized tridactyle footprints exposed in the Boiling Hole cave were likely produced by a shorebird species common today in the Bahamas. It is suggested that the trackmaker belonged to the Order Charadriiformes and was quite possibly one of the following: American oystercatcher (*Haematopus palliates*), greater yellowlegs (*Tringa melanoleuca*), black-necked stilt (*Himantopus mexicanus*), or stilt sandpiper (*Calidris himantopus*). Nonetheless, the precise trackmaker species cannot be identified with the evidence presently in hand. The preservation of the bird footprints in an oolitic grainstone is surprising, as is the conservation of the large polygonal prism or desiccation cracks in the associated eolianites (Kindler and Hearty, 1995). Figure 12 shows that such footprints remain discernible for a few hours to days in cohesive sand, just a few centimeters above the normal high tide line. Subsequent burial by younger (? subtidal) sediment in a low-energy setting could ensure their preservation in the fossil record. In the Boiling Hole case, the footprint-bearing sands could have been quickly cemented by halite crystals precipitated out of marine pore waters, as documented in upper intertidal deposits of Holocene age from Bimini (Davaud and Strasser, 1984), and then rapidly buried and preserved, by a younger sediment layer. The rare occurrence of square pores (Figure 11), possibly resulting from the dissolution of early halite crystals, appears to support this hypothesis.

Origin of Ooids and Sediment Transport

The dip of MIS 5e beach deposits (Figure 7) strongly suggests that their constituent grains originated from the interior of the bank, to the southwest. The eolian strata dip in the same direction. However, they are not foresets, as figured earlier in Kindler and Hearty (1995) and Hearty (1998), but backsets draped over the pre-existing middle Pleistocene topography. Thus, their component particles were also brought up from the bank interior from the west, and not from the open ocean side by the prevailing easterly winds, as previously interpreted. Further, the unusual occurrence of radial ooids (Figure 5b) in these deposits suggests a relatively low-energy production locus (Land et al., 1979; Flügel, 2004), thus strengthening a bank-side source for these deposits. The case is even clearer at Cotton Hole (Figure 2), 1 km to the northwest, where bankward-dipping beach sediments exposed on the ocean-facing cliffs can be traced all the way to the bank-facing shoreline of the island. The Boiling Hole outcrop reveals that a large amount of sediments dating from the last interglacial period has been transported onto the island from the west, opposite to the main transport vector (from east to west) that is prevailing on GBB today. Moreover, ooids were not carried eastward during a single and catastrophic depositional event, such as a storm or a northwesterly gale, but by a sustained flux from the west that lasted long enough for the shoreline to prograde significantly towards the southwest.

CONCLUSIONS

The MIS 5e deposits exposed at the Boiling Hole cove on Eleuthera comprise two superimposed shallowing-upward sequences of coastal deposits separated by an erosional surface and exhibiting beach facies beds at about 3 and 6 m, respectively. These beach beds dip towards the southwest, i.e. towards the bank interior. A bedding plane surface at 5 m displays a 2 m long bird trackway consisting of moderately well-preserved tridactyle footprints that we tentatively assign to the ichnotaxon *Avipeda*. These footprints are the first report of fossil footprints from the Bahama Archipelago, and they were likely formed by an extant shorebird of the Order Charadriiformes. The occurrence of two MIS 5e depositional sequences at the Boiling Hole site adds further evidence to confirm that the last interglacial period was characterized by two sedimentation events corresponding to distinct highstands of sea level, and one erosional phase corresponding to an intervening regression. The Boiling Hole sequences can thus probably be correlated to the 5eII and 5eI sequences defined by White et al. (2001), and further record eustatic sea-level highstands at about +5 and +8 m, respectively, that is somewhat higher than the elevations estimated so far from coral-age data. The dip of the beach beds towards the southwest and the presence of radial ooids generated in a low-energy environment show that, at this locality, a fairly large amount of oolitic sediment was transported from west to east during a significant time period of MIS 5e. This transport direction is opposite to the main sediment transport vector operating on GBB today, demonstrating that the present is not necessarily the key to the past.

ACKNOWLEDGMENTS

We would like to thank Dr. Donald T. Gerace, Chief Executive Officer, and Vincent Voegeli, Executive Director of the Gerace Research Center, San Salvador, Bahamas. PK would like to thank F. Gischig, P. Desjacques and J. Metzger (University of Geneva) for their technical help, the Swiss National Science Foundation for supporting his travel expenses to San Salvador (grant n° 200020-107436), and the staff of the Gerace Research Center for logistical support and their friendly welcome. HAC thanks Jennifer Seavey and Tom Litwin (Smith College) and Paul Sweet (Department of Ornithology, American Museum of Natural History) for helpful suggestions for candidate species as makers of the bird tracks.

REFERENCES

Abbassi, N. and Lockley, M.G., 2004, Eocene Bird and Mammal Tracks from the Karaj Formation, Tarom Mountains, Northwestern Iran: Ichnos, v. 11, p. 349-356.

Ball, M.M., 1967, Carbonate sand bodies of Florida and the Bahamas: Journal of Sedimentary Petrology, v. 37, p. 556-591.

Bathurst, R.G.C., 1975, Carbonate sediments and their diagenesis, Amsterdam, Elsevier: Developments in Sedimentology, v. 12, 658 p.

Boss, S.K. and Neumann, A.C., 1993, Impacts of Hurricane Andrew on carbonate platform environments, northern Great Bahama Bank: Geology, v. 21, p. 897-900.

Carew, J.L. and Mylroie, J.E., 1995, Quaternary tectonic stability of the Bahamian archipelago: evidence from fossil coral reefs and flank margin caves: Quaternary Science Reviews, v. 14, p. 145-153.

Carew, J.L. and Mylroie, J.E., 1999, A review of the last interglacial sea-level highstand (oxygen isotope substage 5e): duration, magnitude, and variability from Bahamian data, *in* Curran H.A. and Mylroie J.E., eds, Proceedings of the Ninth Symposium on the Geology of the Bahamas and Other Carbonate Regions: San Salvador, Bahamian Field Station, p. 14-21.

Carew, J.L. and Mylroie, J.E., 2001, Quaternary carbonate eolianites of the Bahamas: useful analogs for the interpretation of ancient rocks?, *in* Abegg, F.E., Loope, D.B. and Harris, P.M., eds, Modern and Ancient Carbonate Eolianites, Sedimentology, Sequence Stratigraphy, and Diagenesis: Tulsa, Oklahoma, SEPM Special Publication, v. 71, p. 33-45.

Chen, J.H., Curran, H.A., White, B. and Wasserburg, G.J., 1991, Precise chronology of the last interglacial period: ^{234}U-^{230}Th data from fossil coral reefs in the Bahamas: Geological Society of America Bulletin, v. 103, p. 82-97.

Davaud, E. and Strasser, A., 1984, Progradation, cimentation, érosion: évolution sédimentaire et diagénétique récente d'un littoral carbonaté (Bimini, Bahamas): Eclogae geologicae Helvetiae, v. 77, p. 449-468.

Demicco, R.V. and Hardie, L.A., 1994, Sedimentary structures and early diagenetic features of shallow marine carbonate deposits: Tulsa, Oklahoma, SEPM Atlas Series n-1, 265 p.

Flügel, E., 2004. Microfacies of carbonate rocks: Berlin, Springer Verlag, 976 p.

Fruijtier, C., Elliott, T. and Schlager, W., 2000, Mass-spectrometric ^{234}U-^{230}Th ages from the Key Largo Formation, Florida Keys, United States: constraints on diagenetic age disturbance: Geological Society of America Bulletin, v. 112, p. 267-277.

Harris, P.M., 1979, Facies anatomy and diagenesis of a Bahamian ooid shoal, University of Miami, Florida: Sedimenta, n° VII, 163 p.

Hearty, P.J., 1997, Boulder deposits from large waves during the last interglaciation on North Eleuthera Island, Bahamas: Quaternary Research, v. 48, p. 326-338.

Hearty, P.J., 1998, The geology of Eleuthera Island, Bahamas: a Rosetta Stone of Quaternary stratigraphy and sea-level history: Quaternary Science Reviews, v. 17, p. 333-355.

Hearty, P.J. and Kaufman, D.S., 2000, Whole-rock aminostratigraphy and Quaternary sea-level history of the Bahamas: Quaternary Research, v. 54, p. 163-173.

Hearty, P.J. and Kindler, P., 1993, New perspectives on Bahamian geology: San Salvador Island, Bahamas: Journal of Coastal Research, v. 9, p. 577-594.

Hearty, P.J. and Kindler, P., 1995, Sea-level highstand chronology from stable carbonate platforms (Bermuda and The Bahamas): Journal of Coastal Research, v. 11, p. 675-689.

Hearty, P.J., Kindler, P., Cheng, H. and Edwards, L., 1999, A +20 m middle Pleistocene sea-level highstand (Bermuda and The Bahamas) due to partial collapse of Antarctic ice: Geology, v. 27, p. 375-378.

Kindler, P. and Hearty, P.J., 1995, Pre-Sangamonian eolianites in the Bahamas? New evidence from Eleuthera Island, Marine Geology, v. 127, p. 73-86.

Kindler, P. and Hearty, P.J., 1997, Geology of The Bahamas: architecture of Bahamian Islands, *in* Vacher, H.L. and Quinn, T.M., eds., Geology and Hydrogeology of carbonate islands: Amsterdam, Elsevier Science B.V., Developments in Sedimentology, v. 54, p. 141-160.

Kindler P. and Hearty. P.J., 2000, Elevated marine terraces from Eleuthera (Bahamas) and Bermuda: sedimentological, petrographic and geochronological evidence for important deglaciation events during the middle Pleistocene: Global and Planetary Change, v. 24, p. 41-58.

Kindler, P. and Hine, A.C., 2008, The paradoxical occurrence of oolitic limestone on the eastern islands of Great Bahama Bank: where do the ooids come from?: IAS Special Publication, in press.

Land, L.S., Behrens, E.W. and Frishman, S.A., 1979, The ooids of Baffin Bay, Texas: Journal of Sedimentary Petrology, v. 49, p. 1269-1278.

Leonardi, G., 1987, Glossary and Manual of Tetrapod Footprint Palaeoichnology: Publicaçao do Departemento Nacional da Produçao Mineral Brasil, 117 p.

Lynts, G.W., 1970, Conceptual model of the Bahamian platform for the last 135 million years: Nature, v. 225, p. 1226-1228.

Mackenzie, F.T., 1964, Bermuda Pleistocene eolianites and paleowinds: Sedimentology, v. 3, p. 52-64.

Mullins, H.T. and Lynts, G.W., 1977, Origin of the northwestern Bahama Platform: review and reinterpretation: Geological Society of America Bulletin, v. 88, p. 1447-1461.

Neumann, A.C. and Hearty, P.J., 1996, Rapid sea-level changes at the close of the last interglacial (substage 5e) recorded in Bahamian island geology: Geology, v. 24, p. 775-778.

Panuska, B.C., Boardman, M.R., Carew, J.L., Mylroie, J.E., Sealey, N.E. and Voegeli, V., 2002, Eleuthera Island Field Trip Guide for Eleventh Symposium on the Geology of the Bahamas and Other Carbonate Regions: San Salvador, Bahamas, Gerace Research Center, San Salvador, 20 p.

Pindell, J.L., 1985, Alleghenian reconstruction and subsequent evolution of the Gulf of Mexico, Bahamas, and proto-Caribbean: Tectonics, v. 4, p. 1-39.

Purdy, E.G., 1963, Recent calcium carbonate facies of the Great Bahama Bank. 2. Sedimentary Facies: Journal of Geology, v. 71, p. 472-497.

Sarjeant, W.A.S. and Langston, W. Jr, 1994, Vertebrate footprints and invertebrate traces from the Chadronian (Late Eocene) of Trans-Pecos Texas: Austin, Texas Memorial Museum Bulletin, v. 36, 86 p.

Sealey, N.E., 1994, Bahamian Landscapes. An Introduction to the Geography of the Bahamas: Nassau, Media Publishing, Nassau, Bahamas, 128 p.

Sheridan, R.E., Mullins, H.T., Austin, J.A. Jr., Ball, M.M. and Ladd, J.W., 1988, Geology and geophysics of the Bahamas, *in* Sheridan, R.E. and Grow, J.A., eds., The Geology of North America, vol. I-2, The Atlantic Continental Margin, US: Boulder, Colorado: Geological Society of America, p. 329-364.

Swart, P.K., Reijmer, J.J.G., Otto, R. and Bauch, T., 2005, A reevaluation of sedimentary facies on Great Bahama Bank: Geological Society of America, Abstracts with Programs, v. 37, n-7, p 401.

Thompson, W.G. and Goldstein, S.L., 2005, Open-system coral ages reveal persistent suborbital sea-level cycles: Science, v. 308, p. 401-404.

White, B., Curran, H.A. and Wilson, M.A., 1998, Bahamian coral reefs yield evidence of a brief sea-level lowstand during the last interglacial: Carbonates and Evaporites, v. 13, p. 10-22.

White, B., Curran, H.A. and Wilson, M.A., 2001, A sea-level lowstand (Devils' Point Event) recorded in Bahamian reefs: comparison with other last interglacial climate proxies, *in* Greenstein, B.J. and Carney, C.K., eds, Proceedings of the Tenth Symposium on the Geology of the Bahamas and other carbonate regions, San Salvador, Bahamas: Gerace Research Center, San Salvador, Bahamas, p. 109-128.

Wilson, M.A., Curran, H.A. and White, B., 1998, Paleontological evidence of a brief global sea-level event during the last interglacial: Lethaia, v. 31, p. 241-250.

FOSSIL PALM FROND AND TREE TRUNK MOLDS: OCCURRENCE AND IMPLICATIONS FOR INTERPRETATION OF BAHAMIAN QUATERNARY CARBONATE EOLIANITES

H. Allen Curran
Department of Geology
Smith College
Northampton, MA 01063
acurran@smith.edu

Mark A. Wilson
Department of Geology
The College of Wooster
Wooster, OH 44691

John E. Mylroie
Department of Geosciences
Mississippi State University
Mississippi State, MS 39762

ABSTRACT

Molds of palm fronds and vertical, cylindrical structures interpreted as molds of palm tree trunks were reported from Holocene and upper Pleistocene carbonate eolianites on several islands in the Bahamas in the early 1990s. As a result of recent discoveries described herein, palm frond and tree trunk molds are now known to be widespread in Bahamian eolianites, including Holocene beds on Cat Island, Eleuthera, Lee Stocking Island of the Exuma Cays, Long Island, and Stocking Island offshore from Georgetown, Exuma. Late Pleistocene occurrences are known from Eleuthera, Long Island, Norman's Pond Cay of the Exuma Cays, and San Salvador Island. Both palm frond and trunk molds also occur in upper Pleistocene eolianites of Bermuda.

Beds with prolific tree trunk molds comprise an eolianite facies that is interpreted to have formed when drifting sands of coastal dunes encroached on and over the trees of a coastal coppice community dominated by the silver thatch palm, *Coccothrinax argentata*. Rapid cementation of these sands by meteoric waters and decay of palm trunks created the large, cylindrical trunk-mold structures and spongiform texture of this distinctive facies, best represented in Holocene strata exposed along the windward coasts of Eleuthera, Long Island, Lee Stocking Island, and Stocking Island.

INTRODUCTION

Quaternary carbonate eolianites are the dominant rock type capping the islands of the Bahama Archipelago (Figure 1), with virtually all bedrock above 7 meters elevation and much of that at lower elevations, even below sea level, being of eolian origin (Carew and Mylroie, 2001). In recent years, interest in carbonate eolianites has grown, as geologists have come to recognize that an eolian interpretation for grainstones may be more commonly warranted than previously thought (Abegg et al., 2001). For the Bahamas, the meso- and macro-scale physical sedimentary structures and trace fossils that characterize the Quaternary eolianites have been described in some detail from various island localities (e.g., White and Curran, 1988; Caputo, 1995; Kindler, 1995; Curran and White, 2001).

Nonetheless, much remains to be learned about Bahamian eolianites, including better characterization of the various facies that may

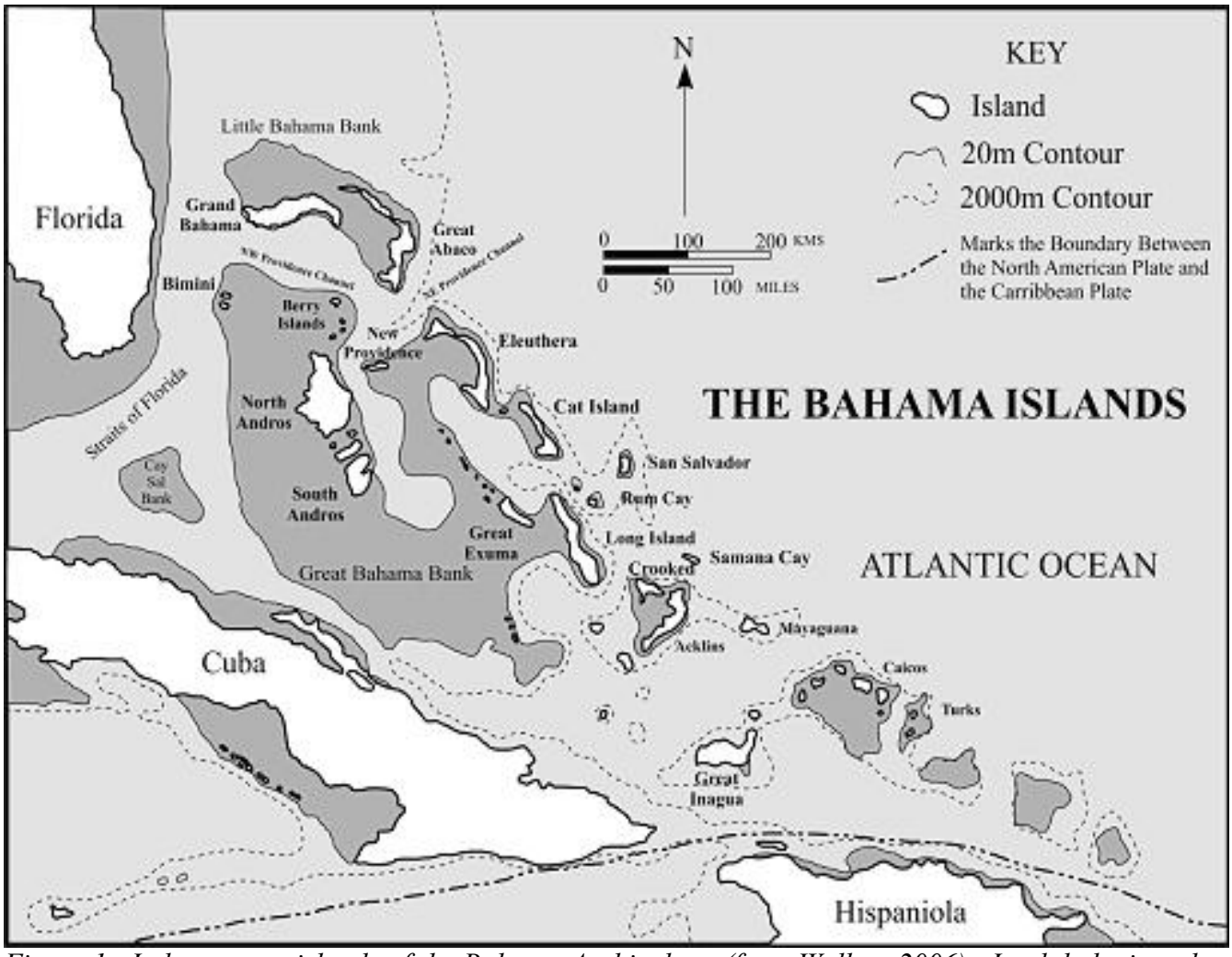

Figure 1. Index map to islands of the Bahama Archipelago (from Walker, 2006). In alphabetic order, fossil palm frond molds presently are known to occur in Quaternary carbonate eolianites on Cat Island, Lee Stocking Island and Norman's Pond Cay of the Exuma Cays (both just north of Great Exuma), and San Salvador Island. Fossil tree trunk molds (and some casts) occur on Cat Island, Eleuthera, Lee Stocking Island, Long Island, and Stocking Island (Atlantic side of Great Exuma, offshore from Georgetown).

be present within any given eolianite unit. The goals of this paper are to describe the occurrence and nature of palm frond and tree trunk molds in eolianites from previously reported and newly discovered localities throughout the Bahamas, to offer an explanation for the formation of such fossils, and to evaluate their implications for paleoenvironmental interpretation.

GEOLOGIC SETTING AND OCCURRENCE

Palm frond and tree trunk molds occur in both upper Pleistocene and Holocene eolianites and have been reported from several of the Bahama islands (Figure 1). Following the Bahamas stratigraphy of Carew and Mylroie (1995, 1997), fossil frond and tree trunk molds are known from Holocene rocks of both the North Point and Hanna Bay members of the Rice Bay Formation, from the regressive eolianites of the Cockburn Town Member of the upper Pleistocene Grotto Beach Formation, and also from transgressive eolianites of the French Bay Member (Figure 2).

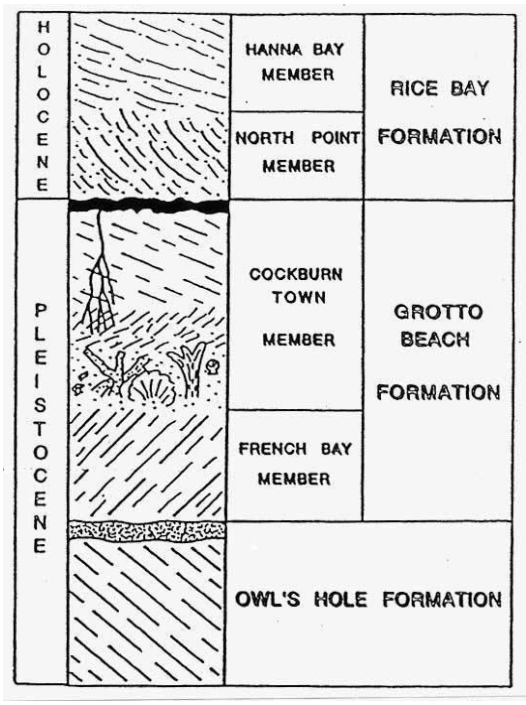

Figure 2. The Carew-Mylroie stratigraphy of the Bahamas (Carew and Mylroie, 1995, 1997).

Interestingly, in occurrences described to date, fossil palm frond molds are not commonly found in direct association with fossil tree trunk molds. Frond molds have been reported previously from Holocene eolianites on Lee Stocking Island of the Exuma Cays (White and Curran, 1993; Kindler, 1995) and Cat Island (Mylroie et al., 2006) and from upper Pleistocene strata in a submarine cave on Norman's Pond Cay of the Exuma Cays (Curran and Dill, 1991). Carew and Mylroie (1994) noted the presence of frond molds in upper Pleistocene beds of the walls of Triple Shaft Cave, a pit cave in the southwestern part of San Salvador, and JEM believes that trunk molds also may be present here. If so, this would mark a first occurrence of both palm frond and trunk molds in close proximity at a single locality.

Fossil tree trunk molds, presumably also from palms, as will be discussed, have been reported from Holocene eolianites on Lee Stocking Island (White and Curran, 1993; Kindler, 1995) and Long Island (Curran et al., 2004). One of us (HAC) found trunk molds similar to those on Long Island in Holocene eolianites of the windward coast of Stocking Island, offshore from Georgetown, Great Exuma. Holocene tree trunk molds also recently were discovered by HAC on the windward coast of Eleuthera, a short distance north of Governor's Harbour, and by JEM on the southern coast of Cat Island. Kindler and Hearty (1996) reported a single trunk mold in upper Pleistocene strata on Eleuthera, also near Governor's Harbour, and JEM found a site on the windward coast of the mid-part of Long Island where trunk casts were common in upper Pleistocene eolianites.

Fossil palm frond and tree trunk molds long have been known to occur in the Pleistocene eolianites of Bermuda (Vacher and Rowe, 1997, and earlier references cited therein). The palm frond and tree trunk molds illustrated by Vacher and Rowe (1997, Fig. 2.7) in the upper Pleistocene Rocky Bay Formation are very similar to those of the Bahamas. Other cylindrical structures, as figured by Vacher and Rowe (1997, Fig. 2-9), were termed soil pipes by Vacher et al. (1995; see Vacher and Rowe, 1997, p. 47-48, for a list of previously applied names). The origin of these structures is more problematic and will be discussed briefly later.

THE FOSSIL PALM FROND AND TREE TRUNK MOLDS

Palm Frond Molds

The most prolific occurrence of fossil palm frond molds reported to date from the Bahamas is within a Holocene eolianite outcrop at Alligator Point on Cat Island. This site was discovered by the Gerace Research Center reconnaissance team in preparation for the 2006 Bahamas Geology Symposium field trip to Cat Island. As Stop 6 of the field trip, details on the location of the outcrop and its description are given in the guidebook (Mylroie et al., 2006, p. 29-33).

This outcrop was generated by excavation for an access road to new home sites, and it cuts the long axis of a fossil dune, revealing a section of well-bedded oolitic eolianite up to 4 m in thickness. There is no calichified paleosol

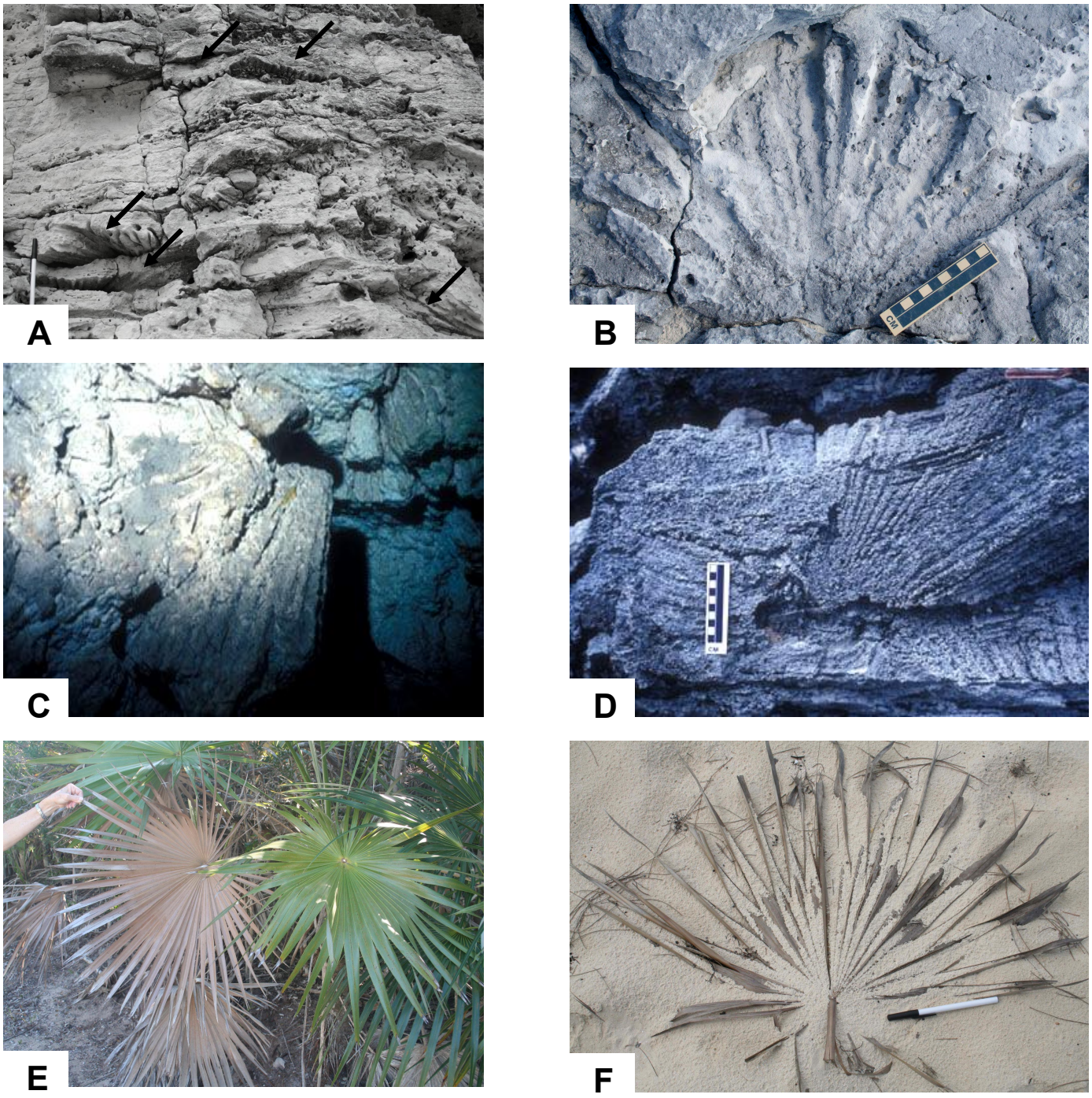

Figure 3. A) Vertical exposure of eolianite beds, North Point Member of Rice Bay Fm., Alligator Point, Cat Island. Arrows indicate palm frond mold fossils. Pen =15 cm. B) Plan view of palm frond mold at Alligator Point. Scale = 10 cm. C) Palm frond molds in late Pleistocene eolianite beds exposed in walls of a submarine cave, Norman's Pond Cay, Exuma Cays. Length of molds up to 40 cm. D) Palm frond mold in the Devonshire Member, late Pleistocene Rocky Bay Fm, Bermuda. Scale = 10 cm. E. Living silver thatch palm fronds, Cat Island. Arm for scale = about 30 cm. F. Silver thatch frond partially buried in proto-dune sands, Cat Island. Pen = 15 cm.

at the top of the dune ridge, confirming a Holocene age for these beds of the North Point Member of the Rice Bay Formation.

Within the outcrop, the palm frond molds are numerous and manifested as coarsely crenulated surfaces along bedding planes (Figure 3A). Parts of frond molds occur commonly in blocks of eolianite lying near this outcrop and along the access road. They can be recognized by the distinctive subparallel to radiate, ridge and groove structure found on the eolianite bedding plane surfaces. A near- perfect palm frond mold fossil (Figure 3B) was found by HAC close to Stop 6 on a bedding plane surface on the Exuma Sound side of Alligator Point during further field study in early 2007.

Similar structures have been found in Holocene eolianites on Lee Stocking Island of the Exuma Cays (White and Curran, 1993, Figure 15; Kindler, 1995). Palm frond molds in upper Pleistocene eolianites also are known to occur in the walls of a submarine cave (Figure 3C) on Norman's Pond Cay of the Exuma Cays, as described by Curran and Dill (1991, Figure 3). On San Salvador, in the walls of Triple Shaft Cave, Sandy Point Pits area, Carew and Mylroie (1994, p. 18), reported the occurrence of palm frond molds in what are thought to be beds of the French Bay Member of the Grotto Beach Formation. Possible trunk molds also may be present in this cave (JEM, not yet described). On Bermuda, similar palm frond molds (Figure 3D) are known from the upper Pleistocene eolianites of the Rocky Bay Formation (Vacher and Rowe, 1997, Fig. 2-7A) and have been observed by HAC in the Southampton Formation.

These fossil molds are interpreted as having formed by the burial of palm fronds in drifting dune sands. With lithification of the dune sediment and decay of organic matter of the frond, the frond mold is generated. As will be discussed further, a likely palm candidate for the frond and tree trunk molds is the silver thatch palm (*Coccothrinax argentata*), common in coastal areas throughout the Bahamas. The fronds of the silver thatch palm are large (can be up to about 1 m in diameter; Figure 3E), accordion-like in form, pliable, and tough. Dead fronds commonly litter the surface around living trees, and easily could be buried in drifting sand (Figure 3F; compare with the fossil mold of 3B).

Trunk Molds

Although fossil tree trunk molds were reported from the Bahamas, on Lee Stocking Island, in the early 1990s (White and Curran, 1993), reconnaissance by a Gerace Research Center team in preparation for a Bahamas Geology Symposium field trip was again the catalyst for a new discovery – this time on Long Island in 2004. The key outcrop section is on the Atlantic side of Long Island, at the north end of Cabana Beach of the Stella Maris Resort (Curran et al., 2004, Stop 3, p. 12-15). A similar sequence of beds occurs at the rocky coast exposures of Stop 1 (Cave Point) of the Long Island field trip guide (Curran et al., 2004), although access to this site is not so easy.

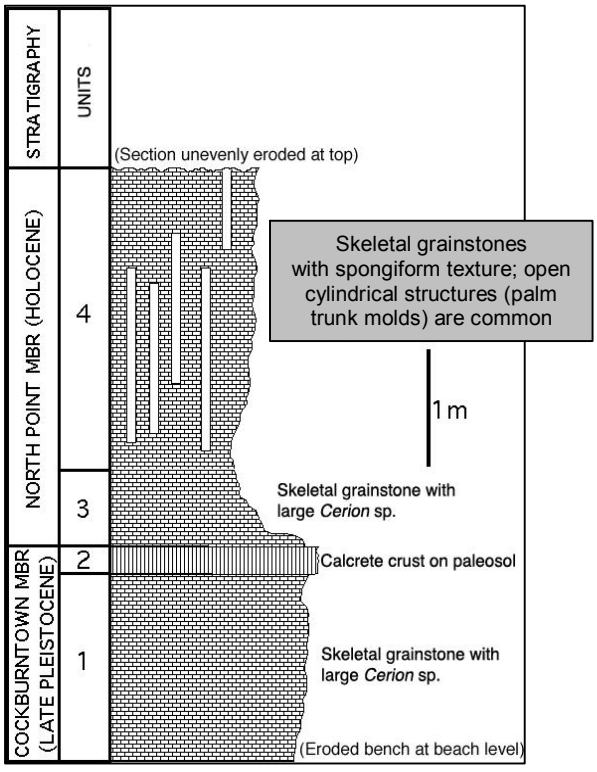

Figure 4. Stratigraphy of the Cabana Beach section, Stella Maris Resort, Long Island, Bahamas (modified from Curran et al., 2004).

The Cabana Beach exposure provides a classic view of the Upper Pleistocene/Holocene contact, as shown in the stratigraphic column of Figure 4. Here Holocene strata of the North Point Member of the Rice Bay Formation lie above a thick, continuous, and very hard caliche layer marking the top of the Pleistocene sequence. The skeletal grainstone beds of Unit 4 of this section are fine grained, not distinctly laminated, and have a friable, spongiform texture (Figure 5A). In addition, they contain numerous well-developed vertical, open cylindrical structures (Figure 5B, D). These cylindrical holes have inside diameters of up to 12 cm, lengths of up to 1.3 m, and are prolific in occurrence. In 2006, HAC measured all holes with inside diameters (not including rind material) of 5 cm or more on several bedding plane surfaces. A total area of 16 m^2 was surveyed, and 44 holes were encountered, for an average of 2.75 holes per m^2.

These cylindrical structures are very similar to the structures reported in equivalent Holocene beds on Lee Stocking Island (White and Curran, 1993; Kindler, 1995) and give no evidence of origin via dissolution. White and Curran (1993, p. 186-187) interpreted the Lee Stocking Island structures as representing palm trunk molds. They also reported finding palm frond imprints in Holocene eolianite talus blocks on Lee Stocking Island and cited supporting evidence for this interpretation from similar structures found on Bermuda that have been interpreted as palm trunk molds (see Vacher and Rowe, 1997, Fig. 2-7B,C for photographs of a comparable example).

An interpretation for Units 3 and 4 of the Cabana Beach section is that Unit 3 represents a protosol layer upon which a coastal coppice palm community developed. Sands from the leeward sides of encroaching dunes buried the palm-dominated community, with the trunks of the palms baffling sediment during deposition and then molded in sand. Rapid cementation of the sands by meteoric waters and decay of the palm trunks created the vertical cylindrical structures (tree trunk molds) and spongiform texture of Unit 4. The hard calichified rind that commonly lines trunk molds likely begins to form early in the burial process, with cementation and diagenesis as meteoric waters run down tree trunks and into the host sediment (Figure 5C). Beds lying above Unit 4 have typical eolianite lamination, contain numerous rhizomorphs, and represent the continued migration of dunes over the coastal palm community.

Several more localities of prolific occurrence of cylindrical structures or palm trunk molds have been discovered in the Bahamas since 2004. These include at Newton Cay on the far north end of the Atlantic coast of Long Island, where HAC found numerous trunk molds in Holocene Hanna Bay Member beds, as well as a similar sequence at Poseidon Point to the south, between Newton Cay and Stella Maris. HAC also observed palm trunk molds on the Atlantic coast of Stocking Island, offshore from Georgetown, Exuma and on the Atlantic side of Eleuthera, just north of the Twin Coves beach estate (on the coast and very near the Two Pines section of Kindler and Hearty (1996) a short distance north of Governor's Harbour). At this locality, trunk molds are prolific in North Point Member beds (Figure 5E). As at the Cabana Beach section on Long Island, the molds occurred in essentially unlaminated skeletal grainstones with a spongiform texture.

Likewise, in a reconnaissance study of the south end of Cat Island, JEM and his students recently discovered numerous trunk molds in Hanna Bay Member beds near Devil's Point, on the southwest coast of the island (Figure 5F). On the mid-Atlantic coast of Long Island, from another reconnaissance study, JEM reported a similar find of trunk molds and casts in upper Pleistocene strata of the Grotto Beach Formation (Figure 5G). This site merits further study because trunk casts have not been observed to date in Holocene strata. Comparison also needs to be made with the fossil tree trunk reported by Kindler and Hearty (1996, Figure 11) in upper Pleistocene eolianites at the Two Pines dune section on Eleuthera and with possibly similar structures on Bermuda. Beyond the Vacher and Rowe (1997) example of a trunk mold cited earlier, most of the "solution pipe" Bermudan

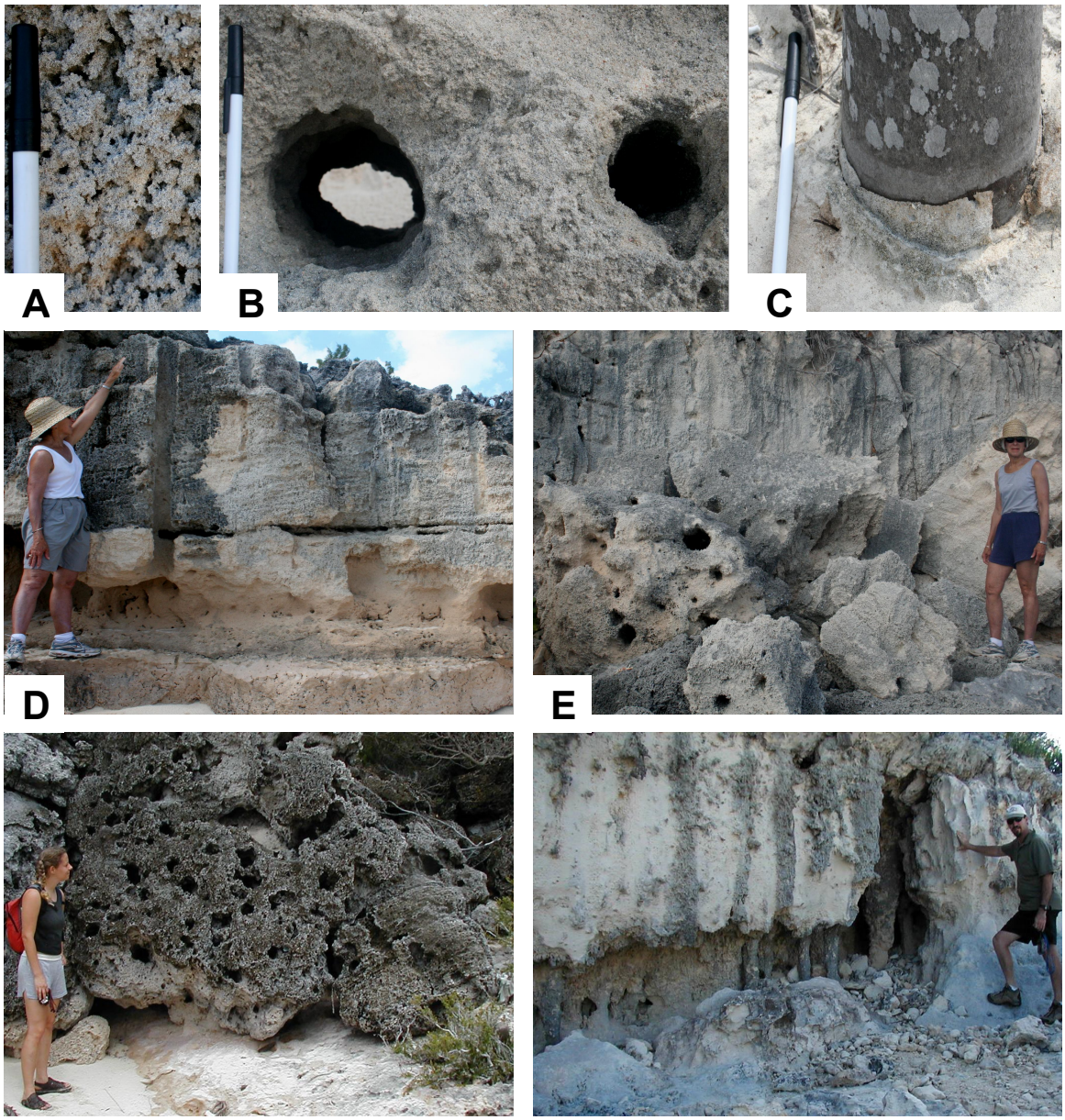

Figure 5. A) Spongioform texture of grainstones, Unit 4 beds, North Point Member, Rice Bay Fm., Cabana Beach section, Long Island. Pen top = 4 cm. B) Open holes of tree trunk molds at Cabana Beach. Pen = 15 cm. C) Silver thatch palm tree with base of trunk encased by a calcified rind and growing in Hanna Bay Member beds of the Rice Bay Fm., Cape Santa Maria, NW Long Island. Pen = 15 cm. D) Multiple tree trunk molds in Unit 4, Cabana Beach section. Trunk molds commonly reach 2-m-length at this site. E) Prolific occurrence of tree trunk molds in beds of the North Point Member, Rice Bay Fm., exposed along the Atlantic coast north of Twin Coves near Governor's Harbor, Eleuthera. F) Tree trunk molds in cross-section of block of Hanna Bay Member eolianite near Devil's Point, Cat Island. G) Tree trunk molds and casts in Upper Pleistocene strata, Grotto Beach Fm., mid-Atlantic coast of Long Island.

examples were reinterpreted by Herwitz (1993) as structures formed by stemflow phenomena, not as the molding of tree trunks by eolian sands. Thus, there is need for critical analysis of all localities where trunk molds and casts occur in the Bahamas and on Bermuda to evaluate further the ways in which these features formed and were preserved.

A MODERN PALM ANALOGUE

Many examples of the occurrence of buried trees, even forests, have been reported in the geologic literature, beginning with the oldest known trees of the Gilboa forest that are preserved *in situ* in middle Devonian sedimentary rocks of upstate New York (Meyer-Berthaud and Decombeix, 2007). Tree trunks preserved in upright position are known to occur in sediments ranging from terrestrial siliciclastics to volcanic ash, with rapid burial as a common theme. Burial with the formation of open molds, as is the case for all of the Holocene examples cited herein, seems less common, but can include interesting examples such as palm preservation as molds in basaltic lava flows, as was recently described from Hawaii (Woodcock and Kalodimos, 2005).

In their field guides to the vegetation of San Salvador, Smith (1993) and Kass (2005) list several species of palms. Our best modern analogue for the fossil palm frond and tree trunk molds found in the Bahamas is the silver thatch palm, *Coccothrinax argentata*, of the Family Arecaceae. The silver thatch palm is a prominent member of the Bahamian coastal coppice community, typically occurring in dry, open areas along the coast (Kass, 2005). Smith (1993) recognized silver thatch palm as the dominant species of a coastal coppice subcommunity and mapped several locations of this subcommunity on San Salvador.

One area of occurrence of the *Coccothrinax argentata* subcommunity is along the northwest coast of San Salvador, just inland from the beach immediately east of Barkers Point and the site of the Haitian boat wreck. Here there is an open silver thatch palm forest with considerable ground litter of palm fronds (Figure 6A). In some places trees have been overturned by storm winds, exposing their root balls (Figure 6B). Interestingly, palm trunks separate cleanly from the root balls. At this location, it is not hard to envision wind-blown sands moving inland from the nearby beach and burying the forest.

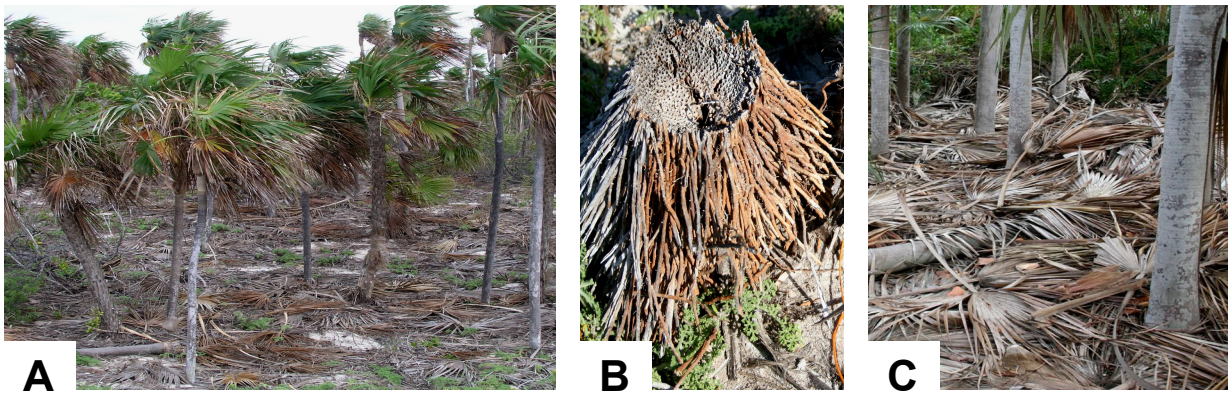

*Figure 6. A) Silver thatch palm (*Coccothrinax argentata*) coastal coppice, northwest coast of San Salvador (just inland from beach immediately east of Barkers Point and site of the wrecked Haitian boat). Note near monospecific occurrence of palm trees (about 3 to 5 m height) and the ground litter of fronds. B) Root ball of a silver thatch palm, showing clean break from the trunk. Diameter at top is about 15 cm. C) Silver thatch coppice just south of Club Med beach, near Governor's Harbour, Eleuthera. Tree trunk diameters here are significantly larger than at the San Salvador site and average about 17 cm. Note the dense litter of fronds. These two sites were used to gather statistical data displayed in Figure 7.*

This is the scenario we propose for formation of the fossil palm frond and tree trunk molds described here. With the formation of eolianites in earlier Holocene and interglacial Pleistocene times, intervals of drifting sand in large quantities must have been much more common throughout the Bahamas than is the case today. This would make the coastal coppice vulnerable to burial, with the fronds and tree trunks of the silver thatch palm being prime candidates for fossilization. Are all fossil trunk molds those of palms? Likely not, but at this stage in our investigations, it is not possible to identify different forms of trunk molds, and palm trunks are the best match for the characteristics of the cylindrical structures that we have observed and measured.

In order to test the coastal coppice burial scenario, HAC and field assistants measured the inside diameters (not including rind material) of fossil trunk molds from five study sites on Long Island and Eleuthera. These data were compared with measurements of modern silver thatch trunk diameters from forest sites on San Salvador and Eleuthera (Figure 6A,C).

The results are shown in Figure 7. Mean diameters for the five fossil sites are similar and

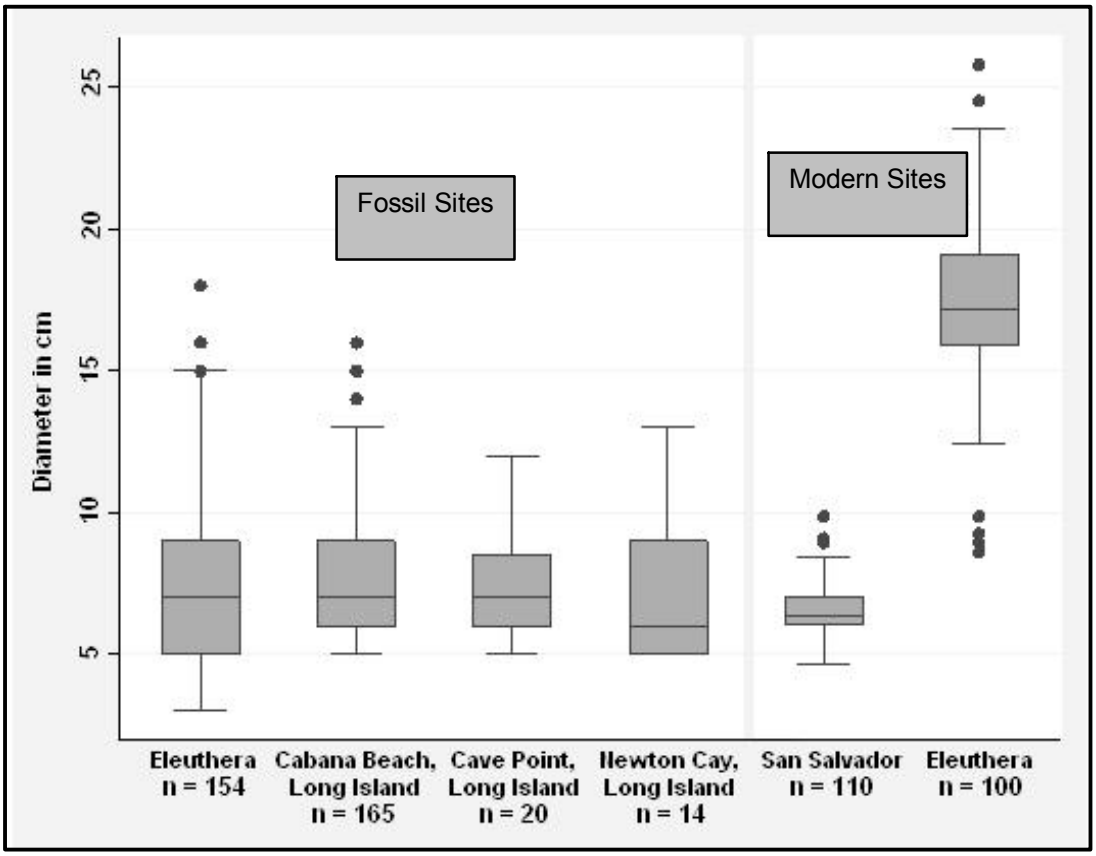

*Figure 7. Box plots for counts of diameters of fossil tree trunk molds and modern silver thatch palm (*Coccothrinax argentata*) trunks at selected sites on Eleuthera, Long Island, and San Salvador.*

suggest a single species of origin. The mean diameters of the fossil sites also matched closely with the mean diameter of the trees at the San Salvador site, supporting silver thatch palm as the modern analogue. However, the modern Eleuthera site does not match well. It was obvious when the measurements were made that this was a much more mature forest with bigger trees than those measured on San Salvador. So, while these results are suggestive, they are by no means conclusive in favor of the silver thatch palm as the one and only analogue. Nonethe-

less, one might speculate that in environmental settings of highly mobile sands, coastal coppice forests would be highly vulnerable to burial. With shorter amounts of time for development, the palm trees would not reach full maturity and would be expected to have and smaller diameter trunks, as at the San Salvador forest site.

DISCUSSION

Although the full distribution and significance of the occurrence of fossil palm tree trunk and frond molds in the carbonate eolianites of the Bahamas remains to be determined, some initial patterns are emerging. At many localities, particularly in Holocene strata, palm trunk molds are the dominant feature characterizing a distinctive eolianite facies. Furthermore, this facies seems to occur most commonly along the windward Atlantic coasts of the more elongate Bahamian islands, with the examples being Eleuthera, Long Island, and Lee Stocking and Stocking islands of the Exuma Cays. Following the island architecture scheme of Kindler and Hearty (1997), all are islands where windward coast sedimentation has been dominant (Class I and III islands). The exception would be the occurrence of fossil tree trunk molds in Holocene Hanna Bay Member beds near Devil's Point, southwest Cat Island. Although the site has not been studied in detail, this reach of coast appears to be subject to at least moderate wind and wave energy.

At present, we know of only two late Pleistocene occurrences of palm trunk molds (and casts), on Long Island (Figure 5G) and Eleuthera (Kindler and Hearty, 1996, Figure 11). Neither of these sites has been studied in detail from the prospective of the significance of palm trunk mold and cast fossils, so it is too early to draw conclusions. Nonetheless, it seems likely that more sites of trunk mold and cast occurrence will be found in upper Pleistocene eolianites with further reconnaissance along the extensive windward coast of Long Island and elsewhere.

Rapid burial by dune sands migrating inland from adjacent beaches during transgression is the most likely explanation for the Holocene sites with prolific occurrences of tree trunks molds as described herein. However, caution is warranted because, as emphasized by Carew and Mylroie (2001), Bahamian eolianites form complex topographies with transgressive, stillstand, and regressive phases. Therefore each case must be evaluated individually with respect to depositional history. The Cabana Beach section on Long Island (Figure 4) is an excellent example of rapid burial of a coastal coppice forest, probably dominated by silver thatch palms (*Coccothrinax argentata*), during mid-Holocene transgression.

We now know that occurrences of fossil palm frond molds in Quaternary Bahamian eolianites are widespread and certainly not uncommon. However, at this point, there seems to be no clear pattern of distribution. The Cat Island site, where the most prolific occurrence of palm frond molds is found, is on the leeward side of the island, although everything about the Holocene geology of the south ridge of Alligator Point suggests the presence of considerable depositional energy in the past. Interestingly, with one possible exception (Triple Shaft Cave on San Salvador), palm frond mold fossils have not been found in close association with tree trunk molds. This may change with future discoveries, but, for now, why this is so remains unknown. Also in need of future study is the role of the megascale porosity and permeability generated by open tree trunk and frond molds on the hydrogeology and diagenesis of the eolianite facies in which they occur.

CONCLUSIONS

As a result of several recent discoveries, fossil palm frond and tree trunk molds now are known to be widespread in the Holocene and upper Pleistocene eolianites of the Bahamas. When occurring in abundance, tree trunk molds

form a distinctive facies, as shown by the Holocene examples cited herein, and this also is likely the case for trunk molds and casts in upper Pleistocene eolianites, although only one site on Long Island with numerous specimens is presently known, and it has not been studied in detail.

The prolific occurrence of trunk molds indicates depositional conditions of rapid burial by drifting dune sands, most likely covering coastal coppice forests dominated by the silver thatch palm, *Coccothrinax argentata*. The Holocene examples that occur on Long Island, Eleuthera, and Lee Stocking and Stocking islands of the Exuma Cays are a direct result of eustatic sea-level transgression. Nonetheless, caution is warranted in the detailed interpretation of depositional environment at any given site because conditions of drifting eolian sands can be present in times of sea-level highstand, still-stand, and regression as well.

Fossil palm frond molds, also attributed to the silver thatch palm, now have been reported from numerous islands and a variety of settings throughout the Bahamas. The most prolific occurrence known to date is in Holocene eolianites at Alligator Point on Cat Island. Interestingly, with one exception (Triple Shaft Cave on San Salvador), fossil palm frond molds have not been found in close association with tree trunk molds.

A number of questions related to the occurrence and significance of fossil palm frond and tree trunk molds remain and should be investigated in the future, including:

1. How widespread is the tree trunk mold facies and does it have a consistent stratigraphic position within Bahamian eolianite sequences?

2. How widespread is palm frond mold occurrence, and why aren't fossil frond and trunk molds consistently found together? Where are the tree root balls, and, if not preserved, why not?

3. What are the implications of the porosity and permeability generated by fossil tree trunk molds for the hydrology and diagenetic processes within the carbonate eolianites in which they occur?

4. How closely do palm frond molds and tree trunk molds and casts from the Bahamas compare with those of Bermuda?

ACKNOWLEDGMENTS

We thank Deborah Freile and Lisa Park for their excellent work in producing this proceedings volume from the 13th Symposium on the Geology of the Bahamas and other Carbonate Regions. HAC thanks Lisa Park for her patience and assistance with the editing of this manuscript. Geology students Abby D'Ambrosia and Anna Lavarreda (Smith College), Drew Feucht (The College of Wooster), and Athena Owen and Will Waterstrat (Mississippi State University) provided valuable field assistance for this project, and Abby and Anna compiled the statistics presented in Figure 7. HAC thanks Aubrey and Tom McDonough for assistance in the field on Eleuthera and Jane Curran for assistance on Cat, Eleuthera, and Long islands. JEM thanks Joan Mylroie for extended field assistance on Cat, Long, Eleuthera, and San Salvador islands. Most of the field work for this project was conducted beyond San Salvador. The significant logistical support provided by the Gerace Research Centre for geologic reconnaissance trips to Long and Cat islands was crucial to this study. For this we are grateful to Vince Voegeli, former Executive Director, Dr. Donald T. Gerace, Chief Executive Officer, and the staff of the GRC.

REFERENCES

Abegg, F.E., Harris, P.M., and Loope, D.B., eds., 2001, Modern and Ancient Carbonate Eolianites: Sedimentology, Sequence Stratigraphy, and Diagenesis: Tulsa, Oklahoma, SEPM (Society for Sedimentary Geology) Special Publication No. 71, 207 p.

Caputo, M.V., 1995, Sedimentary architecture of Pleistocene eolian calcarenites, San Salvador Island, Bahamas, *in* Curran, H.A., and White, B., eds., Terrestrial and Shallow Marine Geology of the Bahamas and Bermuda: Boulder, Colorado, Geological Society of America, Special Paper 300, p. 63-76.

Carew, J.L., and Mylroie, J.E., 1994, Geology and Karst of San Salvador Island, Bahamas: A Field Trip Guidebook: San Salvador, Bahamian Field Station, Ltd., 32 p.

Carew, J.L., and Mylroie, J.E., 1995, Depositional model and stratigraphy for the Quaternary geology of the Bahama Islands, *in* Curran, H.A., and White, B., eds., Terrestrial and Shallow Marine Geology of the Bahamas and Bermuda: Boulder, Colorado, Geological Society of America, Special Paper 300, p. 5-32.

Carew, J.L., and Mylroie, J.E., 1997, Geology of the Bahamas, *in* Vacher, H.L., and Quinn, T.M., eds., Geology and Hydrology of Carbonate Islands: Amsterdam, Developments in Sedimentology 54, Elsevier Science B.V., p. 91-139.

Carew, J.L., and Mylroie, J.E., 2001, Quaternary carbonates of the Bahamas: useful analogues for the interpretation of ancient rocks?, *in* Abegg, F.E., Harris, P.M., and Loope, D.B., eds., Modern and Ancient Carbonate Eolianites: Sedimentology, Sequence Stratigraphy, and Diagenesis: Tulsa, Oklahoma, SEPM (Society for Sedimentary Geology) Special Publication No. 71, p. 33-45.

Curran, H.A., and Dill, R.F., 1991, The stratigraphy and ichnology of a submarine cave in the Exuma Cays, Bahamas, *in* Bain, R.J., ed., Proceedings of the Fifth Symposium on the Geology of the Bahamas: San Salvador, Bahamian Field Station, p. 57-64.

Curran, H.A., and White, B., 2001, The ichnology of Holocene carbonate eolianites of the Bahamas, *in* Abegg, F.E., Harris, P.M., and Loope, D.B., eds., Modern and Ancient Carbonate Eolianites: Sedimentology, Sequence Stratigraphy, and Diagenesis: Tulsa, Oklahoma, SEPM (Society for Sedimentary Geology) Special Publication No. 71, p. 47-56.

Curran, H.A., Mylroie, J.E., Gamble, D.W., Wilson, M.A., Davis, R.L., Sealey, N.E., and Voegeli, V.J., 2004, Geology of Long Island, Bahamas: A Field Trip Guide: San Salvador, Bahamas, Gerace Research Center, 24 p.

Herwitz, S.R., 1993, Stemflow influences on the formation of solution pipes in Bermuda eolianite: Geomorphology, v. 6, p. 253-271.

Kass, L.B., 2005, An Illustrated Guide to Common Plants of San Salvador Island, Bahamas, 2nd edition: San Salvador, Bahamas, Gerace Research Center, 148 p.

Kindler, P., 1995, New data on the Holocene stratigraphy of Lee Stocking Island (Bahamas) and its relation to sea-level history, *in* Curran, H.A., and White, B., eds., Terrestrial and Shallow Marine Geology of the Bahamas and Bermuda: Boulder, Colorado, Geological Society of America, Special Paper 300, p. 105-116.

Kindler, P., and Hearty, P.J., 1996, Carbonate petrography as an indicator of climate and sea-level changes: New data from Bahamian Quaternary units: Sedimentology, v. 43, p. 381-399.

Kindler, P., and Hearty, P.J., 1997, Geology of the Bahamas: architecture of Bahamian islands, *in* Vacher, H.L., and Quinn, T.M., eds., Geology and Hydrology of Carbonate Islands: Developments in Sedimentology 54, Amsterdam, Elsevier Science B.V., p. 141-160.

Meyer-Berthaud, B., and Decombeix, A-L., 2007, A tree without leaves: Nature, v. 446, p. 861-862.

Mylroie, J.E., Carew, J.L., Curran, H.A., Freile, D., Sealey, N.E., and Voegeli, V.J., 2006, Geology of Cat Island, Bahamas: A Field Trip Guide: San Salvador, Bahamas, Gerace Research Center, 44 p.

Smith, R.R., 1993, Field Guide to the Vegetation of San Salvador Island, The Bahamas, 2nd edition: San Salvador, Bahamian Field Station, 120 p.

Vacher, H.L., and Rowe, M.P., 1997, Geology and hydrology of Bermuda, *in* Vacher, H.L., and Quinn, T.M., eds., Geology and Hydrology of Carbonate Islands: Developments in Sedimentology 54, Amsterdam, Elsevier Science B.V., p. 35-90.

Vacher, H.L., Hearty, P.J., and Rowe, M.P., 1995, Stratigraphy of Bermuda: nomenclature, concepts, and status of multiple systems of classification, *in* Curran, H.A., and White, B., eds., Terrestial and Shallow Marine Geology of the Bahamas and Bermuda: Boulder, Colorado, Geological Society of America Special Paper 300, p. 271-294.

Walker, L.N., 2006, The Caves, Karst and Geology of Abaco Island, Bahamas [M.S. Thesis]: Starkville, Mississippi State University, 241 p.

White, B., and Curran, H.A., 1988, Mesoscale physical sedimentary structures and trace fossils in Holocene carbonate eolianites from San Salvador Island, Bahamas: v, 55, Sedimentary Geology, p. 163-184.

White, B., and Curran, H.A., 1993, Sedimentology and ichnology of Holocene dune and backshore deposits, Lee Stocking Island, Bahamas, *in* White, B., ed., Proceedings of the Sixth Symposium on the Geology of the Bahamas: San Salvador, Bahamian Field Station, p. 181-191.

Woodcock, D., and Kalodimos, N., 2005, Tree mold evidence of Loulu palm (*Prichardia* sp.) forest on the Kona Coast, Hawai'i: Pacific Science, v. 59, p. 481-498.

BIOEROSION AND ENCRUSTATION ON CURAÇAO PLEISTOCENE REEFS: EVALUATING GRAZING IN THE FOSSIL RECORD

Halard Lescinsky
Department of Life and Earth Sciences
Otterbein College
Westerville, OH 43081
hlescinsky@otterbein.edu

ABSTRACT

Coral reef bioerosion studies on experimental substrates through time find that grazing bioerosion is an order of magnitude greater than macroboring bioerosion. Geologists working on fossil reefs, on the other hand, have focused primarily on boring bioerosion, largely ignoring grazing which can be more difficult to measure. Here, I assess the relative effects of grazing, macroboring, and encrustation in a well preserved Pleistocene reef, Curaçao, Netherlands Antilles. Taphonomic data from windward reef crest, backreef flat, lagoon, and leeward reef crest facies all suggest that grazing bioerosion was very low. There is a low incidence of surface pitting on the reef, and surface features such as the corallite collars of *Acropora* are well preserved. Boring is estimated to have been <10%, which is similar to rates reported in modern reefs. Encrustation, primarily by coralline algae, is pervasive, occurring in crusts up to 30 mm thick on *Acropora palmata* trunks, and encasing *A. cervicornis* rubble that is sometimes only preserved via bioimmuration on the inner surface of algal rinds. The absence of grazing probably reflects high live coral cover on the living reef, and an overestimation of the importance of grazing in many coral reef settings.

INTRODUCTION

Reefs form where carbonate framework is produced faster than it is removed by either physical transport or the erosive effects of organisms. When Neumann (1966) first proposed the term "bioerosion" for this latter process, he emphasized that both scraping (external) and boring (internal) bioerosion were important to the reef--but the subsequent geological study of bioerosion has focused almost exclusively on the study of borers (e.g., Palmer and Plewes 1993; Perry, 1996, 2000; Weidlich, 1996; Vogel et al., 1987). This is no doubt in part because boring traces are preserved as discrete voids within carbonate substrate and are easy to quantify in fossils. Quantifying the removal of material from the exterior of a surface, as occurs in grazing, is more problematic since successive grazing events remove the evidence of previous events and thus have the primary effect of decreasing substrate size.

The current geological focus on internal bioerosion is at odds with most experimental studies of bioerosion on modern reefs that have found that the intensity of grazing bioerosion is an order of magnitude or more greater than macroboring (Kiene and Hutchings, 1994; Chazottes et al., 1995; Pari et al., 1998). Although, quantifying grazing in fossil reefs is probably inherently impossible if grazing is intense, it is relatively simple if grazing is low. I propose that grazing on fossil reefs can be evaluated using original corallite topography, since external scraping will quickly obliterate any characteristic corallite morphology. This paper addresses grazing prevalence across several different facies of a Pleistocene fossil reef in Curaçao. The observed low rates of grazing bioerosion in the Pleistocene of the Caribbean suggest a need to re-evaluate experimental results, at least as they apply to the Caribbean prior to human impact.

Geological Setting

Curaçao, Netherlands Antilles, lies approximately 60 km north of Venezuela and is composed of a Cretaceous diabase core that was subsequently covered around the margins by carbonate reef deposits. Slow regional uplift (.06

m/1000 yr over the last 1-200 kyr, Schellmann et al., 2004) has resulted in 5 raised carbonate terraces around most of the island (Figures 1, 2). The top of the Lower Terrace (de Buisonjé, 1974) sits 10-12 m above sea level and is composed of a lower Cortalein Unit (216 Ka) and an upper Hato Unit (122 Ka) (Schellmann et al., 2004). The semi-arid climate results in little diagenetic alteration (Bries et al., 2004); and the infrequency of hurricanes has resulted in a high percentage of the corals remaining in life position and comparatively little rubble making up the reef interior (Meyer et al., 2003). The reef corals and constituent grains suggest that there has been little mixing within environments and that several well preserved reef facies are exposed (Pandolfi and Jackson, 2001; Pandolfi et al., 1999). Together, previous work (and this study) suggests that Curaçao fossil reefs preserve a high level of ecological integrity and will give an accurate reflection of coral reef processes that occurred within the living reef community.

METHODS

Bioerosion information was collected on the Curaçao Pleistocene (123 Ka) reef within 4 reef facies: windward reef crest, windward back reef, windward lagoon, and leeward reef flat. Two representative sites of each facies were chosen within the Hato Unit along the northwest end of Curaçao (Figures 3, 4, Table 1). The top of the Hato Unit forms the distinct Lower Terrace whose oceanward edge is marked by a sea cliff that rises from about 10 m below sea level to about 10 m above sea level. Because there is no recent reef along the windward coast (van Duyl, 1985), large waves pound the terrace, making its edge largely inaccessible. The fossil reef interior is only accessible at infrequent "bocas" that cut perpendicular to shoreline and expose cross-sectional views of the reef interior up to 100 m long in cliffs along both sides of the cut. Although bocas occur at mouths of intermittent stream channels, their origin remains a "problem" (Scheffers, 2004).

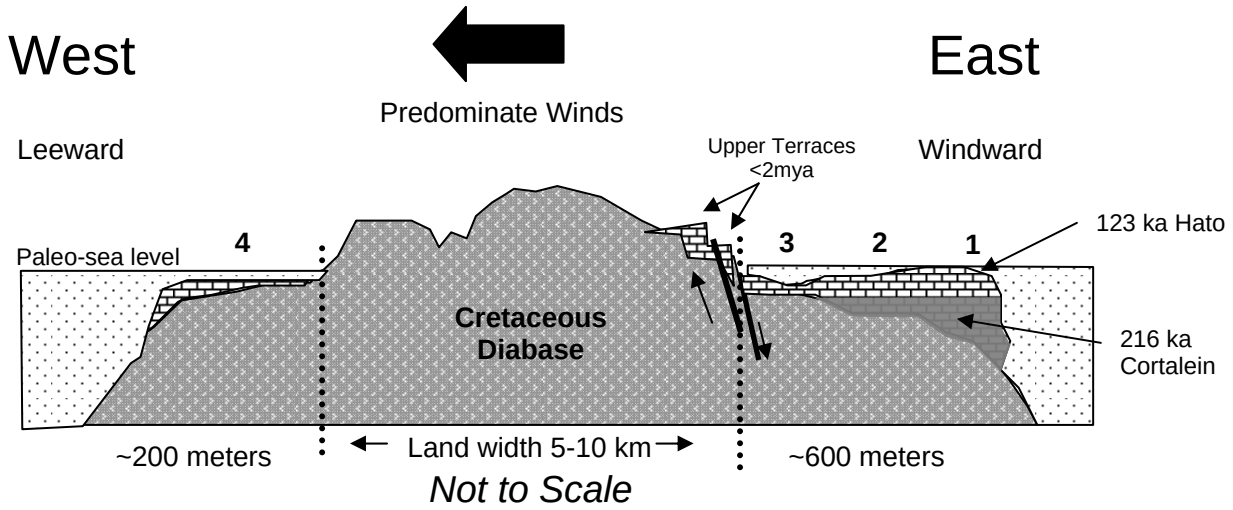

Figure 1. Generalized cross-section through the north end of Curaçao during the Pleistocene. Note that Pleistocene reefs and limestones rest on the Cretaceous volcanic bedrock in several discrete terraces. The Lower Terrace is composed of the upper Hato Unit (123 Ka) and the underlying Cortalein Unit (216 Ka). Windward reef development is far more extensive than leeward. Facies examined include 1) windward reef crest, 2) windward reef flat, 3) lagoon, and 4) leeward reef crest. Subsequent uplift has elevated the Hato Unit (and upper Cortalein) above modern sea level.

Figure 2. Pleistocene reef terraces, Curaçao. View southwest from coast, 5 km north of airport. Photograph taken from the top of Lower Terrace (123 Ka) approximately 10 m above sea level. Limestones of the Middle Terrace 1 are 400 Ka (Schellmann et al., 2004) and ages of higher terraces are poorly constrained.

Windward reef facies occur along Curaçao's eastern shore and consist of a well-developed *Acropora palmata* crest that preserves many large spectacular colonies in life position (Figure 3A). Landward of the crest is an apparently lower energy reef flat facies in which dome-shaped colonies of massive coral (i.e. *Siderastrea, Diploria, Montastrea annularis*) and large colonies of the extinct organpipe species of *Montastrea* (Pandolfi et al., 2002) are preserved (Figure 3B-D). Between the windward reef and the volcanic shoreline, lagoon deposits are sometimes preserved. These facies have a carbonate mud matrix and preserve highly encrusted coral rubble (Figure 3E). Numerous large conch (*Strombus gigas*) shells (Figure 3F) suggest ancient seagrass beds.

Leeward reef deposits are preserved on the western side of Curaçao and represent a well developed leeward reef flat containing *in situ* fine branching corals such as *Acropora cervicornis* and *Pocillopora* cf. *palmata* (Figure 3G, H), and various massive coral heads (e.g., *Diploria, Montastrea*).

In each of the reef facies, taphonomic/ bioerosion information was collected for 20 samples in each coral-form category, as limited by coral occurrence.

Growth form categories were chosen to allow comparisons between facies with different species composition. The two *Acropora* species (*A. palmata* and *A. cervicornis*) were deemed significantly different from other morphologies and were therefore examined as their own categories. For *A. palmata*, separate data was collected for upright colonies and rubble in order to examine the effect of breakage and transport on taphonomy. All *A. cervicornis* were considered to be potentially rubble because of the difficulty in determining life position for this coral. Massive corals were primarily hemispherical domes including *Diploria strigosa*, *Diploria labyrinthiformis*, *Colpophyllia natans*, *Montastrea cavernosa*, and *Siderastrea siderea*. *Montastrea annularis*, a lumpy massive species, was also included here. The branching coral category included primarily organ pipe *Montastrea* in windward sections and organpipe *Montastrea*

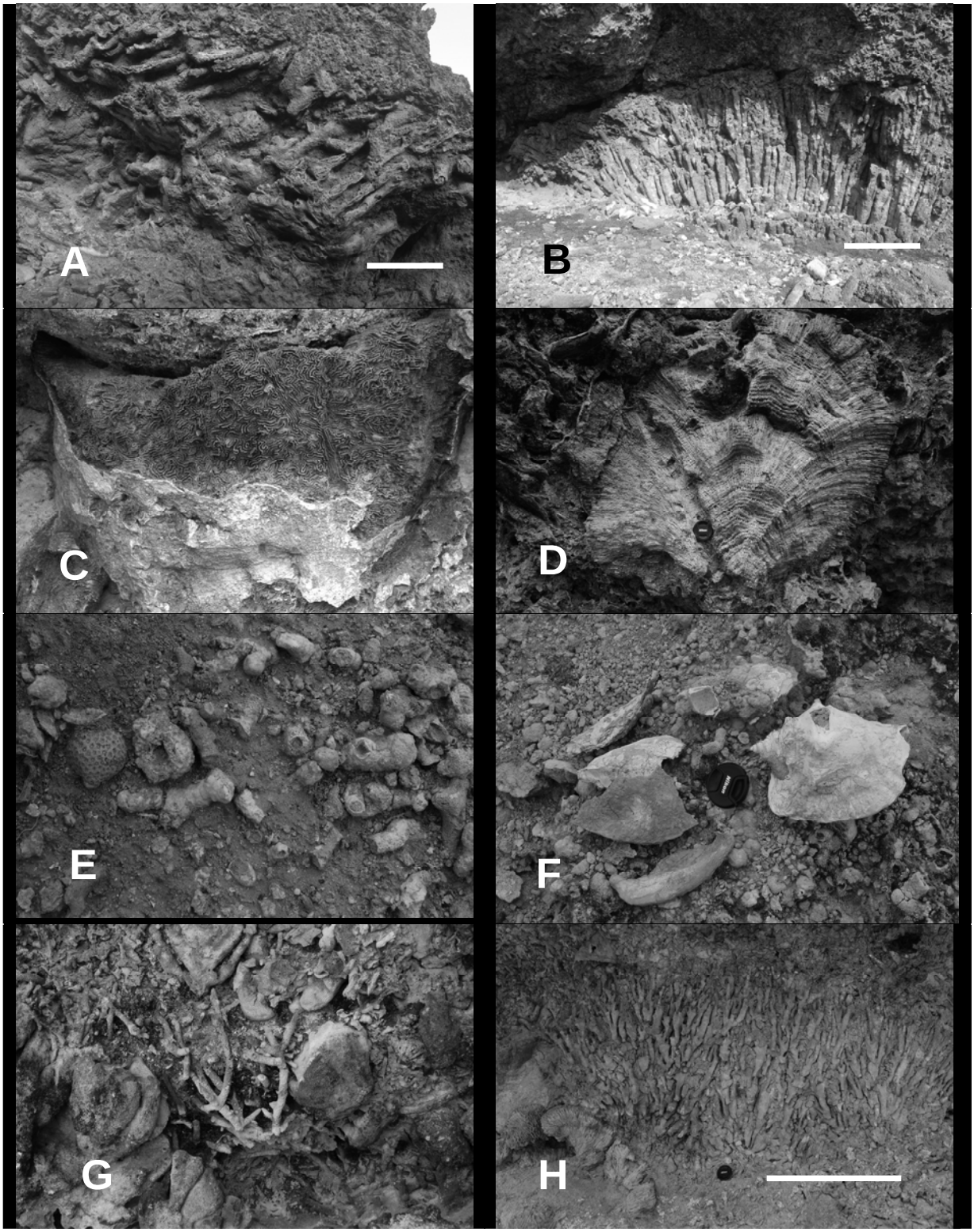

Figure 3. Examples of four Curaçao reef facies. A and B, windward reef crest facies : A) In situ A. palmata*, B) Large organ pipe* Montastrea *colony. C and D) windward back reef facies: C) Coralline algae crust on* Diploria strigosa*, D)* Montastrea annularis *with macroboring. E and F) windward lagoon/sea grass facies: E) heavily encrusted* Porites *rubble, F) Numerous* Strombus gigas*. G and H) Leeward reef flat facies. In situ* A. cervicornis *(G) and* Pocillopora *(H). Scale bar 1 m, Lens cap 7 cm.*

and *Pocillopora* in leeward sections.

At each site, a 30 m transect line was laid out horizontally on the outcrop and corals of particular growth forms were examined along the transect. If less than 20 colonies of a particular growth form were encountered, additional colonies were sought within 1 m above and below the transect, or a second transect at the same height was positioned on the opposite wall of the Boca in an effort to reach 20 colonies. Specimens of *A. cervicornis* were collected and returned to lab for analysis.

Each coral colony was first examined for its orientation in 15 degree intervals (life position = 0, on side=90). Next, the average thickness of encrustation (almost entirely by coralline algae) was recorded in mm, and the % cover of bioerosion was estimated from the cross sectional area in outcrop, and by searching the exposed colony surface. This measure is considered a minimum estimate, since encrustation and lack of exposure makes macroboring difficult to estimate in some situations. Finally, the external surface of the coral was examined for signs of pitting that could have been attributed to grazing and external bioerosion. The percent cover of the pitted or irregular surface was estimated and recorded.

Table 1. Study site with four reef facies. Letters in parentheses refer to site letters in Figure 4.

Facies	**Locality**	**Growth Forms**
WW Crest	Boca Un (C)	*A. palmata, in situ*, N=20
		A. palmata, rubble, N=20
		domes, N=20
		branching (*Montastrea*), N=20
		A. cervicornis, N=16
	Boca Degu (A)	*A. palmata, in situ*, N=20
		A. palmata, rubble, N=20
		domes, N=20
Back Reef	Boca Un (C)	branching (*Montastrea*), N=20
		domes, N=12
		A. palmata, rubble, N=20
		A. cervicornis, N=16
	Boca Degu (A)	branching (*Montastrea*), N=16
		domes, N=16
	Boca Plate (B)	*A. cervicornis*, N=20
Lagoon	Boca Mansalina (B)	*Porites, A. cervicornis*, N=10
Leeward	Punta Halvedag (F)	*A. palmata, in situ*, N=20
		A. palmata, rubble, N=24
		domes, N=23
		branching, N=13
	Playa Lagun (E)	*A. palmata*, rubble, N=22
		domes, N=20
		branching, N=21
	Wamaloa (D)	*A. cervicornis*, N=15

In the lab, *A. cervicornis* specimens were assigned a taphonomic grade based on their surface texture (5= pristine, 4= corallite collars present, 3= corallite collars mostly gone, surface texture more or less smooth, cylindrical, 2= corallum wall eroded/pitted on one side, 1= pitting on more than one side). Specimens were then cross-sectioned in three cuts and the average percent of skeleton missing was recorded. Maximum thickness of encrustation (coralline algae) was also measured in cross-section and considered a minimum estimate, since encrustation and lack of exposure makes macroboring difficult to estimate in some situations. Finally, the external surface of the coral was examined for signs of pitting that could have been attributed to grazing and external bioerosion. The percent cover of the pitted or irregular surface was estimated and recorded.

Figure 4. Study sites along northwest end of Curaçao. Letters refer to sites in Table 1.

RESULTS

Colony Orientation

80-94% of coral colonies in windward and leeward reef settings were preserved in upright position (Figure 5). The high *in situ* rate-for corals was true for massive coral heads and large branching colonies such as organ pipe *Montastrea*. Even examples of *in situ* vertically oriented *A. cervicornis* were seen in outcrop (Figure 3G).

Encrustation

Encrustation by coralline algae was the rule at all sites (Figure 6). More than 80% of the colonies of most coral types were encrusted with coralline algal crusts between 3 and 10 mm (Figure 7). The exception was *in situ A. palmata* colonies in the reef crest zone that were coated, on average, by crusts 30-40 mm thick. Rubble from *A. palmata* and *A. cervicornis* were not more heavily encrusted than in *in situ* colonies.

One interesting result of the intense encrustation of most corals is that in some settings the coralline crust is better preserved than the coral and at times the coral itself has been lost. In these cases the coral's presence can be inferred from the encrusting algae's internal surface which is in effect an internal mold of the coral surface (Figure 8). This effect is termed bioimmuration (Taylor, 1990).

Boring

Most coral substrates examined did not have extensive boring bioerosion (Figure 9). Less than 20% of specimens of most facies and growth forms showed any boring, and most specimens that were bored had less than 10% bioerosion. The highest incidence of boring occurred in *A. palmata* rubble, and the least occurred in branching corals.

A. cervicornis rubble, measured in cross-section also showed a relatively high incidence of boring bioerosion (Figure 10), although rates of bioerosion were low (<10%).

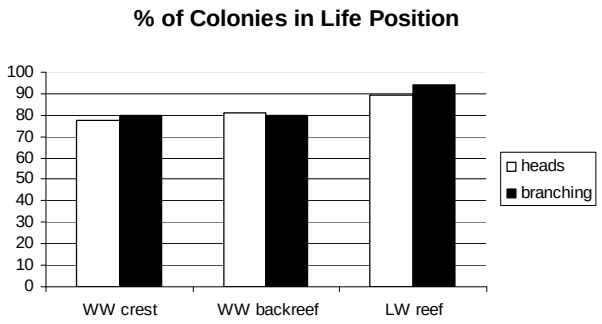

Figure 5. Orientation of massive coral heads and branching colonies. Very few were toppled, suggesting little storm reworking.

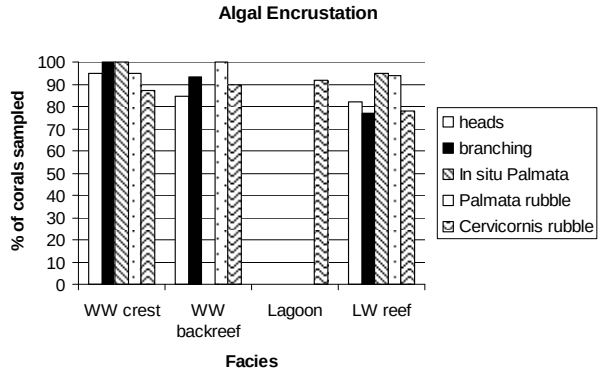

Figure 6. Percentage of coral colonies of various types that were encrusted with coralline algae. In all environments, most substrates were encrusted.

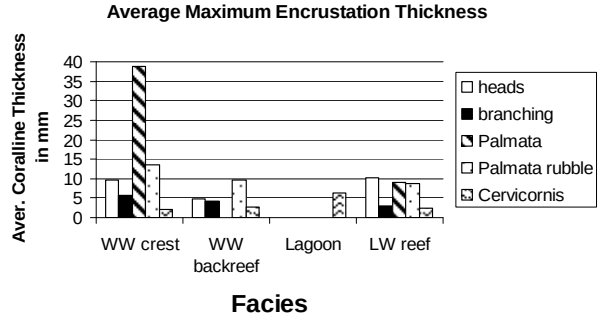

Figure 7. Algal thicknesses on various substrates and in various facies. Thicknesses (in mm) are the average of the maximum thicknesses of each coral piece.

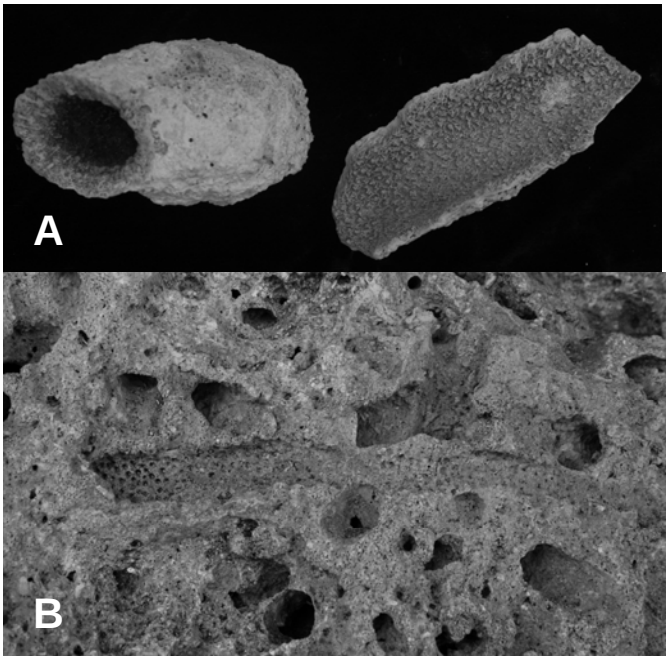

Figure 8. Examples of bioimmuration. A) Coralline algal ring remaining after A. cervicornis *is dissolved (left), inside view of ring showing impressions of corallite necks (right). B) Impression of* A. cervicornis *left in coralline algae in the outcrop.*

External Bioerosion

There was little evidence for the removal of the outer wall of the coral colonies as would be expected through scraping and biting during grazing or physical abrasion. The incidence of pitting of the external coral wall was low (< 20%, Figure 11). *In situ A. palmata* were the least pitted and leeward coral heads had the greatest frequency of pitting, although even here the pitting was generally over only a small proportion of the coral surface.

Taphograde analysis of *A. cervicornis* also suggests a low incidence of grazing (Figure 12). Grades 4 and 5 preserve the fragile corallite collars and thus indicate little external bioerosion. Grade 3 likewise shows some original surface texture and contains no pitting of the surface. Grades 1 and 2 indicate external erosion from either biological or physical (e.g., abrasion) processes. The greatest incidence of pitting is 40% in the windward reef crest setting,

and the least is in the lagoon where heavy coralline encrustation apparently limited external bioerosion.

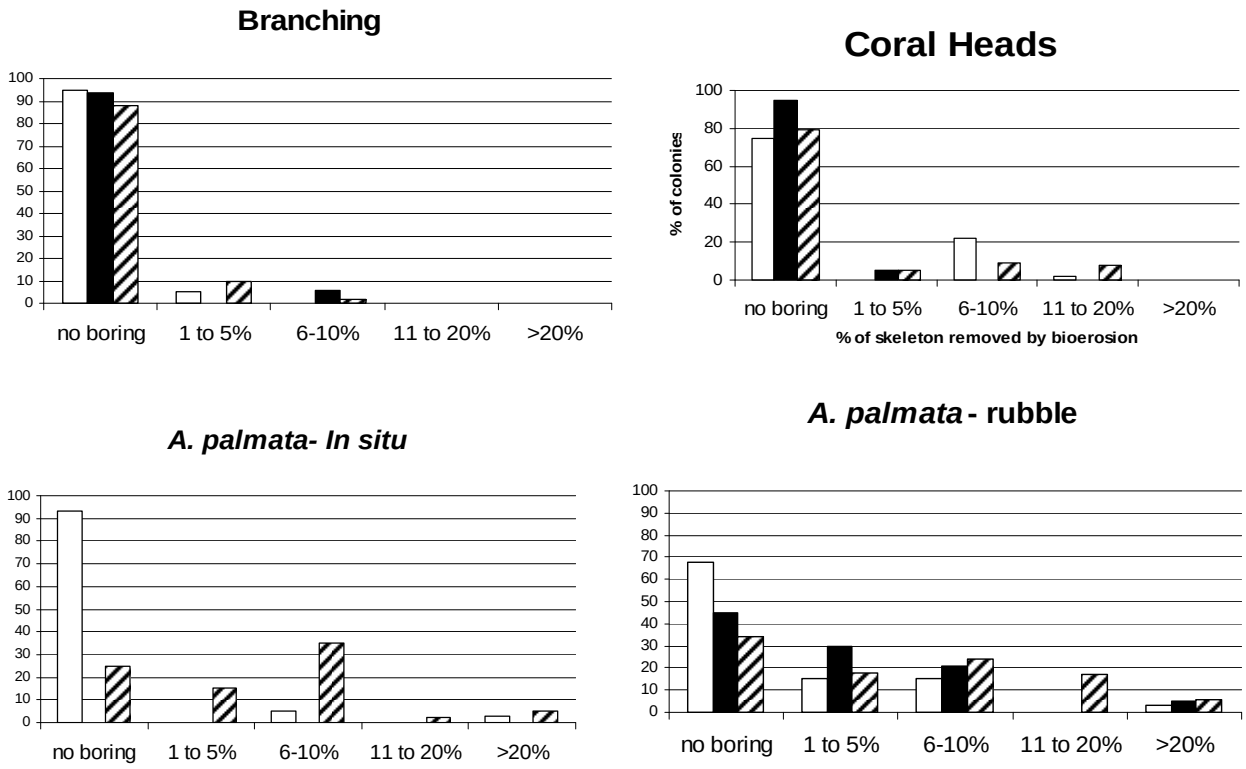

Figure 9. Boring incidence and intensity in various growth forms and facies. White bars are windward reef crest, black bars are windward back reef, and striped bars are leeward reef. Most branching and head colonies have > 80% of specimens without evidence of internal boring. Those that were bored typically had <10% bioerosion. A. palmata *rubble had a higher incidence of bioerosion, but it was still low.*

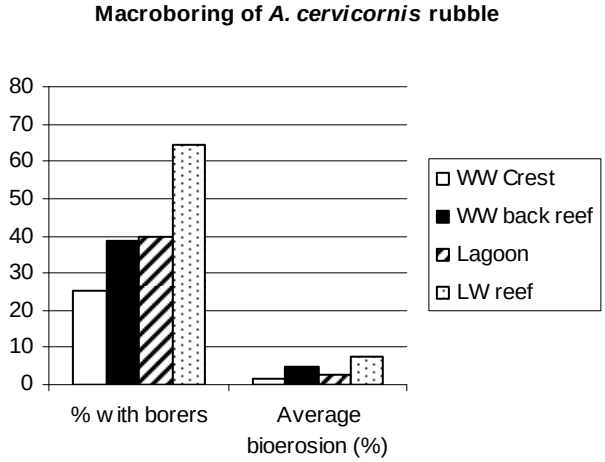

Figure 10. Boring in A. cervicornis *rubble, examined in cross-section. Rubble from leeward reefs had a greater incidence of boring than other facies, but the % of bioerosion was <10% in all facies.*

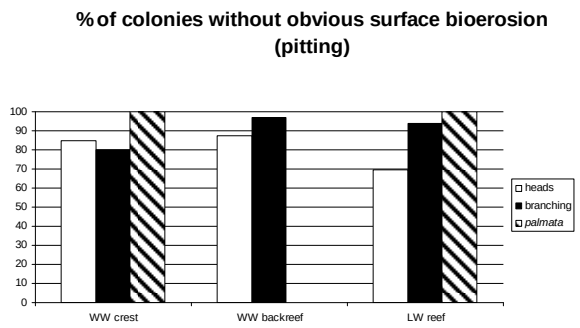

Figure 11. Incidence of external bioerosion on in various substrates and facies.

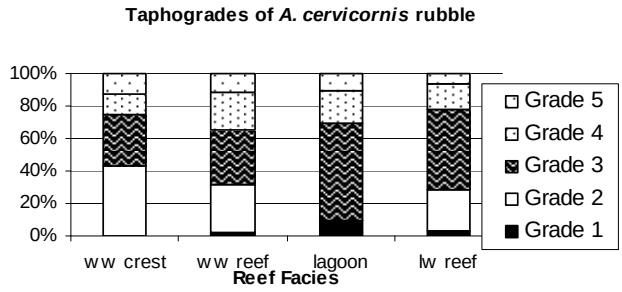

Figure 12. Taphograde analysis of A. cervicornis rubble. Grades 3-5 (pristine) preserve surface texture and indicate little external bioerosion.

DISCUSSION

Little external (grazing) erosion of most coral colonies was evident from the low incidence of surficial pitting and the preservation of fine corallite morphology (e.g., the thin tubes of *Acropora* polyps). This data, coupled with the near ubiquitous encrustation by coralline algae suggest that grazing bioerosion was rare in Curaçao Pleistocene reefs.

Possible explanations for why these results are apparently at odds with the results of most experimental studies may include the loss of grazing evidence in the fossil record, differences in setting from previous studies, and an over-estimation of the importance of grazing bioerosion in previous experimental studies.

Geological Biases

It is unlikely that the Curaçao Pleistocene provided a highly biased measure of grazing excavation because the coral surfaces were so well preserved. Post-mortem reworking, burial, and diagenesis may all degrade coral surface texture, creating a potential taphonomic bias towards greater, not lesser, external bioerosion. In addition, although external scraping can destroy the evidence of previous grazing bioerosion, the lack of highly bored surfaces suggests that substrates were not reduced in size until ultimately being removed from the fossil record.

Some types of grazing bioerosion are more difficult to evaluate and will probably be generally overlooked in fossil studies. For example, many parrotfish take bites of live coral skeleton, and this bioerosion is rapidly masked by coral regeneration (Henry and Hart, 2005). The magnitude of this type of external bioerosion has not been quantified but is expected to be small since corallivory by Caribbean parrotfish is less than 10 bites/m^2/day, and makes up generally <1% of parrotfish bites (Rotjan and Lewis, 2006).

Bioerosion of coralline algae crusts is also difficult to evaluate in the fossil record. While the net rate of coralline algal growth on the reef was positive, this does not imply an absence of algal grazing; parrotfish and echinoids would certainly remove some of the gross coralline algae production. While it is possible to evaluate coral bioerosion in fossil studies, it is difficult or impossible to estimate bioerosion of coralline algae or other secondary substrates in fossil studies.

Importance of Grazing Bioerosion

Low rates of grazing in this fossil study could simply reflect that the living reef had a very high proportion of live coral cover, and most external bioeroders (with the exception of some parrotfish, as mentioned above) scrape substrates other than live coral. On the other hand, the high incidence and thickness of coralline algae encrustation on corals in all

environments suggest that the colonies were exposed for a period of time prior to burial. The absence of substantial grazing during that interval requires a different explanation. I suggest that grazing is less important than has been generally reported.

The presumed high importance of grazing vs. boring bioerosion can be attributed to studies that took cut blocks of *Porites* and fastened them to hard reef substrates and monitored the experimental blocks through time (e.g., Kiene and Hutchings, 1994; Chazottes et al., 1995; Pari et al., 1998). Studies that have used more natural substrates have received less attention but have found that boring, rather than grazing, is generally greater. For example, naturally killed acroporid colonies showed little evidence of external bioerosion after 9 months, except for what was attributed to wave breakage in fragile plate colonies (Musso, 1992). Coral bleaching has also provided "natural" experiments of bioerosion of entire coral colonies. Results from Belize (Lescinsky, 2004) and the Indian Ocean (Sheppard et al., 2002; Zahir, 2002; Schuhumacher et al., 2005) have found boring to be intense after 1-5 years, and that coralline encrustation, rather than surficial erosion was observed.

It is unclear why cut-block and "natural" bioerosion studies have yielded such different results, although differences in the type of substrates examined may play a part. Whereas "natural" studies have focused primarily on branching colonies and coral rubble, the cut-block studies have focused on reef framework independent of individual coral colonies. This study, however, examined various coral growth forms in several different shallow facies and found few differences, suggesting that the observed patterns were generally applicable across the Pleistocene reef. Deeper reef zones were not preserved, but can be expected to have had even lower rates of grazing bioerosion, based on the well-documented trend towards decreasing grazing bioerosion with depth (e.g., Kiene and Hutchings, 1994; Bruggemann et al., 1996).

It is possible that cut-block studies overestimate grazing bioerosion because they focus on a type of substrate that is relatively rare on the reef--a clean, dead, immobile hard surface. While such surfaces do occur on reefs (e.g., a single freshly bleached coral head), they are probably not the norm. When these types of substrates occur *en mass*, as during a regional bleaching event, the extensive area of available substrate may overwhelm grazers leading to a prevalence of encrustation and ultimately boring (Sheppard et al., 2002; Lescinsky, 2004).

In reefs with high live coral cover, such as the Pleistocene reef in this study, it is probable that much of the coral death occurs in lower, older parts of the colony that are shaded and experience higher sedimentation. Although no studies have quantified bioerosion in the coral understory vs. exposed flat surfaces, several observations suggest that grazing bioerosion in crypts is minimal. For example, bioeroding sea urchins are most common on partially alive coral colonies and are absent from patches of rubble and fine sediment (Bak, 1990) and in parrotfish, bioerosion rate is strongly tied to fish size. Smaller parrotfish that might be better able to reach reef recesses account for little to no bioerosion until an ontogenetic diet shift around 20 cm in length for common Caribbean species (Bruggemann et al., 1996). Larger individuals have more frequent, deeper bites and are responsible for most of the bioerosion, but are limited to feeding on more open surfaces.

Macroboring Bioerosion

Macroboring bioerosion, in contrast, will be favored in more cryptic settings, where early recruits are not scraped away. The rates of bioerosion noted in this study (generally <10%) are comparable to annual rates previously reported for bioerosion studies of entire reef corals (e.g., 8%, Lescinsky, 2004; 4-14%, Zahir, 2002, 1-8%, Musso, 1992), and are also within the range of natural macroboring rates reported on reef substrates in different environments where macroboring intensity has been shown to be related to productivity and burial (e.g., Risk et al., 1995; Holmes et al., 2000; Lescinsky et al., 2002). The observed rates of bioerosion, are

comparable to those on modern reefs and substrates that have been exposed for about a year.

Are Curaçao Reefs Unusual?

Curaçao reefs are unusual in their ecological integrity. Unlike many reefs that are composed primarily of stabilized rubble (Blanchon et al., 1997), the Curaçao reefs are composed largely of in place coral colonies with little breakage. In addition, Curaçao reefs probably had very high rates of live coral cover, judging from corallite surface texture, although this deserves further quantification--perhaps using microborer assemblages as markers of post mortem exposure.

High live coral cover in the Pleistocene reef is at odds with current reef conditions throughout most of the Caribbean, that is due in part to recent anthropogenic causes (Gardner et al., 2003). Sea-level transgression during the Pleistocene also would have contributed to rapid reef accretion and perhaps to overall live coral cover, although in recent reefs, live coral cover is dependent on physical disturbance and ecological factors (e.g., bioerosion) that would have functioned independent of the rate of sea-level rise.

CONCLUSIONS

Pleistocene coral reefs of Curaçao are unusually intact ecologically and form a good basis for evaluating external bioerosion from grazers in the fossil record. The data presented here show that grazing bioerosion in each of the four coral types and four facies examined was low, while boring bioerosion was comparable to that described on modern reefs. Previously observed high rates of grazing bioerosion in modern studies is in part a design bias and in part reflects anthropogenic changes to live coral cover in modern reefs. Low grazing, as observed in the Curaçao Pleistocene reef is probably a reflection of normal bioerosion patterns in a healthy (high percentage live coral cover) reef.

ACKNOWLEDGMENTS

I thank Adophe Debrot and the rest of the CARMABI Staff for logistical support in Curaçao and Otterbein College's White Fund, and Sabbatical-Leave Program for funds to conduct this research.

REFERENCES

Bak, R.P.M., 1990, Patterns of echinoid bioerosion in two Pacific coral reef lagoons: Marine Ecological Progress Series, v. 66, p. 267-272.

Blanchon, P., Jones, B., and Kalbfleisch, W., 1997, Anatomy of a fringing reef around Grand Cayman: storm rubble, not coral framework: Journal of Sedimentary Research, v. 67, p. 1-16.

Bries, J.M., Debrot, A.O., and Meyer, D.L., 2004, Damage to the leeward reefs of Curaçao and Bonaire, Netherlands Antilles from a rare storm event: Hurricane Lenny, November 1999: Coral Reefs, v. 23, p. 297-307.

Bruggemann, J.H., van Kessel, A.M., van Rooij, J.M., and Breeman, A.M., 1996, Bioerosion and sediment ingestion by the Caribbean parrotfish *Scarus vetula* and *Sparisoma viride*: implications of fish size, feeding mode, and habitat use: Marine Ecological Progress Series, v. 134, p. 59-71.

Buisonjé P.H. de, 1974, Neogene and Quaternary Atlas of Aruba, Curaçao, and Bonaire (Netherlands Antilles): Foundation for Scientific Research in Surinam and the Netherlands Antilles, v. 78, Utrecht, 291 p.

Chazottes, V., LeCampion-Alsumard, T., and Peyrot-Clausade, M., 1995, Bioerosion rates on coral reefs: interactions between macroborers, microborers, and grazers (Moorea, French Polynesia): Palaeogeography, Palaeoclimatology, Palaeoecology, v. 113, p. 189-198.

Gardner T.A., Cote, I.M., Gill, J.A., Grant, A., and Watkinson, A.R., 2003, Long-term region-wide declines in Caribbean corals: Science, v. 301, p. 958-960.

Henry, L.A., and Hart, M., 2005, Regeneration from injury and resource allocation in sponges and corals- a review: International Review of Hydrobiology, v. 90, p. 125-158.

Holmes, K. E., Edinger, E., Hariyadi, Limmon, H.G., and Risk, M.J., 2000, Bioerosion of live massive corals and branching coral rubble on Indonesian coral reefs: Marine Pollution Bulletin, v. 40, p. 606-617.

Kiene, W.E., and Hutchings, P.A. 1994, Bioerosion experiments at Lizard Island, Great Barrier Reef: Coral Reefs, v. 13, p. 91-98.

Lescinsky, H.L., 2004, Bioerosion in the Caribbean: using coral bleaching as a natural experiment, *in* Lewis, R.D., and Panuska, B.C., eds. Proceedings of the Eleventh Symposium on the Geology of the Bahamas and other Carbonate Regions: San Salvador, Bahamian Field Station, p. 25-34.

Lescinsky, H.L., Edinger, E., and Risk, M., 2002, Mollusc shell encrustation and bioerosion rates in a modern epeiric sea: taphonomy experiments in the Java Sea, Indonesia: Palaios, v. 17, p. 171-191.

Meyer, D.L., Bries, J.M., Greenstein, B.J., and Debrot, A.O., 2003, Preservation of *in situ* reef framework in regions of low hurricane frequency: Pleistocene of Curaçao and Bonaire, southern Caribbean: Lethaia, v. 36. p. 273-286.

Musso, B.M., 1992, Rates of skeletal degradation following death in three species of *Acropora*: Proceeding of the Seventh International Coral Reef Symposium, Guam, v. 1, p. 413-418.

Neumann, A. C., 1966, Observations on coastal erosion in Bermuda and measurements of the boring rate of the sponge, *Cliona lampa*: Limnology and Oceanography, v. 11, p. 92-108.

Palmer. T., and Plewes, C., 1993, Borings and bioerosion in fossils: Geology Today, v. 9, p. 138-142.

Pandolfi, J.M., Llewellyn, G., and Jackson, J.B.C., 1999, Pleistocene reef environments, constituent grains, and coral community structure: Curaçao, Netherlands Antilles: Coral Reefs, v. 18, p. 107-122.

Pandolfi, J.M., and Jackson, J.B.C., 2001, Community structure of Pleistocene coral reefs of Curaçao, Netherlands Antilles: Ecological Monographs, v. 71, p. 49-67.

Pandolfi, J.M., Lovelock, C.E., and Budd, A.F., 2002, Character release following extinction in a Caribbean reef coral species complex: Evolution, v. 56, p. 479-501.

Pari, N., Peyrot-Clausade, M., LeCampion-Alsumard, T., Hutchings, P.A., Chazoootes, V., Golubic, S., LeCampion, T., and Fontaine, M.F., 1998, Bioerosion of experimental substrates on high islands and atoll lagoons (French Polynesia) after two years exposure: Marine Ecology Progress Series, v. 166, p. 119-130.

Perry, C.T., 1996, Distribution and abundance of macroborers in an upper Miocene reef system, Mallorca, Spain: Implications for reef development and framework destruction: Palaios, v. 11, p. 40-56.

Perry, C.T., 2000, Macroboring of Pleistocene coral communities, Falmouth Formation, Jamaica: Palaios, v. 15, p. 483-491.

Risk, M. J., Sammarco, P. W., and Edinger, E. N., 1995, Bioerosion in *Acropora* across the continental shelf of the Great Barrier Reef: Coral Reefs, v. 14, p. 79-86.

Rotjan, R.D., and Lewis, S.M., 2006, Parrotfish abundance and selective corallivory on a Belizean coral reef: Journal of Experimental Marine Biology and Ecology, v. 335, p. 292-301.

Scheffers, A., 2004, Tsunami imprints on the Leeward Netherlands Antilles (Aruba, Curaçao, Bonaire) and their relation to other coastal problems: Quaternary International, v. 120, p. 163-172.

Schellmann, G., Radtke, U., Scheffers, A., Whelan, F., and Kelletat, D., 2004, ESR dating of coral reef terraces on Curaçao (Netherlands Antilles) with estimates of younger Pleistocene sea level elevations: Journal of Coastal Research, v. 20, p. 947-957.

Schuhmacher, H., Loch, K., Loch, W., and See, W.R., 2005, The aftermath of coral bleaching on a Maldivian reef- a quantitative study: Facies, v. 51, p. 80-92.

Sheppard, C.R.C., Spalding, M., Bradshaw, C. and Wilson, S., 2002, Erosion vs. recovery of coral reefs after 1998 El Nino, Chagos Reefs, Indian Ocean: Ambio, v. 31, p. 40-48.

Taylor, P. D., 1990, Preservation of soft-bodied and other organisms by bioimmuration a review: Palaeontology, v. 33, p. 1-17.

van Duyl, F.C., 1985, Atlas of living reefs of Curaçao and Bonaire (Netherlands Antilles). Foundation for Scientific Research in Surinam and the Netherlands Antilles, 117, Utrecht, 37 pp.

Vogel, K., Golubric, S., Brett, C.E., 1987, Endolith associations and their relation to facies distribution in the Middle Devonian of New York State, USA: Lethaia, v. 20, p. 263-290.

Weidlich, O., 1996, Bioerosion in Late Permian Rugosa from reefal blocks (Hawasina Complex, Oman Mountains): Implications for reef degradation: Facies, v. 35, p. 133-142.

Zahir, H., 2002, Assessing bioerosion and its effect on reef structure following a bleaching event in the Maldives, *in* Linden, O., Souter, D., Wilhelmsson, D., and Obura, D., Coral Degradation in the Indian Ocean, Status Report 2002, CORDIO: Department of Biology and Environmental Science, University of Kalmar, Sweden, p. 135-138.

INTEGRATING FIELD EXPERIENCES IN ENVIRONMENTAL SCIENCE AND COMMUNITY SERVICE: LESSONS LEARNED FROM SAN SALVADOR, BAHAMAS

Deborah Freile
Department of Geoscience
New Jersey City University
Jersey City, NJ 07305
Dfreile@NJCU.edu

Melanie DeVore
Department of Biological and Environmental Sciences
Georgia College & State University
Milledgeville, GA 31061

ABSTRACT

Environmental science courses are an attractive option for infusing science across disciplines and within the context of a cross-cultural experience. San Salvador Island, Bahamas, is an ideal site to engage students in all aspects of environmental science. It is a small, remote outer island with a population of roughly 900--located away from the large population centers and heavy tourist areas of New Providence and Grand Bahama Islands. However, San Salvador is not immune from development, and one of the goals of this course is to focus on teaching concepts of sustainable resource utilization to students from the United States as well as from San Salvador. There are several case studies based on recent construction projects on the island where students can apply basic geological principles, while assessing short term and long term gains and losses these facilities provide the community.

In this contribution, we provide examples from our respective environmental science courses illustrating the use of case studies, including pertinent background information and student exercises and assessment. Because service learning is becoming an integral part of undergraduate curricula, we provide examples of service learning activities that we have integrated into our courses. Finally, we provide an example of course outcomes and assessment criteria used for environmental science courses.

INTRODUCTION

The Course

Environmental Science encompasses a number of fields within the natural and social sciences (Figure 1). A course in environmental science taught on San Salvador Island (Figure 2) is by nature a field-oriented course that emphasizes human impacts on the fragile tropical reef and carbonate island ecosystems. This course is a combination of evening lectures and site visits during the mornings and afternoons. The course is often "front loaded"; that is, it demands writing assignments based on papers and reports from students before departing to the island.

In this paper, we present some of the exercises we have used in our courses, along with applicable background content regarding several environmental issues used in class. It is our objective to not present a detailed, scholarship of the teaching and learning approach, but rather to provide a set of activities and issues that faculty from other institutions could extract and use in their own classes.

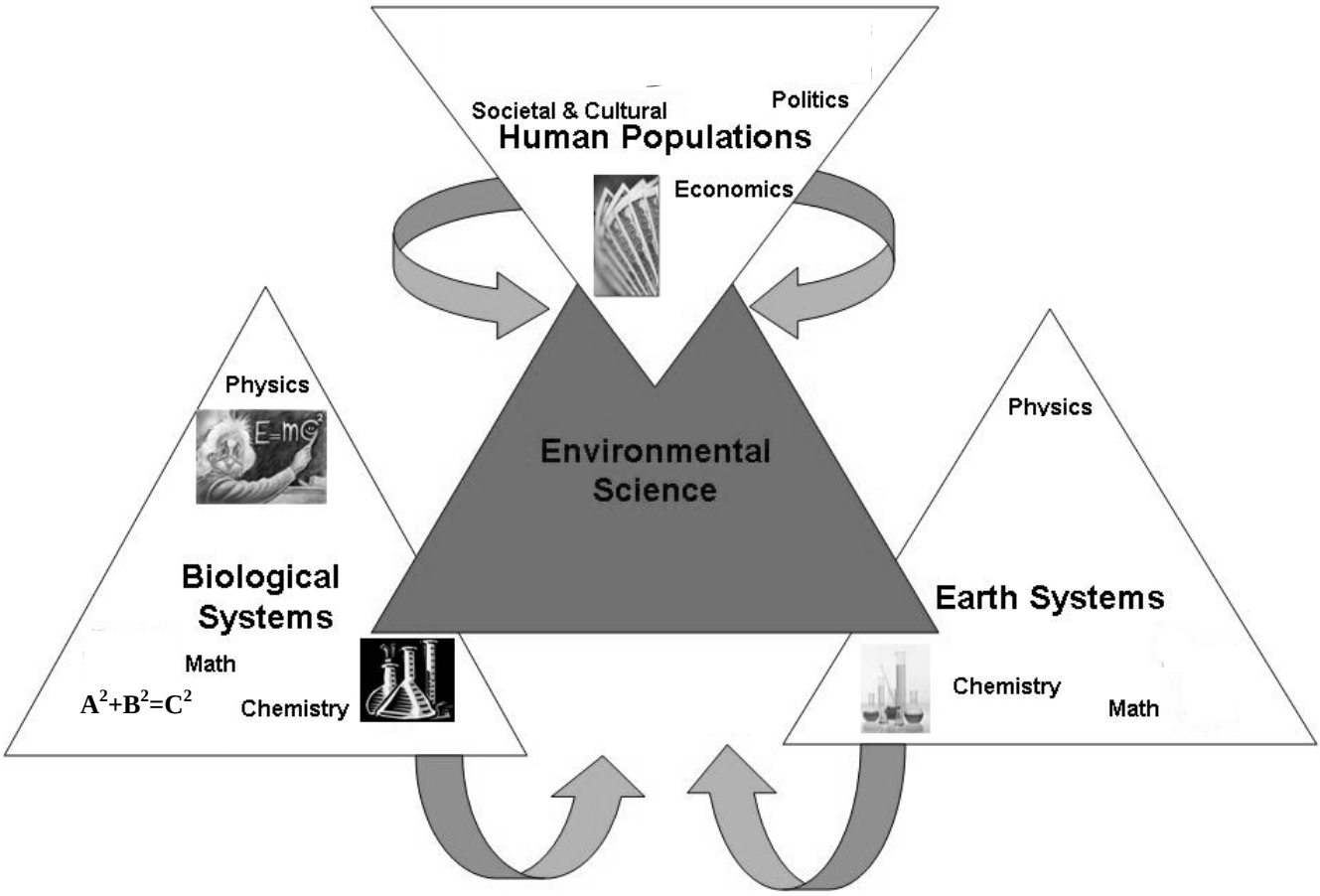

Figure 1. Interrelationships of fields that constitute Environmental Science.

Location and Environmental Issues

The course is held at the Gerace Research Centre (GRC), a former U.S. Navy submarine tracking station on San Salvador Island (Figure 3), Bahamas. The GRC is a well-known marine field station that provides housing and prepared meals for students, excellent laboratory and teaching facilities, and field vehicles. There are a number of sites (Figure 3) that are ideal for illustrating a wide range of environmental issues.

The Bahamas Environment, Science & Technology Commission (BEST) manages the implementation of multilateral environmental agreements and reviews environmental impact assessments and environmental management plans for development projects within The Bahamas. BEST conducted a survey on 13 Family Islands to determine environmental issues as part of the National Capacity Needs Self Assessment Project (2004). The following issues where identified on San Salvador:

1) Lack of emergency infrastructure for fires
2) Poaching
3) Sand mining
4) Lack of safe disposal methods for medical wastes, motor oils and other hazardous household wastes
5) Stability and impact of the new seawall

6) Destruction and/or deterioration of historical sites
7) Lack of disposal options for sewage sludge
8) The unfinished marina and its destruction of the groundwater lens

Surprisingly, freshwater availability was not listed as a major environmental issue for San Salvador in this study.

Figure 2. Map of the Bahamas showing location of San Salvador, a 15km by 8km eastern most island of the Bahamian archipelago. (From: http://www.unesco.org/csi/pub/papers/gerace.htm)

COURSE STRUCTURE

The environmental science courses offered by both authors utilize many different resources and methodologies to make it an enriching and integrative experience:

1) The island and its residents--the students benefit the most from experiencing the sites and people of the island
2) Lectures covering principles needed to understand environmental issues pertaining to the island
3) Documents and reports available on government and non-governmental organization websites
4) Guest lecturers (i.e. fellow colleagues at the station);
5) Field notebooks
6) Debriefing sessions
7) Outreach and service learning activities

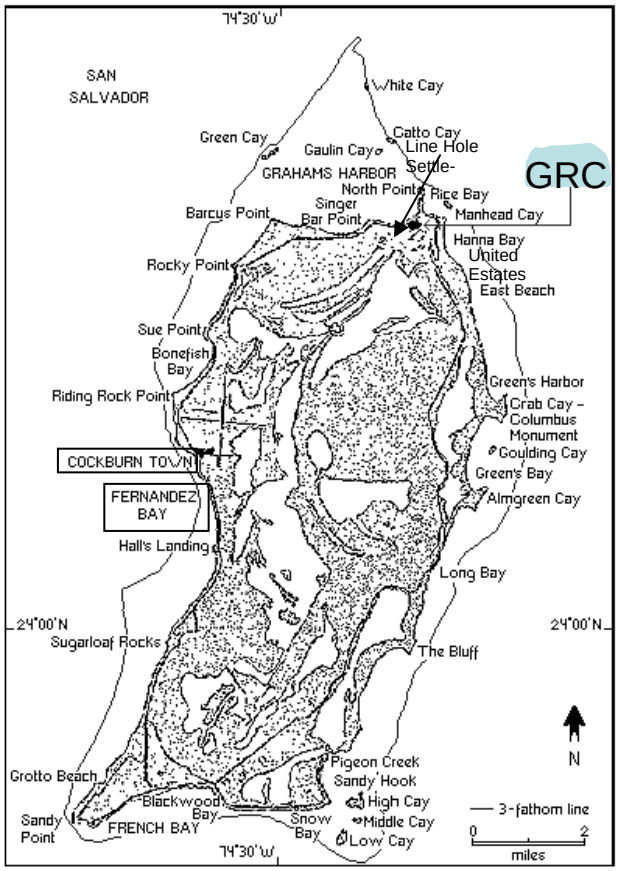

Figure 3. Map of San Salvador showing areas of interest-including Gerace Research Centre, United Estates, Landfill, East Beach, Line Hole Settlement, Riding Rocks, Cockburn Town and Fernandez Bay (modified from http://www.unesco.org/csi/pub/papers/gerace.htm)

Students are provided with readings and lectures on various topics, including coastal processes, groundwater resources and karst geology and geomorphology. Evaluation is based

on responses to questions using sound geological principles and integration of the human dimension of environmental issues covered in the course. Open-ended essay questions are used as a tool to determine student competence in the following skill areas: 1) presentation of accurate scientific content; 2) application of scientific principles to environmental issues; 3) ability to generate multiple "solutions" to an issue; 4) evaluation of potential solutions and selection of one to employ; 5) ability to estimate human responses and factors that could deter employing the "best" practice, and 6) ability to communicate orally and in writing.

Case Study 1: Background on Coastal Erosion Issues

Students learn the basic concepts of coastal processes and the impacts of hurricanes and storm surges on shorelines. They are also taught three approaches to controlling coastal erosion: 1) hard stabilization (i.e. seawalls, groins, jetties); 2) soft stabilization (i.e. beach re-nourishment) and 3) relocation, the approach favored by many coastal geologists (e.g. Orrin Pilkey *Living with the Shore Series*), but not always a feasible one for an island community where area for road placement is extremely limited.

Economics. The Queen's Highway is the major and only road accessible to the entire island and is vital for commerce and transportation on San Salvador. As such, it needs to be protected from the effects of coastal erosion. To do so, a seawall capable of withstanding hurricane-force winds and storm surges needs to be built and maintained on parts of the island to ensure that slumping and undercutting does not damage the roadway and disrupt transportation. The 'new' seawall, which is really more of a bulkhead (a relatively low wall designed to hold land) was built in 2004 after Hurricane Floyd hit the island in 1999. This construction effort was the result of a $21 million loan to the Bahamas in March, 2001 by the Inter-American Development Bank for the reconstruction and rehabilitation of infrastructure in the Family Islands (anonymous, 2001). Additionally, the then-Minister of Agriculture, His Excellency Alfred Gray (2001), mentioned in a speech given to the Food and Agriculture Organization of the United Nations in 2001, "Damages to boats, bridges, docks, seawalls, warehouses and electrical supplies limited our ability to import, store and transport food effectively. Moreover, funds which were earmarked for national development in other areas had to be diverted to rebuilding, repairing and reconditioning infrastructure, including seawalls, roads, storage buildings, and restoring electricity and other communication systems".

Seawalls; Help or Hindrance. A report (USACOE, 2004) based on a study by the Organization of American States entitled *The Bahamas National Report Integrating Management of Watersheds and Coastal Areas in Small Island Developing States (SIDS) of the Caribbean,* stated that "in some cases, waves overtopping the sea defenses caused shoulder and road washouts on the landside of the seawall. The conditions worsened as the seawalls acted as a barrier to the wave surges returning to the ocean. Waves and surges also caused erosion and destruction of the natural vegetation cover." In other words, the seawalls were more of a hindrance than a help to the islands.

Student Involvement and Reflection. Given this information, students are asked to carefully observe and compare the seawall in Cockburn Town with the wall located south along Fernandez Bay. Classes stop at several points along the seawall and are asked to describe its condition at Cockburn Town (Site 1) (Figure 4), Bamboo Point (Site 2) (Figure 5) and Fernandez Bay (3-5) (Figure 6). After careful observations and reflection, students assess the effectiveness of the seawall. In their field notebooks, they respond to the following questions related to where they see slumping, potential for road washouts and the destruction of dune vegetation.

Students also compare seawall and coastal protections measures between San Salvador Island and their own state (Georgia or New Jersey). The students are told to compare the use of seawalls in the United States to San Salvador, specifically addressing the following questions.

- Are there cases where seawalls are effective? If yes, describe the circumstances?
- Can you think of any examples of carbonate dominated beaches (think Florida Keys) where seawalls have been used?
- Why can't carbonate coastal environments be managed the same way as clastic, terrigenous beaches?

Figure 4. Seawall at Cockburn Town looking northward toward the radio towers and Catholic Church. Beachrock is in foreground .

Figure 5. Broken seawall near Rocky Point.

Figure 6. Seawall at Fernandez Bay looking south. Queens' Highway is on left. White poles demarcate the wall edge.

Case Study Two:
Water Use History for San Salvador Island

In this exercise, students are provided with a timeline describing the water resource use on San Salvador Island since the 1950's. This information is based on an April 28, 2006 – address by Bradley B. Roberts M.P., Minister of Works and Utilities, who outlined freshwater availability on the island during the contract signing ceremony for the water main extension into United Estates. The title of his presentation was *Water Relief for San Salvador* (2006a). The information about water usage on the island is summarized below:

1) 1955, 1967, 1971, 1972, and 1974 - groundwater surveys found freshwater sources scarce or lacking. Freshwater sources for the island were recognized at Cockburn Town airfield; the region near the development of Columbus Landing; and smaller bodies near Hard Bargain and Line Hole Settlement.

2) Late 1970's - A line of wells was installed on the north side of Cockburn Town airfield; the wells and the old catchment basin near the airport were used as water sources for Cockburn Town and nearby areas.

3) 1988 - some test drilling performed to explore for additional freshwater resources.

4) 1989 - installation of a well field and distribution system in Line Hole Settlement area to provide water for United Estates.

5) Approximately 1990, Bahamian Government agrees to enlarge the airstrip and create a water supply (>90,000 gallons/day) to encourage Club Med to make a major investment in San Salvador Island.

6) 1992 - After the airfield is constructed, groundwater resources are capable of producing a maximum of 80,000 gallons/day. Club Med, Cockburn Town and North Victoria Hill's water needs cannot be supported in a sustainable way, resulting in gross over pumping.

7) 1990's - The freshwater lens continues to be compromised and the salinity of both Cockburn Town's and United Estates' water rapidly increases becoming non-potable.

8) 2005 - Aqua Design Bahamas Limited (now GE) signs an agreement with the Corporation to provide water produced by reverse osmosis in a plant located in Cockburn Town well field. The plant is currently producing approximately 120,000 gallons/day.

9) 2006 - An agreement with Mr. Ian Greene (San Salvador Island) and his company Big N' Better to install some 12000 ft of 6 inch PVC pipe to connect the reverse osmosis water in North Victoria Hill to the system that serves United Estates is signed in April. The PVC pipes are slated to arrive on San Salvador before the end of May. Projected completion deadline is mid-August. The Bahamian Government estimates the cost of the project to be approximately $350,000, including trenching, materials, site supervision, and modifications to the system now in place in United Estates. Future plans include extending this system to provide water to Sugar Loaf and Long Bay.

With this information about the modern water availability and usage, students are also taken on field trips to observe 19th century plantation wells (Figures 7 and 8) and the field station's catchment area (Figure 9) and water treatment plant and water tanks (Figure 10) as well as the groundwater wells along line hole settlement, airport and across from the marina (Figure 12).

Figure 7. Plantation well at the southern end of the island, at the far edge of the estate associated with Watlings' Castle.

Figure 8. Plantation well, Line Hole Settlement well road.

Figure 9. Catchment at Gerace Research Centre looking southeast. Conduit is located towards the northern end of the basin (left in photo).

Figure 10. New water tank at Gerace Research Centre, constructed in 2006-2007.

Figure 11. Groundwater well across the street from new marina.

Questions Pertaining To Water Resources

Given the information on the water usage and history of the island and field trips to historical areas around the island, students then are asked to assess the various scenarios proposed in 2004 by the US Army Corps of Engineers, for meeting water needs in the Bahamas:

- Groundwater provided via water authority on a large scale
- Private water wells
- Freshwater blended with brackish groundwater
- Groundwater barged in from one island to another
- Groundwater piped from one island to another by underwater lines
- Desalination (i.e. reverse osmosis) plants
- Transporting water from one part of the island to another
- Bottled water for drinking and cooking

Students respond to the following questions and directions in their field notebooks:

- How many of these means of meeting San Salvador Islands water needs have you observed on the island?
- Explain and describe the circumstances.
- Is there another option in use on the island that provides a significant source of freshwater?
- On a map of San Salvador, draw in the major areas of freshwater marshes and water-filled sinkholes.
- Indicate the major development sites of the last 25 years.
- What impact has development had on freshwater resources on the island?
- What has been the history of wetland use on San Salvador?
- Describe the value of wetlands and why they are so important for maintaining aquifers.

Case Study Three:
Solid Waste Disposal--
Using a Historical Perspective
Field Trips and Outreach

Historical Perspective.

Lucayan Occupation

While quite a bit is known about the Lucayan agricultural and fishing resource use, little is known about Lucayan solid waste disposal. Conch piles accreted in beach rock at Barker's Point and refuse piles elsewhere provide one of the few records of Lucayan life.

Loyalist Plantation

The Loyalist Farquharson plantation site can easily be seen from the road traveling along Queen's Highway adjacent to Pigeon Creek. Although the site is not accessible to a student group, students can get a sense waste disposal on the plantation. In general, waste was washed over the hill and there was no latrine (K. Gerace, personal communication). Sometimes visible piles of stones, removed during working the land after fences were completed, served as dump sites. Excavation of these dump sites have provided some invaluable clues to plantation life.

Fortune Hill is a plantation site that is suitable for a class visit. One of the octagon buildings covers a sinkhole that was used as a dump. The building itself may have been constructed to prevent animals from falling into the sinkhole (Kathy Gerace, personal communication).

The Loyalists modified sinkholes for water resources and an excellent well can be viewed on the west side of the dirt road to the Line Hole Settlement well field (Figure 8). Other sinkholes in the vicinity were modified to provide water sources for horses and other livestock.

Cold War Era

Burning solid waste has long been a common practice and is still observed today in some of the outer islands. However, evidence exists that the various military bases on the island used sinkholes as dump sites. A series of sinkholes just north of the dirt road leading to the Line Hole Settlement well field contains the remains of vehicles and occasionally drum remnants.

The Modern Tourism Boom

The San Salvador Island Landfill (Figure 13) was built in 2000-01 with support from the Bahamian Government and the Inter-American Development Bank. The new landfill is used extensively by all members of the community on San Salvador. Prior to the new landfill, different methods were used to dispose of waste depending on where one lived on the island. Below is the assessment of the disposal methods used prior to establishing the landfill (Environmental and Social Impact Report BH-0008: 2.10):

Three main dump sites were found on San Salvador, with the main site serving Cockburn Town, Club Med and Victoria Hill Settlement located about one-half mile from the airport in a depression along the shore of Little Lake. The site was poorly maintained and was seen by arriving passengers at the airport. Not only did it have solids and leachates overflowing into Little Lake, but it also flowed into the groundwater supply wells. This site also had numerous flies around it. The other two sites also had fly problems, as well as debris blowing across the landscape. These sites were located along roadsides and could be easily seen by visitors to the island. Solid waste collection was provided to island residents by contractors and was reasonably reliable, although indiscriminate dumping was and is still fairly common. Club Med used to recycles some of their wastes and incinerated the rest. Today trash haulers are a constant site on the island and waste segregation at the dump is maintained.

Figure 12. Active landfill north of Dixon Hill.

Figure 13. Leachate Pond at modern landfill.

<u>Students are taken to visit these various waste disposal sites and asked to answer questions and make directed observations.</u>

- Draw and label a diagram showing the layout of the San Salvador Landfill.
- Draw an overview and a cross-section that clearly shows the relationship between the cells and the leachate pond.
- What is used as a lining in the leachate pond?
- After a rain, the leachate pond fills and is usually empty within a couple of days. Do you think all of the water evaporates or can you describe another means of why the water disappears so quickly?
- Is there a thick evaporative crust on the lining of the landfill?
- What impact does the leachate pond have on individual wells, like the one Bernie Storrs has, located near the landfill?
- Examine the contents of the active cell. According to the Barbados Report (2004), Bahamians and visitors generate 264,000 tons of solid waste annually; Estimate what percentage of the items dumped in the landfills on San Salvador represents waste that was generated by residents vs. visitors?
- Why do you think cars and other large, steel items are simply discarded and not shipped off the island to be sold as scrap?

In addition to these questions and observations, the students also complete a beach clean-up. The activity is based on a lesson plan for Trash on Texas Beaches: An Investigative Field Trip/Lab Activity (2006b). Items are sorted based on whether they are plastic (including nylon rope), glass, aluminum, metal, or paper and cardboard. All items are weighed and subsequently taken to the landfill.

Figure 14. Debris found along East Beach (A.K.A. Junk Beach).

Figure 15. Collected materials along East Beach (i.e. Junk Beach) being weighed.

Table 1. Weight of items from the designated waste categories collected at Junk Beach. Total weight of all items collected was 257 pounds. Wastes were collected by 19 individuals (students and faculty) in 2.5 hours. Decay time based upon Pennsylvania Department of Natural Resources Beach Debris exercise (Anonymous, 2000).

Materials	Weight(Lbs)	Decay Time (yrs)
Plastics*	226	450
Glass	18	1000000
Metals(non Al)	3	80
Aluminum	2	150
Paper & Cardboard	2	0.8
* including nylon rope (18 Lbs)		

SCHOOL OUTREACH AND COMMUNITY ACTIVITIES

Community involvement began in 2004 when undergraduate students from our courses helped to paint the high school and dispose of trash. In 2005, each university student teamed up with two high school students and completed a beach clean-up. Large items were taken to the landfill and several bags of smaller items were taken to the school to be sorted based on the amount of time it took for the material to degrade. Both 10th graders and college students calculated the percentage of each class of waste and displayed the results in the form of a bar graph. Students also determined the source of discarded items.

In addition to the beach clean up activities, students from NJCU visited the San Salvador primary school. They went into the different classrooms and either helped the teachers with their daily lesson plans or they gave special presentations to the classes. Because many students in the NJCU program are obtaining their undergraduate degrees in Geoscience and either elementary/middle school or high school education, interacting with the primary school was important both culturally and as part of their teacher training (Figure 17). The Primary School was also given recycle containers for aluminum cans (provided by Georgia College & State University) (Figure 18). The class that collected the most cans received a prize at the end of the school year. A plaque was awarded

Figure 16. NJCU student, Justin Raia, teaching astronomy to students in the 5th Grade class at the local school.

Figure 17. NJCU Student, Michelle Chmura helping 2nd Grade students.

Figure 18. Students with the recycle program at the Primary School.

to the 5th grade class in May, 2007 for collecting the most cans. This outreach and service learning could be easily replicated by other groups visiting the GRC, ensuring that the aluminum can recycling program continues on the island.

CONCLUSIONS

Student Assessment

One of the challenges of any course and particularly an intensive week-long field course in the Bahamas is how to assess student performance. In order to do this, we developed the following rubric (Table 2) and outcomes. These outcomes can be assessed using a rubric or other tool to evaluate student presentations, reflective statements as presented in field notebooks, and also the written exercises based on the questions given to them in this program.

Learning Outcomes

Each student is graded numerically (1-3) by having the following outcomes (1-11) placed in a rubric (Table 2).

1. Gather, analyze and synthesize data independently and in groups.

2. Use appropriate graphic displays of data (tables, graphs). (Are the graphs and tables properly labeled with captions; ease that the reader can grasp the concept based on the way data is visually presented).

3. Demonstrate proficiency in oral and written communication. (Are complete sentences, properly constructed and ordered paragraphs used).

4. Demonstrate cultural understanding and appreciation and how it relates to addressing environmental issues (e.g. student may recognize the role religion plays in the lives of Bahamians and addresses issues within the context of caring for the environment is also caring for God's world).

5. Utilize principles from multiple fields of science when addressing environmental issues. (Can the student understand why a certain organic molecule has a long residence time in the environment and how that relates to the way that compound travels in the groundwater and is absorbed by organisms).

6. Employ multiple working hypotheses when assessing environmental processes (student understands that there is not a single cause for the effect they see).

7. Uses accurate scientific content when assessing environmental issues; (is the scientific content both accurate and appropriate to describe the environmental issue).

8. Critique proposed solutions to environmental problems and project possible outcomes to those actions (student can offer a single solution, however, students who perform the best offer multiple "solutions" along with possible benefits and disadvantages of those solutions)

9. Develop and use knowledge of Bahamian economics, political science and other social sciences when assessing environmental issues. (Does the student include an accurate social or cultural factor that could either help or hinder a proposed "solution").

10. Present all points of view and interests of all shareholders when assessing environmental issues. (Does the student realize that a solution is not a solution unless a majority of shareholders can accept the consequences of its implementation?).

11. Demonstrate ability to mediate differences in opinions (does the student try to find a commonality among shareholders?).

Table 2. Rubric used for grading student outcomes. Learning outcomes 1-11 correlate with those explained in text. Assessment is graded numerically 1-3 or U if unable to determine for each student for each learning outcome.

Sample Assessment Data											
	Learning Outcome #										
Student	1	2	3	4	5	6	7	8	9	10	11
	3	3	3	3	3	3	3	3	3	3	3
	1	1	1	1	1	1	U	1	2	U	U
	2	3	1	2	U	1	U	2	2	2	1
	2	1	1	3	1	1	2	1	2	2	2
	1	3	3	1	1	1	U	1	2	2	3
	1	1	3	3	1	3	3	1	3	U	U
	2	2	2	2	2	2	2	2	2	2	1
Average	1.71	2.00	2.00	2.14	1.50	1.71	2.50	1.57	2.29	2.20	2.00
#U = uncertainity	0	0	0	0	1	0	3	0	0	2	2

Assessment Scale
3- High Level of Attainment
2-Moderate level of Attainment
1- Low Level of Attainment
U- Unable to determine

ACKNOWLEDGMENTS

We would like to thank Dr. Donald T. Gerace, Chief Executive Officer, and Vincent Voegeli, Executive Director of the Gerace Research Center, San Salvador, Bahamas and Sandy Voegeli for facilitating working relationships between our classes and the school systems. We would also like to thank the Administration and Faculty of San Salvador High School and Primary School and all the undergraduate students, from a multitude of colleges and universities (University of St. Thomas (Houston), Berry College (Rome, GA), New Jersey City University, University System of Georgia Schools) who have taken part in our courses during the years. Special thanks are extended to Dr. Dwight Call, Liz Havey and Libby Davis (GCSU International Office) for their role

in developing and supporting both of our programs on San Salvador Island.

REFERENCES

Anonymous, 2001, Bahamas, IDB, sign $21 million to assist in rehabilitating works damaged by Hurricane Floyd, Inter-American Development Bank (IDB); Date: 21 Mar, 2001. Retrieved May 5, 2006.http://www.reliefweb.int/rw/RWB.NSF/db900SID/ACOS-64C395?OpenDocument

Anonymous, 2006a, *Water Relief for San Salvador,* Retrieved May 10, 2006. http://www.bahamasuncensored.com/april06.html#WATER%20RELIEF%20FOR%20SA

Anonymous, 2006b, Trash on Texas Beaches An Investigative Field Trip/LabActivity. Retrieved on May 5, 2006. http://teachertech.rice.edu/participants/louviere/Lessons/les5.html

Anonymous, 2000, DCNR-PA Bureau of State Parks, Retrieved on May 10, 2006. http://www.trecpi.org/pdfs/BeachDebris%20pb2000.pdf,

The Bahamas National Assessment Report, 2004, The ten-year review for the implementation of the Barbados Programme of Action. Retrieved May 5, 2006. http://www.Bahamasuncensored.com.

Environmental and Social Impact Report, 2004, The Bahamas Solid Waste Management Program (BH-0008); Distributed by the Inter-American Development Bank.

Gray, Alfred, 2001, Minister for Agriculture, Fisheries and Local Government of the Commonwealth of The Bahamas , Retrieved May 5, 2006, from http://www.fao.org/documents/show_cdr.asp?url_file=/DOCREP/005/Y4172M/rep2/bahamas.htm

Pilkey, Orrin H., and Neal, William J., Editors Living with the Shore- (17 volume series on coastal management), Duke University Press. Durham, North Carolina

Water Resources Assessment of The Bahamas, 2004, Report, US Army Corps of Engineers, Mobile District & Topographic Engineering Center. Retrieved May 6, 2006. http://www.sam.usace.army.mil/en/wra/Bahamas/Bahamas.html